

LIGHT AVAILABILITY AND AQUATIC PRIMARY PRODUCTION:
COLORADO RIVER, GLEN AND GRAND CANYONS, AZ.

By Michael Davis Yard

A Dissertation

Submitted in Partial Fulfillment

Of the Requirements for the degree of

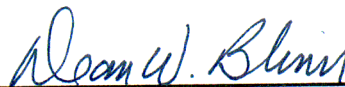
Doctor of Philosophy

In Biology

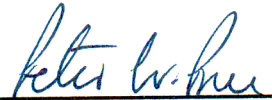
Northern Arizona University

May 2003

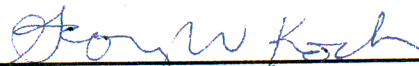
Approved:



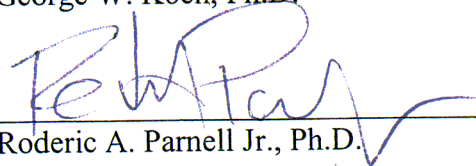
Dean W. Blinn, Ph.D., Chair



Peter W. Price, Ph.D.



George W. Koch, Ph.D.



Roderic A. Parnell Jr., Ph.D.

565.00
ENV-4.00
Y278

ABSTRACT

LIGHT AVAILABILITY AND AQUATIC PRIMARY PRODUCTION:
COLORADO RIVER, GLEN AND GRAND CANYONS, AZ.

Rugged topography is common to southwestern canyon-bound streams and rivers and affects solar insolation received. This is a predictable consequence of canyon and channel orientation, elevation angles and viewshed. Modeled estimates corresponded to measurements for instantaneous photosynthetic photon flux density and daily solar insolation levels. Depending on outlying topography, canyons having east-west orientations exhibited greater seasonal variation, and ranged from 8.1 – 61.4 mol m⁻² d⁻¹. For east-west orientations, 70% of mid-channel sites were seasonally obscured from direct solar incidence.

In Glen Canyon, optical properties were regulated by dissolved organic carbon (DOC) and particulate organic matter. Results suggested that physiochemical and biotic processes occurring in the reservoir and river regulated light-attenuation coefficients (K_N normalized for solar zenith angle). Average K_N differed among years (1991-1998) and seasons, and were correlated to water quality parameters (pH, specific conductance). Spatial differences in K_N were correlated to DOC and appeared related to autotrophic production. Experimental results assessing algal production effects on optical properties indicated that DOC and K_N differed significantly among treatments (algal and non-algal).

In Grand Canyon, PPF_D is regulated by sediment supply and interactions arising from other hydraulic processes that regulate sediment transport. Suspended-sediment

(SS) is the primary causal factor in light-attenuation, K_N ranged from 0.221 to 126 (m^{-1}) and correlated to SS ranging from 0.0003 to 7.0 (g l^{-1}). Significant interactions occurred between SS and discharge, channel geometry, and stream length. Frequency analysis for median estimates of K_N coefficients (1963-2002) were: 0.25 m^{-1} for Glen Canyon; 0.65 m^{-1} for Marble Canyon; 1.35 m^{-1} for Central Grand Canyon; and 2.02 m^{-1} and for Western Grand Canyon.

Primary production measuring oxygen generation was correlated to light, temperature, and biomass. Simulated estimates made under constant K_N (0.24 m^{-1}) and depth (0.5m), resulted in maximum net primary production (*NPP*) (11-16°C) at intermediate biomass levels, ranging from 23.56 to 10.39 $\text{gO}_2 \text{m}^{-2} \text{da}^{-1}$, for summer and winter, respectively. Conversely, under elevated light-attenuation ($K_N > 1$, depths $\geq 2.5\text{m}$), *NPP* reduced to 0.55 and 0.10 $\text{gO}_2 \text{m}^{-2} \text{da}^{-1}$ for 11°C and 16°C, respectively. Modeled estimates were consistent with independent production measurements published for this ecosystem.

ACKNOWLEDGEMENTS

Research findings presented in this dissertation would not have been possible without the assistance, suggestions and encouragement from my major professor, mentor and above all else friend, Dean Blinn. Additionally, I would like to thank the other members of my dissertation advisory committee that include: George Koch, Peter Price, and Rod Parnell who have provided thoughtful perspectives, ideas, improvements and directions for navigating through this academic terrain. However, this dissertation would not have been realized had it not been for the thoughts, assistance, and support from so many other individuals involved. I am very indebted to my family, friends, colleagues, faculty, students and volunteers who have graciously given of their time toward this end.

I dedicate this dissertation to two special people, for without their support, this body of work would not have been. First, my beloved Helen, friend, companion and wife, who has been a constant inspiration throughout this journey, deserves so much of the credit. She has been selfless, supportive and when needed a very persistent goad. As she once stated, "she has managed to persevere through some of the most mundane and monotonous science ever conceived." In defense, I imagine that these types of projects are the ones that we can only selectively share or partially inflict upon our loved ones. For it is certain that no one else in his or her right mind would have done it. Thank you, I am forever indebted. The other person, Glen Bennett has been an unbelievable friend and technical resource. I have relied heavily on his computer programming skills and his ability to ruminate over certain ideas, concepts and

relationships that were later translated into numeric code. This dissertation does not reflect the countless hours directed toward programming, tangential discussions, and immeasurable libations consumed in the process. Also, a thanks goes to Annie Bennett, his wife, whose consent was always forthcoming. I look forward to the near future where we might be able to collaboratively develop a simulation model for estimating primary production in the Colorado River from the research described in this dissertation. Of course the development of this simulation model will need to be libated with an occasional swish from a highland kilt.

Gratitude and fondness is extended to members of my immediate family who actively encouraged my academic pursuit, and were sometimes indentured participants, they are: Renee and John Caswell; Jennifer Diaz; Arline and Phil Miller; Stephanie, Charlie and Tom Moody; Mary and Victor Nackard; Helen Yard; Sharon and George Yard; and Tom Yard. A special thanks goes to my sister Stephanie for her computational tutelage owing to certain mathematical inequities of mine. Ah, the mysteries of recombinant DNA.

Recognition goes to USGS, Grand Canyon and Monitoring and Research Center (GCMRC) that financially supported the proposed research effort through a cooperative agreement 98-FC-40-0540 with Northern Arizona University. A special thanks goes to Barry Gold and Barbara Ralston who understood and believed in the underlying purpose and utility of funding this research. Also, I am thankful for all of the assistance, data, computer and logistical support provided by GCMRC personnel and other people associated with the countless research studies in the Colorado River. Special thanks goes to Dave Baker, Dale Blank, Lew Coggins, Renee Davis, Denny

Finn, Chris Flacus, Carol Fritzinger, Elizabeth Fuller, Dave Garrett, Steve Gloss, Barry Gold, Mark Gonzales, Tom Gushue, Susan Hueftle, Keith Kohl, Ben Komada, Jeanie Korn, Serena Mankiller, Ted Melis, Steve Mietz, Bill Person (AGF), Richard Quartaroli, Barbara Ralston, Park Stephenson, Dennis Stone (FWS), Jake Tieg, David Topping, Randy VanHaverbecke (FWS), Bill Vernieu, Rich Valdez (SWCA), Nick Voichick, and Stephanie Wyse. Additional thanks to other USGS personnel with Water Resource Division: Don Bills, Greg Fisk, Julie Graf, Bob Hart, Nancy Hornewer, and Mike Dai. Also, thanks and appreciation goes to Dave McKinnon a USGS astrophysicist who provided technical assistance and advice regarding irradiometric and photometric analysis.

Certain faculty, students and staff of Northern Arizona University (NAU) should be recognized for their field and laboratory assistance, especially the NAU Aquatic Ecology Lab, thanks goes to Joe Bailey, Emma Benenati, Daniel Boughregard, Steve Earl, Allen and Carol Haden, Ally Martinez, Molly McCormick, Ian McKinnon, Chris O'Brien, Nicky Preston, Kim Pomeroy, Mike Shaver, Joseph Shannon, Amy Welty, Kevin Wilson, and Nathan Zorich; and NAU Geophysical Lab, Jeff Bennett, Joe Hazel, Matt Kaplinski, and Mark Manone. In addition to my committee, I would like to also recognize other faculty members such as Sylvester Allred, Tina Ayers, Bill Gaud, Bruce Hungate, Steven Hempleman, Ron Markle, Jane Marks, Lynn Montgomery, Nancy Johnson, Randy Scott, Tom Sisk, and Tom Whitham for providing either advice or all around encouragement and support. Also, special thanks are extended to Michael Kearsley, Phil Service and Vicky Meretsky (IU) for their statistical advice.

David Wegner deserves special thanks and gratitude for providing me the opportunity to become directly involved in scientific research in Grand Canyon as part of the Glen Canyon Environmental Studies. He exemplifies what a combination of commitment and persistence may accomplish, and has been influential in directing my scientific interest. Also, Larry Stevens who conceived of the idea of phytobenthic light limitation; as well as, Steve Carothers who convinced me of the utility in characterizing the apparent optical properties of the Colorado River. Again, Allen Haden for his collaboration, friendship and being such a stoic and dependable character on all of our river trips. I am also grateful to Ally Martinez for her field and laboratory support. Additionally, I would like to thank Carl Walters (UBC) and Josh Korman (Eco-Metrics) for their insight, advice and demonstrations on conceptual and numerical modeling, spreadsheets, nicotine, and sleep deprivation. Thanks to Margaret Palmer (UMD) and David Topping for their additional review.

Thanks to Charlie Britton (NAU Instrumentation Lab); Frank Mayorga (Mayorga's Welding); Danny Martinez, Eric Brown, Matt Sayre and Bruce Helin (Professional River Outfitters); and Alida Dierker (Sew This) in designing and fabricating many of the novel sampling devices I used in this research study; and Mary Williams for her artistic flare and graphic design. Also, special recognition goes to all of the volunteers who participated on these field trips Sylvester and Donna Allred, Annie Bennett, Dave Brown, Lydia Brunig, Kenny Carothers, Haydee Hampton and George Koch, Lanie Johnstone, Diana Kimberling, Clay Nelson, Chris Mactosh, Nicky Preston, Frank and Barbara Protiva, and Valerie Sailor.

Thanks to all of the wonderful river-guides: Jeff Behan, Jim Boles, Steve Bledsoe, Dugald Bremner, Dave Brown, Brad Dimock, Dave Edwards, Carol "Fritz" Fritzinger, Kenton Grua, Bob Grusy, Curtis "whale" Hansen, Joe Hazel, Nancy and Bruce Helin, Matt Kaplinski, Chris Macintosh, Tom Moody, Lars and Nels Nemi, Peter Reznick, Andre Potochnik, Dirk Pratley, Sue Rhodes, Stewart Rieder, Richard Quartaroli, Tim and Pam Whitney, Mary Williams, and Peter Weiss that were involved and showed interest in this project, especially both Brian and Dan Dierker. Brian Dierker was solely responsible for providing me the opportunity 30-years ago to mess around in little boats, while experiencing the mysteries of the Colorado River. In turn, Dan Dierker has always been a wealth of information by providing thoughtful advice, critique, assistance, and the occasional dollop of sarcasm that has more often than naught been questionably delivered, but appropriately timed. I have and will always remain in all of your debt; thanks I would not have approached it any differently.

Thank you all!

TABLE OF CONTENTS

LIST OF TABLES	xii
LIST OF FIGURES	xiv
PREFACE	xviii
DATA	xix
CHAPTER 1. INTRODUCTION AND SYNTHESIS OF DISSERTATION	
Introduction	1
Literature Cited	7
CHAPTER 2. SEASONAL INFLUENCE OF TOPOGRAPHIC COMPLEXITY ON AQUATIC ECOSYSTEMS: SOLAR INSOLATION ESTIMATES FOR THE COLORADO RIVER, GLEN AND GRAND CANYONS, AZ.	
Abstract	10
Introduction	11
Methods	13
Results	22
Discussion	27
Literature Cited	32

CHAPTER 3. LINKAGES BETWEEN RESERVOIR AND IN-STREAM
PROCESSES REGULATING DISSOLVED ORGANIC CARBON
AND LIGHT-ATTENUATION IN A RIVER ECOSYSTEM.

Abstract	52
Introduction	53
Methods	55
Results	60
Discussion	65
Literature Cited	74

CHAPTER 4. APPARENT OPTICAL PROPERTIES IN A FLUVIAL RIVER
SYSTEM: COLORADO RIVER, GRAND CANYON, AZ

Abstract	96
Introduction	97
Methods	99
Results	104
Discussion	109
Literature Cited	117

CHAPTER 5. MODELING PHOTOSYNTHETIC PHOTON FLUX DENSITY IN A FLUVIAL RIVER SYSTEM: LIGHT-ATTENUATION ESTIMATES FOR THE COLORADO RIVER, GLEN AND GRAND CANYONS, AZ.

Abstract	134
Introduction	135
Methods	137
Results	147
Discussion	161
Literature Cited	156

CHAPTER 6. PRIMARY PRODUCTION MODEL FOR THE COLORADO RIVER, GLEN AND GRAND CANYONS, AZ: INTERDEPENDENCE OF LIGHT, TEMPERATURE AND BIOMASS

Abstract	169
Introduction	170
Methods	172
Results	178
Discussion	182
Literature Cited	190

LIST OF TABLES

CHAPTER 2

Table 1.	Location of major canyon sections and geomorphic reaches of the Colorado River from Glen Canyon Dam to Grand Wash Cliffs, Lake Mead, AZ.	37
Table 2.	Annual and seasonal (21-June and 21-December) estimates of mean daily solar insolation levels for different canyon sections and geomorphic.	38
Table 3.	Mean daily insolation levels ($\text{mol quanta m}^{-2} \text{d}^{-1}$) estimated for summer and winter seasons (21-June and 21-December) along primary channel orientations.	39

CHAPTER 3

Table 1.	ANOVA type II random effects model, for suspended inorganic (SS) and organic (POM) particles in response to sampling date, time, and sites.	82
Table 2.	Summarized data for depth-integrated suspended samples (mg L^{-1}) collected during 1997-1998.	83
Table 3.	Mallows C_p criterion used as for selecting appropriate statistical model to estimate normalized light-attenuation.	84

CHAPTER 4

Table 1.	Suspended-sediment and organic particulate loads measured during different sampling periods (sediment limited and sediment enriched periods) and canyon sections.	123
Table 2.	Light-attenuation coefficients (K_D) measured during different sampling periods (sediment limited and sediment enriched conditions) and canyon sections.	124

CHAPTER 5

Table 1.	Frequency analysis distribution of underwater light attenuation coefficients in the major canyon sections.	160
Table 2.	Total wetted area, mean channel depth, light-attenuation coefficient, photosynthetically available area, and areal percent (PAA%) calculated for the different geomorphic reaches	161

CHAPTER 6

Table 1.	Estimates of net daily photosynthesis, community respiration, hourly biomass-specific gross primary production, daily area-specific gross primary production, and net primary production.	197
Table 2.	Production estimates for measured and predicted: area-specific gross primary production, biomass-specific gross primary production, net photosynthesis, daily community respiration, and net primary production	198

LIST OF FIGURES

CHAPTER 2

Figure 1. Map showing major canyon sections, geomorphic reaches, and tributaries of the Colorado River	40
Figure 2. Schematic drawing illustrating the major topographic and solar altitude angles used in estimating instantaneous ground incidence	41
Figure 3. Predicted and observed daily solar insolation estimates (mol quanta $m^{-2} d^{-1}$) for summer (22 June 1992) and winter (21 December 1993)	43
Figure 4. Graphical results generated from GIS coverage using Arc-Info Hillshade routine (ESRI 1994) for mean illumination angles (Ψ_i , degrees) distributed over the cardinal directions along the entire river length in hectometers from Glen Canyon Dam to Lake Mead	45
Figure 5. Planar view representing mean daily solar insolation (mol quanta $m^{-2} d^{-1}$) distributed over the entire year from Glen Canyon Dam to Lake Mead.	47
Figure 6. Seasonal range of mean daily solar insolation (mol quanta $m^{-2} d^{-1}$) distributed over the entire year from Glen Canyon Dam to Lake Mead.	49
Figure 7. Daily solar insolation (mol $m^{-2} d^{-1}$) comparisons made among winter (21 December) and summer (21 June) seasons from Glen Canyon Dam to Cave Canyon	51

CHAPTER 3

Figure 1. Glen Canyon study area.	85
Figure 2a. Scalar light-attenuation coefficients (K_o , m^{-1}) measured at Site 3 (25.2 km) on 20 September 1998	86
Figure 2b. Average scalar light-attenuation coefficients (\pm SE) measured seasonally in Glen Canyon during 1997-1998	87

Figure 3. Mean annual light-attenuation coefficients measured between 1991-1998 (scalar light-attenuation and normalized light-attenuation coefficients) averaged across all sites in Glen Canyon.	88
Figure 4. Seasonal (1997-1998) and spatial variability of mean dissolved organic carbon ($\text{mgL}^{-1} \pm \text{SE}$).	91
Figure 5a. Total suspended-sediment measured during a sediment supply event.	93
Figure 5b. Normalized light attenuation coefficients during a sediment supply event.	93
Figure 6a. One-way ANOVA for diffuse light-attenuation coefficients (K_d, m^{-1}) carbon exposed to natural sunlight conditions (48-h period) for algal and non-algal treatments	95
Figure 6b. One-way ANOVA for dissolved organic carbon (DOC, mg l^{-1}) exposed to natural sunlight conditions (48-h period) for algal and non-algal treatments	95
 CHAPTER 4. 	
Figure 1. Map of the major canyon sections and geomorphic reaches of Glen and Grand canyons	125
Figure 2. Normalized light-attenuation coefficients plotted in relation to suspended-sediment concentrations	127
Figure 3a. Sediment-light regression coefficients plotted for different hydrological events for sediment-limited conditions	129
Figure 3b. Sediment-light regression coefficients plotted for different hydrological events for sediment enriched conditions	129
Figure 4. Width/depth ratios estimated for both minimum and maximum flow discharge levels ($142 \text{ to } 710 \text{ m}^3 \text{ s}^{-1}$) averaged across multiple cross-sections and plotted against stream length downstream from Glen Canyon Dam	131
Figure 5a. Spatial variability of mean normalized light-attenuation coefficients.	133
Figure 5b. Spatial variability of mean suspended sediment.	133

CHAPTER 5.

Figure 1. Map of the major canyon sections and geomorphic reaches of Glen and Grand canyons	163
Figure 2. Schematic drawing of a cross-sectional profile of the river for two different flow discharges (142 and $568 \text{ m}^3\text{s}^{-1}$)	164
Figure 3. Comparisons of light-depth penetration among observed and estimated underwater depths for 1% of photosynthetic photon flux density	166
Figure 4. Cumulative frequency distribution of estimated mean daily scalar light-attenuation coefficients for Glen Canyon, Marble Canyon, Central Grand Canyon, and Western Grand Canyon sections	168

CHAPTER 6.

Figure 1. Map of the Colorado River and the major canyon sections and tributaries between Lake Powell and Lake Mead reservoirs	199
Figure 2a. At 11°C , measured and predicted rates of net photosynthesis normalized per unit biomass (NP : $\text{mgO}_2 \text{ gC}^{-1} \text{ m}^{-2} \text{ h}^{-1}$) and varying levels of underwater photosynthetic photon flux density	201
Figure 2b. At 16°C , measured and predicted rates of net photosynthesis normalized per unit biomass (NP : $\text{mgO}_2 \text{ gC}^{-1} \text{ m}^{-2} \text{ h}^{-1}$) and varying levels of underwater photosynthetic photon flux density	201
Figure 3. At 11°C and 16°C , predicted area-specific gross primary production ($ASGP$: $\text{mgO}_2 \text{ m}^{-2} \text{ h}^{-1}$) and community respiration (CR_D : $\text{mgO}_2 \text{ m}^{-2} \text{ h}^{-1}$) over a range of standing biomass	203
Figure 4a. Predicted response for daily net primary production (NPP : $\text{gO}_2 \text{ m}^{-2} \text{ d}^{-1}$), and total community respiration, day and night (CR_{D+N} : $\text{gO}_2 \text{ m}^{-2} \text{ d}^{-1}$) distributed over a range of standing biomass during summer at 16°C	205
Figure 4b. Predicted response for daily net primary production (NPP : $\text{gO}_2 \text{ m}^{-2} \text{ d}^{-1}$), and total community respiration, day and night (CR_{D+N} : $\text{gO}_2 \text{ m}^{-2} \text{ d}^{-1}$) distributed over a range of standing biomass during winter at 16°C	205

- Figure 4c. Predicted response for daily net primary production (NPP : $\text{gO}_2 \text{ m}^{-2} \text{ d}^{-1}$), and total community respiration, day and night (CR_{D+N} : $\text{gO}_2 \text{ m}^{-2} \text{ d}^{-1}$) distributed over a range of standing biomass during summer at 11°C 205
- Figure 4d. Predicted response for daily net primary production (NPP : $\text{gO}_2 \text{ m}^{-2} \text{ d}^{-1}$), and total community respiration, day and night (CR_{D+N} : $\text{gO}_2 \text{ m}^{-2} \text{ d}^{-1}$) distributed over a range of standing biomass during winter at 11°C 205

PREFACE

This dissertation has been organized as a set of six chapters, five of which are prepared as manuscripts for publication and appear in the appropriate format style of that respective journal. Relevant titles and submission sites are listed below:

CHAPTER 1. INTRODUCTION AND SYNTHESIS OF DISSERTATION

CHAPTER 2. SEASONAL INFLUENCE OF TOPOGRAPHIC COMPLEXITY ON AQUATIC ECOSYSTEMS: SOLAR INSOLATION ESTIMATES FOR THE COLORADO RIVER, GLEN AND GRAND CANYONS, AZ.

To be submitted to Ecological Modeling.

CHAPTER 3. LINKAGES BETWEEN RESERVOIR AND IN-STREAM PROCESSES REGULATING DISSOLVED ORGANIC CARBON AND LIGHT-ATTENUATION IN A RIVER ECOSYSTEM.

To be submitted to Limnology and Oceanography

CHAPTER 4. APPARENT OPTICAL PROPERTIES IN A FLUVIAL RIVER SYSTEM: COLORADO RIVER, GRAND CANYON, AZ.

To be submitted to Hydrobiologia.

CHAPTER 5. MODELING PHOTOSYNTHETIC PHOTON FLUX DENSITY IN A FLUVIAL RIVER SYSTEM: LIGHT-ATTENUATION ESTIMATES FOR THE COLORADO RIVER, GLEN AND GRAND CANYONS, AZ.

To be submitted to Hydrobiologia.

CHAPTER 6 PRIMARY PRODUCTION MODEL FOR THE COLORADO RIVER, GLEN AND GRAND CANYONS, AZ: INTERDEPENDENCE OF LIGHT, TEMPERATURE AND BIOMASS.

To be submitted to Regulated Rivers.

DATA

All raw and processed data, field notes, samples, and sample collection forms that were generated or collected under the cooperative agreement (98-FC-40-0540) with Northern Arizona University are considered the property of the U. S. Government and have been delivered to United States Geological Survey, Grand Canyon Monitoring and Research Center in accordance with the stipulations of the research and collecting permits for this project. These data are available to the public as specified in the Release of Data section <ftp://ftp.gcmrc.gov/data/>.

Raw and processed data have been delivered and are available in electronic format. Accompanying this archived data set is the metadata that conforms to the Federal Geographic Data Committee (FGDC) metadata standards. Metadata standards are found at: <http://www.fgdc.gov/metadata/constan.html>. The database measurements are in Standard International units and year 2000 compliant.

CHAPTER 1
INTRODUCTION AND SYNTHESIS
OF DISSERTATION

In lotic systems, the structure and function of aquatic communities is regulated by interactions occurring among different abiotic and biotic factors: growth rates are typically influenced by a combination of temperature, light and nutrients (Cuker 1983; Mulholland *et al.* 1991; Hogg and Williams 1996; Falkowski and Raven 1997); whereas loss rates are often affected by herbivory, pathogens and hydrological disturbance (Cuker 1983; Stewart 1987; Blinn *et al.* 1995). The counter acting effect between rates of growth and loss ultimately determines a community's persistence (Peterson 1986; Stewart 1987; Peterson and Boulton 1999).

Globally, very few river systems remain unaltered from land-use practices, flow regulation, flow diversion, and impoundments (Petts 1984). The Colorado River is strongly influenced by human-activities (Stevens *et al.* 1997_a, 1997_b; Blinn *et al.* 1998) and is one of the most regulated rivers in the world (Fradkin 1981). The construction and operation of Glen Canyon Dam (GCD) altered the annual and seasonal characteristics of discharge, temperature and sediment transport (Blinn and Cole 1991; Stevens *et al.* 1997_a). Many of the native fishes of the Colorado River are presently listed as threatened or endangered (Minckley 1991), and the resulting changes to abiotic (i.e., temperature and sediment flux) and biotic (i.e., food availability and non-native fish introductions) factors have been implicated in their decline and/or extirpation (Schmidt *et al.* 1998; Minckley *et al.* 2003).

Although often overlooked, GCD physically disrupted the mass movement and transport of allochthonous organic material through this ecosystem (Haden *et al.* 1999). The conveyance of this organic material had once structurally defined the trophic food-web and linkages of this pre-dam aquatic environment. Aquatic primary production has become the trophic substitute, and now dominates the flow of energy through this once allochthonously based ecosystem (Angradi 1994; Shannon *et al.* 2001).

Photosynthetically photon flux density (PPFD, 400-700 nm) is considered to be the fundamental determinant of phytobenthic productivity in the post-dam Colorado River (Usher and Blinn 1990; Blinn and Cole 1991; Hardwick *et al.* 1992; Shannon *et al.* 1994; Shaver *et al.* 1997).

In response to these ecological changes, the present ecosystem supports a phytobenthic community that consists primarily of macroalgae, *Cladophora glomerata*, *Ulothrix sp.*, *Mougeotia sp.*, *Spirogyra sp.*, *Chara contraria*, bryophytes, *Fontinalis sp.*, and macrophyte, *Potamogeton pectinatus*. *Cladophora glomerata*, a branched green filamentous alga, functions as the structural attachment for epiphytes and habitat for macroinvertebrates (Shannon *et al.* 1994; Blinn *et al.* 1995) and has now become widely established in this ecosystem (Blinn and Cole 1991). The epiphytic assemblage is composed almost entirely of diatomaceous species (*Diatoma vulgare*, *Cocconeis placentula*, and *Rhoicosphenia curvata*) (Hardwick *et al.* 1992; Benenati *et al.* 1998), and appear to be the primary source of autotrophic energy for higher trophic levels and comprise the majority of the invertebrate diet (Blinn and Cole 1991; Blinn *et al.* 1995).

The underlying purpose of this dissertation has been to determine interrelationships among various factors influencing primary production in this lotic

ecosystem. A number of investigators have evaluated the effects of desiccation (Usher and Blinn 1990; Blinn *et al.* 1995) and phytobenthic response to long-term atmospheric exposure. Results have demonstrated how temporary reduction in total wetted area negatively affects the phytobenthos (Peterson 1986; Blinn *et al.* 1995; Shaver *et al.* 1997; Benenati *et al.* 1998). Although information exists on the phytobenthic response to fluctuating flow patterns, little data however is available on how the phytobenthos might respond to varying light environments.

Determining the mechanistic role and biotic responses to these regulating factors is important for understanding limitations to aquatic primary production and the flow of energy in this ecosystem. Consequently, characterizing underwater light environment and its availability for primary production has been central to this research project. This dissertation is organized around the primary factors that regulate: 1) the solar incidence reaching the surface of the water (topographic complexity), 2) apparent optical properties that regulate underwater light-attenuation (dissolved organic carbon and suspended-sediment), and 3) photosynthetic response by the phytobenthic community to these limiting factors.

I examine in chapter 2 the role that complex topography and canyon orientation has on regulating daily, seasonal and annual solar insolation reaching the Colorado River. It was hypothesized that incoming solar incidence available to this aquatic ecosystem would be affected by topographic obstructions, and that the resultant variability would generate a spatial mosaic of varying solar insolation levels throughout the Colorado River. This geographic region extends over 475 km in length and contains four major canyon sections (i.e., Glen, Marble and Central Grand and Western Grand canyons). The

major objectives were: 1) develop a model for estimating instantaneous solar flux for large rivers flowing through topographically complex environments; and 2) determine where differences in daily, seasonal and annual solar insolation occurred along the Colorado River, 3) describe the analytical approach and inherent assumptions used in the model.

It was hypothesized in chapter 3 that: 1) dissolved organic carbon (DOC) was the primary constituent responsible for light-attenuation in the Colorado River tailwater (Glen Canyon); 2) limnological processes occurring in Lake Powell were initially regulating the apparent optical properties of the river, and 3) loss of extracellular photosynthates and particulate organic matter (POM) from in-stream autotrophic production secondarily influenced the apparent optical properties further downstream in Glen Canyon.

A combination of observational studies and experimental manipulations were used to determine the mechanisms responsible for regulating photosynthetic photon flux density available for primary production in this aquatic ecosystem. The major study objectives were: 1) determine the temporal and spatial variability of apparent optical properties of the Colorado River in the regulated tailwater section of Glen Canyon, 2) identify factors and regulating mechanisms potentially responsible, 3) develop a regression model that estimated apparent optical properties for predicting PPFD availability at channel depth for primary production.

I examined in chapter 4 the relationship between suspended-sediment and light-attenuation. In streams and rivers, certain hydraulic forces interact with sediment-supply and geomorphology in regulating sediment transport rates (Howard and Dolan 1981;

Reid *et al.* 1997; Rubin *et al.* 1998; Topping *et al.* 2000a). Suspended-sediment is a major factor that determines underwater light-attenuation, especially in fluvial river systems, and I sought to determine if there was a predictive relationship between suspended concentrations (total suspended, inorganic and organic) and the apparent optical properties of water in the Colorado River.

The major objectives of chapter 5 were: 1) determine the degree to which suspended-sediment (total, inorganic, and organic) affected apparent optical properties of water; 2) determine how discharge, channel morphology, and stream length influenced suspended loads; 3) develop a predictive relationship for estimating suspended-sediment under clear, sediment-limited conditions; and 4) address how underwater light-attenuation in the Colorado River mainstream may be influenced by the hydrodynamic processes regulating suspended loads.

The major study objectives in chapter 5 were: 1) develop a light-sediment model that is regulated by sediment transport and tributary supply processes; 2) validate the light-sediment model by comparing estimated and observed light-attenuation coefficients collected throughout the Colorado River; 3) determine the frequency distribution of light-attenuation in the different canyon sections for the period of record (1963 to 2002); and 4) estimate photosynthetically available area for different canyon sections and geomorphic reaches under varying discharge levels and seasons. I used a combination of predictive relationships, some from previous chapters (Chapter 2, 3, 4 and 6), and other published relationships and models for tributary sediment discharge (Randle and Pemberton 1987; Topping 1997), channel morphology (Randle and Pemberton 1987), and unsteady flow routing (Wiele and Smith 1996).

In chapter 6, a primary production model was constructed to address certain ecological questions that might arise regarding potential effects to the phyto-benthic community by implementing flow scenarios, sediment augmentation and/or temperature modification in the Colorado River. Using simulation modeling as a strategy is a very powerful tool to understand large-scale, complex ecological processes and systems (Oreskes *et al.* 1994). Simulations from this model may provide a conceptual framework for developing testable hypotheses, as well as identifying unrecognized gaps in our present knowledge base. I sought to understand how the phyto-benthic community, composed predominantly of *C. glomerata* would likely respond to varying physical (light and temperature) and biotic (biomass) factors as a result of management actions. A series of primary production experiments were conducted under *in situ* conditions using oxygen-metabolic chambers exposed to different temperature, light, and biomass levels (Brock 2000).

My study objectives were to: 1) determine if net photosynthesis and community respiration rates varied under different levels of temperature, light, and biomass; 2) develop a predictive model for estimating primary production rates (gross, respiration and net photosynthesis); 3) based on environmental conditions compare modeled production estimates against previously measured production estimates for the system; and 4) infer how certain prescriptive changes might influence the autotrophic community in this altered ecosystem.

Literature Cited

- Angradi, T. R. 1994. 'Trophic linkages in the lower Colorado River: multiple stable isotope evidence', *N. Amer. Benth. Soc.* 13: 479-495.
- Benenati, P., J.P. Shannon, and D.W. Blinn. 1998. Desiccation and recolonization of phytobenthos in a regulated desert river: Colorado River at Lees Ferry, Arizona, USA. *Regul. Rivers: Res. Mgmt.* 14:519-532.
- Blinn, D.W., and G.A. Cole. 1991. Algal and invertebrate biota in the Colorado River: Comparison of Pre- and Post-Dam Conditions. *In*. Marzolf, G.R. (Ed.), *Colorado River Ecology and Dam Management: Proceedings of a Symposium*. National Academy Press, Washington D.C.
- Blinn, D.W., J.P. Shannon, L.E. Stevens, and J.P. Carder. 1995. Consequences of fluctuating discharge for lotic communities. *J. N. Am. Benthol. Soc.* 14:233-248.
- Blinn, D.W., J.P. Shannon, P.C. Benenati and K.P. Wilson. 1998. Algal ecology in tailwater stream communities: Colorado River below Glen Canyon Dam, Arizona. *J. Phycol.* 34:734-740.
- Brock, J. T., T. V. Royer, E. B. Snyder, and S. A. Thomas. 2000. 'Periphyton metabolism: A chamber method', *In*. Webb, R. H., J. C. Schmidt, G. R. Marzolf, and R. A. Valdez (Eds), *The controlled flood in Grand Canyon*. Geophysical Monograph, Am. Geophys. Union, Washington, D. C. 110:217-223.
- Cuker, B. E. 1983. 'Grazing and nutrient interactions in controlling the activity and composition of the epilithic algal community of an arctic lake. *Limnol. Oceanogr.* 28: 133-141.
- Falkowski, P. G., and J. A. Raven. 1997. *Aquatic photosynthesis*. Blackwell Science, Malden, Mass.
- Fradkin, P. L. 1981. *A river no more: The Colorado River and the west*. University of Arizona Press, Tucson, AZ.
- Haden, G.A., D.W. Blinn, J.P. Shannon, and K.P. Wilson. 1999. Driftwood: an alternative habitat for macroinvertebrates in a large desert river. *Hydrobiologia.* 397:179-186.
- Hardwick, G.G., D.W. Blinn, and H.D. Usher. 1992. Epiphytic diatoms on *Cladophora glomerata* in the Colorado River, Arizona: longitudinal and vertical distribution in a regulated river.
- Hogg, I.D., and D.D. Williams. Response of stream invertebrates to a global-warming thermal regime: an ecosystem-level manipulation. *Ecology.* 77:395-407.

- Howard, A. and R. Dolan. 1981. Geomorphology of the Colorado River in Grand Canyon. *J. Geol.* 89:269-298.
- Jassby, A. D. and T. Platt. 1976. Mathematical formulation of the relationship between photosynthesis and light for phytoplankton, *Limnol Oecnaogr.*, 21:540-547.
- Minckley, W. L. 1991. 'Native fishes of the Grand Canyon region: an obituary?' *In*. National Academy of Sciences (eds.) *Colorado River ecology and dam management*. NAS Press, Washington, D.C. pp. 124-177.
- Mulholland, P.J., A.D. Steinman, A.V. Palumbo, J.W. Elwood and D.B. Kirschtel. 1991. Role of nutrient cycling and herbivory in regulating periphyton communities in laboratory streams. *Ecology*. 72:966-982.
- Oreskes, N., K. Shrader-Frechette, and K. Belitz. 1994. Verification, validation, and confirmation of numerical models in the earth sciences. *Science*. 263: 641-646.
- Peterson, C.G. 1986. Effects of discharge reductions on diatom colonization below a large hydroelectric dam. *J. N. Am. Benthol. Soc.*, 5:278-289.
- Peterson, C.G. and A.J. Boulton. 1999. Stream permanence influences microalgal food availability to grazing tadpoles in arid-zone springs. *Oecologia* 118:340-352.
- Petts, G. E. 1984. *Impounded rivers*. Wiley Press, Chichester, England.
- Randle, T.J. and E.L. Pemberton. 1987. Results and analysis of STARS (Sediment Transport and River Simulation) modeling efforts of Colorado River in Grand Canyon. Glen Canyon Environmental Studies Technical Report, NTIS No. PB88-183421.
- Reid, I. J.C. Bathurst, P.A. Carling, D.E. Walling and B.W. Webb. 1997. Sediment erosion, transport and deposition. *In*. Thorne, C.R., R.D. Hey and M.D. Newson (Eds.) *Applied fluvial geomorphology for river engineering and management*. John Wiley and Sons, New York, NY.
- Rubin, D.M., J.M. Nelson, and D.J. Topping. 1998. Relation of inversely graded deposits to suspended-sediment grain-size evolution during the 1996 flood experiment in Grand Canyon. *Geology*. 26:99-102.
- Schmidt, J.C., R.H. Webb, R.A. Valdez, G.R. Marzolf, and L.E. Stevens. 1998. Science and values in river restoration in the Grand Canyon: There is no restoration or rehabilitation strategy that will improve the status of every riverine resource. *Bioscience*. 48:735-750

- Shannon, J.P., Blinn, D.W. and L.E. Stevens. 1994. Trophic interactions and benthic animal community structure in the Colorado River, AZ, USA. *Freshwat. Biol.* 31:213-220.
- Shannon, J.P., D.W. Blinn, G.A. Haden, E.P. Benenati, and K.P. Wilson. 2001. Food web implications of $\delta^{13}\text{C}$ and $\delta^{15}\text{N}$ variability over 370 km of the regulated Colorado River USA. *Isotopes Environ. Health Stud.* 37:179-191.
- Shaver, M.L., J.P. Shannon, K.P. Wilson, P.L. Benenati and D.W. Blinn. 1997. Effects of suspended sediment and desiccation on the benthic tailwater community in the Colorado River, USA. *Hydrobiologia.* 357: 63-72.
- Stevens, L.E., K.A. Buck, B.T. Brown, and N.C. Kline. 1997a. Dam and geomorphological influences on Colorado River waterbird distribution, Grand Canyon, Arizona, USA. *Regul. Riv.* 13:151-169.
- Stevens, L.E., J.P. Shannon, and D.W. Blinn. 1997b. Colorado River benthic ecology in Grand Canyon, Arizona, USA: Dam, tributary and geomorphological influences. *Regul. Riv.* 13:129-149.
- Stewart, A.J. 1987. Responses of stream algae to grazing minnows and nutrients: a field test for interactions. *Oecologia.* 72:1-7.
- Topping, D.J. 1997. Physics of flow, sediment transport, hydraulic geometry, and channel geomorphic adjustment during flash floods in an ephemeral river, the Paria River, Utah and Arizona. Ph.D. dissertation. Univ. of Wash. Seattle, WA.
- Topping, D.J., D.M. Rubin, and L.E. Vierra, Jr. 2000a. Colorado River sediment transport 1. natural sediment supply limitation and the influence of Glen Canyon Dam. *Water Resources Research.* 36:515-542.
- Topping, D.J., D.M. Rubin, J.M. Nelson, P.J. Kinzell III, and I.C. Corson. 2000b. Colorado River sediment transport 2. Systematic bed-elevation and grain-size effects of sand supply limitation. *Water Resources Research.* 36:543-570.
- Usher, H.D., and D.W. Blinn. 1990. Influence of various exposure periods on the biomass and chlorophyll A of *Cladophora glomerata* (Chlorophyta). *J. Phycol.* 26:244-249.
- Wiele, S. M., and J. D. Smith, 1996. A reach-averaged model of diurnal discharge wave propagation down the Colorado River through the Grand Canyon. *Water Resources Research.* 32: 1375-1386.

CHAPTER 2

SEASONAL INFLUENCE OF TOPOGRAPHIC COMPLEXITY
ON AQUATIC ECOSYSTEMS: SOLAR INSOLATION ESTIMATES
FOR THE COLORADO RIVER, GLEN AND GRAND CANYONS, AZ.

Abstract

Rugged topography along the Colorado River in Glen and Grand canyons, exemplifies features common to canyon-bound streams and rivers of the arid southwest. Physical relief influences regulated river systems, especially those that are trophically altered and dependent on aquatic primary production. We measured and modeled instantaneous solar flux in a topographically complex environment to determine where differences in daily, seasonal and annual solar insolation occurred in this river system. At a system-wide scale, topographic complexity generates a spatial and temporal mosaic of varying solar insolation. This solar variation is a predictable consequence of canyon and channel orientation, geomorphology, elevation angles and viewshed. Modeled estimates for clear conditions corresponded closely with observed measurements for both instantaneous photosynthetic photon flux density (PPFD: $\mu\text{mol m}^{-2} \text{s}^{-1}$) and daily insolation levels (relative error 2.3%, CI ± 0.45 , std 0.3, n = 29,813). Mean annual daily insolation levels system-wide were estimated to be $36 \text{ mol m}^{-2} \text{ d}^{-1}$ (17.5 std), and varied seasonally from $13.4 - 57.4 \text{ mol m}^{-2} \text{ d}^{-1}$, for winter and summer, respectively. In comparison, mean daily insolation for environmental conditions lacking topographic effect (idealized plane) were reduced by 22% during summer, and as much as 53%

during winter. Also, depending on outlying topography, canyon bound regions having east-west (EW) orientations had higher seasonal variation, averaging from 8.1 – 61.4 mol m⁻² d⁻¹, for winter and summer, respectively. For EW orientations, 70% of mid-channel sites were obscured from direct incidence during part of the year; and of these sites, average diffuse light conditions persisted for 19.3% of the year (70.5-d), and extended upwards to 194-d.

1. Introduction

Vertical relief interferes with incoming solar incidence and can dramatically affect ecosystem energetics, particularly in canyon-bound regions or along densely vegetated streams (Vanote *et al.* 1980; Hawkins *et al.* 1982; Monteith and Unsworth 1990). Physical obstructions are recognized for having pronounced effects on daily, seasonal, and annual solar insolation levels (Hill 1996). Subtle differences in altitude angles, elevation surface gradients, viewshed, and orientation generate varying levels of spatio/temporal complexity (Kumar *et al.* 1997; Dozier and Frew 1990). In GIS-modeled environments, solar radiation models have been used effectively to estimate insolation differences on large-scale geographic surfaces (mountainous and canyon terrain) (Dozier and Outclat 1979; Rich *et al.* 1995). However, topographic effects in river ecosystems remain poorly studied, owing perhaps to methodological constraints (e.g., grid-size limitations, sampling devices) used to determine photosynthetic photon flux density (PPFD: $\mu\text{mol m}^{-2} \text{s}^{-1}$).

The Colorado River (CR) in Glen and Grand canyons is representative of topographically complex riverine environment in the arid southwest. Because of dam-

regulation, some of the biological resources in the CR ecosystem are highly affected (Blinn and Cole 1991; Stevens *et al.* 1997a, 1997b), and its trophic structure appears linked to and dependent on aquatic primary production (Blinn *et al.* 1998, Shannon *et al.* 2001). This trophic condition is unusual, because most large unregulated river systems have an allochthonous energy base (Haden *et al.* 1999); therefore, understanding the physical factors limiting PPF_D has considerable ecological significance for this and other regulated rivers.

The CR is one of the most regulated large rivers in the United States that flows 475 km through northern Arizona between two large reservoirs, Lake Powell and Lake Mead (Stevens *et al.* 1997a, 1997b). Because suspended-sediment is now sequestered in Lake Powell reservoir, hypolimnetic flows released from Glen Canyon Dam (GCD) are highly transparent (Chapter 3). Dam releases typically fluctuate from 142 to 708 m³s⁻¹ on a diurnal schedule. This is a very turbulent river that flows through an extensive geographic region where suspended-sediment supplied from tributaries limits subaqueous PPF_D (Shaver *et al.* 1997). Yet, these light-attenuation effects are subsequent to the initial influence that topographic relief has on determining the quantity of incoming solar incidence.

We examined the role topographic relief had on regulating daily, seasonal and annual solar insolation reaching the CR surface. Geomorphic control functions at regional and local scales to influence the incised characteristics of this canyon dominated river ecosystem by regulating channel meanders, orientation and topography (Schmidt and Graf 1990; Gregory *et al.* 1991; Stevens *et al.* 1997a; Schmidt *et al.* 1998). Stream ecologists have faced similar problems in other aquatic systems; yet, the paucity of

studies on this subject indicates that such research is rarely undertaken. A number of predictive solar models are available (Dubayah and Rich 1995, Kumar *et al.* 1997), although some are incomplete, costly, complicated, or have considerable data requirements. Thus, our study had multiple objectives, 1) develop a model for estimating instantaneous solar flux for large rivers containing topographically complex environment; and 2) determine where differences in daily, seasonal and annual solar insolation occurred along the CR. Here we describe the analytical approach and inherent assumptions used in this model, as well as predicted results.

2. Methods

The study area includes four major canyon sections: Glen Canyon, Marble Canyon Central Grand Canyon, and Western Grand Canyon (Fig 1). All site locations are described in relationship to the distance in river kilometers (Rkm) downstream from GCD (0.0 Rkm). The outer lying rims of these larger canyon sections and geomorphic reaches have varying channel widths, heights, and orientations (Stevens *et al.* 1997a, 1997b). Contained within these major canyon sections are a number of subunits described as geomorphic reaches, each having different topographic, stratigraphic and erosive characteristics (Howard and Dolan 1981; Schmidt and Graf 1990; Stevens *et al.* 1997a) (Table 1).

2.1 Solar and Ground Incidence

Solar flux is distributed over a broad range of wavelengths and peaks within the visible band (400-700 nm), constituting 38.15 % of the total solar spectrum (Kirk 1983).

Solar radiation impinging on the earth's outer atmosphere is relatively constant, with exceptions due to differences in solar surface temperature and the earth's elliptical orbit (Jones 1992). Incidence received at ground level, however, is far from constant and is small relative to the total extraterrestrial solar flux. In general, net atmospheric solar flux measured at ground level is less than 5% because of light absorption and scattering from ozone, water vapor, and air-borne particles (Cole 1983; McCullough and Porter 1971; List 1971). This ground level intensity is regulated by geometric orientation of the sun relative to the incidental surface. Angular departures from normal (perpendicular to the surface) functions to increase the solar zenith angle (θ), which results in decreasing the total solar flux received at the earth's surface (Jones 1992; Rosenberg *et al.* 1983).

Simple estimates of solar flux (SF) are determined as:

$$SF = SF_N \cdot \cos\theta \quad (1)$$

where SF_N is solar flux normal to surface, and θ is zenith angle, representing the angle between the direct beam and normal; therefore as θ increase, SF decreases.

In addition to solar zenith angle, the depth of the overlying air-mass influences the degree of atmospheric absorption, reflection, and refraction, such that solar flux decreases exponentially as a function of optical depth (Page and Sharples 1988; Kasten and Young 1989). Beer's law describes this relationship as:

$$SF = SF_0 e^{(-Kz)} \quad (2)$$

where SF_0 is initial solar flux, K is coefficient of atmospheric light-attenuation, and SF is resulting intensity after a known optical depth (z) through a given air-mass (Stine and Harrigan 1985; Kasten and Young 1989). Yet, accounting for multiple-light attenuating factors requires considerable knowledge of atmospheric conditions (e.g., climate,

transmissivity, atmospheric pressure, and cloud cover), and for all practicality atmospheric data are not sufficiently robust or available for most localities (List 1971; Gutman 1998). This often precludes using more conventional methods for estimating SF . We used an alternative approach whereby we substituted SF_N for a parameter called normalized ground incidence (GI_N). This parameter represents maximum solar flux received at ground surface following atmospheric light-attenuation if solar zenith angles are normal ($\theta = 0^\circ$) and assumes that factors contributing to light-attenuation remain constant. Validity of this assumption is contingent on the variability of local atmospheric conditions. Therefore, constancy of GI_N requires some empirical grounding to determine whether the error varies systematically (spatio/temporal) or within levels acceptable to researchers.

To address this, we used data measured at water surface (LiCor, Inc., LI-190SA) representing PPFD for a wide range of θ angles collected at multiple sites for different years, seasons, and times. We solved for the best estimate of GI_N using a linear optimization program and applying a minimization technique that reduced the sum of squared residuals (Frontlines Systems, Inc. 1999).

2.2 Solar Coordinates and Zenith Angle

The above relationships indicate that zenith angle (θ) is important for estimating daily solar insolation because the mathematical coordinate system used to estimate solar angles requires knowing the spatio/temporal relationships specific to a site location. Solar coordinates are based on solar time (ST), thus differences among local standard time (LST) and ST must be considered. Converting LST to ST requires two types of

adjustments. The first adjustment accounts for differences in longitude among standard meridian L_{st} and observation location L_{ob} . We used a correction of ± 4 -min (i.e., positive east and negative west) for every degree longitude (Rapp 1981). Secondly, seasonal differences among LST and ST (± 16 -min) are related to the earth's elliptical orbit and inclination relative to solar orbital plane. The equation of time (E) accounts for the earth-sun geometric relationship, and is calculated from:

$$E = 9.87 \sin \left[\frac{2(360(Jday - 81))}{365} \right] - 7.53 \cos \left[\frac{360(Jday - 81)}{365} \right] - 1.5 \sin \left[\frac{360(Jday - 81)}{365} \right] \quad (3)$$

in which daily differences in ST relative to LST were corrected by Julian date ($Jday$) (Cousins 1969). By combining temporal adjustments, ST is calculated from

$$ST = LST + 3.989(L_{ST} - L_{OB}) + E \quad (4)$$

where LST is local standard time, L_{ST} is standard meridian, L_{OB} is observed meridian, and E is equation of time.

Solar declination (δ) represents the earth's angular tilt to the sun, which seasonally shifts $\pm 23^\circ 26'$ among vernal and autumnal equinoxes (Duffie and Beckman 1980). Declination is calculated using:

$$\delta = 23.439 \sin \left[360 \left(\frac{283 + Jday}{365} \right) \right] \quad (5)$$

The hour angle (ω) represents the angle of departure from solar noon (0°), which varies $\pm 15^\circ \text{ h}^{-1}$, (i.e., positive east and negative west) and is used to correct for temporal deviations due to differences in longitude among sites, and seasonal differences that occur between LST and ST. Since ST is needed to accurately estimate solar coordinates, ω allows the solar zenith angle (θ) to be estimated from:

$$\theta = \cos^{-1} (\sin \delta \sin \phi + \cos \delta \cos \phi \cos \omega), \quad (6)$$

where δ is declination angle, ϕ is observed latitude for the observed site, and ω is hour angle. For a more rigorous explanation of these predictive relationships refer to Mueller (1977), Rapp (1981), Stine and Harrigan (1985), and Campbell and Norman (1998).

2.3 Estimating photosynthetic photon flux density

Following effects from atmospheric light-attenuation, normal ground incidence GI_N is partitioned into sub-components, representing direct beam $GI_{DB} = GI_N (x)$ and diffuse incidence $GI_{DI} = GI_N (1 - x)$. The variable “ x ” is equivalent to a proportion of direct solar beam in relation to total solar incidence. The proportion of ground incidence ($x = GI_{DB} / GI_N$) received directly from direct solar beam is considered to be approximately 75% of the total solar flux (Monteith and Unsworth 1990). Even though GI_{DB} is highly directional relative to GI_{DI} (downward angle across the skylight) an estimate of total ground incidence (GI) can be calculated using

$$GI = \cos \theta (GI_{DB} + GI_{DI}) \quad (7)$$

where θ is zenith angle, GI_{DB} is direct beam component, and GI_{DI} is diffuse incidence. The temporal reference used for sunrise and sunset is a geometric definition based on the solar disc center perpendicular to normal ($\theta = 90^\circ$). Yet, unlike direct solar beam, atmospheric scattering of diffuse incidence is measurable prior to sunrise and sunset time. Therefore, the reference angle defined as civil twilight (CT) was used to regulate direct beam exposure. The CT occurs when the center of the sun is 6° below horizon and has approximately a 24-min time difference from geometric sunrise and sunset time. The temporal term initiating GI_{DB} is based on geometric sunrise and sunset ($\theta_{DB} = \theta$)

(temporal differences due to refraction are not considered). However, to account for temporal differences among diffuse and direct incidence, we define onset and end time for GI_{DI} based on CT ($\theta_{DI} = \theta - 6^\circ$). Our relationship for estimating ground incidence does not differentiate between proportions of reflected albedo to reflected skylight.

At northern latitudes, the shortest distance of the radius vector (earth center to sun center) occurs during winter periods. Because of earth's asymmetric orbit, an adjustment to GI_N must be made to account for daily differences in solar distance. This is expressed by:

$$sd = 1 + \cos \left[\left((Jday - 3) \cdot \frac{360}{365.2422} \right) \cdot 0.0344 \right] \quad (8)$$

where, 360 represents the earth's solar rotation, 365.2442 is number of days for an annual rotation, and $\pm 3.44\%$ is a distance offset. This results in a linear correction (astronomical units) to GI_N between 1.0344% on 3 January, to 0.9674% by 5 July (Thekaekara 1977).

Although solar coordinates for the geometric center of sunrise and sunset can be derived, topographic relief is important when obstructive features vary in elevation along the azimuth-arc of the skyline, as well as its influence on the proportion of visible skylight, here after referred to as viewshed (V_P). For this reason we estimated 1) solar times for direct-rise and direct-set of the GI_{DB} for each $Jday$, 2) viewshed, and 3) canyon orientation. Elevation angles associated with topography were estimated using a Geographical Information System (GIS) hillshade function (ESRI 2002) on a digital elevation model (DEM) with a 10-m cell size for sites located along the CR centerline at 100-m intervals from Glen Canyon Dam to Pierce Ferry in Lake Mead (Mietz and Gushue 2002).

Diffuse incidence increases at angles adjacent to direct angular beam, and conversely decreases with greater zenith angles. Any decrease in viewshed reduces the quantity of diffuse incidence, even though the overall proportion may be small ($\leq 25\%$) in relation to the direct beam (Monteith and Unsworth 1990). Clearly, GI_{DI} is not evenly distributed across the viewshed, although we assume that $V_P \approx GI_{DI}$. The total ground incidence is estimated by:

$$GI = \left[(\cos \theta_{DB} \cdot GI_{DB}) + (\cos \theta_{DI} \cdot GI_{DI} \cdot V_P) \right] \quad (9)$$

2.4 Topographic Complexity

We used an Arc-Info routine referred to as hillshade function (ESRI 2002) to generate binary grids that represented areas of shadow and illumination for a given set of azimuths and altitude angles. To avoid confusion, we distinguish between two types of altitude angles. Elevation angles (Ψ_E) refer to angles measured from a horizontal surface relative to a topographic feature, whereas illumination angles (Ψ_I) refer to the maximal angle between the topography and skyline. Ψ_I angles were sequentially searched incrementally over a 360° azimuth circle. For every azimuth angle searched, a secondary loop was performed that advanced through the range ($0-90^\circ$) of possible Ψ_E angles above the horizon. Every Ψ_E angle was assessed for illumination using a binary condition that iteratively advanced vertically at 1° increments. Once the condition for illumination occurred, the resulting angle represented the altitude of the topographic skyline (Fig 2). For all possible azimuth angles, 360 illumination angles (Ψ_I) were calculated at each site, this was repeated at 0.1-km increments along the river's centerline for over 4,745 sites.

Although for a given site there were a total of 360 Ψ_I angles, only two of these Ψ_I angles (east and west meridian) for a particular day achieved congruence with the altitude angle of the sun (Ψ_S). These congruent angles represented the topographic point where ground incidence shifted daily from diffuse to direct beam, and back again from direct beam to diffuse conditions. A solar altitude angle (Ψ_S) corresponds to the zenith angle (θ), such that a Ψ_S angle is equivalent to $90^\circ - \theta$. We used a computational routine that initiated a search based on the estimated geometric sunrise and sunset time for a particular day. For every day, topographic direct-rise and direct-set times were determined by sequentially comparing all Ψ_I (direct rise and set) to known Ψ_S angles found within the solar azimuth-arc. This routine was performed in 1-min time increments until the congruent condition of $\Psi_I \geq \Psi_S$ occurred. The resulting Ψ_I angle represented the angular location and solar time when topography no longer obstructed direct solar beam. All estimated times for direct solar beam were site dependent and varied daily due to changes in observed latitude, declination and topographic relief, and based on this temporal condition the term ($\cos \theta_{DB} \cdot GI_{DB}$) was either used or excluded from Eq. 9.

Proportional area of the viewshed (V_p) was determined using analytical geometry (Anton 1984), where for each azimuth angle, arc- or sky angle (α) was determined from the corresponding Ψ_I angle to normal ($\alpha = 90^\circ - \Psi_I$), such that the total proportion of visible sky was described by:

$$V_p = \left(\sum_{i=1}^{360} \alpha / 90 \right) / 360. \quad (10)$$

Only one of four possible channel orientations is assigned to each site, these cardinal directions included: north-south (NS), northwest-southeast (NW-SE), east-west

(EW), and northeast-southwest (NE-SW). Channel orientation was determined for each site using a routine that searched all possible azimuth angles and selected a discrete cardinal direction based on the lowest Ψ_1 angles encountered in the V_P . Ortho-rectified photos were used to validate method for estimating channel orientation.

Empirical data for PPFD ($\mu\text{mol m}^{-2}\text{s}^{-1}$) were adjusted to normal by accounting for differences attributed to zenith angle (θ) (Eq 6) and solar distance (Eq 8). We estimated the parameter GI_N (Eq 9) by regressing observed against estimated incidence and solved for the best fit. Daily solar insolation estimates were derived using a numerical solution that estimated instantaneous PPFD through summation over discrete time steps (1-min intervals). We chose this approach over other methods because our purpose was to estimate aquatic primary production in an optically and hydrologically variable environment using a discrete-state modeling approach that required instantaneous PPFD estimates at smaller time increments. Although, our approach lacks an elegant integration of insolation, it has allowed us to dynamically control other environmental variables operating at smaller time increments.

2.5 Statistical analysis

ANOVA and multiple comparisons were used to test for significant differences in instantaneous incidence and solar insolation among canyon sections, geomorphic reaches, channel orientation and differences among seasons (Sokal and Rohlf 1981). For multiple comparisons, *post-hoc* tests were used to determine group mean differences. Simple linear regressions and bootstrap techniques were used to compare differences among observed and predicted estimates (Neter *et al.* 1995). We determined the relative error of

overestimation in our modeled estimates due to atmospheric influence under clear or cloudy conditions. Using a bootstrap technique, observed data for a range of varying atmospheric conditions were analyzed to determine relative error ($RE = (E - O) / O$) representing the estimated error (E) relative to an observed measurement (O). Data were segregated, representing either clear skies or cloudy conditions. For each resample, 500 random samples were sampled from empirical data for clear skies ($n = 29,813$) cloudy skies ($n = 25,051$), and intermittent clouds ($n = 9,275$). The median RE was iteratively sampled with replacement for 10,000 bootstrap samples. Multiple statistical packages were used (Statistica StatSoft, Inc., 1997; SAS Institute, Inc. 2000; Resampling Stats, Inc., 2001).

3. Results

Our estimated GI_N was $2,326 \mu\text{mol m}^{-2}\text{s}^{-1}$ ($r^2 = 0.94$, $n = 4,312$, $SE \pm 36.3$) that represented clear-sunny daytime conditions characteristic of this large geographical region. Observed data used for estimating this parameter varied from $1,321 - 2,063 \mu\text{mol m}^{-2}\text{s}^{-1}$, and included zenith angles from $12.79^\circ - 49.79^\circ$. Solar distance adjustment to GI_N varied linearly $2326 \pm 80 \mu\text{mol m}^{-2}\text{s}^{-1}$ over a 182.5-da period (Eq 8).

3.1 Relative error in estimation of instantaneous incidence

Data were collected over a range of field conditions, and different years (1992-2001), seasons, and times and sites. Instantaneous PPFD averaged $1052 \mu\text{mol m}^{-2}\text{s}^{-1}$ and varied between 0.15 and $2,100 \mu\text{mol m}^{-2}\text{s}^{-1}$. Although a strong correlation ($p < 0.001$, $r^2 = 0.987$, $n = 58,060$) existed among observed and estimated data, variation in solar

incidence increased during periods of continuous or intermittent cloud cover. Our median RE for observed incidence under clear skies for all seasons was 2.3%, with a 95% bootstrap confidence interval ($CI_{95\%}$) of 1.85-2.75%; whereas, under cloudy conditions median RE was 100%, with a $CI_{95\%}$ of 92.5-107.5%. RE of overestimation was most pronounced during late-July through September monsoons, and winter (December-March) when cloud cover was greatest. However, an inverse response occurred during intermittent cloud cover, which had an estimated incidence less than observed (-2%), and had a $CI_{95\%}$ of -1.8 to -2.2%. This heightened response was perhaps due to enhanced atmospheric scattering (Kirk 1983).

We used a continuous set of logged PPFD measurements (1992-1993), averaged over a 10-min period to compare differences among observed and estimated daily solar insolation ($\text{mol m}^{-2}\text{d}^{-1}$). Under optimal atmospheric conditions, results corresponded linearly among estimated and observed daily insolation ($r^2 = 0.987$, $SE \pm 9.3$: Fig 3).

3.2 Canyon sections and geomorphology

At an ecosystem-scale, annual estimates of average daily insolation for topographically complex environments differed considerably when compared to idealized conditions (no topographic relief, $\Psi_E = 0^\circ$) (Fig 4). Under idealized conditions, mean annual daily insolation levels were estimated at $52.3 \text{ mol m}^{-2} \text{ d}^{-1}$ (15.7 std), and varied seasonally from $28.4 - 73.2 \text{ mol m}^{-2} \text{ d}^{-1}$, for winter and summer, respectively.

Differences in mean daily insolation due to topographic relief varied seasonally, and on average were reduced by 22% during summer, and as much as 53% during winter (Table 2 & 3).

Independent of topographic effects, seasonal changes in day-length and zenith angle were the primary sources of variation responsible for differences in solar insolation (Forsythe *et al.* 1995). Day-length estimates for geometric sunrise to sunset varied seasonally from 568 – 872 min; however, when topographic complexity was taken into account, total day-length for direct beam varied seasonally within and among the different canyon sections, geomorphic reaches, and channel orientations, and day length estimates for direct beam were considerably less. Mean direct beam day-length for the entire CR system averaged 369-min (184 std) annually, and varied seasonally among summer (551-min; 108 std) and winter (161-min; 126 std).

Topographic relief reduced viewshed (V_P), as well as duration of direct solar exposure. For all sites evaluated, V_P ranged from 0.45 - 0.95. Canyon sections and geomorphic reaches having the highest Ψ_1 angles and smallest V_P were: Marble Canyon Section (Supai Gorge, 43.5 to 61.7 km; Redwall Gorge, 61.7 to 83.1 km; and Lower Marble Canyon, 83.1 to 124.3 km), and Western Grand Canyon Section (Muav Gorge, 250.5 to 282.7 km) (Fig 1). *Post-hoc* tests revealed that these two factors influenced the annually average daily insolation levels among geomorphic reaches ($p < 0.05$). Taking into account topographic interference, system-wide estimates for CR had a mean annual daily insolation of $36.0 \text{ mol m}^{-2} \text{ d}^{-1}$ (31% lower than the idealized condition of $52.3 \text{ mol m}^{-2} \text{ d}^{-1}$ ($\Psi_E = 0^\circ$ and $V_P = 1.0$)), and varied from 27.2 - $42.6 \text{ mol m}^{-2} \text{ d}^{-1}$ for different geomorphic reaches, which was 48% to 21% lower than ideal, respectively (Table 2). Thus comparisons among ideal and topographically complex environments demonstrate that varying physical obstructions strongly influence the quantity of annual solar insolation reaching the CR corridor.

3.3 Channel Orientation

Channel orientation relative to outlying topography also strongly affected the seasonal variation in solar insolation (Table 3). Differences in Ψ_1 angles and predominant channel orientation varied among different geomorphic reaches and canyon sections. Mean Ψ_1 angles for all sites in the CR ecosystem (475-km) ranged from 12.6° - 47.4° ($n = 4,745$) and averaged 33.9° (sd 4.43) (Table 2). Variability of Ψ_1 angles within and among sites, geomorphic reaches, and canyon sections influenced the geographical distribution of these angles, and the sequence of repetitive patterns occurring system-wide (Fig 4).

Average annual insolation levels were not significantly different among channel orientations. NS orientation averaged $35.97 \text{ mol m}^{-2} \text{ d}^{-1}$ (14.1 std, $n = 461,892$) and EW was $35.96 \text{ mol m}^{-2} \text{ d}^{-1}$ (21.7 std, $n = 418,338$). Depending on outlying topography in canyon bound regions; NS orientations exhibited far less variation in daily insolation among seasons than did EW ($p < 0.05$) (Fig 5, & Fig 6). Summer solar insolation for EW orientations was significantly higher ($p < 0.05$) than that of NS. Conversely, during winter EW orientations received significantly less solar insolation ($p < 0.05$) than NS (Table 3, Fig 5, & Fig 6). Under idealized conditions (lacking topographic effect) summer and winter estimates for mean daily insolation were 73.1 and $29.1 \text{ mol m}^{-2} \text{ d}^{-1}$. In comparison, summer and winter estimates for mean daily insolation for NS orientation was 52.7 and $17.7 \text{ mol m}^{-2} \text{ d}^{-1}$, respectively; whereas, EW orientation was 61.4 and $8.1 \text{ mol m}^{-2} \text{ d}^{-1}$, respectively. This winter difference due to orientation is considerable,

especially with respect to EW orientation where mean daily insolation levels were on average reduced to 72% from ideal (Table 3).

Direct incidence was topographically obstructed during part of the year for 70% of mid-channel sites having EW orientation and of these sites, average diffuse light conditions persisted for 19.3% of the year (70.5 d). Some sites were exposed solely to diffuse conditions upwards of 194 d. Conditions of diffuse incidence were most prevalent in Redwall Gorge and Muav Gorge, where sites averaged 130 d of diffuse incidence (Fig 5, & Fig 6). In contrast, NS oriented sites that were exposed to only diffuse incidence occurred less than 0.1% of the time and only during winter. Because of the declinational shift during winter season (3-mo), mid-day maximum PPFD levels are 900-1100 $\mu\text{mol m}^{-2} \text{s}^{-1}$ (i.e., winter maximum solar altitude Ψ_I at solar noon varied from 30° - 40°). Duration of diffuse incidence was prevalent system-wide especially for EW orientation because of the higher southerly skyline angles (Ψ_I angles 33.9°, std 13.8) that often exceeded the maximum daily solar altitude angle (Ψ_S) (Fig 4).

Daily insolation was greatly reduced for most sites in winter (Fig 7). Sites having EW orientations, exposed solely to diffuse incidence from October through March, had daily mean instantaneous PPFD levels from 80 - 170 $\mu\text{mol m}^{-2} \text{s}^{-1}$, with maximum mid-day intensities from 125 - 300 $\mu\text{mol m}^{-2} \text{s}^{-1}$. In contrast, sites having NS orientation with direct exposure had daily mean instantaneous PPFD levels from 490 - 810 $\mu\text{mol m}^{-2} \text{s}^{-1}$, with maximum mid-day intensities from 950 - 1725 $\mu\text{mol m}^{-2} \text{s}^{-1}$. Other orientations (NW-SE and NE-SW) were intermediate to these more extremes canyon orientations (Table 3).

4. Discussion

Localized topography strongly affected the availability of daily solar insolation levels received at the Colorado River surface (Fig 5, & Fig 6). At a system-wide scale, topographic complexity generates a spatial and temporal mosaic of varying solar insolation. This variation was a predictable consequence of canyon orientation, elevation angles and viewshed. Canyon sections and geomorphic reaches receiving the greatest quantity of solar insolation were located in reaches having the lowest Ψ_1 angles and largest V_p (Fig 1, Table 2). These same canyon sections and reaches were either adjacent to major tributaries or in the lower extent of the river system.

Topographic relief may influence distribution, biomass, and composition of the phytobenthic community, but also seasonal primary production levels occurring in this system. Suspended-sediment loads are responsible for underwater light-attenuation (Chapter 4) and are governed by sediment-supply and sediment transport processes (Topping and Rubin 2001). If the phytobenthic community is light-limited seasonally as indicated by Stevens *et al.* (1997a) its vertical extent and spatial distribution may be regulated not only by the apparent optical properties of water (i.e., normal light-attenuation coefficients, $K_N > 0.8$) (Chapter 5), but also by the resultant quantity of solar insolation available at the water surface. Spatio-temporal differences in solar incidence are strongly regulated by topographic relief, yet remain independent of other factors that either attenuate underwater light or preclude phytobenthic colonization.

Light-depth limitation should be most evident for EW oriented channels having high elevation angles. We would expect to observe decreased primary production during

winter, and alternately higher production and standing biomass during summer periods when these same channel orientations receive considerably more solar incidence. There is some evidence for this phytobenthic pattern; however, the vertical distribution is further compounded by longitudinal differences in optical properties throughout the CR. Turbidity has been recognized as increasing with downstream distance (Hardwick *et al.* 1992; Shaver *et al.* 1997; Stevens *et al.* 1997a). Suspended-sediment has a strong influence on the distributional patterns (biomass/density) of primary and secondary benthos (Shaver *et al.* 1997; Stevens *et al.* 1997a; Wilson *et al.* 1999), fish (Schmidt *et al.* 1998), waterfowl and piscivorous raptors in this system (Stevens *et al.* 1997b). Also, geomorphology has significant secondary effects on aquatic and aquatically linked biota in the canyon (Stevens *et al.* 1997a, 1997b).

The vertical distribution of the phytobenthic community is likely to adjust in response to seasonal light-depth limitations. Persistence and/or reestablishment at or below compensation point levels for phytobenthic community require either different physiological and metabolic pathways (Blum 1956; Whitton 1970; Sheath *et al.* 1986; Dudley and D'Antonio 1991) or colonization mechanisms (Whitton 1970; Worm *et al.* 2001). Algal colonization rates in this dam-regulated system are slow (> 6-mo) (Shaver *et al.* 1997; Benenati *et al.* 1998) and occur primarily by fragmentation, and are attributed to cold stenothermic conditions (Shannon *et al.* 1994; Shaver *et al.* 1997; Blinn *et al.* 1998).

During winter, estimated maximum daily diffuse incidence at the water surface was 250 - 300 $\mu\text{mol m}^{-2}\text{s}^{-1}$, and is at or below onset of light saturation for *Cladophora glomerata* (Graham *et al.* 1982). Deeper benthic establishment and persistence is likely

to be precluded during winter (Worm *et al.* 2001), owing to the increased duration of diffuse light conditions. Additionally, it must be realized that these winter insolation estimates are overestimated during this period of reduced seasonal insolation owing to an increased frequency of cloud interference. However, because of reduced colonization rates, algal growth may be constrained or non-existent during optimal solar conditions. Lastly, because of the exponential decrease in PPFD as a function of depth, depth distribution of algae persisting at or above metabolic maintenance may be limited solely to the varial zone (Blinn *et al.* 1995). Growth in this zone is susceptible to diel flow fluctuations and desiccation (Blinn *et al.* 1995; Shaver *et al.* 1997; Stevens *et al.* 1997a).

We demonstrate that topographic relief affects daily and seasonal solar incidence in different canyon sections and geomorphic reaches; and we hypothesize that system-wide primary production varies spatially and temporally (Fig 5, & Fig 6). Secondly, we argue that the phytobenthic response is regulated by interactions between solar insolation, colonization constraints, underwater light-attenuation, and desiccation by regulated flow fluctuations (Blinn *et al.* 1995; Shaver *et al.* 1997; Worm *et al.* 2001). Additionally, solar insolation has broader ecological implications to the Colorado River ecosystem. Patterns of daily solar insolation correspond to total radiation transmission, and probably explain some of the distribution and flowering patterns of xeric and riparian vegetation in the deep canyon ecosystem (Clover and Jotter 1944; Jones 1992; Evett *et al.* 1994; Stevens *et al.* 1995). These findings suggest that future comparisons made among different regulating mechanisms (turbidity and geomorphology) should also include temporal variation in solar insolation, as both local and canyon-wide geomorphology, and canyon orientation are inter-correlated with observed seasonal differences in solar insolation.

5. Conclusion

Determining the availability of daily, seasonal and annual solar insolation levels should be considered when characterizing aquatic primary production, especially in topographically complex riverine environments. The approach we used is one such method, and provides an effective means to quantify spatio/temporal variability of incoming solar insolation. We developed and make available a computational program that numerically solves for solar time, spatial coordinates and solar insolation so that other researchers may resolve similar questions in this and other topographically complex systems. The solar insolation model was written in Visual Basic for applications (Microsoft Visual Basic 1999), with several subroutines designed for an Excel worksheet environment (Microsoft Excel 2000), and available from an FTP site: /data/model/light/solar at ftp.gcmrc.gov. Documentation, downloading page and access to updates are available at: <http://www.gcmrc.gov>.

We recommend that users determine whether or not our estimated GI_N is an appropriate estimate for their locality, partly because transmissivity differences may require adjustments to GI_N , or seasonal conditions in its use other than those presented here. Additionally, the model does not account for subtle differences in solar incidence when the ephemeris follows the topographic skyline and/or multiple topographic direct-rise and direct-set times during a single day. Even though altitude angles at specific sites were determined using 10-m DEM in a GIS-environment, other alternate methods are just as practical for geo-referencing and calculating elevation angles. Technological methods range from conventional surveying to handheld protractors.

6. Acknowledgements

Many of the geographic data presented in this paper were collected and analyzed by the Grand Canyon Monitoring and Research Center at US Geological Survey, Flagstaff, AZ. We thank the individuals (alphabetically) that have assisted and supported certain aspects of this study, including D. Baker, S. Gloss, B. Gold, T. Gushue, G. A. Haden, B. Hungate, G. Koch, A. Martinez, D. McKinnon, B. Ralston, M. Williams, and many others. Partial funding for this research was obtained through a cooperative agreement 98-FC-40-0540 to Northern Arizona University, Flagstaff, AZ. Additional thanks and appreciation are extended to the National Park Service at Glen Canyon National Recreational Area and Grand Canyon National Park.

References

- Anton, H. 1984. *Calculus with analytical geometry*. 2nd Edition. John Wiley and Sons. New York, NY.
- Belsley, D.A., Kuh, D. and Welsch, R.E. 1980. *Regression diagnostics: Identifying influential data and sources of collinearity*. John Wiley and Sons. NY.
- Benenati, P.L., Shannon, J.P. and Blinn, D.W. 1998. Desiccation and recolonization of phytobenthos in a regulated desert river: Colorado River at Lees Ferry, Arizona, USA. *Regul. Riv.*, 14:519-532.
- Blinn, D.W. and Cole, G.A. 1991. Algal and invertebrate biota in the Colorado River: comparison of pre- and post-dam conditions. *In*. Marzolf, G.R. (Ed.), *Colorado River ecology and dam management: proceedings of a symposium*. National Academy Press, Washington D.C. pp. 102-123.
- Blinn, D.W., Shannon, J.P., Stevens, L.E., and Carver, J.P. 1995. Consequences of fluctuating discharge for lotic communities. *J.N. Am. Benthol. Soc.* 14:233-248.
- Blinn, D.W., Shannon, J.P., Benenati, P.L., and Wilson, K.P. 1998. Algal ecology in tailwater stream communities: the Colorado River below Glen Canyon Dam, Arizona. *J. Phycol.* 34:734-740.
- Blum, J.L. 1956. *The ecology of river algae*. *Botanical Review.* 22:291-341.
- Campbell, G.S., and Norman, J.M.. 1998. *An introduction to environmental biophysics*. 2nd ed. Springer-Verlag, New York.
- Clover, E. and Jotter, L. 1994. Floristic studies in the canyon of the Colorado and tributaries. *Amer. Midl. Nat.*, 32:591-642.
- Cole, G.A. 1983. *Textbook of limnology*. 3rd ed. Waveland Press, Inc., Prospect Heights, IL.
- Cousins, F.W. 1969. *Sundials: A simplified approach by means of the equatorial dial*. John Baker Publishers, London.
- Dozier, J., and Frew, J. 1990. Rapid calculation of terrain parameters for radiation modeling from digital elevation data. *IEEE Transactions on Geoscience and Remote Sensing.* 28:963-969.
- Dozier, J., and Outclat, S.I.. 1979. An approach toward energy balance simulation over rugged terrain. *Geograph. Anal.*, 11:65-85

Dubayah, R. and Rich, P.M. 1995. Topographic solar radiation models for GIS. *Inter. J. Geogr. Infor. Syst.* 9:405-413.

Dudley, T.L., and D'Antonio, C.M. 1991. The effects of substrate texture, grazing and disturbance on macroalgal establishment in streams. *Ecology.* 72:297-309.

Duffie, J.A., and Beckman, W.A. 1980. *Solar engineering of thermal processes.* John Wiley and Sons, New York, NY.

Environmental Systems Research Institute, Inc. 2002. ARC/INFO Version 8.21. Redlands, CA, USA.

Evet, S.R., A.W. Warrick, and A.D. Matthias. 1994. Energy balance model of spatially variable evaporation from bare soil. *Soil. Sci. Soc. Amer. J.* 58:1604-1611.

Forsythe, W.C., Rykiel, Jr., E.J., Stahl, R.S., Wu, H., and Schoolfield, R.M. 1995. A model comparison for daylength as a function of latitude and day of year. *Ecological Modeling* 80:87-95.

Frontline Systems, Inc. 1999. NLP/NSP Solver DLL Version 3.5. Incline Village, NV.

Graham, J.M., Auer, M.T., Canale, R.P., and Hoffman, J.P. 1982. Ecological studies and mathematical modeling of *Cladophora* in Lake Huron: 4. Photosynthesis and respiration as functions of light and temperature. *J. Great Lakes Res.*, 8:100-111.

Gregory, S.V., Swanson, F.J., McKee, W.A., and Cummins, K.W. 1991. An ecosystem perspective of riparian zones, focus on links between land and water. *Bioscience* 41:540-551.

Haden, G.A., Blinn, D.W., Shannon, J.P., and Wilson, K.P. 1999. Driftwood: an alternative habitat for macroinvertebrates in a large desert river. *Hydrobiologia.* 397:179-186.

Hardwick, C.G., Blinn, D.W., and Usher, H.D. 1992. Epiphytic diatoms on *Cladophora glomerata* in the Colorado River, Arizona: longitudinal and vertical distribution in a regulated river. *The Southwestern Naturalist.* 37:17-30.

Hill, W. 1996. Factors affecting benthic algae. Effects of light. *In.* Stevenson, R.J., Bothwell, M.I., and Lowe, R.L.. (eds.) *Algal ecology: freshwater benthic ecosystems.* Academic Press, Inc., San Diego, Calif. Pp. 121-144.

Howard, A., and Dolan, R. 1981. Geomorphology of the Colorado River in Grand Canyon. *J. Geol.* 89:269-298.

Hawkins, C.P., Murphy, M.L., and Anderson, N.H. 1982. Effects of canopy, substrate composition, and gradient on the structure of macroinvertebrate communities in Cascade Range streams of Oregon. *Ecology* 63: 1840-1856.

Jones, H.G. 1992. *Plants and microclimate: A quantitative approach to environmental plant physiology*. 2nd Ed. Cambridge University Press, Cambridge, UK.

Kasten, F., and Young, A.T. 1989. Revised optical air mass tables and approximation formula. *Applied Optics* 28: 4735-4738

Kumar, L., Skidmore, A.K., and Knowles, E. 1997. Modeling topographic variation in solar radiation in a GIS environment. *Inter. J. Geogr. Infor. Syst.* 11:475-497.

List, R.J. 1971. *Smithsonian Meteorological Tables*. Smithsonian Institution Press, Washington, USA.

McCullough, E.C., and Porter, W.P. 1971. Computing clear day solar radiation spectra for the terrestrial environment. *Ecology* 52:1008-1015.

Microsoft, Corp. 1999. Microsoft Visual Basic for Windows 6.0, Redmond, WA. USA.

Microsoft, Corp. 2000. Microsoft Excel for Windows 9.0, Redmond, WA. USA.

Mietz, S.N., and Gushue, T. 2002. Colorado River centerline and measurement system. USGS, Grand Canyon Monitoring and Research Center. Flagstaff, AZ.

Monteith, J.L., and Unsworth, M.H. 1990. *Principles of Environmental Physics*. 2nd Ed. Edward Arnold, London, Eng.

Mueller, I.I. 1977. *Spherical and Practical Astronomy as Applied to Geodesy*. Ungar, New York.

Neter, J., Kutner, M.H., Nachtsheim, C.J., and Wasserman, W. 1996. *Applied linear statistical analysis*. 4th Ed. Irwin. Chicago, USA.

Page, J.K., and Sharples, S. 1988. The SERC meteorological data base Volume II: algorithm manual. 2nd Ed. Department of Building Science, University of Sheffield.

Randle, T.J., and Pemberton, E.L. 1987. Results and analysis of STARS (Sediment Transport and River Simulation) modeling efforts of Colorado River in Grand Canyon. Glen Canyon Environmental Studies Technical Report, NTIS No. PB88-183421.

Rapp, D. 1981. *Solar Energy*. Prentice-Hall, Inc., Englewood Cliffs, N.J.

Resampling Stats, Inc. 2001. Arlington, Virginia, USA.

- Rich, P.M., Hetrick, W.A., and Savings, S.C. 1995. *Modeling topographical influences on solar radiation: manual for the SOLARFLUX model*. LA-12989-M, Los Alamos National Laboratories, Los Alamos, N.M.
- Rosenberg, N.J., Blad, B.L., and Verma, S.B. 1983. *Microclimate, the biological environment*. John Wiley & Sons, New York, USA.
- SAS, Inc. 1996. Version 6.12, SAS Institute, Inc. Cary, N.C. USA.
- Schmidt, J.C., Webb, R.H., Valdez, R.A., Marzolf, G.R., and Stevens, L.E. 1998. Science and values in river restoration in the Grand Canyon: There is no restoration or rehabilitation strategy that will improve the status of every riverine resource. *Bioscience*. 48:735-750
- Shaver, M.L., Shannon, J.P., Wilson, K.P., Benenati, P.L., and Blinn, D.W. 1997. Effects of suspended sediment and desiccation on the benthic tailwater community in the Colorado River, USA. *Hydrobiologia* 357: 63-72.
- Shannon, J.P., Blinn, D.W., and Stevens, L.E. 1994. Trophic interactions and benthic animal community structure in the Colorado River, AZ, USA. *Freshwater Biology*. 31:213-220.
- Shannon, J.P., Blinn, D.W., Haden, G.A., Benenati, E.P., and Wilson, K.P. 2001. Food web implications of $\delta^{13}\text{C}$ and $\delta^{15}\text{N}$ variability over 370 km of the regulated Colorado River USA. *Isotopes Environ. Health Stud.*, 37:179-191.
- Sokal, R.R., and Rohlf, F.J. 1995. *Biometry the principles and practice of statistics in biological research*. W.H. Freeman and Company, New York, USA.
- Statsoft, Inc. 1997. Statistica for Windows. Version 5.1, Tulsa, O.K., USA.
- Stevens, L.E., Schmidt, J.C., Ayers, T.J., and Brown, B.T. 1995. Flow regulation, geomorphology and Colorado River marsh development in the Grand Canyon, Arizona. *Ecol. Appl.*, 6:1025-1039.
- Stevens, L.E., Shannon, J.P., and Blinn, D.W. 1997a. Colorado River benthic ecology in Grand Canyon, Arizona, USA: Dam, tributary and geomorphological influences. *Regul. Riv.*, 13:129-149.
- Stevens, L.E., Buck, K.A., Brown, B.T., and Kline, N.C. 1997b. Dam and geomorphological influences on Colorado River waterbird distribution, Grand Canyon, Arizona, USA. *Regul. Riv.*, 13:151-169.
- Stine, W.B., and Harrigan, R.W. 1985. *Solar energy fundamentals and design with computer applications*. John Wiley and Sons, Inc. New York, N.Y.

Thekaekara, M. P. 1977. Solar Irradiance, Total and Spectral, *in* Sayigh, A. A. M. (ed), *Solar Energy Engineering.*, Academic Press, New York, NY.

Vanote, R.L., Minshall, G.W., Cummins, K.W., Sedell, J.R., and Cushing, C.E. 1980. The river continuum concept. *Can. J. Fish. Aquat. Sci.*, 37:130-137.

Whitton, B.A. 1970. Biology of *Cladophora* in freshwaters. *Water Res.*, 4:457-476.

Wilson, K.P., Shannon, J.P., and Blinn, D.W. 1999. Effects of suspended sediment on biomass and cell morphology of *Cladophora glomerata* (Chlorophyta) in the Colorado River, Arizona. *J. Phycol.* 35:35-41.

Worm, B., Lotze, H.K., and Sommer, U. 2001. Algal propagule banks modify competition, consumer and resource control on Baltic rocky shores. *Oecologia.* 128:281-293.

Table 1. Major canyon sections and geomorphic reaches found along the Colorado River from Glen Canyon Dam to Lake Mead. Distances are in kilometers that extend downstream from Glen Canyon Dam.

	River Kilometer	River Kilometer	River Kilometer
Glen Canyon Section	0.00 – 26.8		
Marble Canyon Section		Central Grand Canyon Section	Western Grand Canyon Section
Permian (PE)	26.8 – 43.5	Furnace Flats (FF)	124.3 – 149.9
Supai Gorge (SG)	43.5 – 61.7	Upper Granite Gorge (UGG)	149.9 – 214.9
Redwall Gorge (RG)	61.7 – 83.1	Aisles (AI)	214.9 – 227.3
Lower Marble Canyon (LMC)	83.1 – 124.3	Middle Granite Gorge (MGG)	227.3 – 250.5
			Western Canyon (WC)
			250.5 – 282.7
			Muav Gorge (MG)
			282.7 – 369.4
			Lower Canyon (LC)
			369.4 – 421.2
			Lower Granite Gorge (LGG)
			421.2 – 474.5

Table 2. Annual and seasonal (21-June and 21-December) estimates of mean daily solar insolation levels ($\text{mol quanta m}^{-2} \text{d}^{-1}$) for the Colorado River from Glen Canyon Dam to Grand Wash Cliffs, Lake Mead, AZ. Water surface area (hectares) derived from STARS (Randel and Pemberton 1987) based on mean annual discharge of $323 \text{ m}^3 \text{ s}^{-1}$. Mean illumination angles (Ψ_1) expressed in degrees, and derived from 10-m GIS coverage using Arc-Info Hillshade routine (ESRI 1994) ($n = \text{site} \cdot 360$). Solar insolation levels were calculated on centerline at 100m interval ($n = \text{site} \cdot 366\text{-d}$) and season (summer and winter solstice; $n = \text{site} \cdot 1\text{-d}$).

Major Canyon Sections Geomorphic Reaches	Channel Surface Area (Ha)	Mean Ψ_1 ° (sd)	Min Ψ °	Max Ψ °	Mean V_p (sd)	Mean Annual $\text{mol m}^{-2} \text{d}^{-1}$ (sd)	Mean Winter $\text{mol m}^{-2} \text{d}^{-1}$ (sd)	Mean Summer $\text{mol m}^{-2} \text{d}^{-1}$ (sd)	Min $\text{mol m}^{-2} \text{d}^{-1}$	Max $\text{mol m}^{-2} \text{d}^{-1}$	Sites
Glen Canyon	321.6	31.3° (14.2)	3°	70°	0.65 (0.07)	35.2 (18.3)	11.7 (6.1)	57.0 (6.8)	4.6	69.0	268
Marble Canyon	743.0	35.4° (12.5)	4°	71°	0.61 (0.07)	32.2 (15.4)	12.5 (4.8)	50.9 (7.3)	4.0	68.3	975
Permian Section	156.3	30.1° (13.4)	4°	56°	0.68 (0.06)	36.6 (15.4)	15.2 (4.2)	55.9 (6.0)	5.8	68.3	167
Supai Gorge	103.1	37.7° (11.0)	10°	54°	0.61 (0.03)	31.8 (14.6)	12.3 (4.4)	50.3 (6.3)	5.0	64.3	182
Redwall Gorge	130.9	37.5° (11.4)	11°	53°	0.59 (0.06)	30.6 (14.9)	11.2 (3.7)	48.7 (7.2)	4.6	62.4	214
Lower Marble Canyon	386.2	35.5° (12.8)	5°	71°	0.59 (0.06)	31.5 (15.6)	12.2 (5.4)	50.2 (7.1)	4.0	61.9	412
Central Grand Canyon	886.8	34.2° (13.0)	6°	65°	0.68 (0.06)	37.9 (17.9)	13.3 (6.5)	59.2 (5.3)	4.4	68.7	1,262
Furnace Flats	256.8	36.6° (12.5)	11°	55°	0.75 (0.07)	42.1 (16.0)	19.8 (5.6)	61.6 (5.8)	5.6	68.7	256
Upper Granite Gorge	360.8	35.2° (13.2)	7°	65°	0.65 (0.05)	35.9 (18.7)	10.2 (5.6)	58.1 (5.4)	4.4	65.8	650
Aisles	76.4	29.3° (10.7)	6°	55°	0.67 (0.01)	38.0 (17.0)	13.7 (4.9)	58.5 (5.1)	5.8	64.4	124
Middle Granite Gorge	125.9	31.5° (12.9)	6°	60°	0.69 (0.03)	38.8 (17.2)	14.2 (5.1)	60.2 (3.2)	5.6	64.8	232
Western Grand Canyon	857.3	34.7° (14.8)	8°	69°	0.66 (0.10)	36.7 (17.8)	14.0 (7.0)	57.6 (7.3)	4.1	71.7	2,240
Muav Gorge	170.4	36.7° (14.4)	11°	66°	0.53 (0.03)	27.2 (17.8)	7.0 (3.1)	48.6 (9.5)	4.1	63.2	322
Lower Canyon	662.5	36.0° (14.8)	8°	69°	0.64 (0.09)	35.0 (18.0)	12.1 (6.5)	56.8 (6.4)	4.2	67.0	867
Lower Granite Gorge	142.5	32.4° (15.2)	8°	59°	0.70 (0.05)	39.4 (17.0)	15.2 (6.4)	60.0 (4.0)	5.1	65.7	518
Western Canyon	586.3	30.8° (13.8)	8°	54°	0.75 (0.05)	42.6 (15.3)	20.1 (4.1)	61.9 (4.2)	6.3	71.7	533
Colorado River Ecosystem	3,721	33.9° (13.8)	3°	71°	0.66 (0.09)	36.0 (17.5)	13.4 (6.5)	57.4 (6.8)	4.0	71.7	4,745

Table 3. Summary data of mean daily insolation levels ($\text{mol m}^{-2} \text{d}^{-1}$) have been estimated for summer and winter seasons (21-June and 21-December) for the primary channel orientations, north south (NS), northwest southeast (NW/SE), east west (EW), and northeast southwest (NE/SW), and distributed within the different canyon sections and geomorphic reaches of the Colorado River (total distance of 474.5-km from Glen Canyon Dam to Grand Wash Cliffs, Lake Mead, AZ). The standard deviation (sd) and site frequency (n) are indicated.

	NS - Orientation		EW - Orientation		NW/SE - Orientation		NE/SW - Orientation	
	Summer	Winter	Summer	Winter	Summer	Winter	Summer	Winter
	$\text{mol m}^{-2} \text{d}^{-1}$ (sd, n)		$\text{mol m}^{-2} \text{d}^{-1}$ (sd, n)		$\text{mol m}^{-2} \text{d}^{-1}$ (sd, n)		$\text{mol m}^{-2} \text{d}^{-1}$ (sd, n)	
GC	50.5 (5.4)	15.6 (3.3, n = 41)	61.2 (2.9)	8.4 (5.0, n = 91)	55.6 (6.3)	15.5 (6.1, n = 71)	56.5 (7.2)	9.2 (4.7, n = 65)
MC	47.3 (6.8)	15.1 (3.3, n = 349)	58.1 (3.5)	5.5 (2.3, n = 96)	49.6 (6.1)	14.1 (3.9, n = 160)	52.9 (6.8)	11.3 (4.7, n = 370)
PS	53.1 (5.2)	17.4 (2.6, n = 54)	66.8 (0.5)	11.2 (6.3, n = 4)	-	-	56.9 (5.8)	14.3 (4.3, n = 109)
SG	47.0 (4.1)	14.8 (2.3, n = 109)	61.2 (1.3)	13.6 (0.7, n = 3)	-	-	55.0 (5.7)	8.3 (4.1, n = 69)
RG	41.6 (5.5)	12.6 (2.4, n = 40)	57.2 (2.7)	4.8 (0.1, n = 12)	40.0 (7.8)	8.8 (2.3, n = 20)	51.2 (5.8)	11.7 (3.7, n = 142)
LMC	46.9 (7.6)	15.1 (3.8, n = 146)	57.7 (3.1)	5.0 (0.8, n = 77)	51.0 (4.5)	14.9 (3.5, n = 139)	46.0 (6.0)	7.8 (3.9, n = 50)
GCG	55.4 (5.4)	18.6 (3.2, n = 278)	62.9 (2.1)	8.3 (4.5, n = 385)	57.0 (4.9)	12.9 (6.1, n = 322)	60.6 (4.7)	15.6 (6.5, n = 277)
FF	58.8 (5.7)	20.7 (3.5, n = 108)	65.0 (2.4)	13.0 (7.4, n = 31)	58.3 (4.5)	23.8 (1.1, n = 6)	63.6 (5.3)	20.7 (5.6, n = 111)
UGG	52.5 (4.4)	16.6 (2.3, n = 107)	62.4 (2.2)	7.3 (3.7, n = 252)	55.7 (5.0)	11.3 (5.8, n = 232)	59.6 (2.5)	8.4 (3.3, n = 59)
AI	53.1 (2.1)	17.7 (0.8, n = 44)	63.5 (1.0)	9.4 (4.2, n = 55)	58.4 (2.2)	17.1 (2.2, n = 16)	54.1 (2.0)	14.4 (1.7, n = 9)
MGG	57.5 (2.4)	19.3 (1.1, n = 19)	63.7 (1.1)	9.0 (4.3, n = 47)	60.9 (2.4)	16.3 (5.6, n = 68)	58.4 (2.8)	14.3 (3.8, n = 98)
WGC	54.9 (9.0)	18.9 (4.4, n = 594)	60.8 (4.1)	8.3 (5.7, n = 571)	59.5 (5.0)	16.7 (5.6, n = 480)	55.6 (7.9)	12.2 (6.8, n = 595)
MG	37.4 (4.0)	10.7 (2.1, n = 93)	57.8 (2.9)	4.9 (1.0, n = 119)	48.6 (6.1)	4.6 (0.5, n = 21)	48.2 (6.6)	6.5 (2.6, n = 89)
LC	54.9 (5.7)	18.6 (3.0, n = 175)	59.6 (4.0)	7.4 (4.8, n = 256)	61.8 (4.9)	19.0 (5.7, n = 78)	54.5 (6.9)	10.6 (5.1, n = 358)
LGG	60.1 (4.4)	21.7 (2.2, n = 124)	62.8 (1.3)	7.2 (2.6, n = 111)	57.9 (4.3)	14.2 (4.9, n = 172)	60.5 (2.8)	17.5 (4.8, n = 111)
WC	59.7 (3.0)	21.2 (1.8, n = 202)	65.8 (1.3)	17.4 (5.6, n = 85)	61.0 (3.3)	19.1 (3.4, n = 209)	69.6 (3.0)	25.7 (5.4, n = 37)
CR	52.7 (8.4)	17.7 (4.2, n = 1,262)	61.4 (3.7)	8.1 (5.1, n = 1,143)	56.9 (6.2)	15.0 (5.8, n = 1,033)	55.9 (7.4)	12.6 (6.3, n = 1,307)

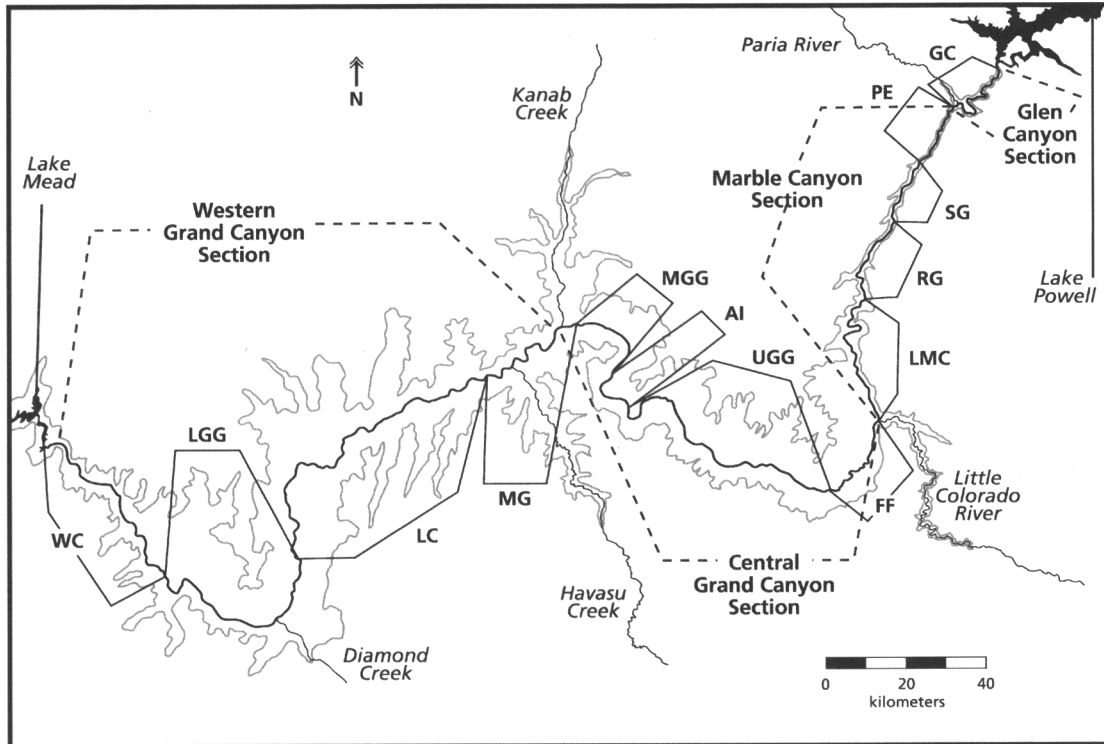


Figure 1. Map showing major canyon sections, geomorphic reaches, and tributaries of the Colorado River. Estimates of daily solar insolation were calculated at 100 m intervals along the entire river centerline for 474.5 river kilometers (Rkm) from Glen Canyon Dam to Lake Mead, AZ.

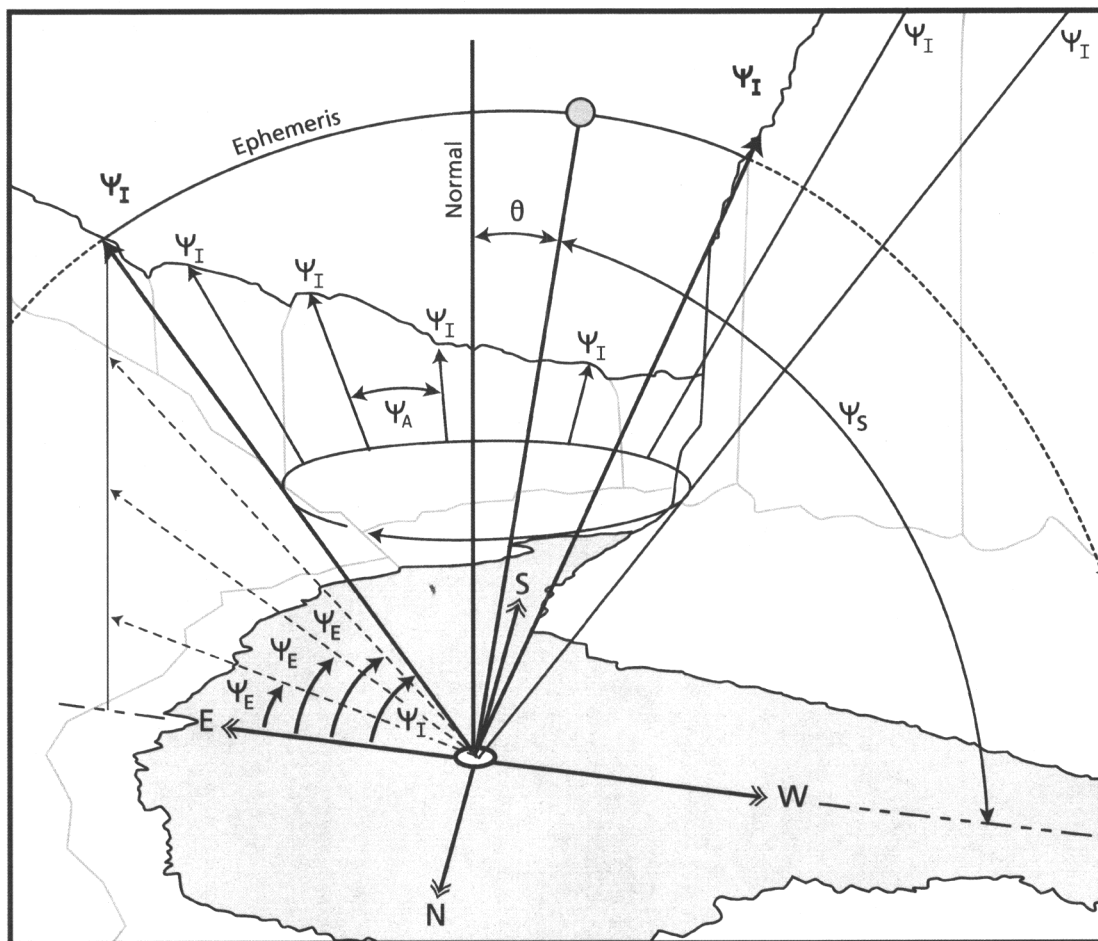


Figure 2. A schematic, illustrating the major topographic and solar altitude angles used for estimating instantaneous total ground incidence (GI). Illustrated angles depicted are: zenith angle (θ) representing the angle between the sun and normal (N) a reference line perpendicular to the incidental water surface; elevation angle (Ψ_E) represents the angle measured from a horizontal surface relative to a topographic feature (i.e., angles are used to vertically search for the illumination angle in single-degree increments); whereas, an illumination angles (Ψ_I) is the maximum elevation angle between the topographic skyline and the horizon; solar altitude angle (Ψ_S) represent the solar angles between the sun and the horizon (i.e., Ψ_S angles are equivalent to $90^\circ - \theta$); and azimuth angles (Ψ_A), are angles that correspond to the cardinal directions (N, E, S, and W) measured within the horizontal plane. Direct solar beam occurs when $\Psi_I \leq \Psi_S$, that $GI = [(\cos \theta_{DB} \cdot GI_{DB}) + (\cos \theta_{DI} \cdot GI_{DI} \cdot V_P)$, (refer to text).

Figure 3. Predicted and observed daily solar insolation estimates ($\text{mol quanta m}^{-2} \text{d}^{-1}$) for summer (22 June 1992) and winter (21 December 1993). Observation site was located 76.5-km downstream in Marble Canyon Gorge ($36^{\circ}12'6.6''\text{N}$, $111^{\circ}48'0.3''\text{W}$) with a north-south channel orientation. Data collected on 23 December 1992 demonstrates the influence atmospheric interference has on mean daily solar insolation.

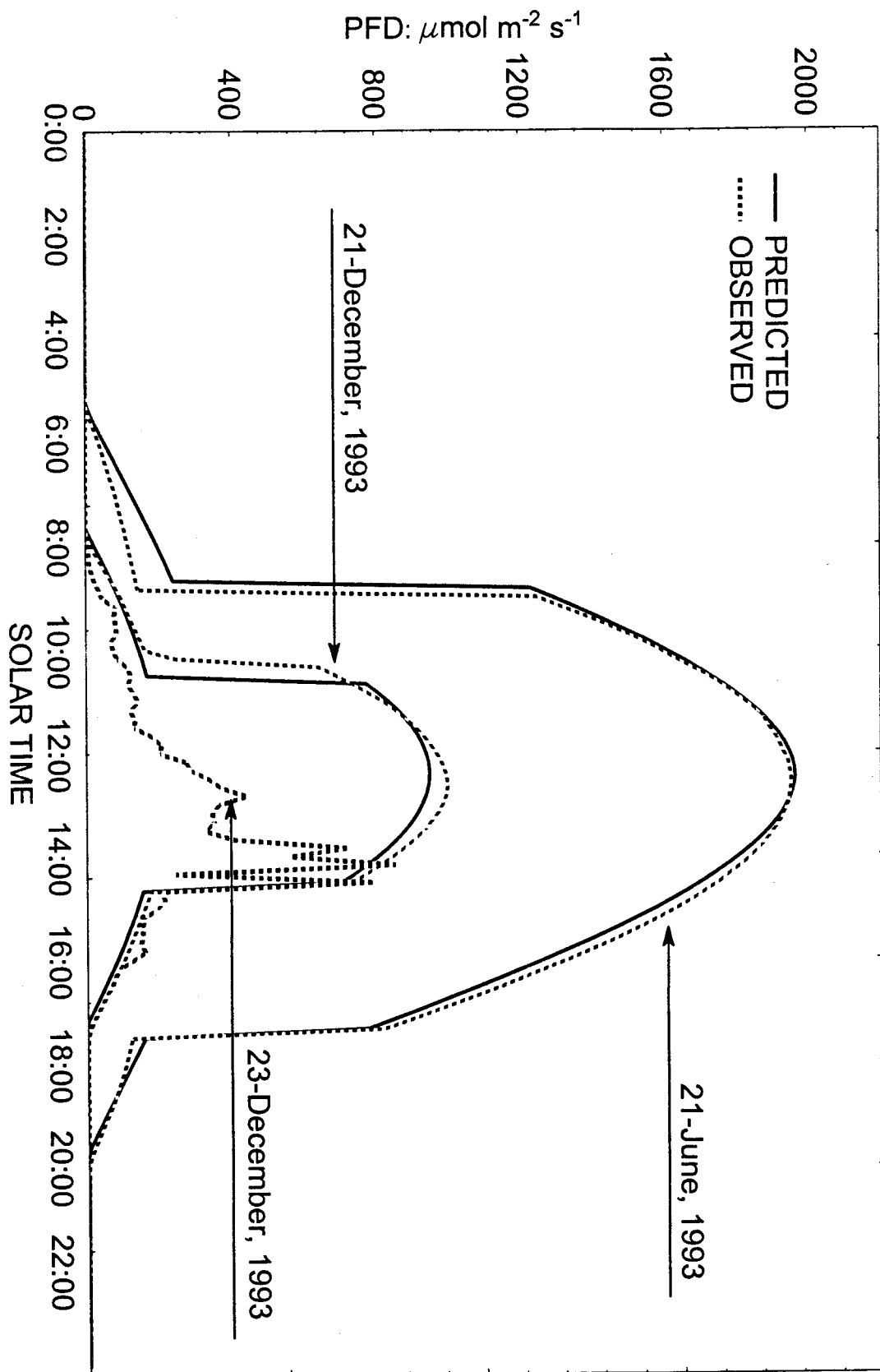


Figure 4. Graphical results generated from GIS coverage using Arc-Info Hillshade routine (ESRI 1994) for spatial distribution of mean illumination angles (Ψ_1 , degrees) distributed over cardinal directions, (i.e., north, east, south and west) (y-axis, 360° azimuth) along the entire river length (x-axis) in hectometers from Glen Canyon Dam to Lake Mead (474.5 km).

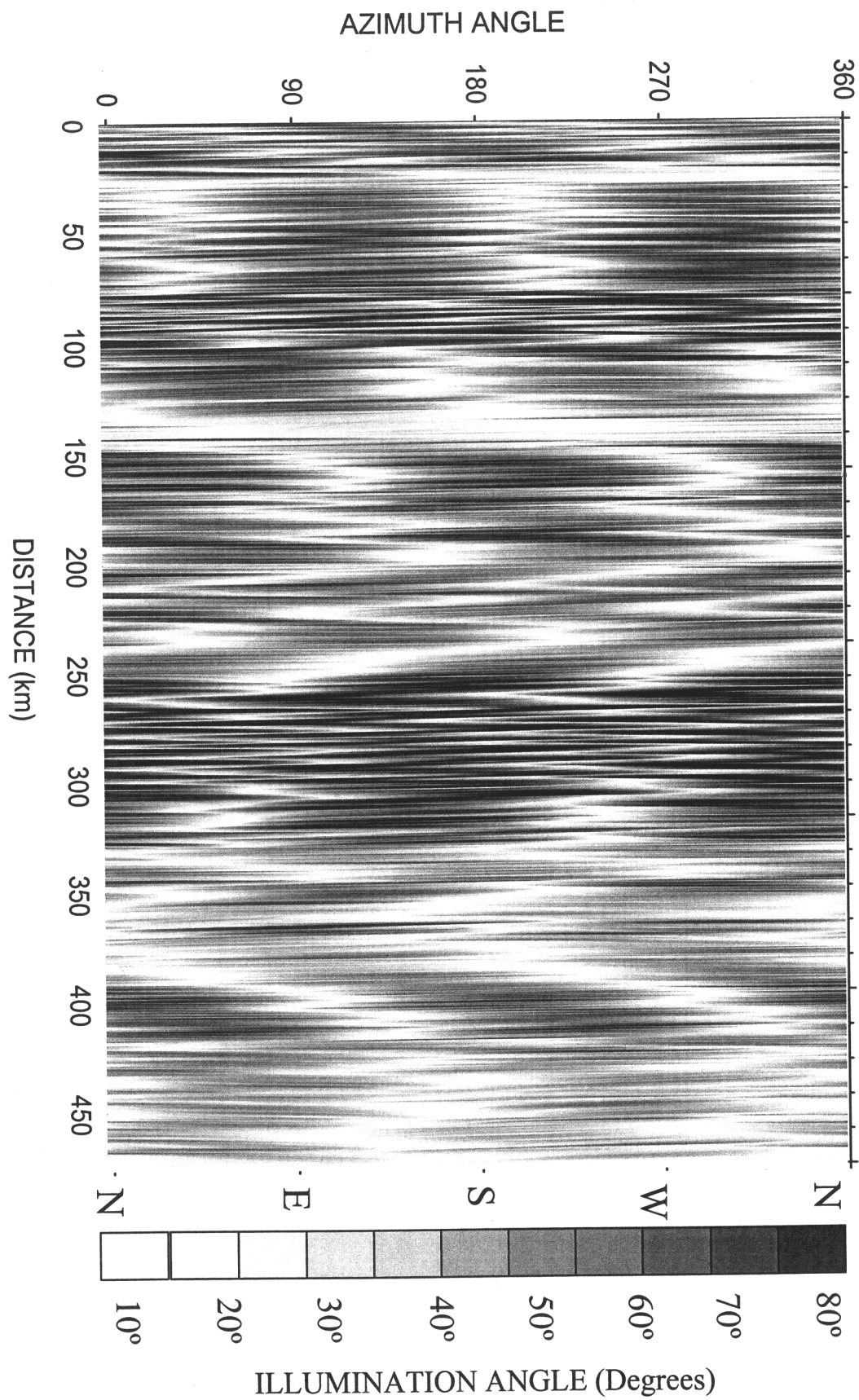


Figure 5. Planar view representing the spatial and temporal distribution of mean daily solar insolation ($\text{mol quanta m}^{-2} \text{d}^{-1}$) for the entire year (y-axis) along the entire river length (x-axis) in hectometers from Glen Canyon Dam to Lake Mead (474.5 km). Graphical results generated from GIS coverage using Arc-Info Hillshade routine (ESRI 1994)

Figure 6. Lateral view representing the annual range of mean daily solar insolation (mol quanta $\text{m}^{-2} \text{d}^{-1}$) distributed along the entire river length (x-axis) in hectometers from Glen Canyon Dam to Lake Mead (474.5 km). Graphical results generated from GIS coverage using Arc-Info Hillshade routine (ESRI 1994)

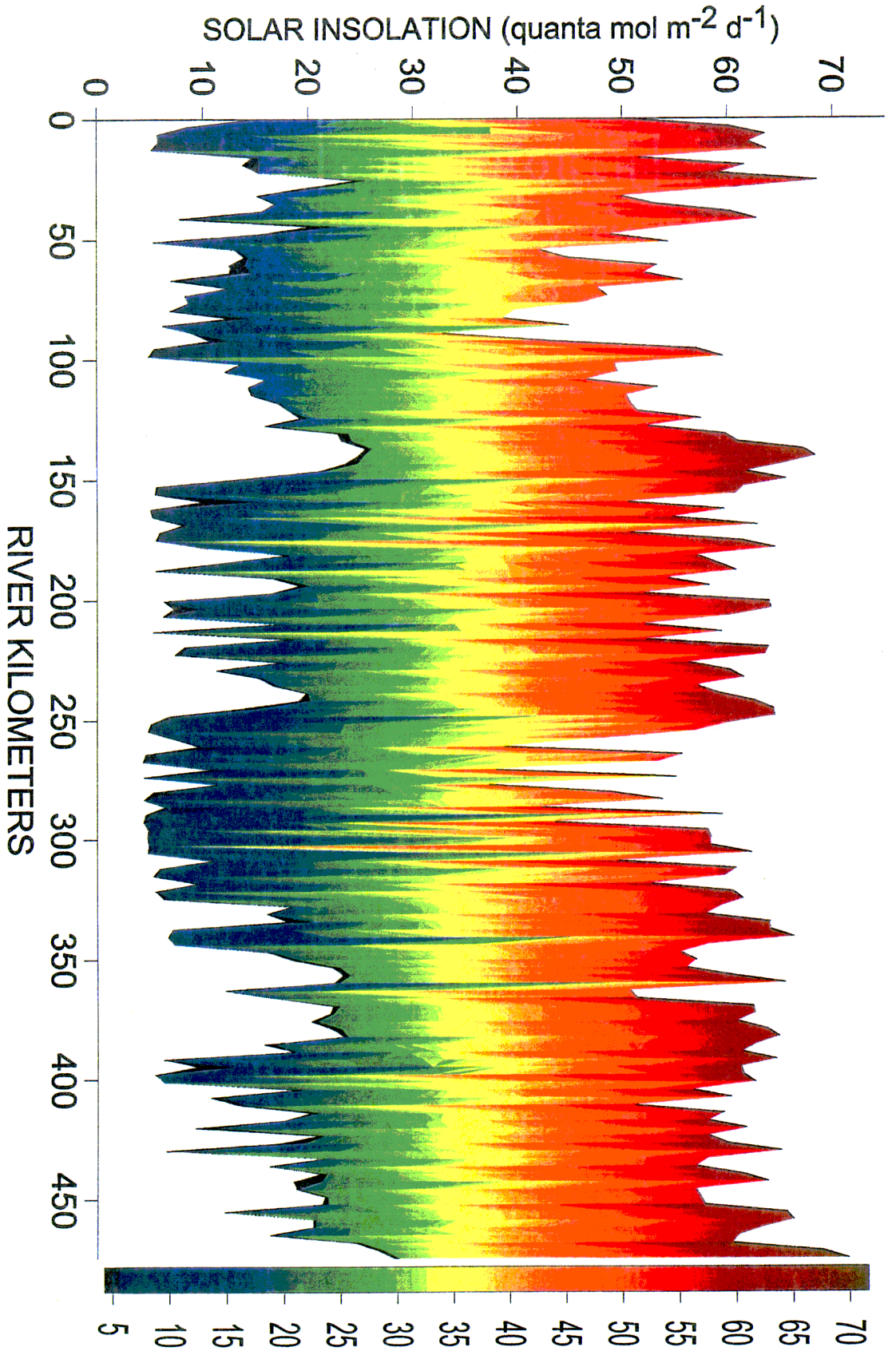
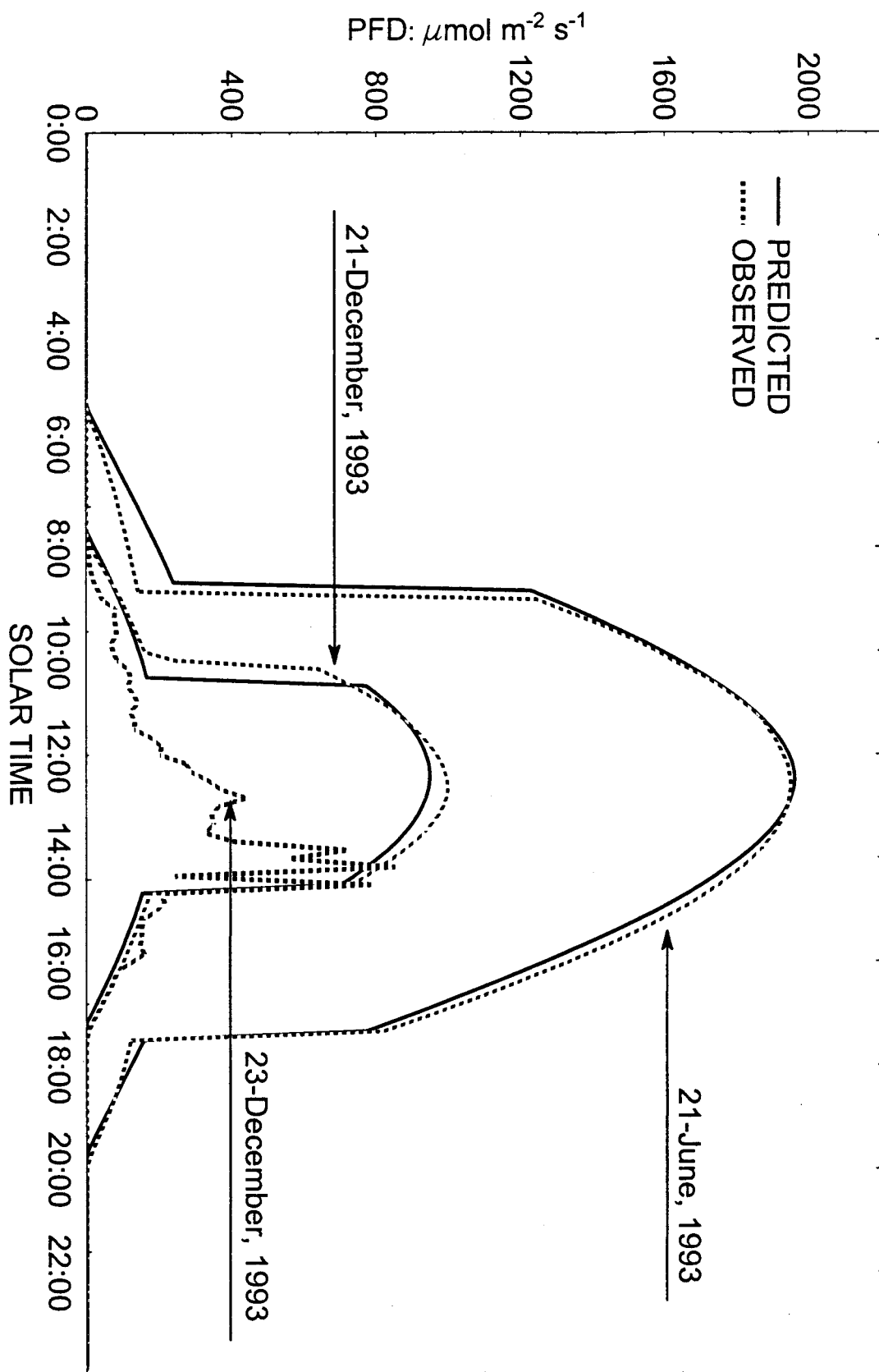


Figure 7. Daily solar insolation ($\text{mol m}^{-2} \text{d}^{-1}$) for winter (21 December) and summer (21 June) seasons over a 20 km distance for a NE-SW trending stretch of the Colorado River below Glen Canyon Dam (0.0-km) to Cave Canyon (20.0-km).



CHAPTER 3

LINKAGES BETWEEN RESERVOIR AND IN-STREAM PROCESSES
REGULATING DISSOLVED ORGANIC CARBON AND
LIGHT-ATTENUATION IN A RIVER ECOSYSTEM.*Abstract*

We hypothesized that dissolved organic carbon (DOC) and particulate organic matter derived from *in situ* autotrophic production influenced underwater light-attenuation. Our study site was located in the Colorado River, Glen Canyon; sediment-limited tailwater section influenced by cold, clear hypolimnetic releases from Lake Powell reservoir. Observations indicated that significant temporal (diel, seasonal) variability in riverine light-attenuation were related to differences in solar zenith angles. Light-attenuation coefficients (K_N) were normalized to control for solar zenith angles and refraction. Results indicated that DOC was the primary light-attenuating constituent. These studies indicated that K_N and DOC were spatially different among sites and significantly correlated; where secondary sources of DOC appear to be originating from autotrophic production. Experiments exposing algae to natural light conditions (48-h) exhibited significantly higher DOC and light-attenuation, where and alternate treatment lacking algae exhibited an opposite response. This indicated that variation in light-attenuation was perhaps strongly linked to local autotrophic production. Inter-annual comparisons (1991-1998) indicated that a significant increase in K_N had occurred in the river, which amounted to a 30% reduction in optical depth; yet, this increase in K_N was not related to solar zenith angles that remain constant between years. Limited data for

DOC were available for assessing affect on light-attenuation among years; therefore, other water quality parameters were tested. Results indicated that parameters such as pH, and specific conductance explained 60% of the observed inter-annual and seasonal differences in K_N . Results suggest that physiochemical processes in Lake Powell reservoir and biotic processes occurring in the Colorado River were strongly linked, and were potentially regulating the quantity of photosynthetic photon flux density available for the phytobenthic community in Glen Canyon.

Introduction

The importance of photosynthetically active radiation (PAR) for primary production is universally recognized, yet for freshwater streams and rivers few studies have attempted to characterize apparent optical properties, or those factors and processes regulating underwater light availability (Roos and Pieterse 1994; Kimber *et al.* 1995). Extensive research has been conducted on light transmission in marine ecosystems (Smith *et al.* 1989; Conversi and McGowan 1994; Berwald *et al.* 1998; Duarte *et al.* 1998), with some emphasis on lentic systems (Blinn *et al.* 1977; Kirk 1979; Roemer and Hoagland 1979; Morris and Hargreaves 1997). Although this optical knowledge is directly applicable to all aquatic systems, differences in regulatory mechanisms between freshwater systems are poorly understood; therefore findings are not entirely transferable, especially for rivers and streams in the arid Southwest.

Biotic and physiochemical processes can significantly alter the concentration and composition of light attenuating constituents in water (Kaplan and Bott 1982; Kirk 1983; Nielsen and Sakshaug 1993; Amon and Benner 1996; Boavida and Wetzel 1998). These

constituents at high concentrations can become photosynthetically limiting, reducing photosynthetic photon flux density (PPFD) available for primary production (Kirk 1980, 1994). Response of algae and macrophytes to varying levels of PPFD may have considerable ecological implications for photosynthetic yields, growth rates, composition, distribution, and trophic linkages in pelagic and benthic communities (Ganf 1973; Jewson and Taylor 1978; Ward and Stanford 1983; Steinman *et al.* 1990; Moorhead *et al.* 1997; Shaver *et al.* 1997).

The unregulated Colorado River, once an allochthonous-based ecosystem (Stanford and Ward 1991), was sediment laden, and varied seasonally in flow and temperature, typifying characteristics associated with most other southwestern fluvial rivers (Stevens *et al.* 1997; Haden *et al.* 1999). In 1963, the trophic structure was altered with the construction of Glen Canyon Dam and suspended loads (inorganic and organic) began to be sequestered within the confines of the Lake Powell reservoir. In absence of allochthonous organic material, downstream sections of this regulated river have become extremely dependent upon PPFD availability for autotrophic production (Hardwick *et al.* 1992; Shaver *et al.* 1997; Blinn *et al.* 1998). Presently, Glen Canyon may account for up to 50% of the total annual autotrophic production throughout the Colorado River system (390-km) inclusive of Grand Canyon during certain periods (Angradi and Kubly 1994; Blinn *et al.* 1995). Areally, it is the most productive section of the Colorado River, yet it represents only 7% of total wetted area available for primary production.

Our objectives were to determine through observational studies and experimental manipulations if the apparent optical properties of the Colorado River in the regulated tailwater section of Glen Canyon were temporally and spatially variable. Furthermore we

sought to identify factors and regulating mechanisms potentially responsible, with the purpose of developing a model to predict the underwater light regime and its availability for primary production. We hypothesized that: 1) dissolved organic carbon (DOC) was the primary light attenuating constituent in Glen Canyon; 2) secondary loss of extracellular photosynthates and particulate organic matter (POM) resulting from in-stream autotrophic production would additively decrease PPFD availability in this aquatic ecosystem.

Methods

Study Area - The Colorado River originates from Lake Powell reservoir as a hypolimnetic release ($9 \pm 2^\circ\text{C}$) and flows through Glen Canyon. Flow releases from Glen Canyon Dam (GCD) hydroelectric facility in Glen and Grand canyons create optically transparent conditions in the downstream tailwater section (Blinn and Cole 1991; Shaver *et al.* 1997; Benenati *et al.* 1998). Our study area, Glen Canyon, is a consistently clear-tailwater section located on the Colorado plateau of northern Arizona in a remote incised canyon section, extending a linear distance of 26.3 km downstream to the Paria River. The highly transparent characteristics of the Colorado River are frequently altered downstream from this tributary's confluence by the high-suspended loads of the Paria (Graf *et al.* 1991). We established three data collection stations that included Site 1 (GCD draft tube, hydroelectric facility), Site 2 (GCD outflow, 0.0 km) and Site 3 (Lees Ferry, 25.2 km) (Fig. 1).

Sampling Design - In 1997-1998, we sampled on a quarterly basis to determine if light-attenuation was spatially and temporally variable (diel, seasonal, and inter-annual).

We analytically explored the effects of certain factors potentially linked to light-attenuation, separating variables into four categories: 1) solar angles, 2) light attenuating constituents, 3) incident light characteristics, and 4) water quality parameters. The sampling schedule coincided seasonally with the solstices and solar equinoxes: 17-18 December 1997, 21-22 March 1998, 19-20 June 1998 and 19-20 September 1998. Non-seasonal sampling was also conducted opportunistically at the above sites on 23-24 August 1997, 6-7 September 1997, and 20-21 June 1998. For making inter-annual light comparisons, we supplemented our analysis using other photometric data that we had collected since 1991.

Light-attenuation Measurements - Three types of quanta sensors (LiCor, Inc.) were used to measure PPFD ($\mu\text{mol s}^{-1}\text{m}^{-2}$), which included LI-193SA and LI-192SA sensors, and incident light above the water surface LI-190SA. The type of sensor used was dependent on its application. All sensors measured equally within the entire waveband (400-700 nm) of PAR (Kirk 1983; Thimijan and Heins 1983). During daylight, three profiles were repetitively collected at 0.5-h intervals at Sites 2 and 3, and measured to a maximum depth of 5 m. Five measurements were collected at each 0.5-m interval on the profile and sensors were equilibrated (10-s) between each depth interval to avoid hysteresis.

Underwater irradiance diminishes exponentially as a function of depth, $Q = Q_z e^{-Kz}$, (Kirk 1977, 1983). Although, this depth-dependent relationship can be linearized by a natural log transformation, variability in incident light received at the water surface during the elapsed period of a measured profile may significantly alter the derived coefficient. The effects from atmospheric conditions were corrected for by using a \log_e

transformation of the ratio of quantum scalar irradiance (Q_z) to water surface incidence (Q_i) and then regressed to depth (z). Derived coefficients, K_O (m^{-1}), provide a useful index to characterize light-attenuation in water, as well as a functional term for estimating depth dependent PPF in the water column, $\ln(Q_z) = z \cdot K_O + \ln(Q_i)$.

Because apparent optical properties are influenced by the angular distribution of incident light (Kirk 1977; 1994), all empirical data were temporally corrected using the equation of time by converting from mean standard time to solar time. Temporal conversion accounted for the inclination of the earth's ecliptic and eccentric orbit around the sun (Duffie and Beckman 1974; Brock 1981). Spherical geometry, equation of time, and global coordinates were used to estimate solar angles: hour angle (ω), declination (δ), solar zenith angle (θ_i) that influenced the quantity of solar incidence and the angle of refraction (θ_r) (Chapter 2). For certain types of analysis light-attenuation coefficients were normalized, K_N , using solar zenith angle (θ_i) by estimating the refractive photic pathlength traveled relative to the vertical depth measured based on refractive index of water (1.33) (Kirk 1983; Denny 1993). The expression used to normalize measured scalar light-attenuation coefficients was, $K_N = \cos(\sin \theta_i / 1.33) \cdot K_O$.

Light Attenuating Factors - Three replicate water samples were collected hourly for light attenuating constituents using a depth-integrated sampler, and sampled concurrently at all sites over a 24-h period (Pemberton 1987, Rubin *et al.* 1998). Each integrated sample was analyzed for dissolved organic carbon (DOC), total suspended load (TSL), inorganic suspended-sediment (SS) and particulate organic matter (POM) concentration ($mg L^{-1}$). Suspended particles were extracted onto glass filters (Whatman 934-AH 1.5 μm pore), desiccated for 24-h at 60°C, weighed (± 0.01 mg), ashed for 1-h at

500°C, and reweighed (Greenberg *et al.* 1992). DOC samples (60 ml) were withdrawn and filtered (Whatman GF/F 0.7 µm pore), preserved by acidification (pH 2 - H₂SO₄) and refrigerated for storage. DOC determinations were performed using UV oxidation process (Phoenix 8000, Dohrman).

Additionally, we determined the effects from other categorical variables measured during the profile. Incident light characteristics were one such group, and included continuous data as minimum, maximum, percent flux ($Q_{\text{Min}}/Q_{\text{Max}}$), mean solar incidence, and nominal data, such as insolation (topographic obstruction) and atmospheric conditions (clouds and rain). Water quality data (Surveyor II, Hydrolab, Inc.) have been continuously monitored at 0.5-h intervals at each of the three sampling sites for a 10-y minimum period. USGS Grand Canyon Monitoring and Research Center and Water Resource Division provided the data used (Hart and Sherman 1996; Vernieu 2000). Discontinuities in the period of record were rectified by combining different data sets and pairing variables to the nearest time interval, parameters included: dissolved oxygen (mg L⁻¹), pH, specific conductance (µS cm⁻¹) and temperature (°C).

Vertical Light-attenuation Chamber Experiment - We hypothesized that DOC regulated light-attenuation in a freshwater river ecosystem through a combination of in-stream processes of algal/macrophytic production and losses through photo-oxidation and bacterial degradation. A total of six experiments were conducted using two treatments, one with algae and one without. Each experimental run required three circular steel tanks for each treatment (1.22 m x 0.76 m) lined with clear polyvinyl plastic. All tanks were simultaneously filled with filtered river water (375-L). Coarse particulate matter was removed using a filter (0.25-mm) on a submersible pump. Algal treatment consisted of

120 algal covered cobbles collected locally at Site 3 (Fig 1), which were covered with a filamentous green alga, *Cladophora glomerata* and associated epiphytes; 40 cobbles were randomly selected for each of the three replicate tanks. Six experimental replicates were suspended in the river, each with a recirculating pump and exposed to natural light conditions and low temperatures (10-14°C) for a 48-h period. Total solar irradiance ($\mu\text{mol s}^{-1} \text{m}^{-2}$) was remotely logged (LI-1000, LiCor, Inc.) during the entire treatment period.

Light-attenuation coefficients and associated parameters (DOC, TSL, SS and POM) were determined for each replicate sample (control and treatments) using the same measuring and analytical methods previously described. Initially for each experimental run, light-attenuation characteristics and suspended and dissolved constituents were determined. This process was then repeated upon completion of the experiment to determine if either treatment type departed from the initial condition. The filtrate (375-L) used for the initial control and treatments was pumped into a vertical light-attenuation chamber (VLAC), (5 x 0.31 m, PVC Sched-40). A halogen lamp (Sylvania, Metalarc M1000/U) was used as the artificial light source ($2100\text{-}2000 \mu\text{mol s}^{-1} \text{m}^{-2}$) by vertically suspending over the chamber opening at 0.5 m above water surface. Irradiometric measurements for diffuse light-attenuation, K_d (LI-192SA), were conducted similar to *in situ* observations previously described. Chamber walls were washed clean between replicates with de-ionized and distilled water. Upon completion of each experimental run, algal samples were removed, desiccated, and analyzed for total biomass.

Statistical Analyses - Variables were separated into four categories (solar angles, light-attenuating constituents, incidental light characteristics, and water quality

parameters) and evaluated for their individual and group effect on light-attenuation, using a combination of statistical methods including ANOVA, ANCOVA, simple (SLR) and multiple linear regressions (MLR). We selected K_O values used in our analyses based on $R^2 \geq 0.95$ and solar zenith angle (θ_i) $< 75^\circ$, and were temporally paired to explanatory variables. Through an elimination process based on *post-hoc* findings, an overall pool of possible variables was initially selected to include in an all-possible regression procedure. We used Mallows' C_p as the final criterion for selecting our desired statistical model (Chatterjee and Price 1977; Netter *et al.* 1996). The statistical packages used for our analyses included SAS, Inc., (1996) and StatSoft, Inc., (1997).

Results

Solar angles and incidence - Diel patterns in light-attenuation for Glen Canyon have a sinusoidal response, exhibiting the least amount of attenuation at solar zenith and greatest during crepuscular periods. Considerable seasonal variation did occur, with greatest attenuation during winter solstice, and conversely so during the summer when solar altitude was at the highest (Fig 2). We tested for the effects of solar angles, as a possible source of this temporal variation. Solar angles, such as declination (δ), solar zenith angle (θ_i), and hour angle (ω) regressed to K_O were significantly correlated by season ($F_{3, 439} = 91.3$, $p < 0.001$). *Post-hoc* tests (SLR) demonstrated that the diel variation in K_O was significantly correlated to ω ($p < 0.001$) and θ_i ($p < 0.001$). Seasonal differences in mean K_O were explained by θ_i ($p < 0.001$) and δ ($p < 0.001$), thus demonstrating that periodicity in the angular distribution of solar incidence and its effect on light-attenuation are temporally deterministic. Our remaining analyses will explain

light-attenuation effects in absence of solar angles through the use of a normalized attenuation coefficient (K_N) due to the predictability and intercorrelatedness of certain explanatory variables to solar time.

Although the departure from normal corresponded directly to an increase in light-attenuation, it only partly accounted for the observed diel and seasonal light variation. In controlling for θ_i , normalized K_N exhibited a significant increase in light-attenuation since 1991, ($F_{1, 441} = 142.5$, $p < 0.001$) (Fig 3). Because solar angles are predictively constant between years, their effect could not be responsible for the inter-annual increase in observed light-attenuation. It was evident that spatial differences also existed for K_N , indicating that an attenuating increase resulted as a function of distance downstream $F_{1, 441} = 21.8$, $p = 0.001$) (Fig 2).

Suspended-sediment and dissolved organic carbon – There were significant spatio/temporal differences in the quantity of suspended and dissolved constituents. ANOVA was performed on the two major components of total suspended load (TSL). These consisted of suspended solids (SS) and particulate organic matter (POM). The factors included sampling period, sampling site, sampling time, and nested effects for different stations at varying levels of sampling period and sampling time. We excluded from our analysis samples collected on 7 September 1997 because of suspended-sediment from ungaged tributary flows. The TSL concentrations were elevated above concentrations characteristic of Glen Canyon. Sampling period and site were significantly influenced ($p < 0.001$) by main factor effects; however, they were unrelated to sampling time (24-h cycle) and the interactions between sampling period and time (Table 1).

Under normal flow conditions, *post-hoc* spatial comparisons, using Tukey HSD test for unequal sample size indicated that mean SS differed significantly for all sampling sites ($p < 0.001$). A SLR indicated a significant and positive difference between sites with SS increasing with downstream distance ($F_{1, 1179} = 50.8, p < 0.001$). This spatial pattern was also true for POM ($F_{1, 1184} = 28.9, p < 0.001$). Comparative tests revealed that mean POM were significantly different ($p < 0.02$) between all sampling sites, increasing with distance from the reservoir to the most downstream river site. No significant spatial difference in DOC was observed between the two upstream sites (Site 1 & 2) indicating that the reservoir and river outflow were initially equivalent, with one notable exception ($p < 0.001$, September 1998). We determined that DOC increased significantly ($F_{1, 784} = 57.1, p < 0.001$) with distance to downstream sites (Fig 4). There were significant differences in DOC between sampling periods ($F_{1, 784} = 5, p = 0.025$), for both upstream ($p = 0.01$) and downstream sites ($p < 0.001$). The spatial and seasonal differences in DOC are illustrated in Fig 4; however, no systematic variability in DOC was observed at a diel level ($p = 0.90$). Also, DOC was significantly and positively correlated to POM ($F_{1, 783} = 8.9, p < 0.003$).

Factors influencing light-attenuation - Spatio/temporal patterns suggested that suspended and dissolved concentrations might be influencing K_O . To determine whether or not these light-attenuating constituents had a direct effect on K_O required controlling for the angular effect. By normalizing light-attenuation, K_N , the regression analysis performed indicated that only DOC and POM were significant ($F_{3, 220} = 3.86, p < 0.01$). *Post-hoc* tests for the inorganic component SS indicated no significance ($p = 0.4$) except for the occasional sediment contribution from small ephemeral catchments. Although

spates were brief in duration and very infrequent (late summer), TSL ($> 500 \text{ mg L}^{-1}$) had a temporary effect on light-attenuation ($F_{1,33} = 185$, $p < .001$) ($r = 0.92$, $\beta = 0.027$). During daylight periods light-attenuation coefficients (K_N) attained elevated values equal to 5.3 m^{-1} , yet returned to nominal attenuation levels within a 12-h period (Fig 5).

Although organics were correlated ($r = 0.16$), individual *post-hoc* tests showed that POM was marginally significant ($p = 0.07$) to this light-attenuation relationship. Yet, despite DOC significant and positive correlation ($\beta = 0.013$) to light-attenuation it lacked a strong 1:1 correspondence as noted for TSL (Fig 5). This in itself indicated that other factors were perhaps influencing light-attenuation due to either the quality of DOC, or other factors that were acting independently on light-attenuation.

Solar characteristics and water quality parameters - We evaluated a suite of variables characterizing solar incidence. Only mean, minimum, percent flux of incidence, and solar insolation were significantly correlated to K_N ($F_{6,433} = 13.7$, $p < 0.001$). Variables excluded were atmospheric conditions (i.e., rain and cloud cover) ($p = 0.26$), and maximum solar intensity ($p = 0.97$). *Post-hoc* tests revealed that each variable was significant ($p < 0.001$). Although these variables accounted for some of the observed variability (diel, seasonal and site) they were not responsible for the inter-annual light-attenuation.

Water quality parameters represented a colligative measure of biotic and physiochemical processes occurring in reservoirs and rivers. The parameters encountered during this study were temperature, $7 - 11.5^\circ\text{C}$, specific conductance, $616 - 978 \mu\text{S cm}^{-1}$, and pH, $7.4 - 8.4$. We included in the analysis Lake Powell's reservoir stage elevation, since water quality parameters respond according to changes in reservoir volume relative

to the stationary withdrawal intake structure. This structure is vertically fixed at 70-m below the surface from full pool elevation (1,130 m). Results indicated that $\mu\text{S (cm}^{-1}\text{)}$ ($r = -0.48$), pH ($r = 0.55$), and stage elevation ($r = 0.09$) were all significantly correlated to K_o ($F_{4, 435} = 67$, $p < 0.001$), even though temperature was excluded ($p = 0.42$).

Vertical Light-attenuation Chamber Experiment (VLAC) - We experimentally removed the effect of θ_i variation using an artificial light system. Results from a 2-way ANCOVA, indicated that K_d covaried as a function of DOC ($F_{2, 28} = 6.39$; $p < 0.005$), and after a 48-h period a significant difference developed between the two treatment types ($p < 0.006$). For comparative purposes separate *post-hoc* tests (ANOVA) were made among treatments. A significant difference existed between algal and non-algal K_d ($p < 0.001$); yet neither algal ($p = 0.14$) nor non-algal ($p = 0.06$) K_d coefficients differed significantly from their initial condition (Fig 6). Also, differences in DOC among treatments indicated that algae had significantly increased in relation to both the initial condition ($p < 0.??$), as well as the non-algal treatment ($p < 0.??$). But no significant difference in concentration was detected between initial and the non-algae treatment ($p = 0.06$).

Findings suggest that DOC originating from algal production resulted in higher light-attenuation; and conversely, water exposed to natural light conditions (UV and visible light) resulted in higher water transparency. Mean DOC for the initial condition and the two treatments (non-algal and algal) were 3.57, 3.62, and 4.53 mg L^{-1} , and differences corresponded to mean K_d values, 2.04, 1.96, and 2.13 m^{-1} , respectively. Each of the six experiments were conducted over a 9-mo period; therefore, due to natural seasonal differences in riverine DOC and atmospheric conditions we were unable to control for the variability in our initial starting condition, hence the difference between

experimental runs ($p < 0.04$). Yet, differences between experimental runs in K_d and DOC did not covary significantly as a function of biomass or ambient light conditions and therefore remain unexplained.

Light-attenuation Model - Using an all-possible regression modeling approach and Mallows C_p as selection criterion, we selected a model that included a total of five explanatory variables ($F_{5, 437} = 54.6$, $p < 0.001$). Solar characteristics, water quality parameters and distance accounted for spatio/temporal differences in light-attenuation. The tabulated results (Table 3) identify independent variables, units of measure, coefficients and level of significance. Using this relationship for predicting the normalized light-attenuation coefficient (K_N) we then reconverted to K_O which best characterized the apparent optical properties present in the river at that time. Expression used for reconvertng this coefficient was: $K_O = K_N / \text{Cos}(\text{Sin } \theta_i / 1.33)$, which accounted for the deterministic effect from θ_i and water refraction (1.33). Comparative results for predicted versus measured light-attenuation coefficient had an r^2 of 0.60.

Discussion

Observational and experimental results indicated that inorganic suspended particles did not regulate light-attenuation in the Glen Canyon tail-water section, but rather organic material and solar zenith angle. By normalizing K_O , results indicated that DOC was the primary light-attenuating constituent. Although significant, the high variance indicated that DOC concentration alone lacked a strong predictive correspondence to K_N . Obviously other factors and mechanisms were therefore responsible for some of the observed variance in light-attenuation. This DOC

relationship was expected, though the discordant response between TSL and K_D was surprising since suspended particles are typically known to be the primary determinant in light-attenuation for fluvial streams and rivers (Davies-Colley *et al.* 1992; Hardwick *et al.* 1992; Roos and Pieterse 1994; Shaver *et al.* 1997). Such is the case in Grand Canyon (Chapter 4 and 5), where the frequency and quantity of TSL loads are regulated by tributary supply, particle size, sediment transport capacity and channel morphology (Andrews 1991; Topping *et al.* 2000).

Although TSL upstream in Glen Canyon differed spatially and seasonally, under normal climatic and flow conditions ($140\text{-}700\text{ m}^3\text{ s}^{-1}$) the mean TSL was extremely low (Table 3) and equivalent to those of low order streams (Thurman 1985). In the 1960-70's, the annual median TSL for Glen Canyon was 7 mgL^{-1} (Howard and Dolan 1981). Our findings now would indicate that suspended loads have become further reduced in this upstream reach ($< 2\text{ mgL}^{-1}$). Whether or not the more elevated TSL loads were the primary light-attenuating constituent during early post-dam construction remains unknown. However, the change in TSL loads does demonstrate the chronic effect dam regulation has on sediment-supply through time, as local supply continues to be depleted due to cumulative suspended-sediment transport (Dolan *et al.* 1974; Gore and Petts 1989).

Thurman (1985) identifies that organic carbon in lakes resides primarily in the form of DOC, and that POM typically contributes 10% of the total organic carbon. In this system, POM represents 15-20% of the total carbon, and annual concentrations were roughly comparable to that of the St. Lawrence 0.4 mgL^{-1} , Yukon 1.2 mgL^{-1} , and Columbia 0.6 mgL^{-1} rivers (Thurman 1985). Although the majority of carbon entering

the Colorado River resides in a dissolved state, under normal flow conditions mean annual TSL from the Lake Powell reservoir was 70% organics. This high organic proportion contrasts with other river systems where typical POM percentages vary between 2 - 4% of TSL (Meybeck 1981, 1983).

We observed a strong interference interaction, where decreased DOC negatively corresponds to an increase in θ_i . Outwardly, this was problematic since as solar zenith angle increased, reductions in DOC were potentially ameliorating for seasonal light-attenuation. Light absorptive systems dominated by DOC are sensitive to the angular orientation of solar incidence and display higher light-attenuation as θ_i increases towards the nadir (Kirk 1980, 1983, and 1994). Since refraction increases the photic pathlength relative to the vertical depth measured, any angular departure from normal increases the probability of absorption. Therefore, a gain in photosynthesis may result seasonally from this temporal interference owing to a reduction in DOC (Fig 4), even though the net effect from θ_i leads to an overall increase in light-attenuation during winter (Fig 2).

Although solar zenith angle explains diel and seasonal patterns in K_O variation, its temporal predictability precluded any relationship to the systematic increase in inter-annual variation (Fig 3). The increase in mean annual K_N from 0.231 m^{-1} (1991) to 0.327 m^{-1} (1998) represented approximately a 30% reduction in optical depth (Kirk 1983). Whether or not decreased PPFD had an overall effect on underwater photosynthetic yield (Fisher and La Voy 1972) cannot be ascertained, since changes in light-attenuation in Glen Canyon corresponded to periods of flow stabilization (BOR 1996) confounding benthic comparisons between years (Blinn *et al.* 1995; Benenati *et al.* 1998). It is also plausible that qualitative rather than a quantitative difference in DOC have occurred

(Morris and Hargreaves 1997) since seasonal patterns for DOC collected in 1990-91 (Hart and Sherman 1996) are similar to our recent observations (1997-98).

Unfortunately, owing to the lack of a continuous time series we are unable to perform seasonal and inter-annual comparisons of DOC.

Regulating Mechanisms - Our experimental findings indicate that algal production under exposure to natural light (UV & PAR) increased DOC and light-attenuation. Conversely, treatments exposed to similar conditions, yet lacking algal production showed the inverse. Since no significant change in DOC concentration was detected between the initial condition and the non-algal treatment would suggest that increased light transparency for the non-algal treatment was perhaps due to a qualitative change in DOC and not due to a loss from microbial mineralization. The resultant mean increase in DOC for algal treatments represented an actual net gain of $0.48 \text{ mg L}^{-1} \text{ d}^{-1}$, similar to the mean spatial difference in DOC (0.37 mg L^{-1}) between Sites 2 and 3 (Table 2). This variation in light-attenuation demonstrates the potential biotic feedback for regulating the underwater light environment of autotrophs.

In most clear water systems, humic substances (i.e., fulvic and humic acids) are the major component of DOC, and are the primary light attenuating constituent (Kirk 1980; Thurman 1985; Hoge et al. 1993). In large rivers at mid-latitudes DOC ranges from 2-6 mg L^{-1} , and consists of 60 to 80% humics (Thurman 1985). Freshwater and marine systems dominated by humics have high light absorption and low scattering characteristics (Kirk 1980), and are instrumental in absorbing short wavelength, especially UV (Neale et al. 1998; Kirk 1994; Wetzel et al. 1995). As a result, plankton and benthic communities are afforded some level of UV-protection (Thurman 1985; Morris et al. 1995). In addition

to the photoreactive characteristics of these substances, their effects on light-attenuation have been reported to be proportionate to the overall DOC concentration (Hoge *et al.* 1993; Duarte *et al.* 1998; Arts *et al.* 2000).

In freshwater systems the largest DOC component is humic substances (Kirk 1994; Wetzel *et al.* 1995). Conventional thought identifies photochemical and microbial decomposition of terrestrial vegetation as the humic source (Thurman 1985; McDowell and Likens 1988; Moran and Hodson 1994). Alternately, it has been proposed that humic sources in oceanic and inland systems are derived primarily from phytoplankton and secondary linkages to bacterial decomposition rather than terrestrial inputs (Kaplan and Bott 1982; McKnight *et al.* 1991; Wetzel *et al.* 1995). In support of this, very little organic contribution originates from the xeric upland vegetation or along riparian margins because of reduced net primary production in semi-arid systems (Jones *et al.* 1996); except during episodic flooding (Blinn *et al.* 1999; Parnell and Bennett 1999) and high flows during runoff events (Jones *et al.* 1996).

We had hypothesized that the additional contribution of extracellular DOC from *in situ* algal/macrophytic production may contribute to light-attenuation observed further downstream (Kaplan and Bott 1982). Spatial and seasonal patterns in DOC and K_D for Glen Canyon suggests a strong linkage to local autotrophic production, yet algal derived substances absorb less light than equivalent concentrations of DOC from terrigenous sources (McKnight *et al.* 1991). As observed in other systems, our results indicate that exposure to natural sunlight inclusive of the entire spectral band may increase water transparency (De Hann 1993; Morris and Hargreaves 1997; Ibelings and Maberly 1998). Photodegradation rates for humics can be equivalent to photosynthesis (de Hann 1993) as

demonstrated by studies evaluating mean DOC loss for full sunlight over a 7-d period (Morris and Hargreaves 1997).

Humic chromophores appear to be the major factor regulating UVR transmission (Kirk 1994; Morris et al. 1995) though little information is available about the molecular type and fate of these algal derived compounds (Kaplan and Bott 1982; Biddanda and Benner 1997). Lacking terrestrial inputs both high boreal lakes with small or isolated catchments and Antarctic desert systems appear unusually transparent to UVR transmission (Morris et al. 1995; Schindler *et al.* 1997; Vincent et al. 1998). In other studies, photolytic reductions or molecular alteration of these chromophores result from exposure to UVR and PAR, (Manny et al. 1971; Stewart and Wetzel 1981; De Hann 1993) and oxidative and/or microbial loss (De Hann 1993; Morris et al. 1995; Wetzel et al. 1995; Neale et al. 1998).

Reservoir and riverine primary production are at highest levels by mid-summer (Stewart and Blinn 1979; Gloss *et al.* 1980; Angradi and Kubly 1994). Microbial activity in marine systems is strongly linked to phytoplankton blooms (Biddanda and Benner 1997; Carlson *et al.* 1998). Therefore, one would suspect that considerable organic material and microbial activity are linked to reservoir surface production, resulting in organic fallout into the hypolimnion (Johnson and Merritt 1979; Hueftle and Stevens 2000) having low oxygen and temperature levels. This potentially reduces the effectiveness of aerobic bacteria metabolizing available organics (Thurman 1985). During our study period, Benenati *et al.* (2000) identified a decrease in nutrient concentration for Glen Canyon, a pattern that was positively correlated to changes in specific conductance ($\mu\text{S cm}^{-1}$). It has been shown that substantial amounts of DOC can

be produced in response to nutrient limitations, attributed to differential leakage by phytoplankton and decoupling of autotrophic production from microbial consumption in phosphorous limited systems (Karl *et al.* 1998).

DOC originating from Lake Powell reservoir (Site 1) attained its highest mean concentration (3.18 mg L^{-1}) by September. The Green, Colorado, and San Juan Rivers have a combined drainage area of $181,800 \text{ km}^2$ (Stanford and Ward 1986), and each annually contribute sizeable quantities of organic material to the Lake Powell's inflow areas. Seasonal runoff (May-June) advectively flows 300 km (i.e., within the metalimnion due to an extensive chemocline) to Glen Canyon Dam, and typically arrives by late summer (Gloss *et al.* 1980; Hueftle and Stevens 2000). Advective arrival corresponds to elevated levels of DOC entering the river. Hydrodynamic and physical characteristics (i.e., storage capacity, hydraulic retention, advective flow and thermal stratification) of the reservoir may be responsible for regulating the availability and qualitative characteristics of organics leaving the reservoir (Johnson and Merritt 1979; Stanford and Ward 1991).

The source, quantity and quality of DOC in large reservoir systems especially in the semi-arid western U.S. are understudied and remain problematic. It is interesting to note that our seasonal observations contrasted with most other arid western rivers and streams, where the lowest concentrations occur in autumn, and are followed later by an increase in DOC during winter or spring runoff (Naiman 1974; Jones *et al.* 1996). This seasonal shift in DOC may reflect an inherent difference in regulating mechanisms for streams and rivers over lakes and reservoirs.

Lake Powell reservoir becomes heavily stratified due to morphology and a density chemocline (Johnson and Merritt 1979; Gloss *et al.* 1980), where typically upwelling and partial reservoir mixing occur as of winter, owing to the maximum reservoir depth (160 m) (Stewart and Blinn 1976; Hueftle and Stevens 2000). The river reflects hypolimnetic characteristics during periods of lower surface elevation (early 1990's) due to the dense chemocline. Yet, within a decade it had become more metalimnetic in character owing to higher reservoir levels, volumetric dilution and flushing (Hueftle and Stevens 2000).

Conceptually if physiochemical processes were regulating organic constituents such as DOC, we would hypothesize that a corresponding pattern in inter-annual light-attenuation would occur. We observed a significant correlation between conductivity and pH to seasonal and inter-annual K_O . It has been shown that changes in pH and ionic composition influence DOC characteristics by modifying adsorption rates, scavenging, particulate size fraction, and precipitation losses (Curtis 1993; De Hann 1993; Shaw 1994; Schindler *et al.* 1997). Studies in saline lakes and wetlands have shown that DOC and diffuse light-attenuation (K_d) coefficients covaried under elevated conductivity (Arts *et al.* 2000). Leenheer *et al.* (1974) showed that DOC was significantly correlated to conductivity and alkalinity, but these parameters accounted for a small part of the observed variation in humic substances. Additionally, particulate and colloidal organic matter typically flocculates at higher pH or salinity levels (Thurman 1985; Meade 1972; Shaw 1994; Schindler *et al.* 1997).

In summary, there was considerable spatio/temporal variability in light-attenuation observed for Glen Canyon. Experimental and observational studies indicated that DOC functioned as the primary light attenuating constituent and that an interaction

with solar zenith angle determined light-attenuation. It appears also quite likely that autochthonous production of riverine derived DOC increased light-attenuation. Although the exact regulatory mechanism(s) in the reservoir remains uncertain, water quality parameters appear to be useful as a set of predictor variables owing to the interrelationship that exists for any of the mechanisms proposed herein. This study identifies the potential for a feedback system to be operating; where DOC is regulated by reservoir supply and in-stream autochthonous production, and changes are offset by secondary losses from hydraulic conveyance, mineralization, microbial degradation, and photo-oxidation.

We propose, that light-attenuation was a consequence of light behavior interacting with DOC, regulated by reservoir and in-stream processes, and that certain correlates can be predictively used to quantitatively model underwater PPFD availability for benthic primary production in this river ecosystem. The statistical model used provides a conceptual framework to explore and test the mechanisms hypothesized to be causally responsible for observed light-attenuation, and a means to computationally examine and validate predicted outcomes from continued observations.

References

- AMON, R.M.W., AND R. BENNER. 1996. Photochemical and microbial consumption of dissolved organic carbon and dissolved oxygen in the Amazon River system. *Geochim. Cosmochim. Acta.* 60:1783-1792.
- ANDREWS, 1991. Sediment transport on the Colorado River basin. *In.* Marzolf, G.R. (Ed.), *Colorado River ecology and dam management: proceedings of a symposium.* National Academy Press, Washington D.C.
- ANGRADI, T.R. AND D.M. KUBLY. 1994. Concentration and transport of particulate organic matter below Glen Canyon Dam on the Colorado River, Arizona. *J. Arizona/Nevada Acad. Sci.* 28:12-22.
- BENENATI, P., J.P. SHANNON, AND D.W. BLINN. 1998. Desiccation and recolonization of phytobenthos in a regulated desert river: Colorado River at Lees Ferry, Arizona, USA. *Regul. Rivers: Res. Mgmt.* 14:519-532.
- BENENATI, P.E., J.P. SHANNON, D.W. BLINN, K.P. WILSON AND S.J. HUEFTLE. 2000. Reservoir-river linkages: Lake Powell and the Colorado River, Arizona. *N. Amer. Benth. Soc.* 19:742-755.
- BERWALD, J., D. STRAMSKI, C.D. MOBLEY, D.A. KIEFER. 1998. Effect of Raman scattering on the average cosine and diffuse attenuation coefficient of irradiance in the ocean. *Limnol. Oceanogr.* 43:564-576.
- BIDDANDA, B., AND R. BENNER. 1997. Carbon, nitrogen, and carbohydrate fluxes during production of particulate and dissolved organic matter by marine phytoplankton. *Limnol. Oceanogr.* 42:506-518.
- BLINN, D.W., T. TOMPKINS, AND A.J. STEWART. 1977. Seasonal light characteristics for newly formed reservoir in Southwestern USA. *Hydrobiologia.* 51:77-84.
- BLINN, D.W., AND G.A. COLE. 1991. Algal and invertebrate biota in the Colorado River: Comparison of Pre- and Post-Dam Conditions. *In.* Marzolf, G.R. (Ed.), *Colorado River ecology and dam management: proceedings of a symposium.* National Academy Press, Washington D.C.
- BLINN, D.W., J.P. SHANNON, L.E. STEVENS, AND J.P. CARDER. 1995. Consequences of fluctuating discharge for lotic communities. *N. Amer. Benth. Soc.* 14:233-248.
- BLINN, D.W., J.P. SHANNON, P.L. BENENATI AND K.P. WILSON. 1998. Algal ecology in tailwater stream communities: Colorado River below Glen Canyon Dam, Arizona. *J. Phycol.* 34:734-740.

- BLINN, D.W., J.P. SHANNON, K.P. WILSON, C. O'BRIEN, AND P.L. BENENATI. 1999. Response of benthos and organic drift to a controlled flood. *In*. Webb, R.H., J.C. Schmidt, G.R. Marzolf, and R.A. Valdez. (Eds.), *The controlled flood in Grand Canyon*. Amer. Geophys. Union., Washington, D.C.
- BOAVIDA, M.J., AND R.G. WETZEL. 1998. Inhibition of phosphatase activity by dissolved humic substances and hydrolytic reactivation by natural ultraviolet light. *Freshwat. Biol.* 40:285-293.
- BROCK, T.D. 1981. Calculating solar radiation for ecological studies. *Ecol. Model.* 14:1-19.
- BUREAU OF RECLAMATION. 1996. Operation of Glen Canyon Dam Colorado River storage project, Arizona: final environmental impact statement. U.S.DOI. BOR.
- CARLSON, C.A, H.W. DUCKLOW, D.A. HANSELL AND W.O. SMITH, Jr. 1998. Organic carbon partitioning during spring phytoplankton blooms in the Ross Sea polynya and the Sargasso Sea. *Limnol. Oceanogr.* 43:375-386.
- CHATTERJEE, S., AND B. PRICE. 1977. *Regression analysis by example*. John Wiley and Sons., New York, NY.
- CONVERSI, A. AND J.A. MCGOWAN. 1994. Natural versus human-caused variability of water clarity in the Southern California Bight. *Limnol. Oceanogr.* 39:632-648.
- CURTIS, P.J. 1993. Effect of dissolved organic carbon on ⁵⁹Fe scavenging. *Limnol. Oceanogr.* 38:1554-1561.
- DAVIES-COLLEY, R.J., C.W. HICKEY, J.M. QUINN AND P.A. RYAN. 1992. Effects of clay discharges on streams. 1. Optical properties and epilithon. *Hydrobiologia.* 248:215-234.
- DE HANN, H. 1993. Solar UV-light penetration and photodegradation of humic substances in peaty lake water. *Limnol. Oceanogr.* 38:1072-1077.
- DENNY, M.W. 1993. *Air and water, the biology and physics of life's media*. Princeton University Press., Princeton, NJ.
- DOLAN, R., A. HOWARD, AND A. GALLENSON. 1974. Man's Impact on the Colorado River in the Grand Canyon. *Amer. Sci.* 62:392-401.
- DUARTE, C.M., S. AGUSTI, M.P. SATTI, AND D. VAQUE. 1998. Partitioning particulate light absorption: A budget for a Mediterranean bay. *Limnol. Oceanogr.* 43:236-244.

- DUFFIE, J.A. AND W.A. BECKMAN. 1974. *Solar energy thermal processes*. John Wiley, and Sons. Chicago, IL.
- FISHER, S.G. AND A. LA VOY. 1972. Differences in littoral fauna due to fluctuating water levels below a hydroelectric dam. *J. Fish. Res. Brd Can.* 29:1472-1476.
- GANF, G.G. 1973. Incident irradiance and light penetration as factors controlling the chlorophyll (a) content of a shallow equatorial lake (Lake George, Uganda). *J. Ecol.* 62:593-609.
- GLOSS, S.P., L.M. MAYER, AND D.E. KIDD. 1980. Advective control of nutrient dynamics in the epilimnion of a large reservoir. *Limnol. Oceanogr.* 25:219-228.
- GORE, J.A. AND G.E. PETTS. 1989. (Eds.) *Alternatives in regulated river management*. CRC Press, Inc., Boca Raton, FL.
- GRAF, J.B., R.H. WEBB, AND R. HERFORD. 1991. Relation of sediment load and flood-plain formation to climatic variability, Paria River drainage basin, Utah and Arizona. *Geol Soc. Am. Bull.* 103:1405-1415.
- GREENBERG, A.E., L.S. CLESCERI, AND A.D. EATON. 1992. (Eds.) *Standard methods for the examination of water and wastewater*. 18th Edition. American Public Health Assoc.
- HADEN, G.A., D.W. BLINN, J.P. SHANNON AND K.P. WILSON. 1999. Driftwood: an alternate habitat for macroinvertebrates in a large desert river. *Hydrobiologia.* 397:179-186.
- HARDWICK, G.G., D.W. BLINN, AND H.D. USHER. 1992. Epiphytic diatoms on *Cladophora glomerata* in the Colorado River, Arizona: longitudinal and vertical distribution in a regulated river. *Southwest. Nat.* 37:148-156.
- HART, R.J. AND K.M. SHERMAN. 1996. Physical and chemical characteristics of Lake Powell at the forebay and outflows of Glen Canyon Dam, Northeastern Arizona, 1990-1991. U.S. Geological Survey. Water Resources Invest. Report 96-4016.
- HOGUE, F.E., A. VODACEK, AND N.V. BLOUGH. 1993. Inherent optical properties of the ocean: Retrieval of the absorption coefficient of chromophoric dissolved organic matter from fluorescence measurements. *Limnol. Oceanogr.* 38:1394-1402.
- HOWARD, A. AND R. DOLAN. 1981. Geomorphology of the Colorado River in the Grand Canyon. *J. Geology.* 89:269-298.
- HUEFTLE, S.J., AND L.E. STEVENS. 2001. Experimental flood effects on the limnology of Lake Powell reservoir, Southwestern USA. *Ecol. Appl.* 11:644-656.

- IBELINGS, B.W., AND S.C. MABERLY. 1998. Photoinhibition and the availability of inorganic carbon restrict photosynthesis by surface blooms of cyanobacteria. *Limnol. Oceanogr.* 43: 408-419.
- JEWSON, D.H. AND J.A. TAYLOR. 1978. The influences of turbidity on net phytoplankton photosynthesis in some Irish lakes. *Freshwater Biology.* 8:573-584.
- JONES, J.B. JR., S.G. FISHER AND N.B. GRIMM. 1996. A long-term perspective of dissolved organic carbon transport in Sycamore Creek, Arizona, USA. *Hydrobiologia.* 317:183-188.
- JOHNSON, N.M., AND D.H. MERRITT. 1979. Convective and advective circulation of Lake Powell, Utah-Arizona, during 1972-1975. *Water Resour. Res.* 15:873-884.
- KAPLAN, L.A., AND T.L. BOTT. 1982. Diel fluctuations of DOC generated by algae in a piedmont stream. *Limnol. Oceanogr.* 27:1091-1100.
- KARL, D.M., D.V. HEBEL, K. BJORKMAN, AND R.M. LETELIER. 1998. The role of dissolved organic matter release in the productivity of the oligotrophic North Pacific Ocean. *Limnol. Oceanogr.* 43:1270-1286.
- KIMBER, A., J.L. OWENS AND W.G. CRUMPTON. 1995. Light availability and growth of wild celery (*Vallisneria americana*) in upper Mississippi River backwaters. *Regul. Rivers: Res. Mgmt.* 11:167-174.
- KIRK, J.T.O. 1977. Use of a quanta meter to measure attenuation and reflectance of photosynthetically active radiation in some inland and coastal South-eastern Australian waters. *Aust. J. Mar. Freshwat. Res.* 28:9-21.
- KIRK, J.T.O. 1979. Spectral distribution of photosynthetically active radiation in some southeastern Australian waters. *Aust. J. Mar. Freshwater Res.* 30:81-91.
- KIRK, J.T.O. 1980. Spectral absorption properties of natural waters: Contributions of the soluble and particulate fractions to light absorption in some inland fractions of south-eastern Australia. *Aust. J. Mar. Freshwat. Res.*, 31:287-296.
- KIRK, J.T.O. 1983. *Light and photosynthesis in aquatic ecosystems.* Cambridge University Press, Cambridge, London.
- KIRK, J.T.O. 1994. Characteristics of the light field in highly turbid waters: A Monte Carlo study. *Limnol. Oceanogr.* 39:702-706.
- KRAUSE-JENSEN, D. AND K. SAND-JENSEN. 1998. Light attenuation and photosynthesis of aquatic plant communities. *Limnol. Oceanogr.* 43:396-407.

- LEENHEER, J.A., R.L. MALCOLM, P.W. MCKINLEY AND L.A. ECCLES. 1974. Occurrence of dissolved organic carbon in selected groundwater samples in the United States. *USGS. J. Res.* 2:361-369.
- MANNY, B.A., M.C. MILLER AND R.G. WETZEL. 1971. Ultraviolet combustion of dissolved organic nitrogen compounds in lake waters. *Limnol. Oceanogr.* 16:71-85.
- MCDOWELL, W.H. AND G.E. LIKENS. 1988. Origin, composition, and flux of dissolved organic carbon in the Hubbard Brook Valley. *Ecol. Monogr.* 58:177-195.
- MCKNIGHT, D.M., G.R. AIKEN AND R.L. SMITH. 1991. Aquatic fulvic acids in microbially based ecosystems: Results from two desert lakes in Antarctica. *Limnol. Oceanogr.* 36:998-1006.
- MEADE, R.H. 1972. Transport and deposition of sediments in estuaries. *Geol. Soc. Am. Mem.*, 133:91-120.
- MEYBECK, M. 1981. River transport of organic carbon to the ocean. *In*. Likens, G.E. (Ed.) *Flux of organic carbon by rivers to the oceans*. U.S. Dept. Energy., NTIS CONIF-8009140, Springfield, VG.
- MEYBECK, M. 1983. Carbon, nitrogen, and phosphorous transport by rivers. *Okios.* 36:214-220.
- MOORHEAD, D.L., C.F. WOLF AND R.A. WHARTON, JR. 1997. Impact of light regimes on productivity patterns of benthic microbial mats in an Antarctic lake: A modeling study. *Limnol. Oceanogr.* 42:1561-1569.
- MORAN, M.A. AND R.E. HODSON. 1994. Dissolved humic substances of vascular plant origin in a coastal marine environment. *Limnol. Oceanogr.* 39:762-771.
- MORRIS, D.P. AND B.R. HARGREAVES. 1997. The role of photochemical degradation of dissolved organic carbon in regulating the UV transparency of three lakes on the Ponono Plateau. *Limnol. Oceanogr.* 42:239-249.
- MORRIS, D.P., H. ZAGARESE, C.E. WILLIAMSON, E.G. BALSEIRO, B.R. HARGREAVES, B. MODENUTTI, R. MOELLER, AND C. QUEIMALINOS. 1995. The attenuation of solar UV radiation in lakes and the role of dissolved organic carbon. *Limnol. Oceanogr.* 40:1381-1391.
- NAIMAN, J.R. 1974. Bioenergetics of a pupfish population (*Cyprinodon*) and its algal food supply in a thermal stream. Ph.D. Dissertation. Arizona State University, Tempe, AZ.

- NEALE, P.J., J.J. CULLEN AND R.F. DAVIS. 1998. Inhibition of marine photosynthesis by ultraviolet radiation: Variable sensitivity of phytoplankton in the Weddell-Scotia Confluence during austral spring. *Limnol. Oceanogr.* 43:433-448.
- NETTER, J., M.H. KUTNER, C.J. NACHTSHEIM AND W. WASSERMAN. 1996. *Applied linear statistical models*. (4th Ed.) Times Mirror Higher Education Group, Inc., Chicago, US.
- NIELSEN, M.V., AND E. SAKSHAUG. 1993. Photobiological studies of *Skeletonema costatum* adapted to spectrally different light regimes. *Limnol. Oceanogr.* 38:1576-1581.
- PARNELL, R.A., AND J.B. BENNETT. 1999. Mineralization of riparian vegetation buried by the 1996 controlled flood. In: Webb, R.H., J.C. Schmidt, G.R. Marzolf, and R.A. Valdez. (Eds.), *The controlled flood in Grand Canyon*. Amer. Geophys. Union. Washington, D.C.
- PEMBERTON, E.L. 1987. Sediment data collection and analysis for five stations on the Colorado River from Lees Ferry to Diamond Creek. Glen Canyon Environmental Studies Technical Report, NTIS No. PB88-183397.
- ROEMER, S.C. AND K.D. HOAGLAND. 1979. Seasonal attenuation of quantum irradiance (400-700 nm) in three Nebraska reservoirs. *Hydrobiologia.* 63:81-92.
- ROOS, J.C. AND A.J.H. PIETERSE. 1994. Light, temperature and flow regimes of the Vaal River at Balkfontein, South Africa. *Hydrobiologia.* 277:1-15.
- RUBIN, D.M., J.M. NELSON, AND D.J. TOPPING. 1998. Relation of inversely graded deposits to suspended-sediment grain-size evolution during the 1996 flood experiment in Grand Canyon. *Geology.* 26:99-102.
- SAS, Inc., 1996. Version 6.12, SAS Institute, Inc. Cary, N.C. USA.
- SCHINDLER, D.W., P.J. CURTIS, S.E., BAYLEY, B.R. PARKER, K.G. BEATY AND M.P. STANTON. 1997. Climate-induced changes in the dissolved organic carbon budgets of boreal lakes. *Biogeochem.* 36:9-28.
- SHAVER, M.L., J.P. SHANNON, K.P. WILSON, P.L. BENENATI AND D.W. BLINN. 1997. Effects of suspended sediment and desiccation on the benthic tailwater community in the Colorado River, USA. *Hydrobiologia.* 357:63-72.
- SHAW, P.J. 1994. The effect of pH, dissolved humic substances, and ionic composition on the transfer of iron and phosphate to particulate size fractions in epilimnetic lake water. *Limnol. Oceanogr.* 39:1734-1743.

- SMITH, R.C., B.B. PREZELIN, R.R. BIDIGARE AND K.S. BAKER. 1989. Bio-optical modeling of photosynthetic production in coastal waters. *Limnol. Oceanogr.* 34:1524-1544.
- STANFORD, J.A. AND J.V. WARD. 1986. The Colorado River system. *In*. Davies, B.R. and K.F. Walker (Eds.), *The ecology of river systems*. Dr. W. Junk Publishers, Dordrecht, Netherlands.
- STANFORD, J.A. AND J.V. WARD. 1991. Limnology of Lake Powell and the chemistry of the Colorado River. *In*. Marzolf, G.R. (Ed.), *Colorado River ecology and dam management: proceedings of a symposium*. National Academy Press, Washington D.C.
- STATSOFT, INC. 1997. Statistica for Windows., Version 5.1, Tulsa, O.K., USA.
- STEINMAN, A.D., P.J. MULHOLLAND, A.V. PALUMBO, T.F. FLUM, J.W. ELWOOD AND D.L. DEANGELIS. 1990. Resistance of lotic ecosystems to a light elimination disturbance: a laboratory stream study. *Oikos*. 58:80-90.
- STEVENS, L.E., J.P. SHANNON AND D.W. BLINN. 1997. Colorado River benthic ecology in Grand Canyon, Arizona, USA: Dam, tributary, and geomorphological influences. *Regul. Rivers: Res. Mgmt.* 13:129-149.
- STEWART, A.J., AND D.W. BLINN. 1976. Studies on Lake Powell, USA: Environmental factors influencing phytoplankton success in a high desert warm monomictic lake. *Arch. Hydrobiol.* 78:139-164.
- STEWART, A.J. AND R.G. WETZEL. 1981. Dissolved humic materials: Photodegradation, sediment effects, and reactivity with phosphate and calcium carbonate precipitation. *Arch. Hydrobiol.* 92:265-286.
- THIMIYAN, R.W., AND R.D. HEINS. 1983. Photometric, radiometric, and quantum light units of measure: A review of procedures for interconversion. *HortScience*. 18:818-822.
- THURMAN, E.M. 1985. *Organic geochemistry of natural waters*. Martinus Nijhoff/Dr. W Junk, Boston Massachusetts, USA.
- TOPPING, D.J., D.M. RUBIN, AND L.E. VIERRA, Jr. 2000. Colorado River sediment transport 1. Natural sediment supply limitation and the influence of Glen Canyon Dam. *Water Resources Research*. 36:515-542.
- VERNIEU, W.S. 2000. Water quality below Glen Canyon Dam – water year 2000. U.S. Geological Survey. GCMRC Technical Report.

VINCENT, W.F., R. RAE, I. LAURION, C. HOWARD-WILLIAMS, AND J.C. PRISCU. 1998. Transparency of Antarctic ice-covered lakes to solar UV radiation. *Limnol. Oceanogr.* 43:618-624.

WARD, J.V. AND J.A. STANFORD. 1983. The serial discontinuity concept of lotic ecosystems. *In*. Fontaine, T.D. and S.M. Bartell. (Eds.) *Ecology of river systems*. Dr. W. Junk Publishers., Dortrecht., The Neatherlands.

WETZEL, R.G., P.G. HATCHER AND T.S. BIANCHI. 1995. Natural photolysis by ultraviolet irradiance of recalcitrant dissolved organic matter to simple substrates for rapid bacterial metabolism. *Limnol. Oceanogr.* 40:1369-1380.

Table 1. Results of ANOVA type II random effects model, for suspended inorganic (SS) and organic (POM) particles in response to sampling date, sampling time, sampling site and nested effects. Analysis tested the spatio/temporal variability of suspended particles considered responsible for light attenuation.

<i>Source</i>	<i>df</i>	<i>SS</i>	<i>MS</i>		<i>F - ratio</i>	<i>F</i>	<i>P</i>
Model (SS)	353	447.7	0.83	{M1}	M1 / M7	4.53	<0.001
Sampling Date	5	125.1	25.11	{M2}	M2 / M5 + M6	33.70	<0.001
Sampling Time	24	12.5	0.52	{M3}	M3 / M5 + M6	0.71	0.826
Sampling Site	2	54.0	27.02	{M4}	M4 / M6 + M7	5.46	<0.001
Date x Time	94	71.2	0.74	{M5}	M5 / M6 + M7	0.91	0.708
Site (Date Time)	226	184.5	0.82	{M6}	M6 / M7	2.92	<0.001
Error	827	231.3	0.25	{M7}			
Total	1180	334.2					
Model (POM)	353	61.9	0.18	{M1}	M1 / M7	4.53	<0.001
Sampling Date	5	4.4	0.87	{M2}	M2 / M5 + M6	6.59	<0.001
Sampling Time	24	3.0	0.13	{M3}	M3 / M5 + M6	0.97	0.518
Sampling Site	2	4.2	2.10	{M4}	M4 / M6 + M7	12.76	<0.001
Date x Time	94	12.6	0.13	{M5}	M5 / M6 + M7	0.78	0.922
Site (Date Time)	226	38.1	0.17	{M6}	M6 / M7	2.45	<0.001
Error	827	56.2	0.07	{M7}			
Total	1180	118.1					

Table 2. Summarized data includes depth-integrated samples collected during 1997-1998 for suspended concentrations (mg L^{-1}), including: total suspended sediment (TSS), inorganic sediment (IS) and organics (POM).

Location	Mean	Median	Min	Max	N	SD	SE
Site 1 - draft tube Glen Canyon Dam							
TSS	0.88	0.80	0.00	4.47	452	0.53	0.03
SS	0.22	0.00	0.00	4.37	452	0.40	0.02
POM	0.66	0.62	0.00	3.25	452	0.32	0.02
DOC	2.97	2.84	2.08	8.55	279	0.59	0.35
Site 2 - Base Glen Canyon Dam							
TSS	1.19	1.01	0.00	12.41	385	0.84	0.04
SS	0.45	0.20	0.00	10.56	385	0.73	0.04
POM	0.74	0.70	0.00	2.45	385	0.32	0.02
DOC	2.91	2.77	2.22	4.99	220	0.47	0.031
K _O	0.372	0.385	0.242	0.473	167	0.046	0.004
K _N	0.314	0.308	0.205	0.384	167	0.029	0.002
Site 3 - Lees Ferry							
TSS	1.41	1.43	0.20	7.94	344	0.81	0.04
SS	0.62	0.61	0.00	7.13	344	0.71	0.04
POM	0.80	0.81	0.00	2.32	344	0.31	0.02
DOC	3.28	3.07	2.41	6.96	287	0.70	0.04
K _O	0.389	0.406	0.293	0.571	226	0.058	0.004
K _N	0.331	0.325	0.223	0.454	226	0.039	0.003

Table 3. Mallows C_p was used as criterion for selecting an appropriate statistical model for estimating normalized light attenuation, K_N . Solar characteristics, water quality parameters and distance accounted for spatio/temporal differences in light attenuation. The predictive parameters, regression coefficients and statistical results are indicated.

Model Variables	Unit	Min	Max	Mean	β	t (432)	p
Intercept					-1.68754	-3.69	<.001
Reservoir Characteristics							
<i>Conductivity</i>	μS	616	978	698	-0.00018	-6.8	<.001
<i>PH</i>		7.4	8.4	7.9	0.09114	9.0	<.001
<i>Stage Elevation</i>	m	1107	1127	1122	0.00038	3.17	.002
Irradiant Intensities							
<i>% Flux</i>	%	0.002	0.74	0.15	0.03139	2.9	.004
Spatial Characteristics							
<i>Rkm</i>	Km	0.095	25.2		0.00031	2.3	.022

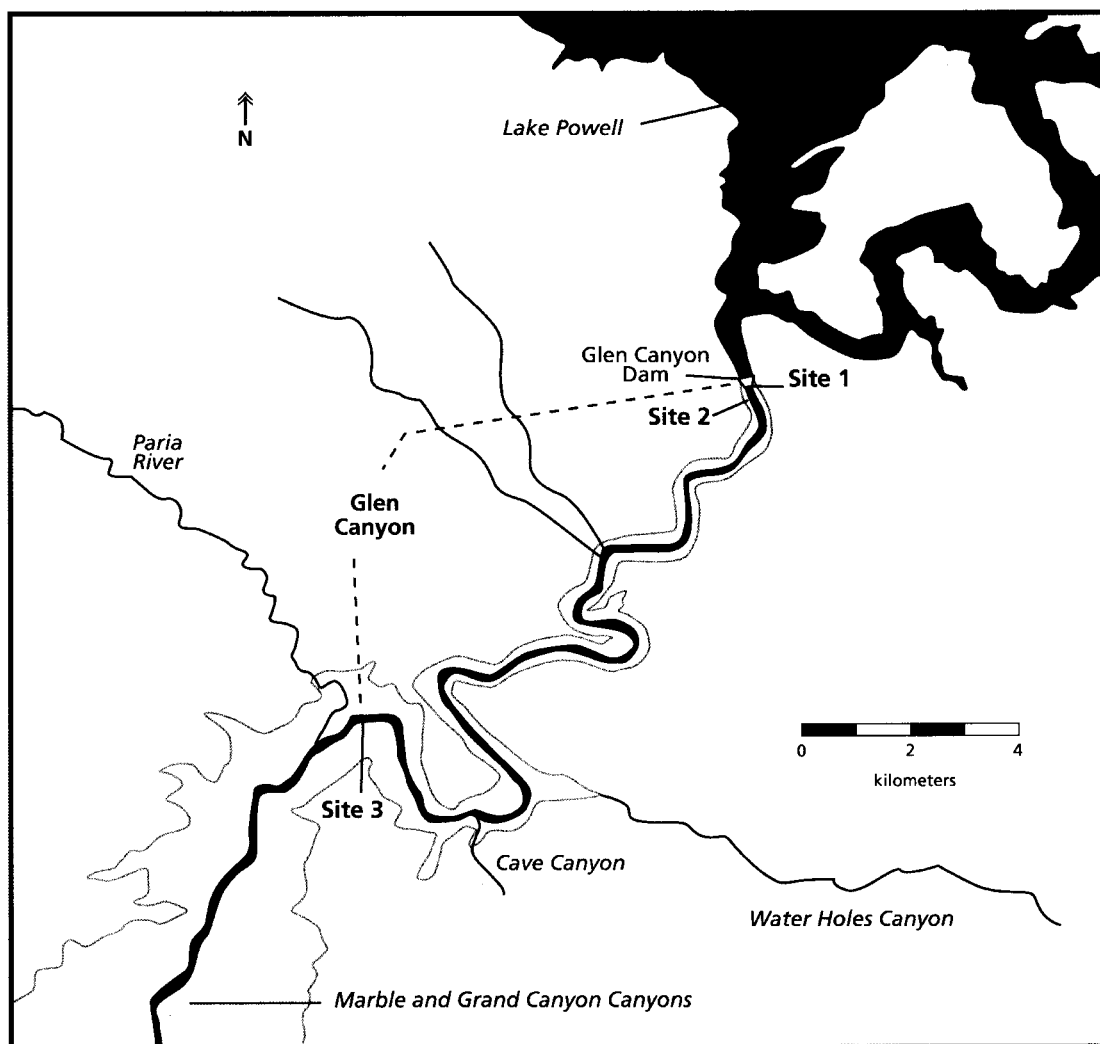


Figure 1. Location of the three data collection stations: Site 1, Glen Canyon Dam hydroelectric facility ($36^{\circ}56'06''\text{N}$, $111^{\circ}28'53''\text{W}$); Site 2, Glen Canyon Dam river outflow 0.0-km; and Site 3, located at Lees Ferry 25.2-km downstream on the Colorado River in Glen Canyon.

Figure 2. Light-attenuation measurements were made at two sites, Site 2 (0.0 km) and Site 3 (25.2 km). Fig 2-A) Scalar light-attenuation coefficients (K_d , m^{-1}) derived from Site 3 (25.2 km) based on measurements made on 20 September 1998. And fig 2-B), average seasonal scalar light-attenuation coefficients (\pm SE) observed in Glen Canyon during 1997-1998.

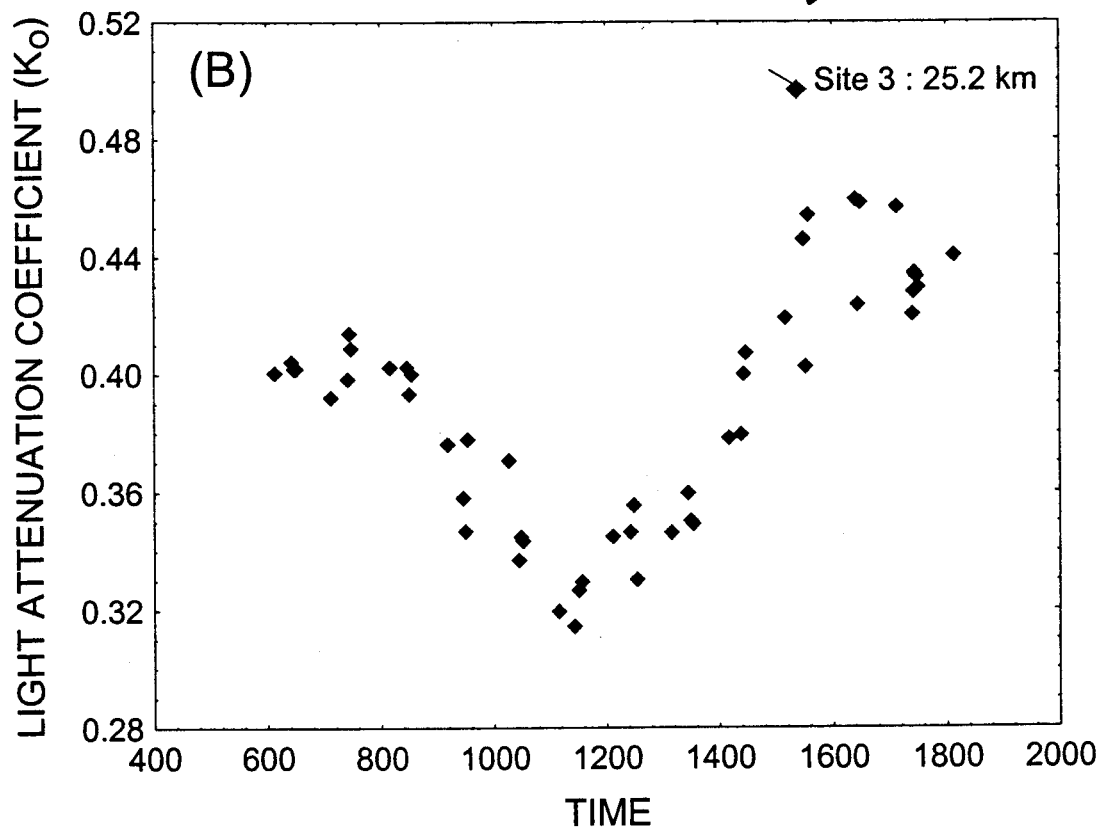
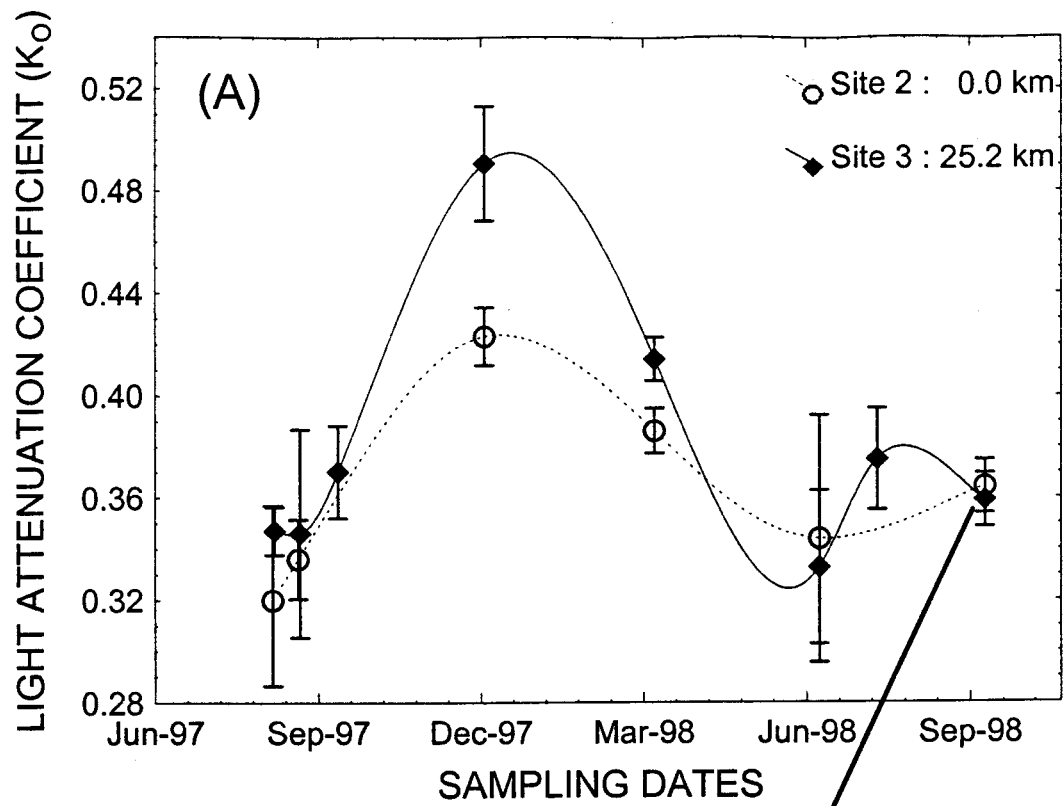


Figure 3. Mean annual light-attenuation coefficients measured between 1991-1998 for scalar light-attenuation (K_O) and normalized light-attenuation (K_N) coefficients averaged across all sites located within Glen Canyon. Data has been excluded for measurements during high suspended-sediment levels (7 September 1997).

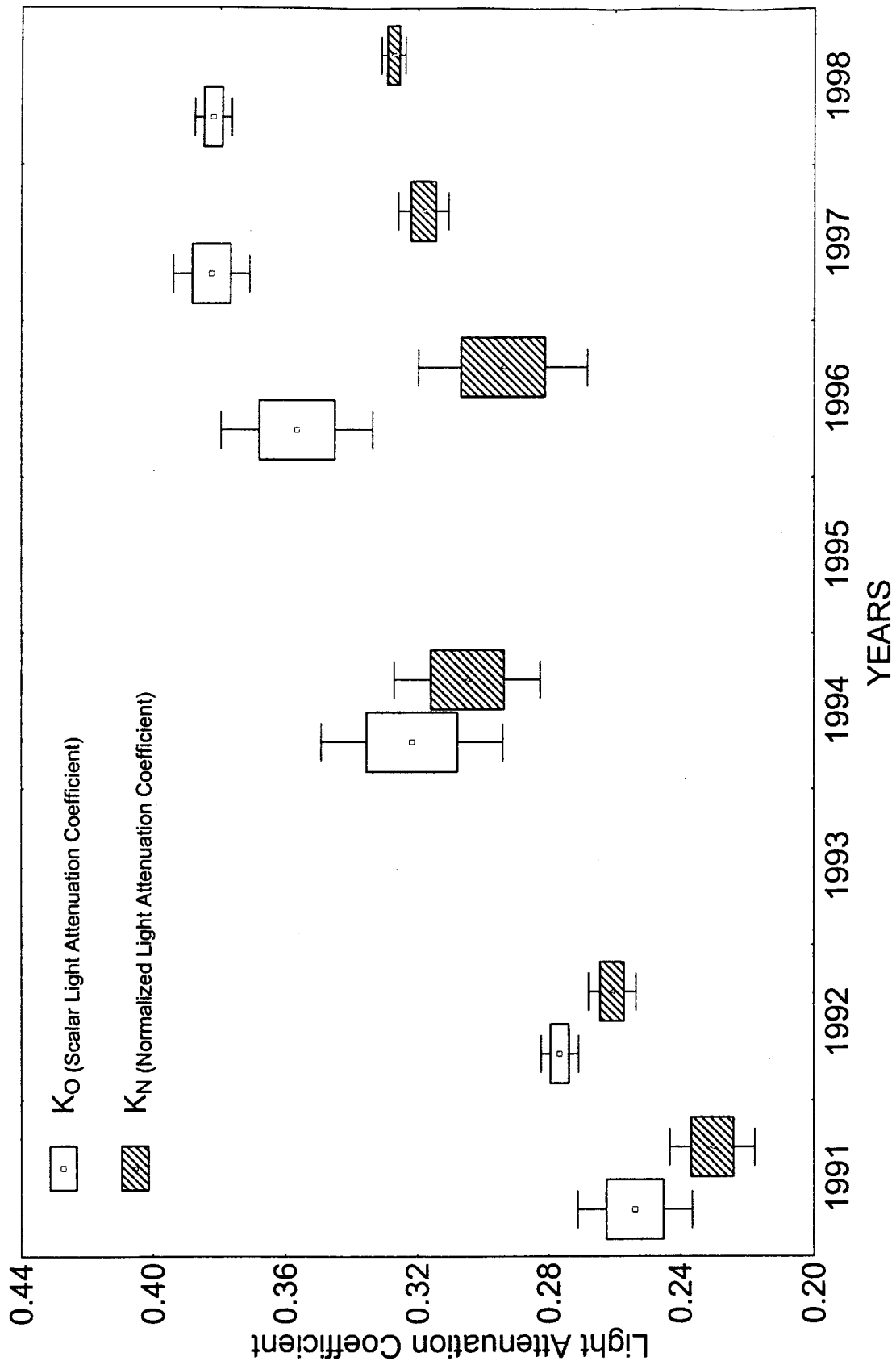


Figure 4. For 1997-1998, spatial distribution of mean seasonal concentration ($\text{mgL}^{-1} \pm \text{SE}$) of dissolved organic carbon (DOC) found at Site 1, Glen Canyon Dam (GCD) hydroelectric facility; Site 2, GCD river outflow 0.0-km; and Site 3, located 25.2-km downstream at Lees Ferry. Outlier observed for Site 1 (September 1998) is considered due to at turbines at GCD.

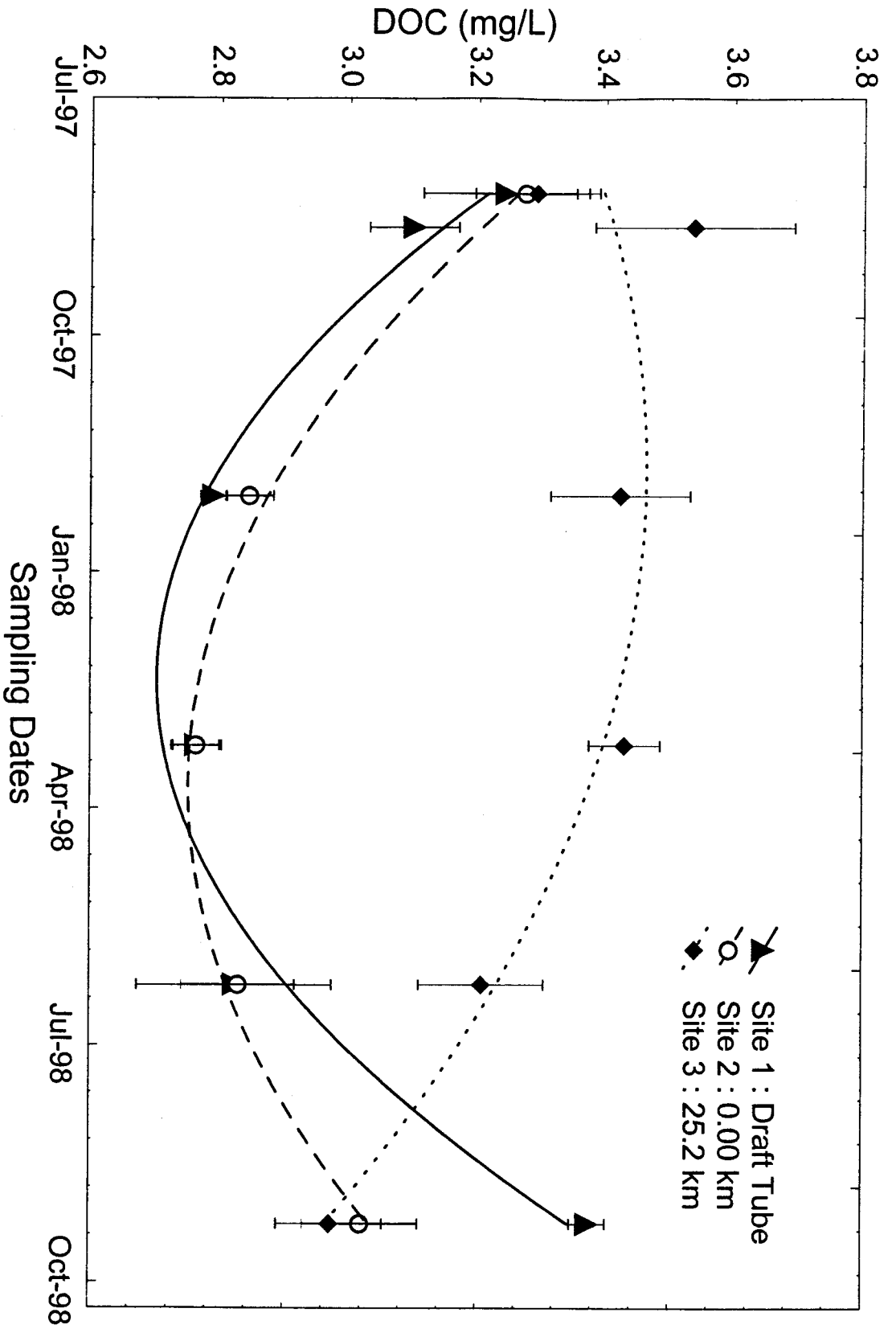


Figure 5. During sediment-supply events a linear relationship exists between A) total suspended-sediment (TSS, mgL^{-1}), and B) normalized light-attenuation coefficients (K_N , m^{-1}). Data collection on 7 September 1997 at Site 3 (25.2 km) during unusually high-suspended loads from ungaged tributaries.

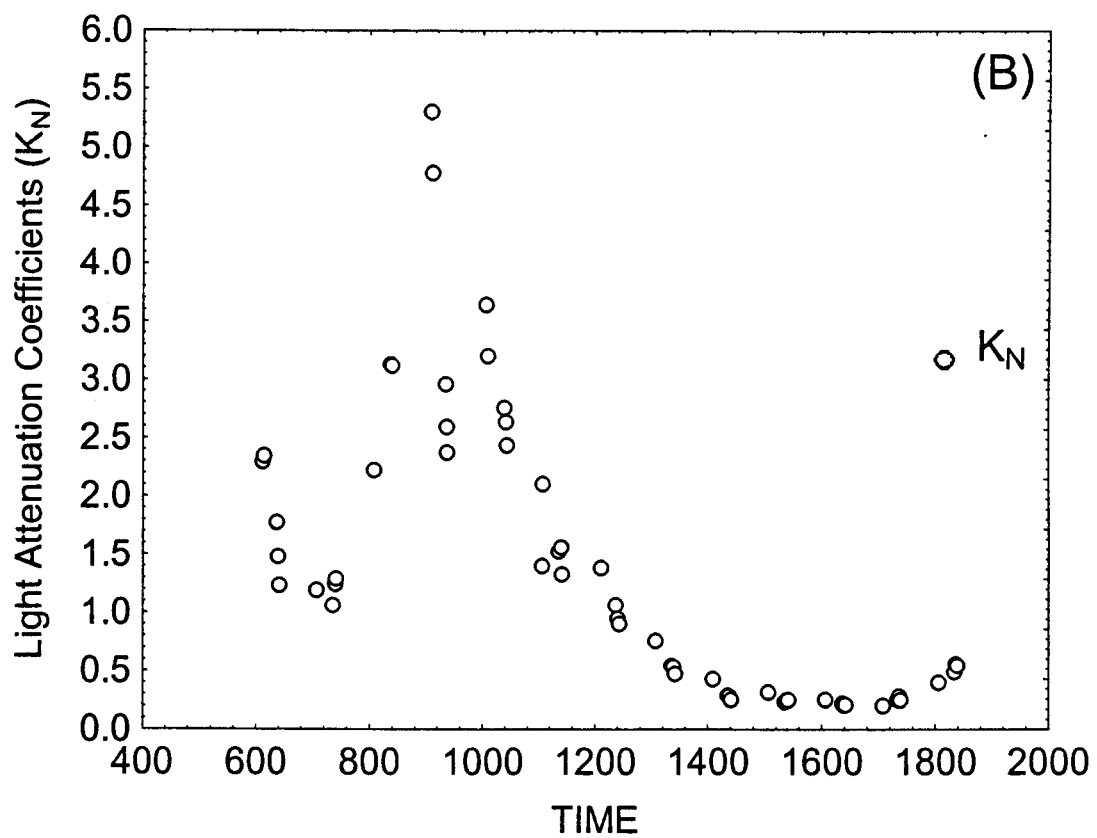
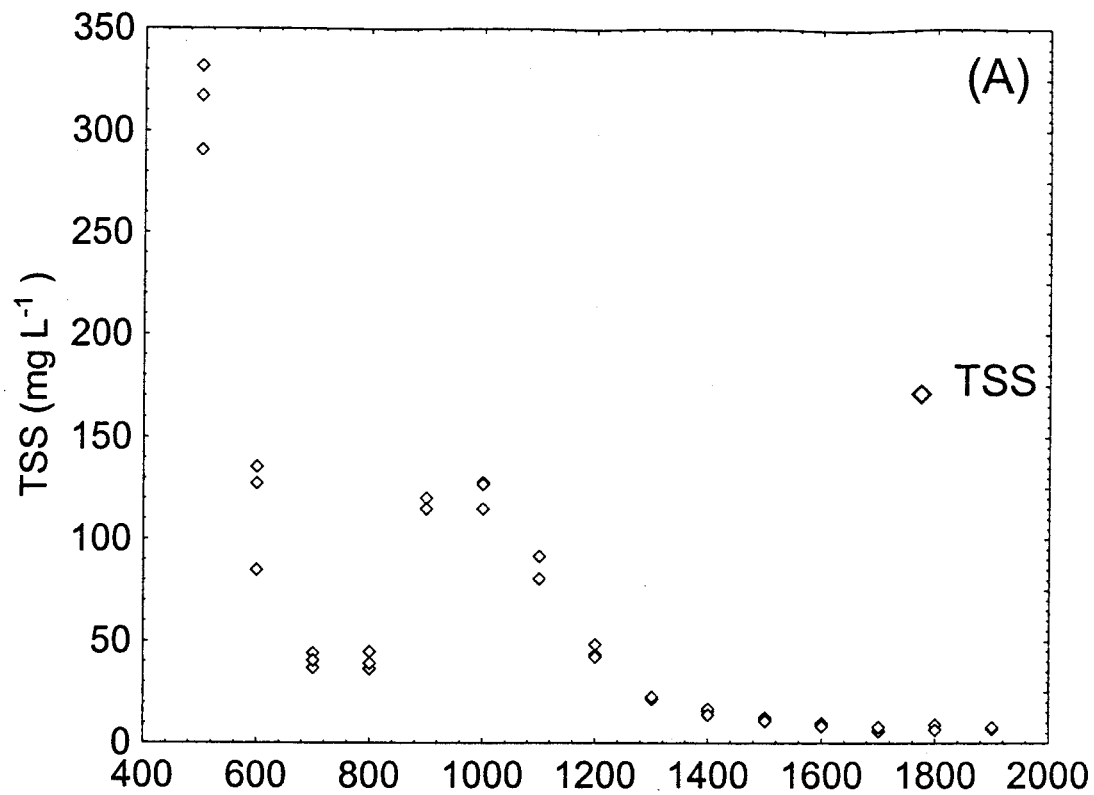
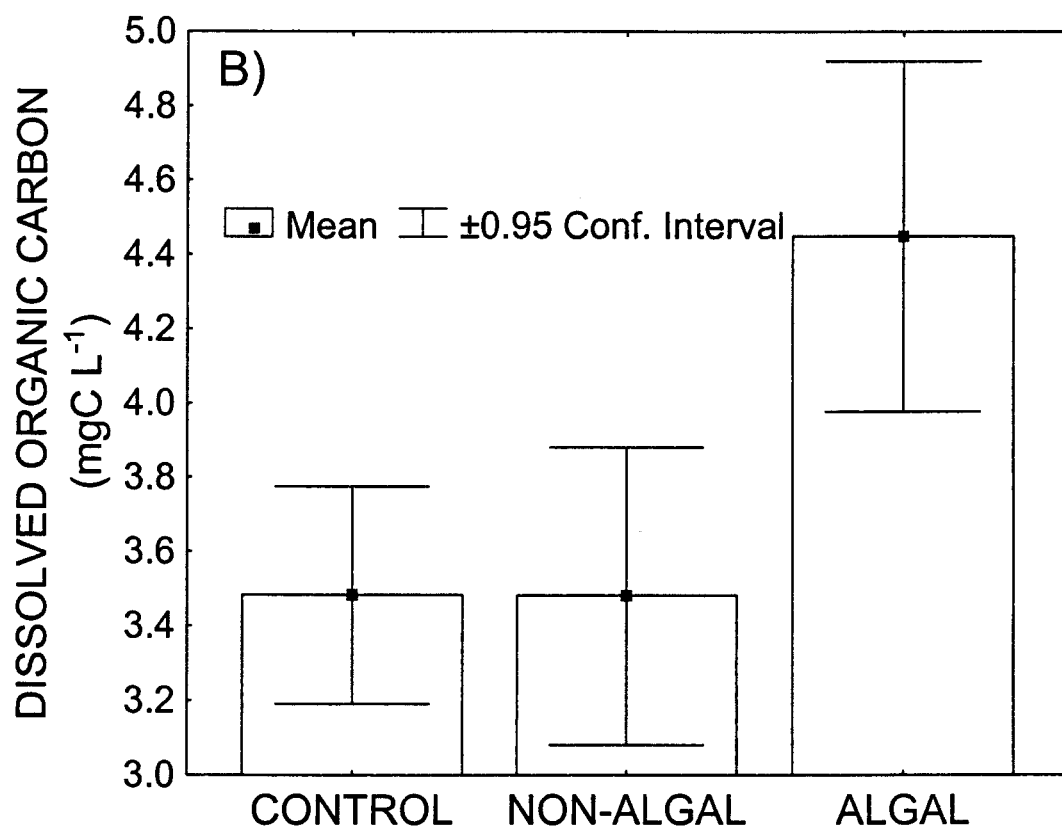
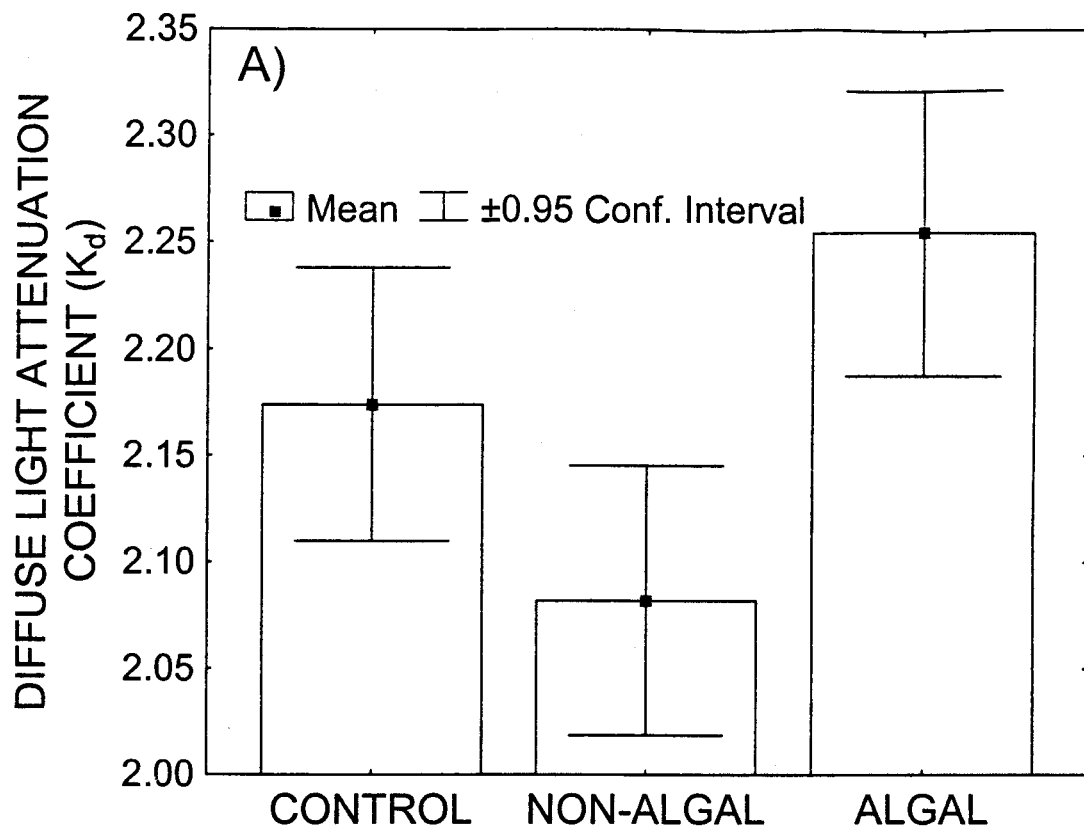


Figure 6 Results using a one-way ANOVA for Fig 6-A) diffuse light-attenuation coefficients (K_d, m^{-1}), and Fig 6-B) dissolved organic carbon (DOC, $mg\ l^{-1}$). Mean values and confidence limits (95% CI) are plotted, showing initial characteristic of the river, and the experimental response to the treatments of non-algal and algal following a 48 hr exposure to natural sun light conditions.



CHAPTER 4

APPARENT OPTICAL PROPERTIES IN A FLUVIAL RIVER SYSTEM:
COLORADO RIVER, GRAND CANYON, AZ.

ABSTRACT

In fluvial systems, the availability of underwater light is a predictable consequence of spatio/temporal limitations of sediment-supply and interactions with other hydraulic processes that regulate sediment transport. A strong linear relationship exists between suspended-sediment concentration (SS) and light-attenuation coefficients (K_N normalized for refraction) for the regulated Colorado River in Glen and Grand Canyons, AZ. Inorganic suspended-sediment was the primary causal factor in light-attenuation during clear, sediment-limited conditions lacking tributary discharge ($R^2 = 0.79$). And only during periods of sediment-enrichment when suspended loads originate from tributaries did organics in combination with SS have a significant effect on K_N coefficients ($R^2 = 0.87$). The optical properties encountered in the Colorado River range from high transparency to conditions of light extinction, such that K_N coefficients range from 0.197 to 166 (m^{-1}) and correspond to sediment concentrations ranging from 0.0002 to 8.6 ($g\ l^{-1}$).

Differences in suspended-sediment (quantity/quality) result in different optical properties. Under sediment-limited conditions, discharge, channel geometry, and stream length explain the observed spatial differences in suspended-sediment levels ($F_{4,145} = 261$, $r^2_{adj} = 0.90$, $p < .001$). The light-sediment relationship between K_N and SS is described

by the regression coefficient (β), however, this β coefficient (8 to 23.5 m⁻¹) shifts in response to differences in discharge, sediment-supply events, residence time, and antecedent flow conditions. We hypothesize that differences observed among β coefficients are due to differences in the grain-size distribution of sediment. All of these factors, including tributary flow events are interacting with suspended-sediment to seasonally reduce or eliminate the availability of light for primary production in certain geomorphic reaches of the Colorado River.

INTRODUCTION

Although our understanding of optical properties in river systems is limited, the underlying processes that regulate sediment transport are well established empirically and theoretically (Einstein 1950; Rubin and Topping 2001). Even so, there is a considerable difference in the quantity of suspended-sediment transported relative to differences in discharge, sediment-supply and other hydraulic characteristics. Suspended-sediment is known to influence phytobenthic production and colonization rates, morphology, physiognomy and photo-trophic linkages (Blinn and Cole 1991; Hardwick *et al.* 1992; Shannon *et al.* 1994; Shaver *et al.* 1997; Wilson *et al.* 1999), however, bio-optical research in freshwater ecosystems remains poorly studied, especially in fluvial streams and rivers (Di Toro 1978; Spinrad *et al.* 1978; Kirk 1985, 1994; Jonasz 1987; Stramski and Mobley 1997; Berwald *et al.* 1998).

Impoundments and other forms of flow regulation have had dramatic ecological effects on river systems worldwide, especially arid regions (Stanford and Ward 1991; Ibanez and Prat 1996). The disruption of seasonal flow patterns (i.e., frequency,

magnitude and duration) and sequestered sediment in impoundments has significantly altered some of the more fundamental trophic characteristics of pre-dam ecologies (Stevens *et al.* 1997b, Marzolf *et al.* 1999; Schmidt *et al.* 2001). Flow-regulated systems have reduced suspended loads and increased water transparency and the availability of underwater light for primary production (Ward and Stanford 1983, Stevens *et al.* 1997a). Reducing suspended-sediment loads transforms low-productive allochthonous systems into highly productive autochthonous systems (Armitage 1984; Shaver *et al.* 1997).

Photosynthetic photon flux density (PPFD: $\mu\text{mol quantum m}^{-2}\text{s}^{-1}$) is suggested to be the most fundamental determinant of phytobenthic productivity in the post-dam Colorado River (Usher and Blinn 1990; Blinn and Cole 1991; Hardwick *et al.* 1992; Shaver *et al.* 1997). The Colorado River is one of the most regulated large rivers in the United States (Dynesius and Nilsson 1994). Prior to flow regulation in 1963, suspended loads transported through Glen and Grand canyons had on average, annual mean concentration of 1.5 gL^{-1} (Stanford and Ward 1991). Yet, because flow discharge was seasonally variable, suspended loads often exceeded concentrations of 28 gL^{-1} (Dolan *et al.* 1974).

Soil erosion coupled with sediment-supply is appreciable in arid regions (Leopold *et al.* 1964) owing to periodic and overland flow (Moore and Burch 1986) where tributary flow events result in variable and sometimes sizeable sediment transport (Andrews 1991). Presently, suspended-sediment loads continue to vary due to tributary supply (Topping *et al.* 2000b); however, disruption of sediment transport by Glen Canyon Dam has eliminated what was once the primary sediment source in the Colorado River (Howard and Dolan 1981; Topping *et al.* 2000a). Differences in sediment-supply

and transport have generated a mosaic of varying suspended-sediment concentrations ranging seasonally and spatially from < 0.001 to $>20 \text{ gL}^{-1}$ (Dolan *et al.* 1974; Garrett *et al.* 1993).

The purpose of this study was to examine the spatial and temporal variation in suspended-sediment loads and their effects on apparent optical properties regulating underwater light in the Colorado River. We focused on hydrodynamic processes to address the following objectives: 1) determine the degree to which suspended-sediment (total, inorganic, and organic) affected apparent optical properties of water; 2) determine how discharge, channel morphometry and stream length mechanistically influenced suspended loads; and 3) address how underwater light-attenuation in the Colorado River mainstream may be influenced spatially by the hydrodynamic processes regulating suspended loads.

MATERIALS AND METHODS

Study Area – The Colorado River is a highly turbulent bedrock river that flows through deeply incised canyons in northern Arizona (Fig 1). Our study area extended 390 km from Glen Canyon Dam (GCD) to Diamond Creek. Site locations herein are described in relationship to the distance in river kilometers (Rkm) downstream from GCD (0.0 Rkm). Normal hydro-electrical operations for Glen Canyon Dam (GCD) generate flows that fluctuate diurnally (142 to $708 \text{ m}^3\text{s}^{-1}$) these hypolimnetic releases emerge highly transparent because suspended-sediment is sequestered in Lake Powell reservoir (Marzolf *et al.* 1999; Topping *et al.* 2000a). Initial clear transparent

characteristics appear to be regulated by physical, chemical and biological processes occurring within the reservoir (Chapter 3).

While over 390 ephemeral and perennial tributaries are distributed along the entire river length (Stevens *et al.* 1997a), three major tributaries supply the majority of suspended-sediment (75-80%) between GCD and Lake Mead (Randle and Pemberton 1987; Topping 1997). Frequency, magnitude and duration of sediment discharges from these tributaries vary due to differences in regional and local climate patterns, geomorphology, and stratigraphy (Hereford 1984; Graf *et al.* 1991; Topping 1997; Webb *et al.* 2000). The foremost upstream tributary is the Paria River; a perennial tributary located 26.8 Rkm downstream from GCD. The Paria River has a mean annual discharge of $0.77 \text{ m}^3 \text{ s}^{-1}$ and a basin area of $3,650 \text{ km}^2$ (Graf *et al.* 1991; Topping 1997). Secondly, the Little Colorado River is an ephemeral river (i.e., discounting karst-spring flow within the lower 21-km section), located downstream at 124.3 Rkm, and has a mean annual discharge of $7.0 \text{ m}^3 \text{ s}^{-1}$ and basin area of $69,810 \text{ km}^2$ (Hereford 1984). Lastly, Kanab Creek is a perennial river located at 255.6 Rkm. It has a mean annual discharge of $0.192 \text{ m}^3 \text{ s}^{-1}$ and basin area of $5,931 \text{ km}^2$ (Webb *et al.* 2000). In Grand Canyon, the remaining ungaged sources of suspended-sediment are supplied from small ephemeral and perennial streams having a cumulative drainage area of $5,100 \text{ km}^2$ (Howard and Dolan 1981; Webb *et al.* 2000). The annual sediment yield for tributaries is quite significant ($12.6 \text{ M mt yr}^{-1}$) even though their combined discharge is $< 2\%$ of the mean annual discharge for the Colorado River ($323 \text{ m}^3 \text{ s}^{-1}$) (Randle and Pemberton 1987; Webb *et al.* 2000; Schmidt *et al.* 2001).

Geomorphic control acting at regional and local scales and outcrop patterns of sedimentary rocks have influenced the erosive and depositional features found within this canyon bound river system (Stevens *et al.* 1997a; Schmidt *et al.* 2001). Channel configuration and hydraulics are quite variable and distinct among the four designated canyon sections. And within each of major canyon sections are a series of sub-units or geomorphic reaches. These canyon sections and geomorphic reaches include: Glen Canyon Section (Glen Canyon; Marble Canyon Section (Permian (PE), Supai Gorge (SG), Redwall Gorge (RG), and Lower Marble Canyon (MCG)); Central Grand Canyon Section (Furnace Flats (FF), Upper Granite Gorge (UGG), Aisles (AI), and Middle Granite Gorge (MGG)); and Western Grand Canyon Section (Muav Gorge (MG), Lower Canyon (LC), and Lower Granite Gorge (LGG). Areas excluded from our data collection and analysis are the geomorphic reaches below Diamond Creek (389.6 Rkm) and include a segment of the Lower Granite Gorge and the entire Western Canyon (WC).

Data collection - Sampling trips were scheduled with specific hydrological events. These events included conditions when the Colorado River had: clear and constant flows, $142 \text{ m}^3 \text{ s}^{-1}$ (28 June to 2 July, and 12-15 July 1991), $227 \text{ m}^3 \text{ s}^{-1}$ (28 May to 1 June 1994, 2-9 August 2000), and $425 \text{ m}^3 \text{ s}^{-1}$ (23-31 May 1991); and clear and variable flows, $300\text{-}540 \text{ m}^3 \text{ s}^{-1}$ (24-31 May 1998), $410\text{-}620 \text{ m}^3 \text{ s}^{-1}$ (15-22 May 1999). Three additional sampling trips were scheduled during sediment discharges from Paria River and Little Colorado River, where Colorado River mainstem flows were turbid and variable, $160\text{-}400 \text{ m}^3 \text{ s}^{-1}$ (30 May to 14 June 1992), $340\text{-}675 \text{ m}^3 \text{ s}^{-1}$ (16-22 August 1998), and $410\text{-}660 \text{ m}^3 \text{ s}^{-1}$ (16-23 August 1999).

Photometric measurements were collected in conjunction with suspended-sediment samples using an underwater quantum scalar sensor (Q_o) (LiCor, Inc., LI-193SA), and cosine corrected quantum sensor (Q_i) (LI-190SZ). Photosynthetic photon flux density (PPFD) represents the visible spectrum (400-700 nm) of light measured in units of $\mu\text{mol quantum m}^{-2}\text{s}^{-1}$. Photometric profiles were measured and replicated three times per sampling site. All measurements were made between 0900-1500. Maximum profile depth was 5 m, and typically for each profile five separate measurements were collected at each depth interval. The depth interval used was contingent on water clarity and varied between 0.5 and 0.05 m depending on turbidity. A 5-s time interval was used for sensor equilibration while lowering and raising quanta sensors between depths.

When calculating scalar attenuation coefficients (K_o) we accounted for effects from varying solar incidence by performing a \log_e transformation of the ratio of quantum PPFD measured at depth (Q_z) and at the water surface (Q_i). Transformed PPFD ratios were then regressed against the depth (z) dependent variable. Attenuation coefficients were normalized to account for differences in light behavior due to in solar zenith angles (θ_i) and water refraction (i.e., 1.33 is the refractive index of water) (Denny 1993). We estimated the photo-pathlength using an estimated refracted angle relative to the vertical depth measured during each profile. The mathematical expression used for normalizing attenuation coefficients (K_N) is, $K_N = \cos(\sin\theta_i \div 1.33) \cdot K_o$. Depth-integrated suspended-sediment was sampled mid-channel using an isokinetic bag-sampler (Pemberton 1987, Rubin *et al.* 1998). For each sampling site mean concentrations were based on 3 to 4 integrated samples. To explain observed differences in light-attenuation we separated inorganic suspended-sediment (SS) and organic particulate matter (POM)

from total suspended load (TSL), and analyzed for their effect on K_N coefficients.

Concentration (mg l^{-1}) was determined for TSL, SS, and POM by extracting samples onto glass filters (Whatman 934-AH 1.5 μm pore), desiccating (24-h, 60°C), weighing (± 0.1 mg), ashing (1-h, 500°C), and reweighing (Greenberg *et al.* 1992).

The environmental conditions that we sampled extended from high transparency to light extinction, defined as a light depth penetration where only 1% of surface PPFD remains following light-attenuation. In most cases, when sediment loads exceeded concentrations of 0.5 gL^{-1} , it was estimated that less than 1% of the solar incidence actually penetrated to depths greater than 0.5m. Under these highly turbid conditions, the availability of underwater PPFD for photosynthesis was considered to be at functional light extinction.

An instantaneous discharge (15-min interval) was estimated at each sampling site using the flow routing CRFSSGUI model (Korman *et al.* 2002) that numerically solves for flow and stage discharge, and channel characteristics in the Colorado River. This application incorporates Wiele and Smith's (1996) reach-averaged one-dimensional unsteady flow model that estimates the propagation of GCD discharge wave downstream; and Randle and Pemberton's (1987) steady state flow model that estimates changes in channel characteristics (hydraulic area, top width, and depth) based on the stage discharge relationship at specific sites throughout Glen and Grand canyons. Hydrological data were acquired for GCD using the US Bureau of Reclamation flow records, and stream flow records (provisional real-time unit values) for the Paria River (station 09382000) and Little Colorado River (station 09402000) from US Geological Survey. For our analysis, we then calculated the channel and hydraulic characteristics by

averaging across all cross-sectional profiles contained within that designated geomorphic reach (e.g., Redwall Gorge, 61.7 to 83.1 km) (Stevens *et al.* 1997).

Statistical analysis was performed using simple, multiple linear regressions, and analysis of variance (ANOVA) to evaluate the effect that mean suspended-sediment (TSL, SS and POM) concentrations had on mean attenuation coefficients (K_N). Multiple linear regression analysis was used with a forward stepwise procedure to evaluate the influence that hydraulic geometry, stream length (Rkm), and discharge (Q) had on SS (Netter *et al.* 1996). We used the coefficient of determination ($r^2 > 0.95$) as a filtering criterion for selecting K_N values used in our regression analysis. Analysis of covariance (ANCOVA) was used to test slope equivalence among different light-sediment regression coefficients estimated from different sampling trips. Several statistical packages were used for our analyses (SAS, Inc. 2001; StatSoft 2002).

RESULTS

Light-sediment relationship - Our empirical data included the range of apparent optical properties (AOP) encountered in the Colorado River. The observed SS concentrations ranged from 0.0002 to 8.8 gL⁻¹ (Table 1), which corresponded to respective mean K_N values of 0.197 to 166 m⁻¹ (Table 2). Multiple linear regression analysis was performed using pooled data for clear sediment-limited conditions. Normalized attenuation coefficients (K_N) varied linearly in response to SS ($F_{2, 147} = 290$, $R^2 = 0.79$, $p < 0.001$) (Fig 2). Inclusion of POM with SS had no significant effect on light-attenuation response ($p = 0.78$). This was unexpected since apparent optical properties are often influenced by the presence of organics in suspended and dissolved forms.

Separate *post-hoc* tests, using simple linear regressions were performed to evaluate independent sampling trips. Results indicated that the light-sediment regression coefficients (β) for the relationship between K_N to SS decreased in response to discharge ($\beta = 15.4$ at $142 \text{ m}^3 \text{ s}^{-1}$, $\beta = 13.5$ at $227 \text{ m}^3 \text{ s}^{-1}$, $\beta = 10.8$ at $425 \text{ m}^3 \text{ s}^{-1}$, and $\beta = 8.0$ at $> 430 \text{ m}^3 \text{ s}^{-1}$) (Fig 3-A, Table 1). Although β coefficients observed under hydraulically clear conditions were dissimilar, tests for slope equivalence using ANCOVA, detected no significant differences between relationships of K_N to SS as it covaried in response to different discharge levels (142 to $> 430 \text{ m}^3 \text{ s}^{-1}$) ($p = 0.2$).

Sediment enriched conditions – A simple linear regression was performed using pooled data collected during periods of tributary flows. Results for hydraulically clear conditions indicated that K_N was significantly correlated to SS ($F_{1, 141} = 977$, $R^2 = 0.87$, $p < 0.001$). Results from pooled data specifically for sediment-enriched conditions indicated that the light-sediment regression coefficient ($\beta = 17.85$) was more elevated than under hydraulically clear conditions. Separate *post-hoc* tests were performed for three separate sampling periods (May/June 1992, August 1998, and August 1999). Results indicated that K_N was significantly correlated to SS for all sampling periods (SLR, $p < 0.001$).

Results testing slope equivalence using ANCOVA indicated that light-sediment regression coefficients (β) differed significantly among turbid sampling periods ($p < 0.04$), ($\beta = 23.5$, 1992; $\beta = 15.6$, 1998; and $\beta = 16.4$, 1999). Variation around β coefficients among turbid sampling periods appeared related to either difference in sediment source (Paria, Little Colorado River and/or ungaged tributaries) or tributary discharge (Fig 3-B). Further tests indicated no significant difference between β

coefficients for August 1998 and August 1999. Because of these similarities we chose to compare β coefficients for sediment enriched and sediment-limited conditions. There was no significant difference among β coefficients (ANCOVA, $p = 0.12$) when slope comparisons were made among turbid (August of 1998 and 1999) and low constant flows (142 and $227 \text{ m}^3\text{s}^{-1}$) conditions. Mean SS concentrations (one-way ANOVA, $p < 0.001$) and mean K_N (one-way ANOVA, $p < 0.001$) were significantly different when sediment-limited ($9.4 \text{ mg l}^{-1} \pm 0.8 \text{ SE}$; $0.422 \text{ m}^{-1} \pm 0.013 \text{ SE}$) and sediment enriched conditions ($1,298 \text{ mg l}^{-1} \pm 212 \text{ SE}$; $25.79 \text{ m}^{-1} \pm 4.1 \text{ SE}$) were compared, however β coefficients were deemed equivalent (Table 2).

Suspended Organics - Under sediment-enriched conditions POM in combination with SS was found to have a significant effect on K_N coefficients (MLR, $F_{2, 140} = 725$, $R^2 = 0.91$, $p < 0.001$). This positive correlation with organics was unlike previous responses observed for hydraulically clear flows. Based on the coefficient of partial determination, inclusion of organics as an additional independent variable resulted in a proportional reduction by 30% of the remaining unexplained variance associated with K_N (Table 2). Under turbid flows, percent POM was found to be significantly (SLR, $p = 0.03$) and inversely correlated to increasing SS concentration, even though it was not correlated to stream length (SLR, $p = 0.7$). Even though POM concentrations were significantly higher, the overall organic proportion for total suspended load (TSL) was considerably less than that found under hydraulically clear conditions. The proportion of organics ranged between 2% and 23%, having a mean of 6.5%. On average for turbid conditions, mean and median POM concentrations were $60 \text{ mg l}^{-1} \pm 7 \text{ SE}$ ($n = 109$), and 23 mg l^{-1} , respectively.

We estimated an annual organic yield based on our findings that the organic proportion was 6.5% of TSL during tributary flows. Using a reported estimate of 12.6 M mt yr⁻¹ as the annual sediment yield inclusive of all Colorado River tributaries (Schmidt *et al.* 2001), our estimated annual organic yield was 0.876 M mt yr⁻¹ {organics = 12.6 / (1 - 0.065) · (0.065)}. This estimate is considered conservative since the proportion of sampled organics under turbid conditions lacks a normal distribution; and secondly, sediment discharge from tributaries and mass balance estimates for sediment yield typically account for the quantity of suspended-sediment rather than the suspended wash-load.

For hydraulically clear conditions, organic loads were found to be extremely low. Mean and median POM concentrations were 3 mg l⁻¹ ± 0.4 SE, and 1.5 mg l⁻¹, respectively. Although organic concentrations were significantly lower during clear conditions, their overall proportion to TSL was considerably higher than those found during turbid conditions. Under hydraulically clear conditions the mean organic proportion of TSL was 29%, and ranged between 13% and 91%. Organics responded significantly to changes in sampling periods (one-way ANOVA, $p < 0.001$), but was not correlated to differences in discharge (SLR, $p = 0.38$). Organics increased significantly in relation to increases in stream length ($p < 0.001$), indicating a cumulative export of POM through the system, and was perhaps related to aquatically derived autotrophic production. Variation in POM may have been due to differences in instream production between sampling trips rather than related to transport as a function of discharge (Table 1).

Hydraulic geometry, stream length and discharge – Geomorphic reaches in the Colorado River have varying channel width, depth, and hydraulic slope. Differences in channel hydraulics and configuration create a series of wide/shallow or narrow/deep channels (Table 2). Variation in W/D ratios as a function of stream length and discharge is graphically apparent in Fig 4. Notable, is the strong response observed for both K_N coefficients and SS levels (Fig 5) to different geomorphic and hydraulic geometry. Under clear sediment-limited conditions, a strong and significant set of interactions occurred between SS and discharge (Q), channel geometry (W/D), and stream length (Rkm) (MLR, $F_{4,145} = 261$, $r^2_{adj} = 0.90$, $p < .001$). Results with the inclusion of Rkm ($p < 0.001$), as well as interactions occurring among other independent variables, such as between Rkm · Q ($p < 0.001$), Rkm · W/D ($p < 0.001$), and Rkm · Q · W/D ($p < 0.001$) were significantly correlated to SS. However, under sediment enriched conditions we were unable to discern any influence that hydraulic geometry had on suspended loads during tributary supply events. During sediment-enriched periods the overriding influence of suspended wash-load appears to have removed or masked any detectable effect associated with differences in channel configuration, discharge, and stream length. The statistical model that best describes the spatial variability in sediment transport (gL^{-1}) is:

$$SS = \left[0.057 + (-0.909 \cdot Rkm) + (0.041 \cdot Rkm \cdot Q_{CR}) + (0.003 \cdot Rkm \cdot WD) + (-0.0001 \cdot Rkm \cdot Q_{CR} \cdot WD) \right] \cdot 1000 .$$

where different interactions occurring between stream length (Rkm), Colorado River discharge (Q_{CR}) and width/depth ratios (WD) are used to predict differences in suspended-sediment.

DISCUSSION

Spatial and temporal patterns observed in apparent optical properties correspond strongly to biotic patterns observed for the distribution of phyto-benthic, macroinvertebrates, fish, and waterfowl in the Colorado River (Shannon *et al.* 1994; Stevens *et al.* 1997a, 1997b; Schmidt *et al.* 2001). In fluvial systems the availability of underwater light is a predictable consequence of spatio/temporal limitations of sediment-supply and interactions between hydraulic processes regulating sediment transport (Rubin *et al.* 1998; Andrews 1991). The primary causal factor in light-attenuation in the downstream sections of the Colorado River is inorganic sediment; although there is evidence suggesting that dissolved organic carbon regulates apparent optical properties in the upstream section of Glen Canyon (0.0 to 26.8 Rkm) (Chapter 3). Sediment concentrations are sometimes problematic when used as a univariate predictor for estimating light-attenuation coefficients.

In fluvial systems apparent optical properties vary in response to sediment-supply limitations and transport processes (Andrews 1991; Rubin *et al.* 1998). Topping (1997) identified that that during episodic flow events the proportion of fines (grain size <0.0625 mm) from the Paria was 50%; whereas, the LCR was $> 80\%$ (Pemberton 1987). Suspended-sediment supplied by tributaries consists predominantly of suspended fine silts and clays referred to as wash-load (Randle and Pemberton 1987; Rubin *et al.* 1998).

In most fluvial systems, wash-load is evenly dispersed through the height of the water column and independent of bed and suspended loads (Van Duin *et al.* 1992; Topping 2000b). In streams and rivers, certain hydraulic forces (discharge) influence as well as interact with other fluvial processes (sediment-supply, grain-size distribution, channel morphometry) in regulating sediment transport rates (Howard and Dolan 1981; Reid *et al.* 1997; Rubin *et al.* 1998; Topping *et al.* 2000a; Rubin and Topping 2001). Sediment-supply from tributaries tends to contribute a higher proportion of fines during turbid flow conditions; conversely, lower flows will tend to discriminate by favoring smaller grain-size in the bed material (Rubin *et al.* 1998; Andrews 1991). Rubin *et al.* (1998) have demonstrated that an increase in turbulent flow entrains large coarser bed material, and once the bed material is scoured of entrainable sized particles, the grain-size distribution then evolves upward toward larger coarser sized particles.

An inverse relationship exists between surface area and grain-size (Webb and Walling 1994) where differences in grain-size for equivalent concentration should invariably result in different light-attenuation coefficients. We hypothesize that the observed differences among light-sediment regression coefficients (β) for the Colorado River were due principally to differences in the grain size distribution of the sample concentration (Jones and Wills 1956; Van Duin *et al.* 1992). As shown by others, particle surface area associated with suspended fines are largely responsible for differences in light scattering characteristics, and that scattering rather than absorption by sediment is the primary mechanism for light-attenuation (Kirk 1985, 1994; Jonasz 1987; Berwald *et al.* 1998). The relationship of AOP to different sediment grain-size appears to vary in response to sediment-supply events. Convergence among light-sediment

regression coefficients during periods of reduced discharge ($142\text{-}227\text{ m}^3\text{ s}^{-1}$); as well as periods of sediment enrichment (1992, 1998, and 1999) are thought to be due to grain-size similarities in suspended-sediment.

Research and monitoring data on the phytobenthic community indicates a positive response in biomass accretion under either chronic sediment-limitation as occurs in Glen Canyon, or during periods of infrequent tributary discharge as frequently occurs in Marble Canyon (Shaver *et al.* 1997; Stevens *et al.* 1997a; Benenati *et al.* 1998). We hypothesize that under sediment-supply limitations, attenuation coefficients should continue to decrease over time as the bed material is winnowed of finer grain-size sediment. Factors such as 1) duration prior to last tributary discharge event, 2) beach habitat building flows (Rubin *et al.* 1998; Schmidt *et al.* 2001), and 3) sustained high or variably high discharges further armor the streambed by selectively winnowing fines (Rubin *et al.* 1998; Topping *et al.* 2000b). Under prolonged periods of sediment-limited conditions the AOP in the Colorado River should result in a long-term decrease in light-attenuation. Coarsening of bed material over extended periods of high flows and minimal tributary supply (Rubin *et al.* 1998) may explain some of the observed differences existing among β coefficients for equivalent discharge (Fig 3), as well as spatial differences in the distribution of light-attenuation coefficients as a function of stream length (Fig 5).

Light-sediment regression coefficients (β) typically respond by shifting from higher to lower slope values, and depending on residence time and antecedent flow events the source of these suspended-sediments are either slowly depleted or completely scoured from the bed. This downward response in β coefficients is immediately reset

once suspended-sediment is re-supplied by tributary flows. This light-sediment response pattern is similar to the hysteresis observed annually in the CR, where with the cessation of tributary flow suspended-sediment concentrations decrease as grain-size increases (Rubin *et al.* 1998; Topping *et al.* 2000a, 2000b).

Organic component - K_N was positively correlated to the presence of organics under turbid conditions. This contrasted with our findings during sediment-limited conditions showing that no significant relationship exists between light-attenuation and organics. This response pattern was notable because under sediment limitations the organic proportion was greater and represented approximately 30% of the overall TSL. Under turbid conditions organics were significantly correlated to inorganic sediment levels; however, this was not the case under sediment-limited conditions. The strong correlation between SS and POM concentrations suggests that this organic sediment relationship is probably due to carbon adsorption to clay and silt particles (Thurman 1985). Based on annual sediment yield for all gaged and ungaged tributaries (Randle and Pemberton 1987; Schmidt *et al.* 2001), the annual organic yield in this system is estimated at $0.876 \text{ M mt yr}^{-1}$, and appears to be originating from high desert plateaus. Yet, retention, trophic linkages, and ultimate fate of these sediment-bound organics remain unknown.

Proportion of organics (30%) under clear non-turbid conditions was considered much higher than those reported for other fluvial systems (Thurman 1985). When comparisons were made among sampling events differences in organic levels were not related to discharge. We found that the quantity of organics was spatially and temporally variable, and that differences within and among sampling trips may have been associated

with local and system-wide autochthonous production. As observed in other regulated river systems (Lieberman and Burke 1993) organics tend to increase with stream length indicating cumulative production. Yet, during sediment enrichment, the average proportion of organics found in TSL was 6.5%. Although these organic proportions were low, mean concentration levels were 15-fold greater than observed under sediment-limited conditions. Organic source of this material may have been associated with phytobenthic disturbance (abrasion and shear forces) (Shannon *et al.* 1996; Shaver *et al.* 1997; Wilson *et al.* 1999); however, it seems more likely that the origin was terrestrial because high organic levels were sustained throughout the duration of the sediment discharge event.

Suspended-sediment - Even though no universal relationship exists between light-attenuation and sediment concentration (Kirk 1985; Han and Rundquist 1994; Stramski and Mobley 1997), developing or using existing methods for estimating suspended-sediment transport and relating these sediment levels to a light-sediment relationship may provide a means to understand phytobenthic response in other regulated river systems. In the Colorado River increased light-attenuation with stream length appears to be explained by interactions with sediment-supply, discharge, spatial storage differences, and hydraulic geometry (Schmidt 1990; Rubin *et al.* 1998). Our results suggest that hydraulic and channel geometry influence suspended-sediment loads in the Colorado River. Channel configuration appears to contract and expand within the major canyon sections (Fig 4) such that suspended loads respond inversely to changes in W/D ratios. Interactions between channel characteristics and stream length initially result in lower sediment loads for upstream reaches having wide/shallow channels. However, as stream

length increases suspended-sediment continues to increase even in downstream reaches having wide/shallow channels. The interaction of stream length and W/D ratios begins to have strong multiplicative effect on suspended loads in Central Grand Canyon and Western Grand Canyon sections.

Increases in discharge results in elevating sediment transport capacity; yet the interactions associated with discharge, channel configuration and stream length further affect suspended loads. Rubin *et al.* (1991) have shown that channel expansion typically occurs under higher discharge in geomorphic reaches having large recirculation zones. Channels with large W/D ratios tend to have lower velocities (Schmidt 1990), and hence less sediment transport; even so under fluctuating or higher discharges, changes to recirculation zones may influence flow and channel configuration, as well as locations for deposition and erosion (Rubin *et al.* 1991; Schmidt *et al.* 2001). Although discharge increases the erosive potential at higher discharge ($>227 \text{ m}^3\text{s}^{-1}$), sediment availability for erosion and transport becomes less for certain canyon sections, especially in narrow/deep channels where large reattachment bars are limited and lateral expansion is constrained (Melis 1997; Stevens *et al.* 1997).

The most decisive factor influencing apparent optical properties for a given site was its spatial relationship to major tributaries in Grand Canyon. In most cases, when sediment loads exceeded concentrations of 0.5 gL^{-1} , it was estimated that less than 1% of the solar incidence actually penetrated and reached depths greater than 0.5m. During these turbid conditions, availability of underwater light for photosynthesis was considered functionally unavailable to the phytobenthic community. Most of the cross-sectional perimeter available for phytobenthic community is disproportionately found in

the deeper regions of the channel, due to the hydraulic radius (Randle and Pemberton 1987). Since visible light diminishes exponentially as a function of depth, any increase in light-attenuation under sediment-limited conditions acts to further reduce or totally eliminate PPFD in deeper channel sections that would have otherwise been photosynthetically available to the phytobenthos.

We expect that the upward extent of the phytobenthic community would be limited by desiccation, whereas the lowest vertical extent would be limited by PPFD availability. We find that once the euphotic depth (depth representing 1% surface incidence) no longer exceeds the mean thalweg depth, that the remaining available area for potential photosynthesis is laterally restricted to the littoral margin (Shaver *et al.* 1997). Conversely, at lower discharge the channel area available for photosynthesis is greater because of reduced light-attenuation and channel depth. Both factors allow for greater light penetration even though total wetted area of the channel is reduced. The colonization and growth occurring in the euphotic zone is exacerbated by variable flow conditions. As Benenati *et al.* (1998) have shown, the effect of desiccation from atmospheric exposure due to normal flow variation further compounds the effect related to increased light-attenuation. The boundaries of this zone collapse inward under extreme fluctuating flows and sediment enriched conditions. These factors coupled together may seasonally reduce or eliminate primary production from occurring in certain geomorphic reaches.

ACKNOWLEDGMENTS

We would like to extend our appreciation to Donna and Sylvester Allred, Dave Baker, Annie Bennett, Lydia Brunswick, Renee Davis, Brian Dierker, Susan Hueftle, Mike Kearsley, Diana Kimberling, Haydee and George Koch, Jeanie Korn, Vickie Meretsky, Nels Niemi, Nicky Preston, Barbara and Frank Protiva, Val Salor, Joe Shannon, Mike Shaver, Bill Vernieu, Alex Wilson, Helen Yard, Stephanie Yard and Tom Yard for their invaluable advice and assistance in the field and laboratory. Special thanks go to George Koch, Rod Parnell, Peter Price, and Dave Topping for their review; as well as David Wegner with Glen Canyon Environmental Studies, U.S. Bureau of Reclamation, and Barry Gold with Grand Canyon Monitoring Research Center, U.S. Geological Survey for providing the funding and logistical support for this project. This study was funded in part by a cooperative agreement through Northern Arizona University (98-FC-40-0540).

LITERATURE CITED

- Andrews, E.D., 1991. Sediment Transport in the Colorado River Basin. *In*. Committee on Glen Canyon Environmental Studies (Eds) *Colorado River ecology and Dam Management*. National Academy Press, Washington D.C.
- Armitage, P.D., 1984. Environmental changes induced by stream regulation and their effects on lotic macroinvertebrate communities. *In*. Lillehammer, A. and S.J. Saltveit. (Eds) *Regulated Rivers*. Universitetsforlaget AS, Oslo.
- Benenati, P., J.P. Shannon, and D.W. Blinn, 1998. Desiccation and recolonization of phyto-benthos in a regulated desert river: Colorado River at Lees Ferry, Arizona, USA. *Regul. Rivers: Res. Mgmt.* 14:519-532.
- Berwald, J., D. Stramski, C.D. Mobley, D.A. Kiefer, 1998. Effect of Raman scattering on the average cosine and diffuse attenuation coefficient of irradiance in the ocean. *Limnol. Oceanogr.* 43:564-576.
- Blinn, D.W., and G.A. Cole, 1991. Algal and invertebrate biota in the Colorado River: comparison of pre- and post-dam conditions. *In*. Committee on Glen Canyon Environmental Studies (Eds.) *Colorado River ecology and Dam Management*. National Academy Press, Washington D.C.
- Colby, B.R., 1961. Effect of depth flow on discharge of bed material. U.S. Geological Survey -Water Supply Paper 1498-D.
- DiToro, D.M., 1978. Optics of turbid estuarine waters: approximation and applications. *Water Research.* 12:1059-1068.
- Dolan, R., A. Howard, and A. Gallenson, 1974. Man's Impact on the Colorado River in the Grand Canyon. *Amer. Scientist.* 62:392-401.
- Duarte, C.M., S. Agusti, M.P. Satta, and D. Vaque, 1998. Partitioning particulate light absorption: A budget for a Mediterranean bay. *Limnol. Oceanogr.* 43: 236-244.
- Dynesius, M., and C. Nilsson, 1994. Fragmentation and flow regulation of river systems in the northern third of the world. *Science.* 266:753-762.
- Einstein, H.A., 1950. The bed-load function for sediment transportation in open channel flows. *Serv. Tech. Bull. U.S. Dep. Agric. Soil Conserv., No. 1026* U.S. Gov. Printing Office, Washington D.C.
- Ganf, G.G., 1973. Incident irradiance and light penetration as factors controlling the chlorophyll (a) content of a shallow equatorial lake (Lake George, Uganda). *J. Ecol.* 62:593-609.

- Garrett, W.B., E.K. Van DeVanter and J.B. Graf, 1993. *Streamflow and sediment-transport data, Colorado River and three tributaries in Grand Canyon, Arizona, 1983 and 1985-86*. US. Geological Survey, Open-File Report 93-174. Denver, CO.
- Graf, J.B., R.H. Webb and R. Hereford, 1991. Relation of sediment load and flood-plain formation to climatic variability, Paria River drainage basin, Utah and Arizona. *Geol. Soc. of Am. Bull.* 103:1405-1415.
- Graf, J.B., 1995. Measured and predicted velocity and longitudinal dispersion at steady and unsteady flow, Colorado River, Glen Canyon Dam to Lake Mead. *Water Resources Bulletin.* 31:265-281.
- Graham, J.M., M.T. Auer, R.P. Canale, and J.P. Hoffman, 1982. Ecological studies and mathematical modeling of *Cladophora* in Lake Huron: 4. Photosynthesis and respiration as functions of light and temperature. *J. Great Lakes Res.* 8:100-111.
- Greenberg, A.E., L.S. Clesceri, A.D. Eaton, 1992. (Eds.) *Standard methods for the examination of water and wastewater*. 18th Edition. American Public Health Assoc.
- Han, L. and D.C. Rundquist, 1994. The response of both surface reflectance and the underwater light field to various levels of suspended sediments: Preliminary results. *Photogrammetric Engineering & Remote Sensing.* 60:1463-1471.
- Hardwick, G.G., D.W. Blinn, and H.D. Usher. 1992. Epiphytic diatoms on *Cladophora glomerata* in the Colorado River, Arizona: longitudinal and vertical distribution in a regulated river. *Southwest. Nat.* 37:148-156.
- Hereford, R., 1984. Climate and ephemeral-stream processes: Twentieth-century geomorphology and alluvial stratigraphy of the Little Colorado River, Arizona. *Geol. Soc. of Am. Bull.* 95:654-668
- Howard, A. and R. Dolan, 1981. Geomorphology of the Colorado River in the Grand Canyon. *J. of Geology.* 89:269-298.
- Ibanez, C. and N. Prat, 1996. Changes in the hydrology and sediment transport produced by large dams on the lower Ebro River and its estuary. *Regul. Rivers: Res. Mgmt.* 12:51-62.
- Jonasz, M., 1987. Nonsphericity of suspended marine particles and its influence on light scattering. *Limnol. Oceanogr.* 32:1059-1065.
- Jones, D. and M.S. Wills, 1956. The attenuation of light in sea and estuarine waters in relation to the concentration of suspended solid matter. *J. Mar. Biol. Ass. U.K.* 35:431-444.

- Kirk, J.T.O., 1983. *Light and photosynthesis in aquatic ecosystems*. Cambridge University Press, Cambridge, London.
- Kirk, J.T.O., 1985. Effects of suspensoids (turbidity) on penetration of solar radiation in aquatic ecosystems. *Hydrobiologia*. 125:195-208.
- Kirk, J.T.O., 1994. Characteristics of the light field in highly turbid waters: A Monte Carlo study. *Limnol. Oceanogr.* 39:702-706.
- Korman, J., S. Wiele, T. Randle, T. Melis, and D. Topping, 2000. User's guide to the graphic interface combining flow, stage and sediment-input models developed for the Colorado River in Grand Canyon. USGS, Grand Canyon Monitoring and Research Center, Flagstaff, AZ.
- Leopold, L.B., M.G. Wolman, and J.P. Miller, 1964. *Fluvial processes in geomorphology*. W.H. Freeman, San Francisco, Calif.
- Lieberman, D.M., and T.A. Burke, 1993. Particulate organic matter transport in the lower Colorado River, south-western USA. *Regul. Rivers: Res. Mgmt.* 8:323-334.
- Marzolf, G.R., C.J. Bowser, R. Hart, D.W. Stephens, and W.S. Vernieu, 1999. Photosynthetic and respiratory processes: an open stream approach. In: J.C. Schmidt, G.R. Marzolf, and R.A. Valdez (eds). *The controlled flood in Grand Canyon*. American Geophysical Union, Geophysical Monograph 110, Washington, D.C.
- Melis, T.S., 1997. Geomorphology of debris flows and alluvial fans in grand Canyon National Park and their influences on the Colorado River below Glen Canyon Dam, Arizona. Ph.D. Dissertation., Univ. of Arizona, Tucson, AZ.
- Moore, I.D. and G.J. Burch, 1986. Sediment transport capacity of sheet and rill flow: application of unit stream power theory. *Water Resources Research*. 22:1350-1360.
- Netter, J., M.H. Kutner, C.J. Nachtsheim and W. Wasserman, 1996. *Applied linear statistical models*. (4th Ed.) Times Mirror Higher Education Group, Inc., Chicago, US.
- Pemberton, E.L., 1987. Sediment data collection and analysis for five stations on the Colorado River from Lees Ferry to Diamond Creek. Glen Canyon Environmental Studies Technical Report, NTIS No. PB88-183397.
- Randle, T.J., and E.L. Pemberton, 1987. Results and analysis of STARS modeling efforts of the Colorado River in Grand Canyon. U.S. Department of Interior, Bureau of Reclamation. NTIS No. PB88-183421/AS.

- Reid, I. J.C. Bathurst, P.A. Carling, D.E. Walling and B.W. Webb, 1997. Sediment erosion, transport and deposition. *In*. Thorne, C.R., R.D. Hey and M.D. Newson (Eds.) *Applied fluvial geomorphology for river engineering and management*. John Wiley and Sons, New York.
- Roos, J.C. and A.J.H. Pieterse, 1994. Light, temperature and flow regimes of the Vaal River at Balkfonteln, South Africa. *Hydrobiologia*. 277:1-15.
- Rubin, D.M., J.M. Nelson, and D.J. Topping, 1998. Relation of inversely graded deposits to suspended-sediment grain-size evolution during the 1996 flood experiment in Grand Canyon. *Geology*. 26:99-102.
- Rubin, D. M., and D. J. Topping. 2001. Quantifying the relative importance of flow regulation and grain size regulation of suspended sediment transport α and tracking changes in grain size of bed sediment β . *Water Resources Research*. 37:133-146.
- SAS Institute, Inc., 2001. SAS V8.02, TS Level O2MO. The SAS System for Windows Version. Cary, N.C., USA.
- Schmidt, J.C., 1990. Recirculating flow and sedimentation in the Colorado River in Grand Canyon, Arizona. *J. of Geology*. 98:709-724.
- Schmidt, J.C., R.A. Parnell, P.E. Grams, J.E. Hazel, M.A. Kaplinski, L.E. Stevens, and T.L. Hoffnagle, 2001. The controlled flood in Grand Canyon: flow, sediment transport, and geomorphic change. *Ecological Applications*. 11:657-671.
- Shannon, J.P., D.W. Blinn and L.E. Stevens, 1994. Trophic interactions and benthic animal community structure in the Colorado River, Arizona, U.S.A. *Freshwat. Biol.* 31:213-2120.
- Shannon, J.P., D.W. Blinn, P.L. Benenati, and K.P. Wilson. 1996. Organic drift in a regulated desert river. *Can. J. Fish. Aquat. Sci.* 53:1360-1369.
- Shaver, M.L., J.P. Shannon, K.P. Wilson, P.L. Benenati and D.W. Blinn, 1997. Effects of suspended sediment and desiccation on the benthic tailwater community in the Colorado River, USA. *Hydrobiologia*. 357:63-72.
- Smith, R.C., B.B. Prezelin, R.R. Bidigare and K.S. Baker, 1989. Bio-optical modeling of photosynthetic production in coastal waters. *Limnol. Oceanogr.* 34:1524-1544.
- Spinrad, R.W., J.R.V. Zaneveld, and H. Pak, 1978. Volume scattering function of suspended particulate matter at near-forward angles: a comparison of experimental and theoretical values. *Applied Optics*. 17:1125-1130.

- Stanford, J.A., and J.V. Ward, 1991. Limnology of Lake Powell and the Chemistry of the Colorado River. *In*. Committee on Glen Canyon Environmental Studies (Eds.) *Colorado River Ecology and Dam Management*. National Academy Press, Washington D.C.
- StatSoft, Inc., 2002. STATISTICA (data analysis software system), V6.1, Tulsa, OK, USA.
- Stevens, L.E., J.P. Shannon and D.W. Blinn, 1997a. Colorado River benthic ecology in Grand Canyon, Arizona, USA: dam, tributary and geomorphic influences. *Regul. Rivers: Res. Mgmt.* 13:129-149.
- Stevens, L.E., A.A. Buck, B.T. Brown, and N.C. Kline, 1997b. Dam and geomorphological influences on Colorado River waterbird distribution, Grand Canyon, Arizona, USA. *Regul. Rivers: Res. Mgmt.* 13:151-169.
- Stramski, D. and C.D. Mobley, 1997. Effects of microbial particles on oceanic optics: A database of single-particle optical properties. *Limnol. Oceanogr.* 42:538-549.
- Thurman, E.M., 1985. *Organic geochemistry of natural waters*. Martinus Nijhoff/Dr. W Junk, Boston Massachusetts, USA. pp. 496.
- Topping, D.J., 1997. Physics of flow, sediment transport, hydraulic geometry, and channel geomorphic adjustment during flash floods in an ephemeral river, the Paria River, Utah and Arizona. Ph.D. dissertation. Univ. of Wash. Seattle, WA.
- Topping, D.J., D.M. Rubin, and L.E. Vierra, Jr., 2000a. Colorado River sediment transport 1. Natural sediment supply limitation and the influence of Glen Canyon Dam. *Water Resources Research.* 36:515-542.
- Topping, D.J., D.M. Rubin, J.M. Nelson, P.J. Kinzell III, and I.C. Corson, 2000b. Colorado River sediment transport 2. Systematic bed-elevation and grain-size effects of sand supply limitation. *Water Resources Research.* 36:543-570.
- Van Duin, E.H.S., G. Blom, L. Lijklema and M.J.M. Scholten, 1992. Aspects of modeling sediment transport and light conditions in Lake Marken. *Hydrobiologia.* 235/236:167-176.
- Usher, H.D., and D.W. Blinn, 1990. Influence of various exposure periods on the biomass and chlorophyll A of *Cladophora glomerata* (Chlorophyta). *J. Phycol.* 26:244-249.
- Ward, J.V., and J.A. Stanford, 1983. The serial discontinuity concept of lotic ecosystems. *In*. Dynamics of Lotic Ecosystems. Ann. Harbor Science Publishers. Ann Arbor, MI.

Webb, B.W. and D.E. Walling, 1994. Water quality II. Chemical characteristics. *In*. Callow, P. and G.E. Petts (Eds.) *The rivers handbook, hydrological and ecological principles*. Blackwell Scientific Publications, London, UK.

Webb, R.H., P.G. Griffiths, T.S. Melis, and D.R. Hartley, 2000. Sediment delivery by ungaged tributaries of the Colorado River in Grand Canyons. US Geological Survey Water Resources Investigations Report 00-4055.

Wiele, S.M., and J.D. Smith, 1996. A reach-averaged model of diurnal discharge wave propagation down the Colorado River through the Grand Canyon. *Water Resources Research*. 32:1375-1386

Wilson, K.P., J.P. Shannon and D.W. Blinn, 1999. Effects of suspended sediment on biomass and cell morphology of *Cladophora glomerata* (Chlorophyta) in the Colorado River, Arizona. *J. Phycol.* 35:35-41.

TABLE 1. Average inorganic suspended-sediment and particulate organic matter (mg L^{-1}) for the Colorado River collected over a range of constant and varying discharge levels in the four major canyon sections of Glen and Grand canyons.

Collection Period	Discharge	n	GLEN CANYON SECTION				MARBLE CANYON SECTION								
			Suspended Sediment		Suspended Organics		Suspended Sediment		Suspended Organics						
			Avg	sd	min - max	n	Avg	sd	min - max	Avg	sd	min - max			
June-July 1991	142 m^3s^{-1}	9	2.0	1.4	0 - 5	8.0	3.3	4.2 - 13.5	14	3.0	2.8	0.2 - 11.9	6.8	2.9	1.8 - 11.8
May-June 1994	227 m^3s^{-1}	8	5.2	1.1	4 - 7	1.2	0.6	0.4 - 2.4	20	8.7	4.4	5.6 - 18.0	1.9	1.6	0.2 - 7.7
August 2000	227 m^3s^{-1}	3	1.3	0.8	0 - 2	0.8	0.6	0.8 - 0.8	24	2.6	1.8	0.3 - 8.2	1.2	0.4	0.8 - 2.0
May 1991	425 m^3s^{-1}	6	1.4	1.3	0 - 3	3.7	2.3	3.7 - 3.7	14	7.7	5.8	0.2 - 17.3	6.1	3.5	1.5 - 12.6
May 1998	300-540 m^3s^{-1}	6	0.3	0.4	0 - 1	0.6	0.3	0.6 - 0.6	59	6.4	4.0	1.0 - 17.2	1.0	0.5	0.2 - 2.4
May 1999	410-620 m^3s^{-1}	18	2.1	2.6	1 - 12	1.1	0.2	1.1 - 1.1	48	92.4	57.2	2.8 - 209	3.1	4.8	0.7 - 24.9
May-June 1992	160-400 m^3s^{-1}	12	1.4	1.3	0 - 4	2.6	1.4	2.6 - 2.6	51	347	233	112.7 - 1088	31.0	31.0	14.0 - 99.8
August 1998	340-675 m^3s^{-1}	3	0.5	0.4	0 - 1	2.0	0.7	2.0 - 2.0	44	38.7	23.3	6.7 - 98.4	1.7	0.7	0.6 - 3.8
August 1999	410-660 m^3s^{-1}	3	1.1	0.3	1 - 1	0.2	0.1	0.2 - 0.2	46	66.1	47.2	8.1 - 207	2.3	1.3	0.0 - 4.6
CENTRAL GRAND CANYON SECTION															
Collection Period	Discharge	n	Suspended Sediment				Suspended Organics								
			Avg	sd	min - max	n	Avg	sd	min - max	n	Avg	sd	min - max		
			Avg	sd	min - max	n	Avg	sd	min - max	n	Avg	sd	min - max		
June-July 1991	142 m^3s^{-1}	21	8.3	5.5	2 - 18	6.2	3.2	1.0 - 12.1	18	16.3	7.8	0.4 - 30.9	9.3	4.0	3.6 - 16.9
May-June 1994	227 m^3s^{-1}	20	10.8	6.4	2 - 26	2.0	1.9	0.2 - 6.6	21	16.7	4.2	10.0 - 23.4	1.2	0.8	0.6 - 3.3
August 2000	227 m^3s^{-1}	54	6.2	2.6	2 - 13	1.5	0.7	0.8 - 4.3	69	16.0	11.1	4.0 - 49.8	2.2	1.2	0.9 - 8.6
May 1991	425 m^3s^{-1}	27	36.4	23.1	2 - 91	11.7	5.4	1.7 - 25.4	24	66.0	17.0	24.6 - 94.6	17.0	6.1	8.6 - 32.6
May 1998	300-540 m^3s^{-1}	48	48.6	27.4	12.7 - 105	2.3	1.7	0.6 - 10.3	48	50.7	24.0	22.5 - 130	2.2	1.7	0.8 - 12.6
May 1999	410-620 m^3s^{-1}	54	403	178	73.2 - 901	7.1	3.0	1.4 - 14.9	53	180	61.6	78.8 - 422	4.7	2.5	2.7 - 20.5
May-June 1992	160-400 m^3s^{-1}	64	417	201	181 - 860	33.3	13.4	16.2 - 77.2	60	183	28.2	129 - 246	28.7	43.1	12.8 - 353
August 1998	340-675 m^3s^{-1}	57	151	59.1	13.5 - 415	6.2	7.0	1.2 - 56.7	62	228	85.1	16.9 - 434	9.8	8.1	1.4 - 68.9
August 1999	410-660 m^3s^{-1}	60	4501	1694	2150 - 8823	205	61	88 - 386	69	4914	1278	2398 - 6830	190	31.7	100 - 256
WESTERN GRAND CANYON SECTION															
Collection Period	Discharge	n	Suspended Sediment				Suspended Organics								
			Avg	sd	min - max	n	Avg	sd	min - max	n	Avg	sd	min - max		
			Avg	sd	min - max	n	Avg	sd	min - max	n	Avg	sd	min - max		

TABLE 2. Average light-attenuation coefficients in the Colorado River measured over a range of constant and varying discharge levels in the four major canyons sections of Glen and Grand canyons.

Collection Period	Discharge	GLEN CANYON SECTION				MARBLE CANYON SECTION			
		Light Attenuation Coefficients				Light Attenuation Coefficients			
		n	Avg	sd	min - max	n	Avg	sd	min - max
June-July 1991	142 m ³ s ⁻¹	9	0.228	0.023	0.197 - 0.261	14	0.304	0.030	0.266 - 0.349
May-June 1994	227 m ³ s ⁻¹	8	0.291	0.010	0.285 - 0.298	20	0.364	0.029	0.321 - 0.406
August 2000	227 m ³ s ⁻¹	3	0.315	0.010	0.305 - 0.325	24	0.322	0.023	0.290 - 0.388
May 1991	425 m ³ s ⁻¹	6	0.217	0.015	0.202 - 0.231	14	0.324	0.048	0.225 - 0.398
May 1998	300-540 m ³ s ⁻¹	6	0.214	0.106	0.239 - 0.270	59	9.582	7.023	3.171 - 25.34
May 1999	410-620 m ³ s ⁻¹	18	0.304	0.021	0.283 - 0.327	48	0.363	0.039	0.274 - 0.498
May-June 1992	160-400 m ³ s ⁻¹	12	0.307	0.019	0.269 - 0.337	51	0.509	0.149	0.013 - 0.720
August 1998	340-675 m ³ s ⁻¹	3	0.325	0.005	0.320 - 0.330	44	0.749	0.188	0.527 - 1.377
August 1999	410-660 m ³ s ⁻¹	3	0.310	0.014	0.300 - 0.320	46	1.221	0.252	0.715 - 1.765
CENTRAL GRAND CANYON SECTION									
Collection Period	Discharge	Light Attenuation Coefficients				WESTERN GRAND CANYON SECTION			
		Light Attenuation Coefficients				Light Attenuation Coefficients			
		n	Avg	sd	min - max	n	Avg	sd	min - max
June-July 1991	142 m ³ s ⁻¹	27	0.470	0.091	0.349 - 0.577	18	0.549	0.078	0.439 - 0.658
May-June 1994	227 m ³ s ⁻¹	20	0.432	0.046	0.371 - 0.527	21	0.479	0.034	0.437 - 0.545
August 2000	227 m ³ s ⁻¹	54	0.380	0.019	0.340 - 0.418	69	0.540	0.181	0.360 - 1.041
May 1991	425 m ³ s ⁻¹	27	0.730	0.246	0.398 - 1.185	24	0.928	0.105	0.699 - 1.088
May 1998	300-540 m ³ s ⁻¹	48	10.21	3.253	6.097 - 17.33	48	4.877	1.067	3.431 - 7.137
May 1999	410-620 m ³ s ⁻¹	54	0.812	0.145	0.585 - 1.136	53	0.870	0.174	0.609 - 1.360
May-June 1992	160-400 m ³ s ⁻¹	64	1.715	0.458	0.700 - 2.632	60	1.404	0.230	0.318 - 1.788
August 1998	340-675 m ³ s ⁻¹	57	2.486	0.742	0.764 - 4.589	62	4.507	1.018	1.899 - 7.082
August 1999	410-660 m ³ s ⁻¹	60	74.18	10.68	54.17 - 97.01	69	110.4	19.44	74.67 - 166.8

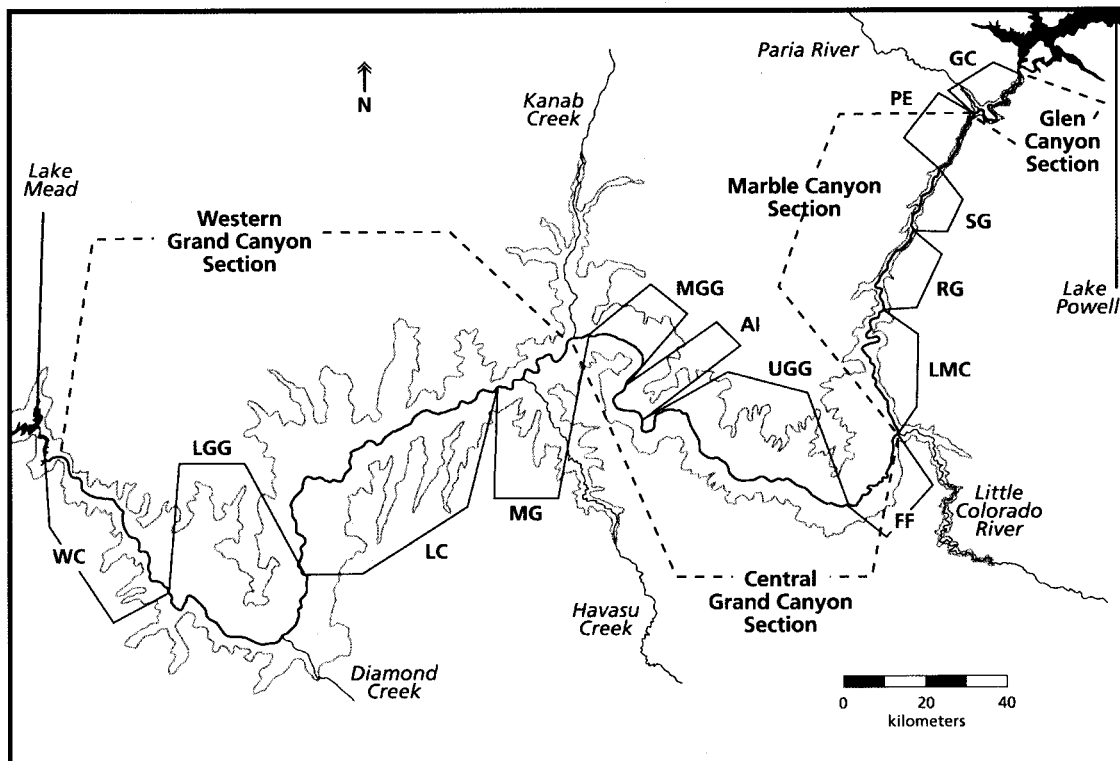


Figure 1. Map showing major canyon sections, geomorphic reaches, and tributaries of the Colorado River. Estimates of daily solar insolation were calculated at hectometer intervals along the entire river centerline for 474.5 km from Glen Canyon Dam to Lake Mead, AZ. Major canyon sections and geomorphic reaches included are: Glen Canyon Section (Glen Canyon (GC), 0 to 26.8 Rkm); Marble Canyon Section (Permian (PE), 26.8 to 43.5 Rkm; Supai Gorge (SG), 43.5 to 61.7 Rkm; Redwall Gorge (RG), 61.7 to 83.1 Rkm; Lower Marble Canyon (LMC), 83.1 to 124.3 Rkm); Central Grand Canyon Section (Furnace Flats (FF), 124.3 to 149.9 Rkm; Upper Granite Gorge (UGG), 149.9 to 214.9 Rkm; Aisles (AI), 214.9 to 227.3 Rkm; Middle Granite Gorge (MGG), 227.3 to 250.5 Rkm); and Western Grand Canyon Section (Muav Gorge (MG), 250.5 to 282.7 Rkm; Lower Canyon (LC), 282.7 to 369.4 Rkm; Lower Granite Gorge (LGG), 369.4 to 421.2 Rkm; Western Canyon (WC), 421.2 to 474.5 Rkm).

Figure 2. Normalized light-attenuation coefficients (K_N, m^{-1}) plotted in relation to suspended-sediment concentrations (gL^{-1}). Data are displayed graphically as a log-log plot to demonstrate the slight curvilinear response in K_N to increasing sediment concentrations in the Colorado River, Glen and Grand canyons.

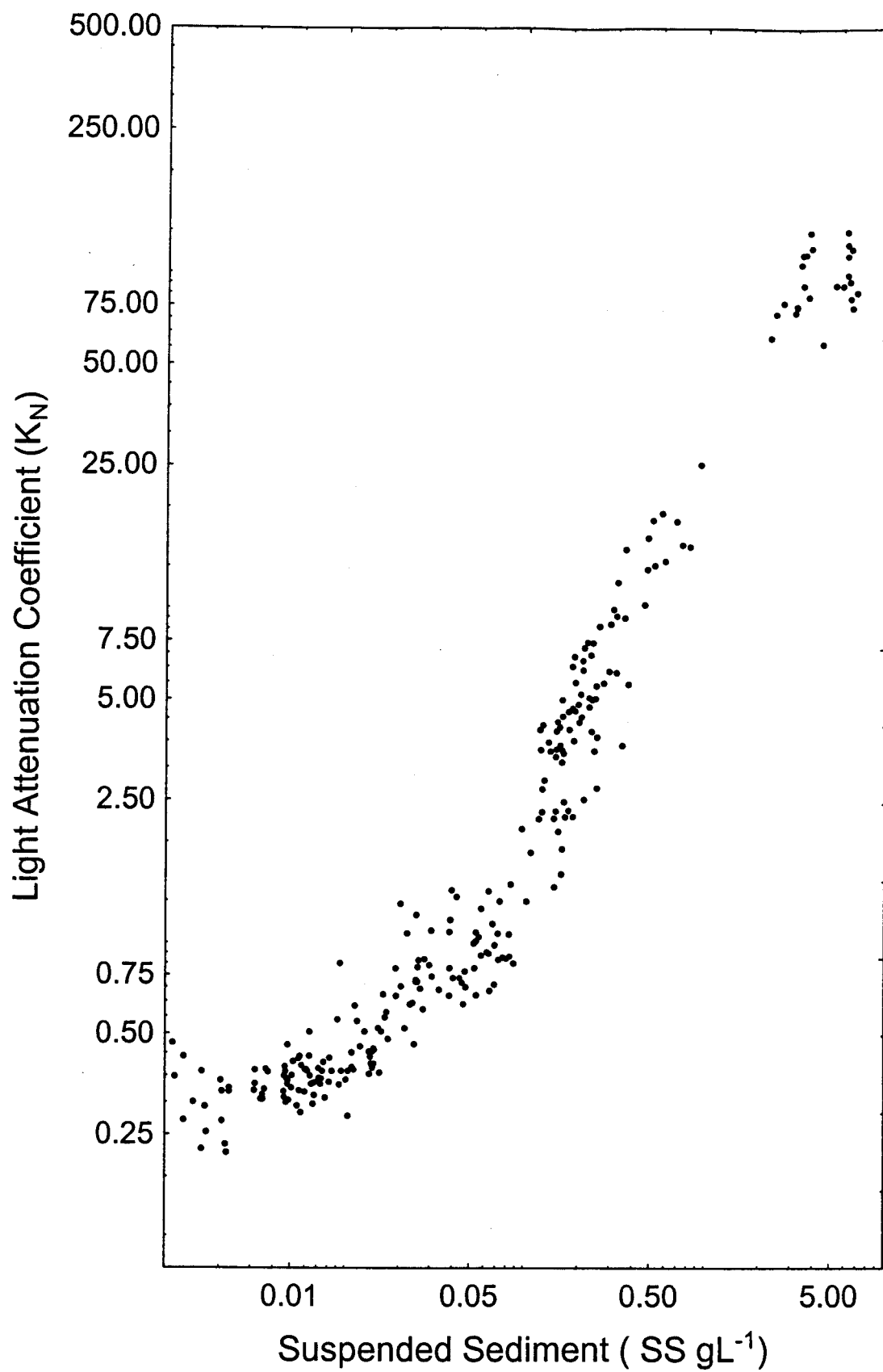


Figure 3. Sediment-light regression coefficients (β) are plotted for different hydrological events. Differences in β coefficients are attributed to differences in discharge among sampling trips. For sediment-limited conditions (Fig3-A), demonstrates a trend of decreasing β coefficients in response to discharge ($\beta = 15.4$ at $142 \text{ m}^3\text{s}^{-1}$, $\beta = 13.5$ at $227 \text{ m}^3\text{s}^{-1}$, $\beta = 10.8$ at $425 \text{ m}^3\text{s}^{-1}$, and $\beta = 8.0$ at $> 430 \text{ m}^3\text{s}^{-1}$). Whereas, under sediment enriched conditions (Fig 3-B), β coefficients become elevated ($\beta = 23.5$, May/June 1992; $\beta = 15.6$, August 1998; and $\beta = 16.4$, August 1999) in response to suspended-sediment supplied from major tributaries. Under these highly turbid conditions difference in β coefficients were independent of discharge.

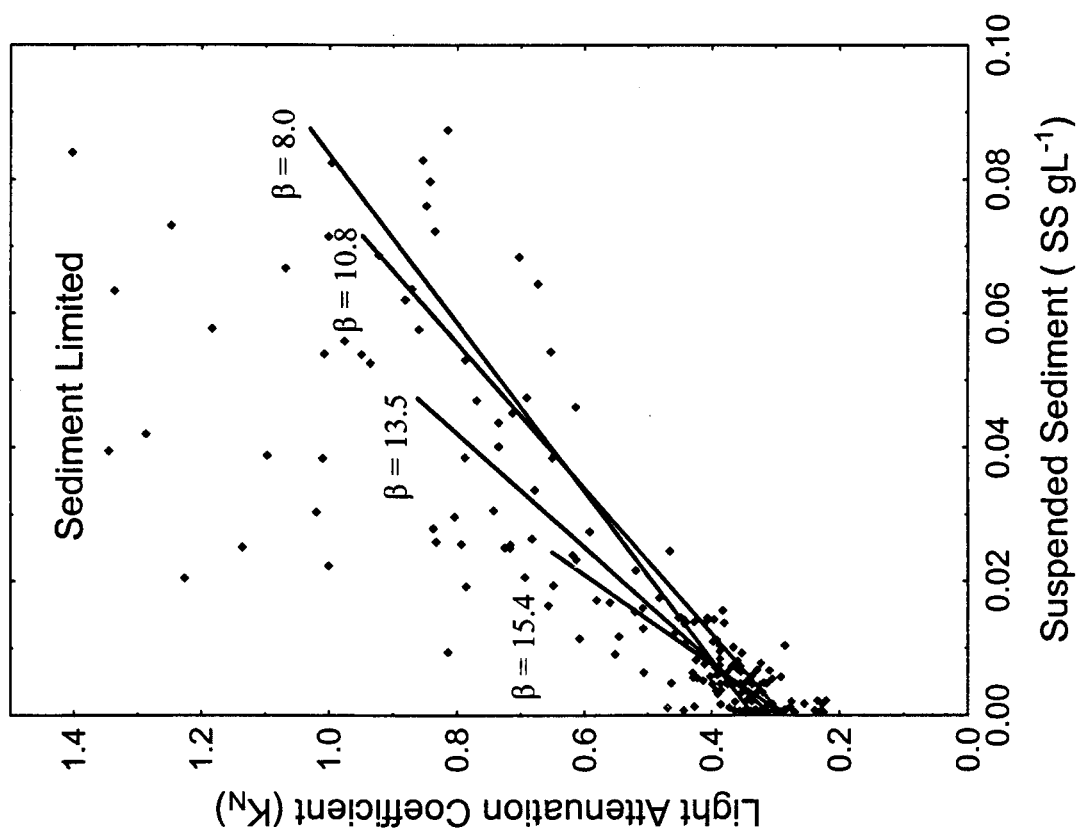
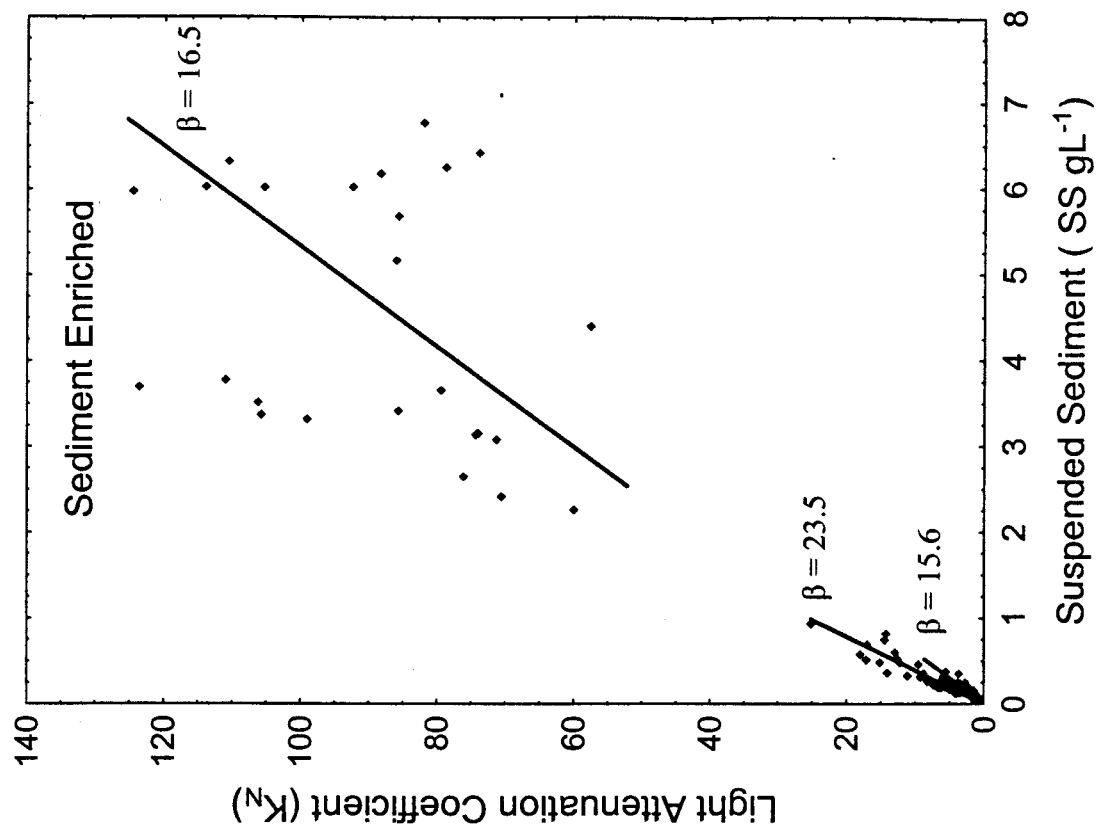


Figure 4. Randle and Pemberton's (1987) steady flow model was used for estimating channel characteristics (hydraulic area, top width, and depth) in Glen and Grand canyons. Based on the stage discharge relationship for a specific channel cross-section, width/depth ratios were estimated for both minimum (solid \blacklozenge) and maximum (open \circ) discharge levels (142 to 710 m^3s^{-1}). Ratios were averaged across multiple cross-sections and plotted against stream length (Rkm) from GCD.

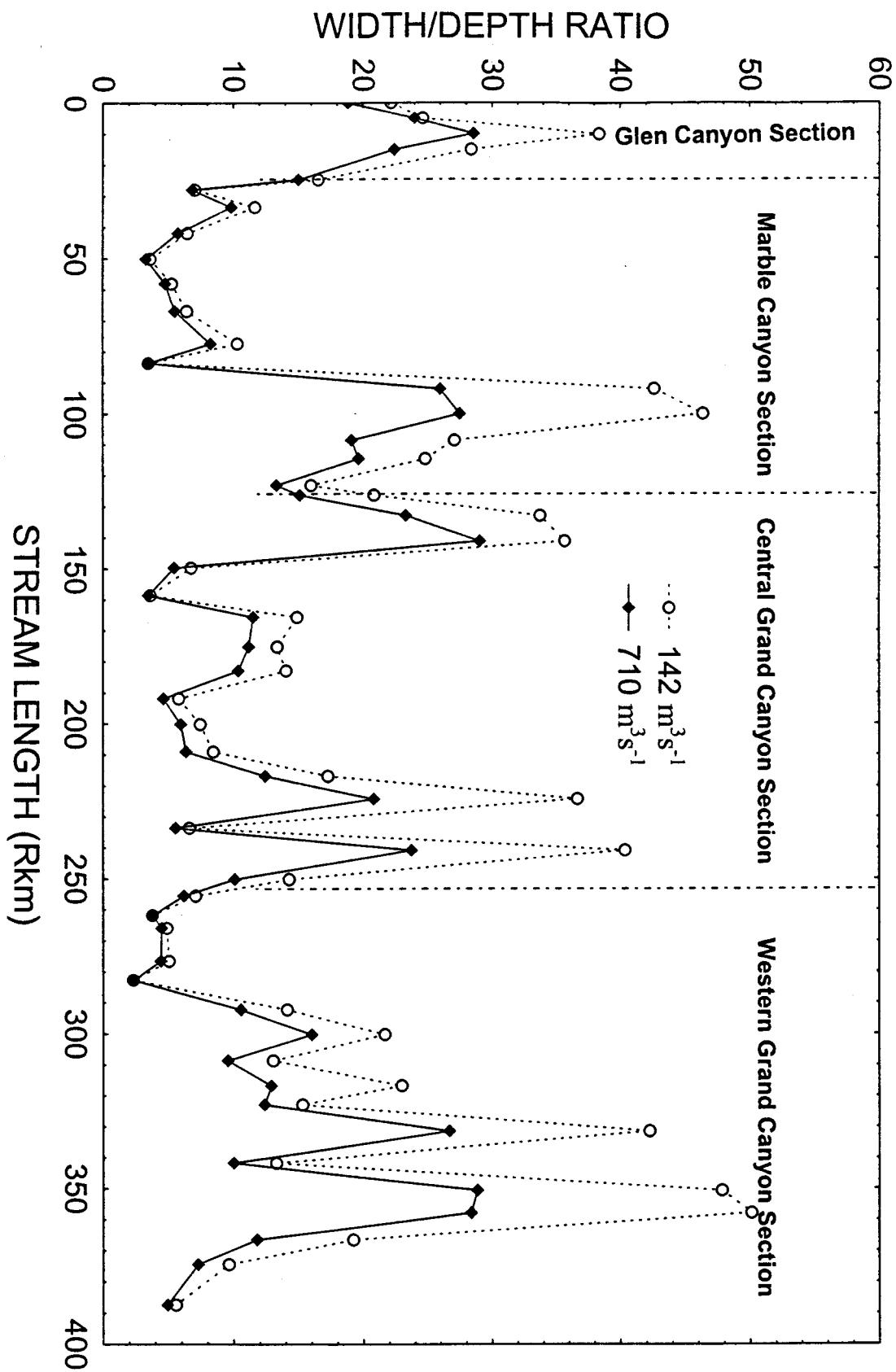
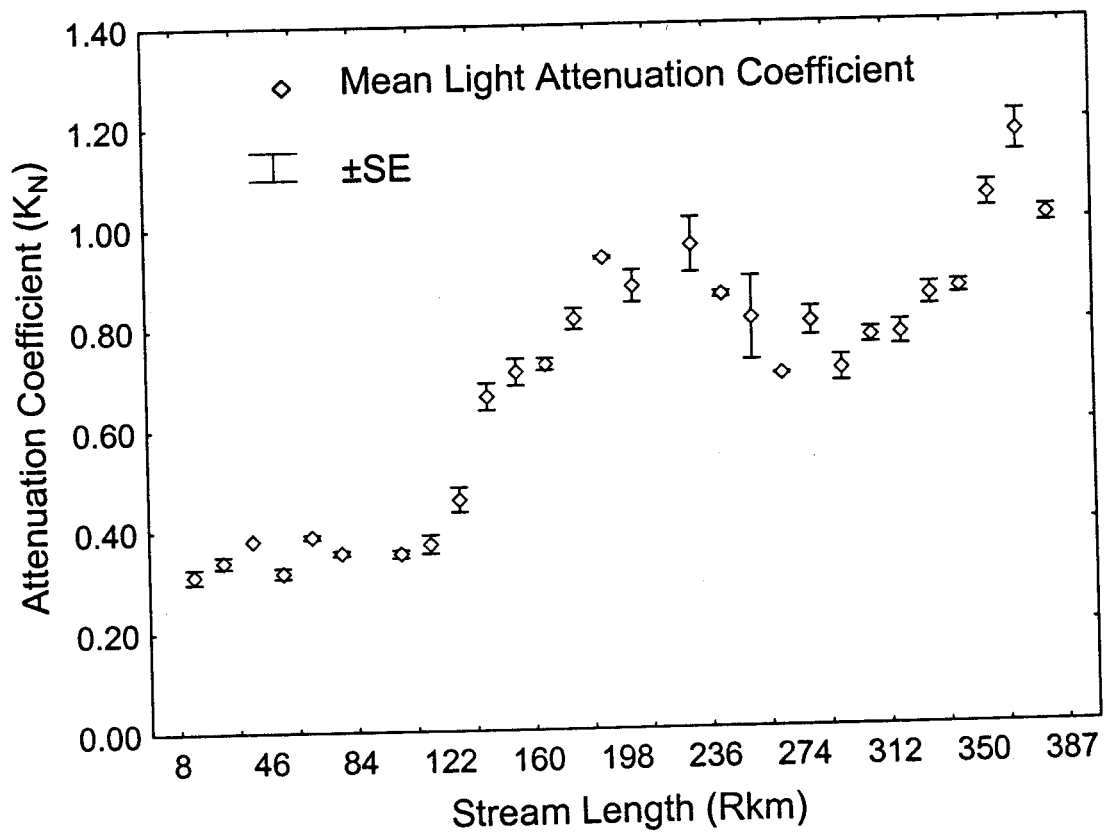
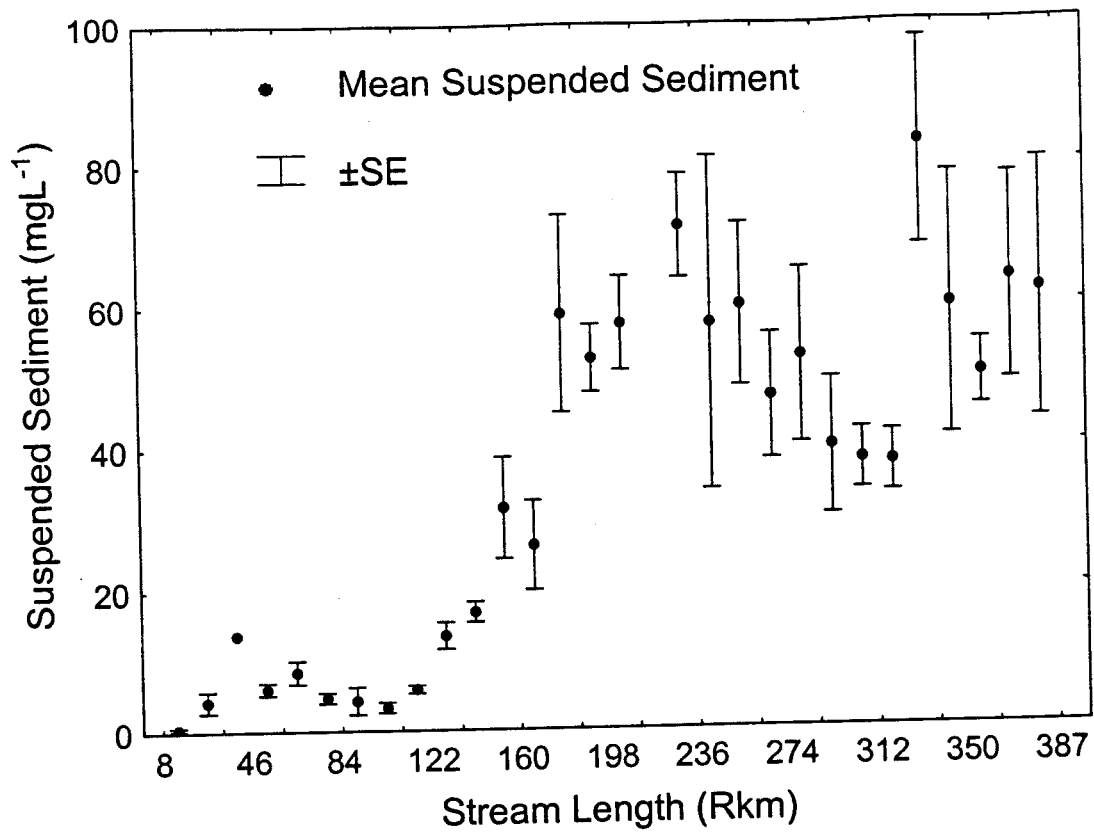


Figure 5. Under sediment-limited conditions, the typical longitudinal pattern observed for mean values ($1 \pm \text{SE}$) for: Fig 5-A, normalized light-attenuation coefficients (K_N); and Fig 5-B, suspended-sediment concentrations (gL^{-1}). This spatial pattern demonstrates the influence stream length and geomorphic characteristics has on apparent optical properties and sediment levels. Data were collected and measured during sediment-limited conditions from 22-31 May 1998, at discharges of $300\text{-}540 \text{ m}^3 \text{ s}^{-1}$.



CHAPTER 5

MODELING PHOTOSYNTHETIC PHOTON FLUX DENSITY IN A
FLUVIAL RIVER SYSTEM: LIGHT-ATTENUATION ESTIMATES FOR
THE COLORADO RIVER, GLEN AND GRAND CANYONS, AZ.

Abstract

In the regulated Colorado River downstream from Glen Canyon Dam, multiple factors are responsible for differences in underwater light availability, and appear primarily related to sediment transport and sediment-supply processes. Light-attenuation increases with increasing distance downstream. This spatial change in optical properties is partly due to sediment-supply events from tributaries, and the cumulative suspension and transport of sand reworked from channel and bar deposits. Spatial and hydrological interactions between stream-length, discharge, and channel characteristics are used to predict differences in suspended-sediment transport. A strong predictive relationship exists between suspended-sediment concentration and light-attenuation coefficients. There was a strong correspondence among light-attenuation estimates derived from this predictive relationship compared to independent data based on observations. Modeled results (1963-2002), indicate that the estimated median mid-day light-attenuation coefficients was 0.25 m^{-1} for Glen Canyon; 0.65 m^{-1} for Marble Canyon; 1.35 m^{-1} for Central Grand Canyon; and 2.02 m^{-1} for Western Grand Canyon. Estimates for total wetted area for the entire Colorado River showed an areal increase with increasing discharge levels, areal estimates ranged from 2,746 ha to 3,308 ha for respective steady

flows of $142 \text{ m}^3\text{s}^{-1}$ and $568 \text{ m}^3\text{s}^{-1}$. Conversely, photosynthetically available area (PAA), based on light penetration representing 1% of water-surface solar incidence under sediment-limited conditions, decreased with elevated discharge such that summer estimates for PAA decreased from 1,961 ha to 1,838 ha for a respective increase in flow from $142 \text{ m}^3\text{s}^{-1}$ to $568 \text{ m}^3\text{s}^{-1}$. However, because of reduced solar incidence during the winter season, estimates for PAA decreased, ranging from 1,813 ha to 1,078 ha for discharges of $142 \text{ m}^3\text{s}^{-1}$ and $568 \text{ m}^3\text{s}^{-1}$, respectively. This represented a 67% reduction in the total wetted area available for the winter season.

Introduction

Reduction of photosynthetic photon flux density (PPFD) in freshwater streams and rivers may impose physiological limitations on the phytobenthic inhabitants. This is especially evident in fluvial systems where apparent optical properties change due to the transport of suspended-sediment (Newcombe and MacDonald 1991; Shaver *et al.* 1997). In the regulated Colorado River downstream from Glen Canyon Dam (GCD), the distribution and abundance patterns for algae-macrophytes, macroinvertebrates, fishes, and water-birds are now strongly correlated to the spatio-temporal differences in suspended-sediment (Hardwick *et al.* 1992; Shaver *et al.* 1997; Stevens *et al.* 1997a, 1997b). In this altered ecosystem, *Cladophora glomerata* (Usher and Blinn 1990) and associated epiphytes (Hardwick *et al.* 1992; Benenati *et al.* 1998) comprise the primary phytobenthic component that relies entirely on availability of PPFD (Blinn and Cole 1991). This macroalgal and epiphytic association is considered the structural and energetic link that supports secondary and tertiary trophic levels in the regulated

Colorado River (Angradi 1994; Shannon *et al.* 1994; Benenati *et al.* 1998; Shannon *et al.* 2001).

Spatial distribution and availability of PPFD may be the most influential factor regulating phyto-benthic production in the Colorado River. Underwater light diminishes exponentially as a function of depth, $Q = Q_z e^{-Kz}$ (Kirk 1983) where K is the attenuation constant. Therefore any increase in light-attenuation acts to further reduce underwater PPFD and its availability for primary production. In the regulated Colorado River, apparent optical properties vary with distance downstream from Glen Canyon Dam, being determined primarily by dissolved organics in Glen Canyon, and by suspended-sediment in the downstream sections in Marble and Grand canyons. For well-mixed homogeneous flows, light-attenuation increase linearly with sediment concentration; therefore estimating sediment concentration is an affective means for characterizing apparent optical properties and estimating underwater PPFD at varying depths.

Most sediment transport models are designed to estimate movement of bed-load and suspended-loads, primarily as a means to predict sediment yield at larger time scales (annual yield) (Andrews 1991; Topping *et al.* 2000a, 2000b). Biotic responses to sediment-transport and sediment-supply can occur at much smaller time scales, and owing to the time-averaged conventions used, certain biological insights are often lost. Additionally, there appears to be no general agreement on selection of independent variables to predict suspended loads at varying temporal scales, this becomes problematic especially for river systems that have different sediment sources and delivery rates (Rubin and Topping 2001).

The purpose of this paper is to understand the nature of light-attenuation in the regulated Colorado River in order to make inferences about possible biological responses to certain types of environmental variability, primarily the effects of suspended-sediment. Our objectives, are: 1) to develop a light-sediment model that is regulated by sediment transport and supply processes; 2) to validate light-sediment model; 3) to determine the frequency distribution of light-attenuation in the different canyon sections; and 4) to estimate photosynthetically available area for different canyon sections and geomorphic reaches under varying discharge levels and seasons.

Method

Study area - The regulated Colorado River (CR) is strongly influenced by flows released from GCD. Operational constraints restrict GCD hourly and daily flow rates (BOR 1996) such that under normal power generation flow releases are diurnally variable, fluctuating between 142 to 710 m³s⁻¹ (minimum-maximum). Our study area extends a linear distance of 390-km downstream from GCD (36°56'06" N, 111°28'53" W) to Diamond Creek (DC, 35°46'15" N, 113°22'06" W; Fig 1). Stream length and site locations are referenced in relation to the distance from GCD measured in river kilometers (Rkm). We used confluence locations of major gaged tributaries to delineate the boundaries of the four major canyon sections (Stevens *et al.* 1997b).

Glen Canyon is the first canyon section that extends downstream from GCD (0 Rkm) to Paria River (PR, 27 Rkm). This canyon section is optically clear, small in length, and located upstream from all major gaged tributaries. Light-attenuation coefficients are primarily influenced by the dissolved organics originating from Lake

Powell reservoir (Chapter 3). In contrast, in downstream canyon sections light-attenuation characteristics are regulated primarily by fluvial rather than limnological processes, and herein will be the primary emphasis of this paper. Canyon sections and boundary locations are: Marble Canyon from PR to Little Colorado River (LCR, 124 Rkm); Central Grand Canyon from LCR to Kanab Creek (KC, 268 Rkm); and Western Grand Canyon from KC to Diamond Creek (DC, 390 Rkm). Areas excluded from our data collection and analysis are the geomorphic reaches below Diamond Creek (389.6 Rkm) and include a segment of the Lower Granite Gorge and the entire Western Canyon (WC) (Fig 1). These gaged tributaries contribute the majority of suspended-sediment, but represent only 2% of this river's mean annual discharge ($323 \text{ m}^3 \text{ s}^{-1}$). Physical and hydrological characteristics for these different gaged tributaries have been well described and studied extensively (Hereford 1984; Randle and Pemberton 1987; Andrews 1991; Graf *et al.* 1991; Topping 1997). Remaining sediment sources are from ungaged perennial and ephemeral tributaries, and at present their periodic contribution remains small but unaccountable (Melis 1997; Webb *et al.* 2000).

Data collection – Data were collected over a wide-range of field conditions, and different years (1992-2002), seasons, times, and sites. Sampling trips coincided with varying hydrological events that ranged from sediment-limited to sediment-enriched periods, and discharge conditions representing constant and variable daily flows. Photosynthetic photon flux density (PPFD) and suspended-sediment were measured and collected respectively, at pre-established sites distributed along the river at 8-km intervals. For each sampling site, three-to-four replicate samples (0.5-L) were collected mid-channel using a depth-integrated sampler (D-77 sampler) (Pemberton 1987; Rubin *et*

al. 1998). Suspended-sediment (SS, gL^{-1}) was determined by filtering samples onto pre-ashed glass filters (Whatman 934-AH 1.5 μm pore), desiccating (24-h, 60°C), weighing (± 0.1 mg), ashing (1-h, 500°C), and reweighing (Greenberg *et al.* 1992). Photometric measurements were collected in conjunction with SS samples using an underwater quantum scalar sensor (LiCor, Inc., LI-193SA), and cosine corrected quantum sensor (LI-190SZ). A series of photometric profiles were used for measuring photosynthetic photon flux density (PPFD), which includes the visible spectrum (400-700 nm) expressed in units of $\mu\text{mol quantum m}^{-2}\text{s}^{-1}$. Scalar light-attenuation coefficients (K_0, m^{-1}) provide a functional means to estimate PPFD integrated over all directions at a given underwater depth. Coefficients were determined by transforming (\log_e) ratios consisting of underwater to surface PPFD intensities and then regressing against the measured underwater depth (z) (Kirk 1983). Scalar attenuation coefficients were normalized (K_N) to account for effects attributed to zenith angle (θ_i) and refraction (i.e., refractive index of water ≈ 1.33), $K_N = \cos(\sin \theta_i \div 1.33) \cdot K_0$.

Light-attenuation suspended-sediment relationship – Sample distributions for sediment and light-attenuation data are considered representative of the environmental conditions encountered in the field. Because light and sediment measurements were not temporally paired during field collection activities, K_N coefficients and SS concentrations were averaged across the sampling period (15-min). Mean values for both variables were subdivided into two strata, representing sediment-limited and sediment-enriched conditions (i.e., tributary discharge exceeding $0.64 \text{ m}^3\text{s}^{-1}$).

We randomly sampled a small sub-set from the entire light-attenuation data set to test the effect that mean suspended-sediment (SS) and instantaneous discharge for the

Colorado River (Q_{CR}), Paria River (Q_{PR}), and the LCR-Cameron (Q_{LCR}) had on light-attenuation using a multiple linear regression. The remaining independent light-attenuation data were used to validate this predictive light-sediment relationship by comparing observed and estimated light-attenuation coefficients.

Hydraulic and Flow Routing Models - Two types of hydrological data were used in our analysis; data included stream flow records for both mean daily discharge and provisional real-time unit values (15-min intervals) from US Geological Survey for the Paria River (USGS 09382000), LCR-Cameron (USGS 09402000), LCR-Confluence (USGS 09402300), and US Bureau of Reclamation for GCD. Flow simulations provide a site-specific method for estimating: 1) instantaneous discharge; 2) average water velocity based on reach average cross-sections; and 3) stage-discharge relationships for specific channel cross-sections. Wiele and Smith (1996) developed a reach-averaged one-dimensional unsteady flow model to estimate the propagation of GCD discharge wave downstream. Additionally, a steady-state flow model developed by Randle and Pemberton (1987) was also used to numerically solve for hydraulic geometry as a function of flow. Both of these models have been combined into a graphic user interface called CRFSSGUI (Korman *et al.* 2000). This numerical model is used for estimating instantaneous water discharge for all sampling sites. Hydraulic parameters (slope, depth, cross-sectional area, stage, and top-width) used in this model were derived from USGS bed material maps. Instantaneous discharge estimates were used for calculating hydraulic characteristics at sampling sites, as well as average channel characteristics across all cross-sectional profiles contained within a designated geomorphic reach or canyon section (Stevens *et al.* 1997b).

Sediment transport and sediment-supply – The empirical relationship that best describes the spatial variability in sediment transport for estimating suspended-sediment (SS, gL⁻¹) in the regulated Colorado River is:

$$SS = \left[\begin{array}{l} 0.057 + (-0.909 \cdot Rkm) + (0.041 \cdot Rkm \cdot Q_{CR}) + \\ (0.003 \cdot Rkm \cdot WD) + (-0.0001 \cdot Rkm \cdot Q_{CR} \cdot WD) \end{array} \right] \cdot 1000 + (Tributary \ WL). \quad (1)$$

where the interactions occurring between stream length (Rkm), Colorado River mainstem discharge (Q_{CR}) and width/depth ratios (WD) are used to predict differences in suspended loads by accounting for spatial and hydrological effects (Chapter 4). The remaining sediment is the wash-load contribution, which originates from primary gaged tributaries and is independent of bed-load and suspended-bed material because it remains in suspension once it is discharged into the Colorado River.

Wash-load consists of fine silts and clays (<0.0625 mm) and represents the largest proportion of sediment (50-90%) supplied by tributaries (Randle and Pemberton 1987; Topping *et al.* 2000a). Physical location of the PR gage station relative to its confluence with the CR allows for wash-load to be routed downstream without accounting for a lag-time prior to routing flow downstream using conventional hydraulic models (Korman *et al.* 2000). However, this is not the case for the LCR-Cameron gage, which is located 95-km upstream from the LCR-Confluence. The differences in flow rate for the LCR (Q_{LCR}) discharge were determined by temporally matching peak discharges between gage stations, and then regressing the log transformed peak Q_{LCR} against travel time to the LCR confluence.

Two different methods were used to disperse suspended-sediment downstream from tributaries. The first method was used when comparisons among observed and estimated light-attenuation coefficients required greater temporal and spatial resolution. An instantaneous suspended-sediment concentration (15-min) was estimated based on sampling location and date-time, by the following series of computational steps: 1) estimate instantaneous discharge at sample site; 2) back-calculate travel time from gaged tributaries using average water velocity (Wiele and Smith 1996); 3) select real-time unit values to nearest 15-min interval; 4) estimate suspended load from tributary using sediment-rating curves (discharge and seasonal conditions) (Randle and Pemberton 1987; Topping 1997); 5) convert density estimate to mass (Kgs^{-1}); 6) convert total SS to an equivalent wash-load proportion; 7) convert to concentration (gL^{-1}) based on instantaneous discharge (Korman *et al.* 2000); 8) combine predicted estimates of SS for tributary wash-load discharge and suspended-sediment transport (Eqn 5); 9) convert the instantaneous total SS estimate to an equivalent K_N coefficient (Eqn 4); and lastly 10) convert K_N coefficients to K_O coefficients based on date-time (Eqn 2).

The second dispersal method used a larger time-scale (one-day average) for estimating and dispersing suspended-sediment. We determined the frequency that each of the major canyon sections were influenced by mean daily sediment discharges when one or more of the gaged tributaries exceeded base flow conditions ($> 0.64 \text{ m}^3\text{s}^{-1}$). Average daily suspended-sediment concentration for post-GCD flows (water-year: 1963-2002) was estimated using mean daily flow records for the major gaged tributaries. Estimates for suspended-sediment in Western Grand section are underestimated and only

include hydrological data for Kanab Creek gage station (USGS 09403780), which was operated only through water-years 1964-1980.

Frequency analysis for modeled light-attenuation coefficients derived from suspended-sediment estimates was performed for each geomorphic reach and canyon section. We used a fixed-discrete approach to spatially route mean daily discharge for tributaries and the Colorado River. Typically for Glen and Marble canyons, flows travel through these canyon sections within the first-day. Further downstream these same flows reach the middle part of Central Grand Canyon by the second-day, and within the third-day have reached the Western Grand Canyon section. This fixed-discrete approach (24-h) is not as computationally robust or precise as the first dispersion method that estimates an instantaneous discharge and average flow velocity (15-min interval) (Wiele and Smith 1996). However, the mean daily dispersion method provides a general characterization of the flow and underwater light-attenuation pattern, although under certain hydrological conditions (i.e., excessively high or low discharges) these rates will depart from this three-day flow pattern.

Light-depth penetration – A light-depth estimate provides a useful parameter to compare modeled results (Kirk 1983). Convention has it that 1% of light-depth corresponds to an attenuation distance of $\zeta = 4.6$ (Falkowski and Raven 1997). Since PPF_D is dependent on light-attenuation, we have estimated the vertical light-depth that represents 1% of the proportion of underwater light remaining after light-attenuation:

$$z_{1\%} = \zeta / K_N \quad (2)$$

where $z_{1\%}$ is light-depth, ζ is the attenuation distance, and K_N is coefficient of normalized light-attenuation. Although these light-depths should not be thought of as an actual measure of the compensation depth for algae, they do provide a general characterization of the vertical extent of the euphotic zone.

Changes in K_N coefficients are independent of angular differences in θ ; therefore, underwater PPF_D is often overestimated unless K_N coefficients are adjusted to represent apparent environmental conditions. In general, light-depth estimates vary in response to diurnal and seasonal differences in solar zenith angle (θ); therefore, in order to estimate apparent underwater PPF_D at depth within the water column, K_N must be converted to K_O . The conversion used is:

$$K_O = K_N / \cos(\sin \theta / 1.33) \quad (3)$$

where K_N represents the normalized light-attenuation coefficient, θ is the solar zenith angle, and 1.33 is the refractive index of water. Mid-day values for solar zenith angle vary seasonally; therefore, estimates used for θ angle varied from 13.5° to 60.4° (i.e., convert zenith angle degrees to radians) for respective summer and winter periods.

Model Validation - Models used for estimating PPF_D in aquatic environments often lack validation studies, which are useful in determining whether or not modeled outputs are accurate, and if the model is a consistent representation of the referent system (Oreskes *et al.* 1994). We compared the performance of this light-sediment model using independent data. Provisional real-time unit values were used for determining relative error around the estimate by comparing differences among measured and estimated K_O

coefficients. The relative error, $RE = (E - O/O)$, is the calculated error relative to the estimated (E) and observed (O) measurement. Using a bootstrap technique, RE and confidence intervals ($CI_{95\%}$) were determined for a range of estimated K_O coefficients. For each resample, 30 random samples were sampled from observed data, stratified for sediment-limited conditions representing high clarity ($K_O \leq 0.8$), and for sediment-enriched conditions representing medium turbidity ($K_O > 0.8$ and ≤ 1.6) and high turbidity ($K_O > 1.6$). The average mean RE was then calculated for K_O by iteratively resampling with replacement for a total of 1,000 bootstrap samples (Resampling Stats, Inc., 2001). Additionally, relative error was also determined for light-depth calculations by comparing differences among measured and estimated light-depth penetration (Eqn 1 & Eqn 2).

Photosynthetically available area – Vertical light penetration has biological significance for photoautotrophs because estimated light-depths (z) correspond to the proportion of solar incidence remaining after PPFD has been attenuated (Kirk 1983). To quantify the photosynthetically available area (PAA) of the euphotic zone we calculated depth representing the specific algal compensation point (z_{CP}) using:

$$z_{CP} = -\ln(Q_0/Q_z)/K_O \quad (4)$$

where Q_0 is the solar incidence at the surface, Q_z is the underwater PPFD at depth, and K_O is the scalar light-attenuation coefficient. In the CR ($11^\circ\text{C} \pm 1^\circ$), *C. glomerata* and its associated epiphytes have a compensation point equivalent to $25\text{-}35 \mu\text{mol quanta m}^{-2}\text{s}^{-1}$ (Chapter 6). We were able to compare differences in euphotic depth in response to

changes in either optics or seasonal solar intensity by using this PPFD level as a threshold value (i.e., compensation point is the PPFD level where gross primary production equals daily metabolic demands). We evaluated seasonal differences in PPFD and mid-day values for Q_0 that were equivalent to maximum solar incidence. Maximum PPFD mid-day values range seasonally between 2020-1980 and 1200-1150 $\mu\text{mol quanta m}^{-2}\text{s}^{-1}$ for summer and winter, respectively.

A one-dimensional steady state simulation model (Randle and Pemberton 1987) was then used to estimate the proportion of total wetted area (TWA) available in the channel for photosynthesis. For comparative purposes, we assumed a steady uniform flow condition and calculated water surface elevations at known cross-sections using established stage-discharge relationships. PAA was estimated for two discharge levels (142 and 568 m^3s^{-1}) representing the normal range of GCD operations. Modeling hydraulic parameters provides a means to quantify the areal extent of the euphotic zone.

It was assumed that the photosynthetic perimeter (PP) was equal to the total wetted perimeter (TWP), if z_{CP} was greater than maximum channel depth (z_{MAX}); conversely, if z_{CP} was less than z_{MAX} we used the trapezoidal characteristics of the channel to estimate PP by using top-width, z_{MAX} , and hydraulic area to estimate the upper segments of the PP (Fig 2). Surface area for the channel-bed was determined by multiplying stream length between cross-sectional perimeter and then summing across all cross-sectional segments along the longitudinal axis of the river.

Statistical analysis – We used a combination of statistical tests, that included: simple (SLR), multiple linear regressions (MLR), and analysis of variance (ANOVA)

(Netter *et al.* 1996; Sokal and Rohlf 1995). Multiple statistical packages were used (SAS Institute, Inc. 2000; StatSoft, Inc., 2002; Resampling Stats, Inc., 2001).

Results

Light-attenuation model – We randomly sampled from our light-sediment data set to test the effect of mean suspended-sediment (SS) and instantaneous discharge ($\text{m}^3 \text{s}^{-1}$) for the Colorado River (Q_{CR}), Paria River (Q_{PR}), and the LCR-Cameron (Q_{LCR}) on light-attenuation. The multiple-linear regression was significant ($F_{4,47} = 71.7$, $p < 0.001$), and the equation for estimating K_N was:

$$K_N = 0.23 + SS \cdot 8.38 + (Q_{CR} \cdot -0.0001 + Q_{PR} \cdot 0.60 + Q_{LCR} \cdot 0.57) \quad (5)$$

where, SS represents concentration levels for suspended-sediment. The flow routing relationship ($F_{1,68} = 152$, $r^2 = 0.69$) used in estimating LCR-Cameron discharge (Q_{LCR}) travel time from the upstream gage station (USGS 09402000) is:

$$LCR \text{ Traveltime} = 64.2 - 15.8(\log Q_{LCR}). \quad (6)$$

Frequency analysis – The frequency (post-GCD, WY 1963-2002) that major canyon sections were influenced by suspended-sediment from tributary discharges that exceeded base flow conditions ($0.64 \text{ m}^3 \text{ s}^{-1}$) occurs 28% of the time for Marble Canyon, and 49% for Central Grand Canyon and Western Grand Canyon sections. This condition represents a period of sediment enrichment due to wash-load contribution. A separate

analysis was performed for Western Grand Canyon to assess the cumulative discharge frequency (temporally and spatially synchronized) from all major gaged tributaries including Kanab Creek (WY 1963-1981). Although the discharge gage for Kanab Creek was discontinued, results indicated that there were no differences in the frequency and duration of turbidity for lower Western Grand Canyon section because of the combined tributaries discharges ($> 0.64 \text{ m}^3 \text{ s}^{-1}$). Kanab Creek's sediment discharge appears to be temporally and spatially synchronized with the additional wash-load contribution from the Paria River and LCR. Because of this the combined discharges for all tributaries above base flow does not change the exceedance frequency for Western Grand Canyon section even though suspended-sediment concentrations appear to increase with additional sediment-supply.

The reciprocal condition occurs during a period of sediment-supply limitations when light-attenuation is not excessive. Although independent of wash-load contribution from tributaries, however due to sediment transport effects from discharge and channel characteristics this sediment-limited condition is not always representative of high water clarity. Notably, only ungaged tributaries influence the Glen Canyon section, and this sediment contribution is very infrequent and probably occurs less than 1% of the time (late summer monsoons) (Howard and Dolan 1981). When ungaged events do occur suspended-sediment might on occasion exceed 0.5 gL^{-1} (Chapter 3); yet, the resulting elevated light-attenuation coefficients ($K_N = 5.3 \text{ m}^{-1}$) have been observed to return to nominal levels ($K_O = 0.200\text{-}0.270 \text{ m}^{-1}$) within a 12-h period. However the frequency that the Colorado River continues to have high water clarity conditions becomes reduced once

the wash-load contribution from tributaries is combined with sediment transport downstream of the Paria River.

Light-attenuation coefficients (i.e., mean mid-day K_O coefficients for WY 1963-2002) for upper and lower canyon sections were significantly different ($p < 0.001$, $n = 14,245$). K_O coefficients exceeded 0.8 m^{-1} 26.2%, 69%, 83.6% of the time for Marble Canyon, Central Grand Canyon and Western Grand Canyon sections, respectively. For each of the four major canyon sections the median and minimum-maximum range for K_O coefficients were equal to: 0.247 m^{-1} ($0.205\text{-}5.38 \text{ m}^{-1}$) for Glen Canyon, 0.648 m^{-1} ($0.235\text{-}59.9 \text{ m}^{-1}$) for Marble Canyon, 1.35 m^{-1} ($0.254\text{-}295 \text{ m}^{-1}$) for Central Grand Canyon, and 2.02 m^{-1} ($0.296\text{-}355 \text{ m}^{-1}$) for Western Grand Canyon. Cumulative frequency distribution of light-attenuation coefficients is graphically displayed for the four major canyon sections (Fig 3). Relative, cumulative, and exceedance frequencies for a range of different light-attenuation coefficients are tabulated for the four major canyon sections (Table 1).

Model Validation – Model validation compared instantaneous observed and estimated light-attenuation coefficients based on the first method. For sediment-limited conditions, average mean relative error (RE) for an estimated instantaneous K_O coefficient $< 0.8 \text{ m}^{-1}$ was 15% ($CI_{95\%}$, 10-21%). Under moderately turbid conditions the average mean RE was 25% ($CI_{95\%}$, 20-29%) for estimated K_O coefficients ranging between $> 0.8 \text{ m}^{-1}$ and $\leq 1.6 \text{ m}^{-1}$. During periods of sediment-enrichment ($> 1.6 \text{ m}^{-1}$), differences among estimated and observed K_O coefficients were considerably larger. The average mean RE was 55% ($CI_{95\%}$, 46-125%).

Modeled results appear to explain much of the spatio-temporal variability in light-attenuation observed in this ecosystem, from sediment-limited to sediment-enriched periods. Observed and estimated values of light-depth penetration ($z_{1\%}$) were strongly and linearly correlated ($R^2 = 0.89$, Fig 4). Overall average mean RE for light-depth penetration ($z_{1\%}$) ranged from 10% RE for high clarity conditions, which are equivalent to light-depth penetrations ranging between 22 m to 5.76 m; 37% RE for moderately turbid conditions having a light-depth penetration of 5.75 m to 2.88 m; and 195% RE for highly turbid conditions with a light-depth penetration of 2.87 m to 0.03 m. For high clarity conditions differences between observed and estimated K_O coefficients ranged from 0.2 m^{-1} to 0.4 m^{-1} , corresponding to a range in $z_{1\%}$ from 23 m to 11.5 m. Thus, high clarity RE of 10% represents a significant difference for estimates of light-depth penetration. Under highly turbid conditions light-depth differences as great as 195% RE for estimated and observed values may not be biologically significant, because for these turbid conditions $z_{1\%}$ represents a range from ? m to ? m.

Photosynthetic Available Area – Overall mean channel depth (z) and TWA increase with discharge from 142 to $568 \text{ m}^3 \text{ s}^{-1}$; however, the resulting channel expansion in the CR failed to result in increasing PAA (Table 2). Although, Glen Canyon and Marble Canyon sections had an increase in PAA with increasing discharge, the cumulative increase in suspended-sediment with increasing discharge results in increasing K_O , which further reduces PAA in the lower canyon sections. This offsets any areal gains made in upstream canyon sections due to an increase in TWA. For summer, system-wide estimates for PAA were 1,961 ha and 1,838 ha for $142 \text{ m}^3 \text{ s}^{-1}$ and $568 \text{ m}^3 \text{ s}^{-1}$, respectively. During winter seasons reduced PAA was due to seasonal shifts in zenith

angle that increased K_D , and reduced mid-day solar maximum PPFD intensities. Higher flows further increased light-attenuation due to increased suspended-sediment loads. For winter, system-wide estimates for PAA were 1,813 ha and 1,078 ha for $142 \text{ m}^3 \text{ s}^{-1}$ and $568 \text{ m}^3 \text{ s}^{-1}$, respectively (Table 2).

Discussion

Simulation models are an effective method for understanding complex and large-scale systems and ecological processes occurring in the Colorado River (Cale *et al.* 1989; Oreskes *et al.* 1994). We integrated a series of predictive yet independent relationships together, such as: hydraulic geometry, unsteady flow routing, sediment transport, and sediment dispersion for making spatio-temporal estimates of light-attenuation (Randle and Pemberton 1987; Pemberton 1987; Wiele and Smith 1996; Topping 1997; Korman *et al.* 2000).

Multiple factors are responsible for differences in underwater light availability, and appear primarily related to sediment transport and supply processes, as well as seasonal differences in solar zenith angle (Chapter 3 & 4). The responsible factors are listed below: 1) sediment transport is a function of discharge; 2) progressive depletion of bed material occurs as finer grain sizes are transported downstream at faster rates than coarser particle-sizes during the time between tributary supply (Rubin *et al.* 1998, Topping *et al.* 2000b, Rubin and Topping 2001); 3) tributaries function as the primary sediment source (Randle and Pemberton 1987; Topping 1997); 4) sediment concentrations are influenced by channel characteristics and stream length (Schmidt 1990; Rubin *et al.* 1998); 5) topography interferes with incoming solar insolation.

Frequent sediment discharges from tributaries are the most significant factor regulating light-attenuation in the Colorado River. Sediment contribution for both the PR and LCR account for over 70% of the annual sediment yield, of which 50-90% consists of fine silts and clays (Randle and Pemberton 1987; Topping *et al.* 2000a). Because wash-load remains in suspension it is rapidly exported, and only settles out once average flow velocities are reduced (Knighton 1984). There is an increase in suspended-sediment transport with stream length (Chapter 4), as well as a decrease in the median grain size distribution of suspended-sediment (Topping 2000a, 2000b, Rubin and Topping 2001). Differences in particle size, shape and refractive characteristics for equivalent suspended concentrations can significantly alter the light-attenuation characteristics of water (Kirk 1994). This trend toward “fining” (Rubin *et al.* 1998; Topping *et al.* 2000a) has resulted in a longitudinal gradient of increasing light-attenuation with distance downstream from GCD (Rubin and Topping 2001).

The method we have used to estimate suspended-sediment is not based on a mass balance approach, but recognizes implicitly that conservation of mass is maintained by tributary events that episodically supply sediment to this river system. Sediment-supply from tributaries functions independently of discharge, such that tributary flows govern the frequency, duration, and magnitude of sediment supplied to this system. Although the quantity of tributary sediment (bed- and suspended-load) is not accounted for in our modeling approach, these periodic contributions are the source of suspended-sediment transported in the CR during sediment-limited conditions. And it is only during these sediment-limited conditions that primary production is most likely to occur. Both of these fluvial processes, sediment transport and sediment-supply influence the spatial and

temporal distribution of suspended-sediment, and hence underwater light availability in the downstream canyon sections (Fig 1).

Although an incorrect assumption, we have for computational convenience assumed that sediment-supply and transport are in equilibrium and that the remaining sediment contributed by tributaries replenishes the bed-load that is being depleted during sediment-limited periods. This assumption is an oversimplification and does not account for effects from seasonal hysteresis, bed depletion or shifts in grain size distribution that may rapidly or chronically occur due to variability in climate and flow operations at GCD (Hereford 1984; Rubin *et al.* 1998; Topping *et al.* 2000a, 2000b; Rubin and Topping 2001). Additionally, the frequency analysis does not account for the cumulative loss of channel and bar deposits over time. It is more likely that continued loss of sand from these downstream canyon sections will only result in a higher frequency of reduced light-attenuation. This has already occurred for Glen Canyon, and a similar response is presently being observed for Marble Canyon (Topping *et al.* 2000a, 2000b; Rubin and Topping 2001). Because of the reduced light-attenuation over the life expectancy of the dam (700-yr) we would predict that the availability of PPFD for primary production would only increase with time.

Growth and productivity of *Cladophora glomerata* contributes significantly to the productivity of the regulated Colorado River, and influences other biotic components of this ecosystem. Therefore, the duration of time that algae are below PPFD threshold levels will restrict growth rates, photosynthetic yield, and colonization (Shaver *et al.* 1997; Benenati *et al.* 1998). Reported compensation points and onset of light saturation (maximum photosynthetic rate) for this algal species range from 25-35 and 300-600 μmol

quanta $\text{m}^{-2}\text{s}^{-1}$ respectively (Chapter 6). Although *C. glomerata* appears photosynthetically adapted to low light levels (Adams and Stone 1973; Graham *et al.* 1982), periods of exclusion below actual compensation point ultimately determine its vertical and longitudinal distribution throughout the overall river channel.

Spatial and temporal patterns in light-attenuation coefficients correspond strongly to distribution and standing biomass patterns of the phytobenthos and macroinvertebrates currently found in Colorado River (Blinn *et al.* 1995; Stevens *et al.* 1997b). Owing to unsteady flow patterns released from GCD, downstream canyon sections and geomorphic reaches are frequently characterized by high light-attenuation. Due to the cross-sectional radius most of the wetted perimeter in the channel is disproportionately found in the deeper regions. For this reason, PPFD availability may not be sufficient to support primary production throughout the entire submerged channel (Fig 2). Since PPFD diminishes exponentially as a function of depth, elevated light-attenuation reduces or totally eliminates what would otherwise be available to the phytobenthos. The contraction of the PAA into the upper region of the cross-sectional area may have significant effects on seasonal growth patterns and overall system-wide production.

A limitation to PPFD availability at different channel depths may not only restrict the vertical distribution of algae, but also colonization rates, thus limiting growth solely to the upper littoral region of the channel margin. This same region, referred to as the varial zone, is often influenced by flow fluctuations, which result in desiccating and reducing algal biomass (Usher and Blinn 1990; Benenati *et al.* 1998). The effect seasonal light-limitation has on the algal community will be entirely dependent on its colonization response rate for the deeper channel areas. Therefore, once light conditions become more

optimal colonization rates appear to be the biotic limitation to primary production. Secondary studies indicate that > 6-mo period is required for colonization (Benenati 1998). These slow colonization rates may result in total exclusion, even though deeper channel regions are seasonally available. When these downstream canyon sections have prolonged periods of variable flows and suspended-sediment, these same sections often become dominated by *Oscillatoria spp* (Shaver *et al.* 1997; Stevens *et al.* 1997b). These blue-green algae are known to be very tolerant of low-light intensities and exposure to desiccation (Shaver *et al.* 1997; Benenati *et al.* 1998). Although, *Oscillatoria* is abundant under these sediment enriched and sub-aerial conditions, and appears not to have any direct linkage to higher trophic levels (Shannon *et al.* 2001).

Although not universally applicable to other rivers systems, our mechanistic approach in modeling potentially provides a method for assessing availability of PPF_D for seasonal phytobenthic production under varying underwater light environments. Recent technological advances using laser diffraction for the continuous monitoring of suspended-sediment concentration and grain size may in the near future provide an alternative means to estimate underwater light-attenuation in a fluvial systems with greater spatial and temporal accuracy (Gartner *et al.* 2001; Melis *et al.* 2002). The framework we have developed to explain causal processes and effects on light-attenuation in the Colorado River provides a conceptual and analytical method that may allow for better understanding of growth dynamics of the phytobenthic community, as it is influenced by operational flow strategies and tributary sediment discharges.

References

- Adams, M. S. & W. Stone, 1973. 'Field studies on photosynthesis of *Cladophora glomerata* (Chlorophyta) in Green Bay, Lake Michigan', *Ecology*. 54: 853-862.
- Andrews, E. D., 1991. Sediment Transport in the Colorado River Basin. *In*. Committee on Glen Canyon Environmental Studies (Eds) *Colorado River ecology and Dam Management*. National Academy Press, Washington D.C. pp. 54-74.
- Angradi, T. R. 1994. 'Trophic linkages in the lower Colorado River: multiple stable isotope evidence', *N. Amer. Benth. Soc.* 13: 479-495.
- Benenati, P., J. P. Shannon, & D. W. Blinn, 1998. Desiccation and recolonization of phyto-benthos in a regulated desert river: Colorado River at Lees Ferry, Arizona, USA. *Regul. Riv.* 14: 519-532.
- Blinn, D. W., Truitt, R. & A. Pickart, 1989. 'Response of epiphytic diatom communities from the tailwaters of Glen Canyon Dam, Arizona, to elevated temperature.' *Regul. Riv.* 4: 91-95.
- Blinn, D. W., & G. A. Cole, 1991. Algal and invertebrate biota in the Colorado River: comparison of pre- and post-dam conditions. *In*. Committee on Glen Canyon Environmental Studies (Eds.) *Colorado River ecology and Dam Management*. National Academy Press, Washington D.C., pp. 102-123.
- Blinn, D. W., J. P. Shannon, L. E. Stevens, & J. P. Carder, 1995. Consequences of fluctuating discharge for lotic communities. *J.N. Am. Benthol. Soc.* 14: 233-248.
- BOR 1996. Operation of Glen Canyon Dam Colorado River storage project, Arizona: final environmental impact statement. U.S.DOI. BOR., pp. 320.
- Cale, W. G., G. M. Henebry & J. A. Yeakley, 1989. Inferring processes from pattern in natural communities. Can we understand what we see? *Bioscience*. 39: 600-605.
- Falkowski, P. G., & J. A. Raven, 1997. *Aquatic photosynthesis*. Blackwell Science, Malden, Mass.
- Gartner, J. W., R. T. Cheng, P. Wang, & K. Richter, 2001. Laboratory and field evaluation of the LISST-100 instrument for suspended particle size determinations. *Mar. Geology*. 175: 199-219.
- Graf, J. B., R. H. Webb & R. Hereford, 1991. Relation of sediment load and flood-plain formation to climatic variability, Paria River drainage basin, Utah and Arizona. *Geol. Soc. of Am. Bull.* 103: 1405-1415.

- Graham, J. M., M. T. Auer, R. P. Canale, & J. P. Hoffman, 1982. Ecological studies and mathematical modeling of *Cladophora* in Lake Huron: 4. Photosynthesis and respiration as functions of light and temperature. *J. Great Lakes Res.* 8: 100-111.
- Greenberg, A. E., L. S. Clesceri, & A. D. Eaton, 1992. (Eds.) *Standard methods for the examination of water and wastewater*. 18th Edition. American Public Health Assoc.
- Hardwick, G. G., D. W. Blinn, & H. D. Usher, 1992. Epiphytic diatoms on *Cladophora glomerata* in the Colorado River, Arizona: longitudinal and vertical distribution in a regulated river. *Southwest. Nat.* 37: 148-156.
- Hereford, R. 1984. Climate and ephemeral-stream processes: Twentieth-century geomorphology and alluvial stratigraphy of the Little Colorado River, Arizona. *Geol. Soc. of Am. Bull.* 95: 654-668
- Howard, A. & R. Dolan, 1981. Geomorphology of the Colorado River in the Grand Canyon. *J. of Geology.* 89: 269-298.
- Kirk, J. T. O. 1983. *Light and photosynthesis in aquatic ecosystems*. Cambridge University Press, Cambridge, London., 401 p.
- Kirk, J. T. O. 1994. Characteristics of the light field in highly turbid waters: A Monte Carlo study. *Limnol. Oceanogr.* 39: 702-706.
- Knighton, D. 1984. *Fluvial forms and processes*. The Chaucer Press Ltd., Bungay, Suffolk. 218 pp.
- Korman, J., S. Wiele, T. Randle, T. Melis, & D. Topping. 2000. User's guide to the graphic interface combining flow, stage and sediment-input models developed for the Colorado River in Grand Canyon. USGS, Grand Canyon Monitoring and Research Center, Flagstaff, AZ.
- Krause-Jensen, D. & K. Sand-Jensen, 1998. Light attenuation and photosynthesis of aquatic plant communities. *Limnol. Oceanogr.* 43: 396-407.
- Melis, T. S. 1997. Geomorphology of debris flows and alluvial fans in grand Canyon National Park and their influences on the Colorado River below Glen Canyon Dam, Arizona. Ph.D. Dissertation., Univ. of Arizona, Tucson, Arizona.
- Melis, T. S., D. J. Topping, D. M. Rubin, & Y. C. Agrawal. 2002. Recent innovations in monitoring suspended-sediment mass balance of the Colorado River ecosystem below Glen Canyon Dam: A laser based approach. *EOS Trans, AGU*, 83:47
- Mobley, C. D., B. Gentili, H. R. Gordon, Z. Jin, G. W. Kattawar, A. Morel, P. Reinersman, K. Stamnes & R. H. Stavn, 1993. Comparison of numerical models for computing underwater light fields. *Applied Optics.* 32: 7484-7504.

- Netter, J., M. H. Kutner, C. J. Nachtsheim & W. Wasserman, 1996. *Applied linear statistical models*. (4th Ed.) Times Mirror Higher Education Group, Inc., Chicago, US. pp 1408.
- Newcombe, C. P., D. D. MacDonald, 1991. Effects of sediments on aquatic ecosystems. *N. Amer. J. Fish. Mang.* 11:72-82.
- Oreskes, N., K. Shrader-Frechette, & K. Belitz, 1994. Verification, validation, and confirmation of numerical models in the earth sciences. *Science*. 263: 641-646.
- Pemberton, E. L. 1987. Sediment data collection and analysis for five stations on the Colorado River from Lees Ferry to Diamond Creek. Glen Canyon Environmental Studies Technical Report, NTIS No. PB88-183397. 156 p.
- Randle, T. J., & E. L. Pemberton, 1987. Results and analysis of STARS modeling efforts of the Colorado River in Grand Canyon. U.S. Department of Interior, Bureau of Reclamation. NTIS No. PB88-183421/AS.
- Resampling Stats, Inc. 2001. Arlington, Virginia, USA.
- Rubin, D. M., J. M. Nelson, & D. J. Topping, 1998. Relation of inversely graded deposits to suspended-sediment grain-size evolution during the 1996 flood experiment in Grand Canyon. *Geology*. 26: 99-102.
- Rubin, D. M., and D. J. Topping. 2001. Quantifying the relative importance of flow regulation and grain size regulation of suspended sediment transport α and tracking changes in grain size of bed sediment β . *Water Resources Research*. 37:133-146.
- SAS Institute, Inc. 2001. SAS V8.02, TS Level O2MO. The SAS System for Windows Version. Cary, N.C., USA.
- Schmidt, J. C. 1990. Recirculating flow and sedimentation in the Colorado River in Grand Canyon, Arizona. *J. of Geology*. 98: 709-724.
- Shannon, J. P., D. W. Blinn & L. E. Stevens, 1994. Trophic interactions and benthic animal community structure in the Colorado River, Arizona, U.S.A. *Freshwat. Biol.* 31: 213-220.
- Shannon, J. P., D. W. Blinn, G. A. Haden, E. P. Benenati, & K. P. Wilson, 2001. Food web implications of $\delta^{13}\text{C}$ and $\delta^{15}\text{N}$ variability over 370 km of the regulated Colorado River USA. *Isotopes Environ. Health Stud.* 37: 179-191.
- Shaver, M. L., J. P. Shannon, K. P. Wilson, P. L. Benenati & D. W. Blinn, 1997. Effects of suspended sediment and desiccation on the benthic tailwater community in the Colorado River, USA. *Hydrobiologia*. 357: 63-72.

Sokal, R. R., & F. J. Rohlf, 1995. *Biometry the principles and practice of statistics in biological research*. W.H. Freeman and Company, New York, USA.

StatSoft, Inc. 2002. STATISTICA (data analysis software system), V6.1, Tulsa, OK, USA.

Stevens, L. E., A. A. Buck, B. T. Brown, & N. C. Kline, 1997a. Dam and geomorphological influences on Colorado River waterbird distribution, Grand Canyon, Arizona, USA. *Regul. Riv.* 13: 151-169.

Stevens, L. E., J. P. Shannon & D. W. Blinn, 1997b. Colorado River benthic ecology in Grand Canyon, Arizona, USA: dam, tributary and geomorphic influences. *Regul. Riv.* 13: 129-149.

Topping, D. J. 1997. Physics of flow, sediment transport, hydraulic geometry, and channel geomorphic adjustment during flash floods in an ephemeral river, the Paria River, Utah and Arizona. Ph.D. dissertation., Seattle, Univ. Wash. 405 p.

Topping, D. J., D. M. Rubin, & L. E. Vierra, Jr., 2000a. Colorado River sediment transport 1. natural sediment supply limitation and the influence of Glen Canyon Dam. *Water Resources Research.* 36: 515-542.

Topping, D. J., D. M. Rubin, J. M. Nelson, P. J. Kinzell III, & I. C. Corson, 2000b. Colorado River sediment transport 2. Systematic bed-elevation and grain-size effects of sand supply limitation. *Water Resources Research.* 36: 543-570.

Usher, H. D., & D. W. Blinn, 1990. Influence of various exposure periods on the biomass and chlorophyll A of *Cladophora glomerata* (Chlorophyta). *J. Phycol.* 26: 244-249.

Webb, R. H., P. G. Griffiths, T. S. Melis, & D. R. Hartley, 2000. Sediment delivery by ungaged tributaries of the Colorado River in Grand Canyons. US Geological Survey Water Resources Investigations Report 00-4055. 67 p.

Wiele, S. M., & J. D. Smith, 1996. A reach-averaged model of diurnal discharge wave propagation down the Colorado River through the Grand Canyon. *Water Resources Research.* 32: 1375-1386.

Table 1. Light attenuation coefficients (K_0), standard deviation (sd), and sample size (N) are estimated for the four major canyon sections, Glen Canyon (0-26.8 Rkm), Marble Canyon (26.8-124.3 Rkm), Central Grand Canyon (124.3-250.5 Rkm), and Western Grand Canyon (250.5-389.6 Rkm). A relative frequency, cumulative frequency (\leq maximum K_0 range) and exceedance frequency ($>$ maximum K_0 range) have been estimated for the canyon sections. Estimates for mean and median K_0 values were based on mid-day solar noon values. Solar zenith angle (θ) varied seasonally from 13.5° to 60.4° (degrees converted to radians) for summer and winter solstice.

MODELED ESTIMATES	MEAN K_0	SD (\pm)	MEDIAN K_0	N	FREQUENCY ANALYSIS		
					Rel.	Cum.	Exc.
GLEN CANYON SECTION							
Average $K_0 < 0.4$	0.250	0.03	0.247	14,189	99.6%	99.6%	0.4%
Average $K_0 > 0.4 \text{ \& } < 0.8$	0.465	0.08	0.425	55	0.4%	100%	0.0%
MARBLE CANYON SECTION							
Average $K_0 < 0.4$	0.328	0.04	0.326	3,145	22%	22%	78%
Average $K_0 > 0.4 \text{ \& } < 0.8$	0.567	0.11	0.552	7,367	52%	74%	26%
Average $K_0 > 0.8 \text{ \& } < 1.6$	1.06	0.21	1.01	2,829	20%	94%	6%
Average $K_0 > 1.6$	4.00	5.52	2.51	903	6%	100%	0%
CENTRAL GRAND CANYON SECTION							
Average $K_0 < 0.4$	0.335	0.04	0.333	895	6%	6%	94%
Average $K_0 > 0.4 \text{ \& } < 0.8$	0.606	0.11	0.607	3,519	25%	31%	69%
Average $K_0 > 0.8 \text{ \& } < 1.6$	1.09	0.22	1.03	3,203	22%	53%	47%
Average $K_0 > 1.6$	46.6	149.6	8.50	6,626	47%	100%	0%
WESTERN GRAND CANYON SECTION							
Average $K_0 < 0.4$	0.359	0.02	0.358	240	4%	4%	96%
Average $K_0 > 0.4 \text{ \& } < 0.8$	0.586	0.12	0.577	838	13%	17%	83%
Average $K_0 > 0.8 \text{ \& } < 1.6$	1.18	0.23	1.17	1,249	20%	37%	63%
Average $K_0 > 1.6$	48.6	172.8	5.35	3,883	63%	100%	0%

Table 2. Areal estimates were calculated for the geomorphic reaches and include: total wetted area (TWA), mean channel depth (Z), light attenuation coefficient (K_0), photosynthetically available area (PAA) and areal percent (PAA%). Zenith angles used for estimating K_0 (mid-day estimate) varied seasonally from 60.4° to 13.5°. Maximum photosynthetic photon flux density (PPFD) for summer and winter seasons range between 2020-1980, and 1200-1150 $\mu\text{mol quanta m}^{-2} \text{s}^{-1}$ respectively. Compensation point used (30 $\mu\text{mol quanta m}^{-2} \text{s}^{-1}$) was specific to *C. glomerata*.

		Flow Discharge 142 $\text{m}^3 \text{s}^{-1}$						Flow Discharge 568 $\text{m}^3 \text{s}^{-1}$									
		SUMMER			WINTER			CHANNEL			SUMMER			WINTER			
CHANNEL		K ₀	PAA	PAA	K ₀	PAA	PAA	TWA	Z	K ₀	PAA	PAA	K ₀	PAA	PAA		
ha		m ⁻¹	ha	%	m ⁻¹	ha	%	ha	m	m ⁻¹	ha	%	m ⁻¹	ha	%		
GLEN CANYON		298	7.2	0.22	297	100%	0.34	284	95%	484	8.9	0.22	474	98%	0.33	331	69%
MARBLE CANYON SECTION																	
Permian		147	6.1	0.39	96	65%	0.59	86	58%	163	7.9	0.42	121	74%	0.65	67	41%
Supai Gorge		105	6.4	0.36	78	74%	0.55	72	68%	120	8.9	0.55	67	56%	0.84	39	32%
Redwall Gorge		127	6.4	0.36	103	81%	0.55	98	77%	146	8.9	0.57	99	68%	0.88	56	38%
Lower Marble Canyon		376	5.2	0.52	241	64%	0.80	221	59%	410	7.1	0.52	319	78%	0.80	177	43%
CENTRAL GRAND CANYON SECTION																	
Furnace Flats		238	3.7	0.76	167	70%	1.18	141	59%	266	5.4	0.52	251	94%	0.80	160	60%
Upper Granite Gorge		352	5.7	0.66	173	49%	1.02	152	43%	416	8.2	0.75	190	46%	1.16	89	21%
Aisles		71	5.7	0.45	50	71%	0.69	47	67%	85	8.1	1.27	25	29%	1.96	12	14%
Middle Granite Gorge		131	7.0	0.45	95	73%	0.69	90	69%	154	9.5	1.38	42	27%	2.12	18	12%
WESTERN GRAND CANYON SECTION																	
Muav Gorge		152	5.4	0.58	95	63%	0.89	84	56%	185	8.1	1.11	53	29%	1.71	28	15%
Lower Canyon		607	3.9	0.59	472	78%	0.91	446	73%	722	6.4	1.36	187	26%	2.09	94	13%
Lower Granite Gorge		143	5.9	0.45	94	66%	0.69	91	63%	157	8.3	2.66	10	7%	4.09	6	4%
TOTAL		2,746	5.3	-	1,961	71%	-	1,813	66%	3,308	7.7	-	1,838	56%	-	1,078	33%

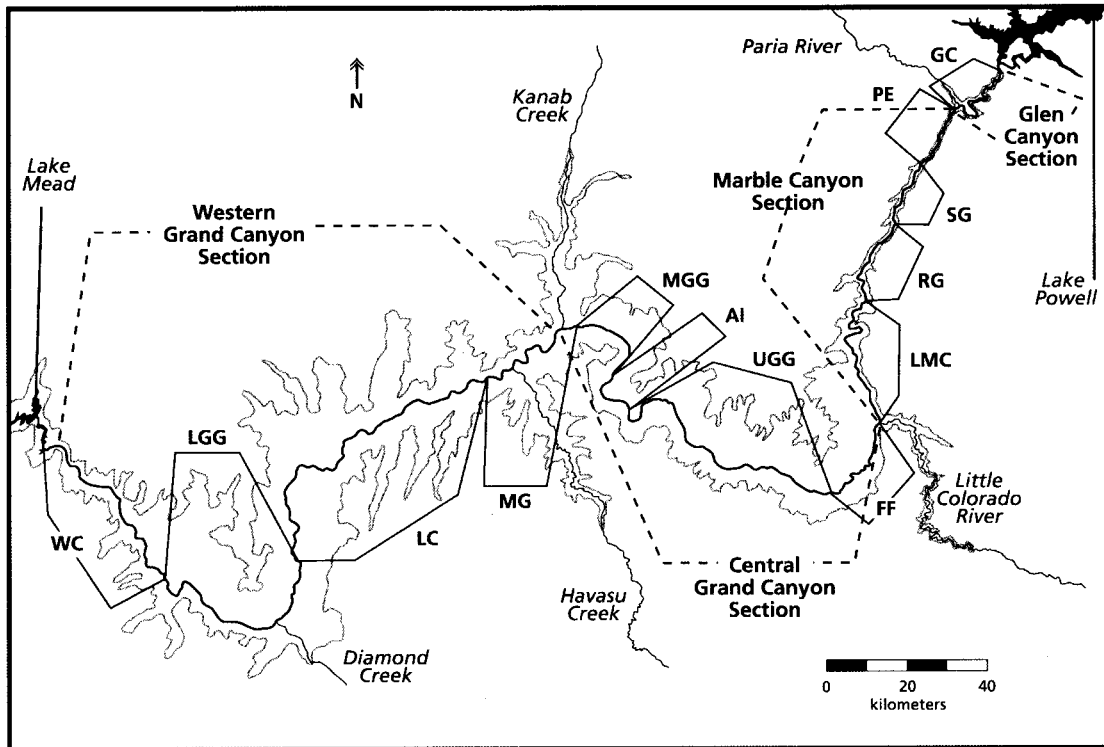


Figure 1. Map showing major canyon sections, geomorphic reaches, and tributaries of the Colorado River. Estimates of daily solar insolation were calculated at hectometer intervals along the entire river centerline for 474.5 km from Glen Canyon Dam to Lake Mead, AZ. Major canyon sections and geomorphic reaches included are: Glen Canyon Section (Glen Canyon (GC), 0 to 26.8 Rkm); Marble Canyon Section (Permian (PE), 26.8 to 43.5 Rkm); Supai Gorge (SG), 43.5 to 61.7 Rkm; Redwall Gorge (RG), 61.7 to 83.1 Rkm; Lower Marble Canyon (LMC), 83.1 to 124.3 Rkm); Central Grand Canyon Section (Furnace Flats (FF), 124.3 to 149.9 Rkm; Upper Granite Gorge (UGG), 149.9 to 214.9 Rkm; Aisles (AI), 214.9 to 227.3 Rkm; Middle Granite Gorge (MGG), 227.3 to 250.5 Rkm); and Western Grand Canyon Section (Muav Gorge (MG), 250.5 to 282.7 Rkm; Lower Canyon (LC), 282.7 to 369.4 Rkm; Lower Granite Gorge (LGG), 369.4 to 421.2 Rkm; Western Canyon (WC), 421.2 to 474.5 Rkm).

Figure 2. Schematic drawing of a cross-sectional profile showing the stage discharge relationship for two different discharges (142 and $568 \text{ m}^3\text{s}^{-1}$). Hydraulic and photometric parameters include: maximum channel depth (z_{MAX}), stage discharge, top-width (channel cross-section), photosynthetic photon flux density level (PPFD), euphotic zone, light extinction zone, photosynthetic perimeter (PP), normal light-attenuation coefficient (K_N), solar zenith angle (θ), and compensation depth (z_{CP}), solar surface incidence (Q_0), algal compensation point ($Q_Z = 30 \mu\text{mol quanta m}^{-2}\text{s}^{-1}$), and refractive index of water (1.33). The PP is affected by changes in apparent optical properties of water, which are influenced by sediment transport, sediment-supply, and by both seasonal and diurnal change in θ angle. The Q_Z represents PPFD level where gross primary production is equal to daily algal metabolic demands. The resulting z_{CP} varies in response to environmental changes in PPFD and underwater K_N . Compensation depth ($z_{CP} = -\ln(Q_0 / Q_Z) / [K_N / \cos(\sin / 1.33)]$), was used to determine PP. Photosynthetically available area was calculated by multiplying stream length and cross-sectional perimeter, and summing segments along the longitudinal axis of the river.

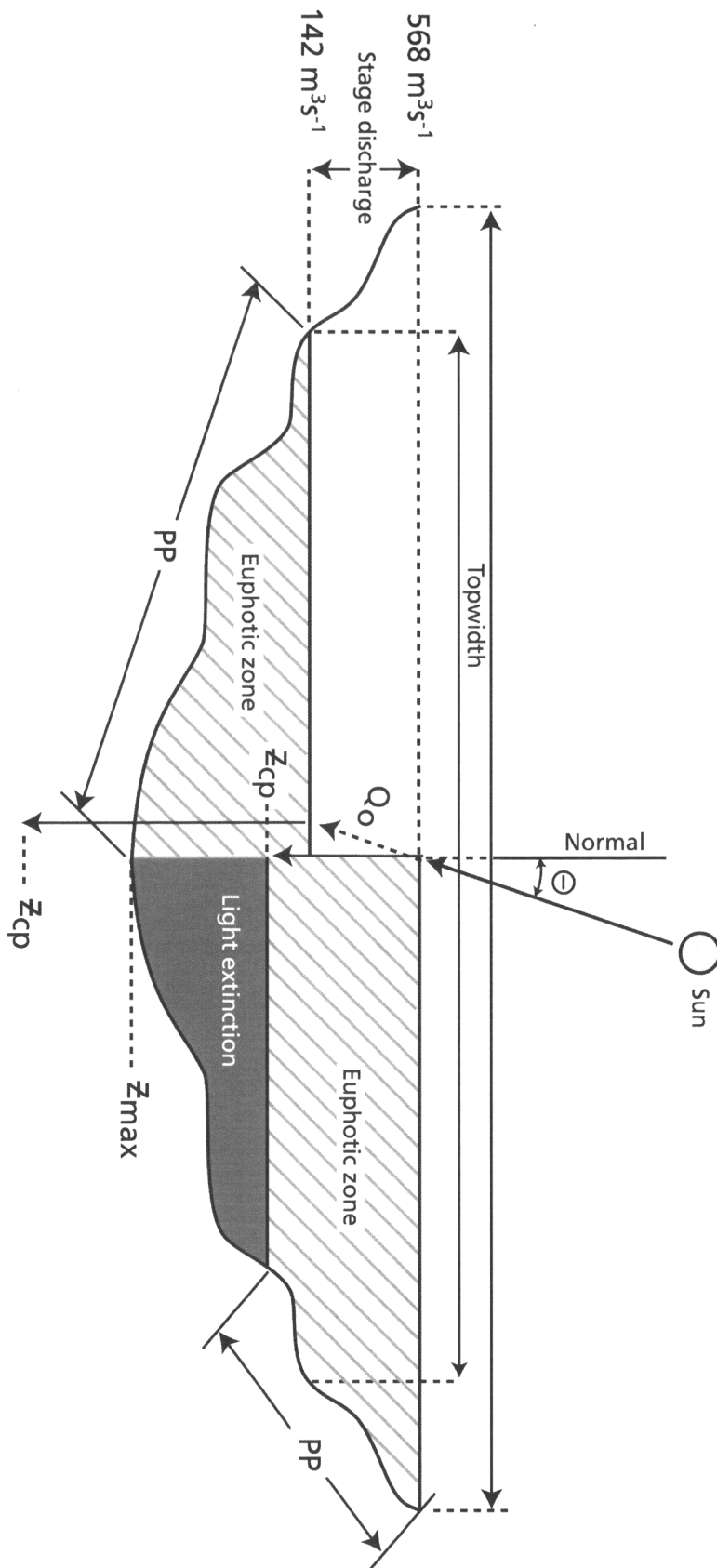


Figure 3. Comparison of observed and estimated light penetration depths ($z_{1\%}$), the depth where 1% of photosynthetic photon flux density (PPFD) remains after light-attenuation. A strong linear correspondence exists among observed and estimated depths at $z_{1\%}$ ($R^2 = 0.89$).

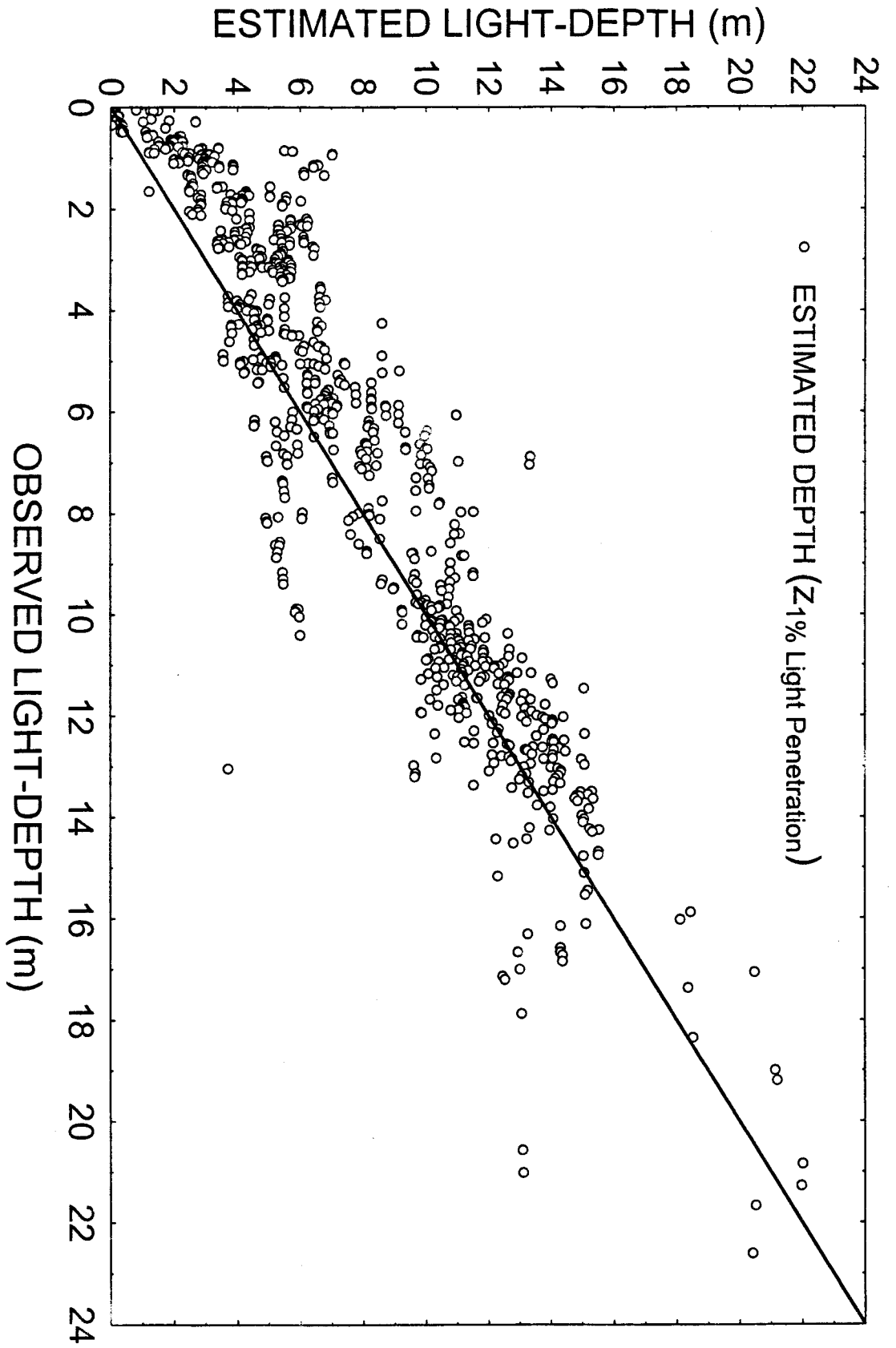
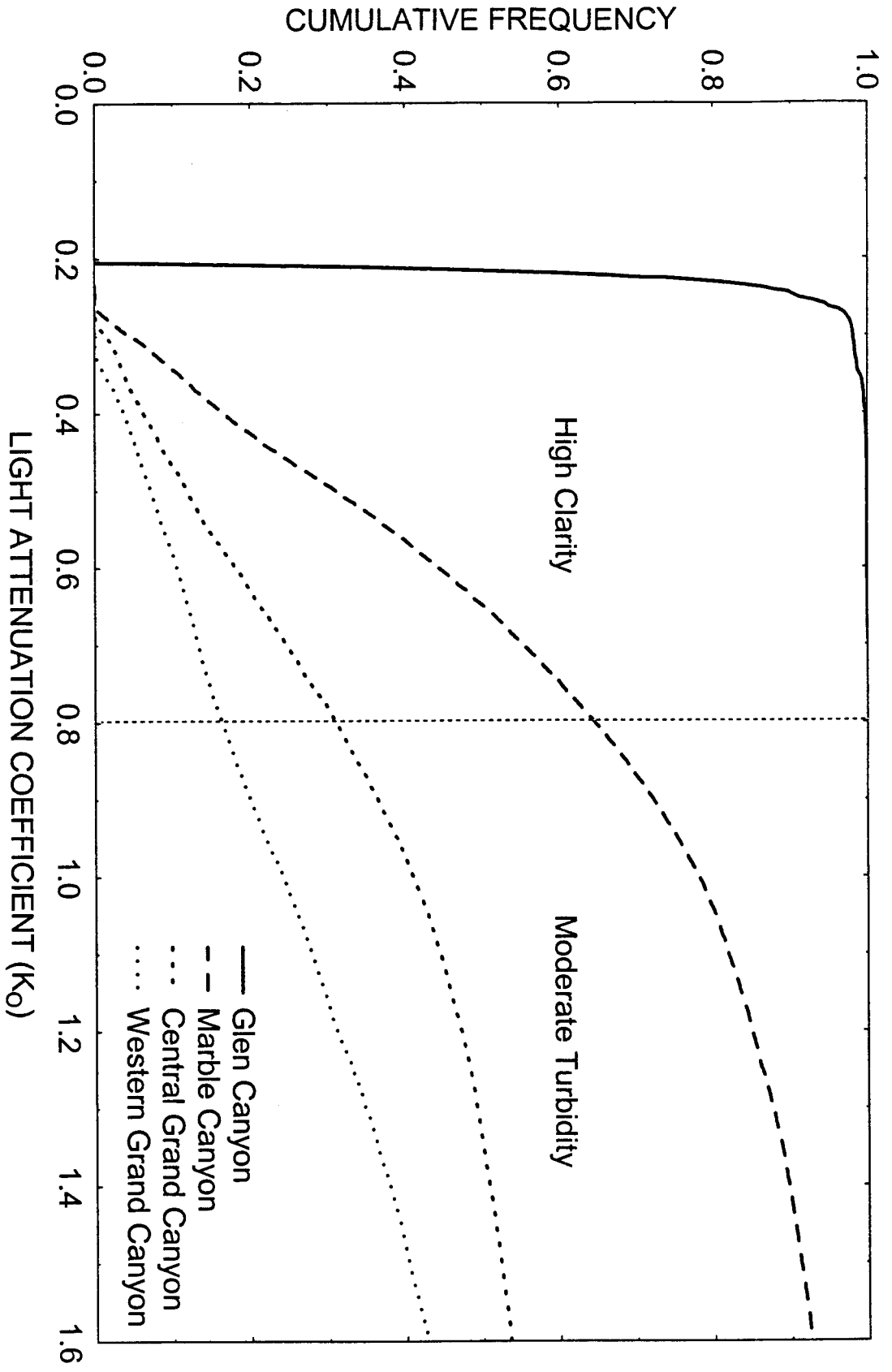


Figure 4. Cumulative frequency analysis showing the distribution of mean daily scalar light-attenuation coefficients (K_D) estimated for Glen Canyon, Marble Canyon, Central Grand Canyon, and Western Grand Canyon sections. The K_D estimates were adjusted for daily and seasonal differences in mid-day solar zenith angles (13.5° in summer to 60.4° to winter). Frequency distribution represents only light-attenuation characteristics considered representative of high clarity ($K_D \leq 0.8 \text{ m}^{-1}$) and moderately turbid conditions ($K_D > 0.8 \text{ m}^{-1}$ and $\leq 1.6 \text{ m}^{-1}$).



CHAPTER 6

PRIMARY PRODUCTION MODEL FOR THE COLORADO RIVER,
GLEN AND GRAND CANYONS, AZ: INTERDEPENDENCE
OF LIGHT, TEMPERATURE AND BIOMASS.

ABSTRACT

We developed a predictive model to evaluate the interdependence of light, temperature and biomass on primary production in the regulated Colorado River, USA. Regulation altered key ecological processes in Glen and Grand canyons, resulting in a trophic transformation from an allochthonous river into an autochthonous-based ecosystem. Simulating pre-dam characteristics are being considered; however, prescriptive changes (flow regulation, sediment augmentation, and thermal control device) might alter the trophic reliance on the existing phytobenthic community. Primary production covaried as a function of light and temperature, but was not independent of algal biomass. Although biomass has been conceptually recognized for its allometric effect (resource acquisition) on net primary production (NPP : $\text{gO}_2 \text{ m}^{-2} \text{ da}^{-1}$) rates, this effect is rarely accounted for in production estimates. Increased temperature (11° to 16°C) resulted in greater algal production. Variable patterns in estimated daily NPP suggested algal biomass and disturbance history were useful predictors for making inferences on production rates. Under optimal normalized light-attenuation ($K_N = 0.24 \text{ m}^{-1}$), depth (0.5m), and temperatures between 11° and 16°C , that maximum NPP occurred at intermediate biomass levels, and ranged from 23.56 to $10.39 \text{ gO}_2 \text{ m}^{-2} \text{ da}^{-1}$, for

summer and winter, respectively. Conversely, for similar temperatures, yet under higher light-attenuation ($K_N > 1$, depths ≥ 2.5 m), modeled *NPP* was reduced, and ranged from 0.55 and 0.10 $\text{gO}_2 \text{ m}^{-2} \text{ da}^{-1}$, for summer and winter, respectively. Predicted maximum phytoplankton carrying capacity (150 to 200 g m^{-2}) corresponded to observed biomass reported for this, and other systems. Our modeled estimates were consistent with independent production measurements published for this ecosystem.

INTRODUCTION

Few river systems remain unaltered due to human land-use practices, flow regulation, diversions, impoundments, and non-native species (Ward and Stanford, 1983; Minckley, 1991; Dynesius and Nilsson, 1994; Ligon *et al.*, 1995). These alterations have changed key natural processes occurring in river systems, and of these, the Colorado River is one of the more altered and regulated rivers in the world (Rader and Ward, 1988; Poff *et al.*, 1997). With the closure of Glen Canyon Dam (GCD), key physical and biological processes have been decoupled as compared to the historical condition. These changes include seasonal variability in flow, temperature, and sediment characteristics (Ward and Stanford, 1983; Stevens *et al.*, 1997); as well as disruption of allochthonous organic transport. Although not well recognized, this allochthonous material had once structurally defined the trophic food web and linkages in this pre-dam aquatic environment (Blinn and Cole, 1991; Haden 1997; Hayden *et al.* 1999; Jordan *et al.*, 1999). A number of endemic fish have become threatened or endangered system-wide, and certain abiotic (i.e., hydrology, temperature and sediment flux) and biotic (i.e.,

predation pressures and parasites) factors are implicated in their decline and/or extirpation (Minckley, 1991; Schmidt *et al.*, 1998).

In response to ecological changes, a branched, filamentous green alga, *Cladophora glomerata*, has now become widely established in Colorado River ecosystem (Blinn and Cole, 1991). Although this alga has often been recognized as a nuisance species in other systems (Wolfe and Sweeney, 1982), it has become a dominant and important trophic component in Colorado River (Blinn *et al.*, 1998), providing structural habitat and surface area for epiphytic attachment (Hardwick *et al.*, 1992; Shannon *et al.*, 1994). Occurrence and importance of *C. glomerata* has been recognized for other regulated rivers (Lowe, 1979). In absence of allochthonous organics, epiphytes comprise the majority of the invertebrate diet and energy supporting higher trophic levels (Pinney, 1991; Thorp and DeLong 1994; Shannon *et al.*, 2001). Notwithstanding high productivity, this ecosystem is depauperate in macroinvertebrate diversity, consisting almost entirely of nearctic dipterans (Stevens *et al.*, 1998; Sublette *et al.*, 1998). Lack of invertebrate diversity is typical of most regulated rivers (Rader and Ward, 1988; Fayolle, 1998); consequently altered ecosystems are less resilient to environmental change (Carpenter *et al.*, 2001).

To reverse some of these environmental changes, a number of conservation efforts are being considered. Some of these actions would not necessarily restore but simulate certain hydrological, thermal, and sediment transport characteristics that had existed prior to disruption of natural flow regime. These management actions are thought to potentially benefit early-life stage survival, recruitment, and spawning of native fishes (Clarkson *et al.*, 1994; Stanford, 1994; Poff *et al.*, 1997; Valdez *et al.*, 2000).

Uncertainty exists however, regarding their effect on the phytobenthic community. Clearly, conflicting resource and conservation issues exist since trophic reliance, structure, and linkages appear dependent on autochthonous rather than allochthonous production (Thorp and Delong, 1994; Shannon *et al.*, 2001).

Toward that purpose, we sought to understand how the autotrophic community might respond to physical and biotic changes as a result of management actions. Our study objectives were to determine the relationship of net photosynthesis and community respiration rates to temperature, light, and biomass; and secondly, based on experimental findings, to develop a predictive model for estimating primary production rates. Lastly, in advance of simulating certain aspects of pre-dam conditions, we sought to infer how certain prescriptive changes might influence the autotrophic community in this altered ecosystem.

MATERIALS AND METHODS

Study area and autotrophic community

Regulated segment of Colorado River is located on Colorado plateau of northern Arizona, flowing 480km through Glen and Grand canyons (Figure 1). Variable flows are released from the GCD hydroelectric facility, where operational constraints limit daily range of discharge fluctuations ($142\text{-}710\text{ m}^3\text{ s}^{-1}$) (BOR, 1995). This is a canyon-bound region where topographic obstructions and canyon orientation regulate quantity of daily and seasonal solar insolation (Chapter 2). Although this river is located in the arid southwest it remains stenothermically cold ($10^\circ \pm 1^\circ$), and variably turbid (light-attenuation coefficients, 0.22 to $>26.0\text{ m}^{-1}$) (Chapter 4). The river's nutrient levels for

dissolved orthophosphate are depleted ($<10 \mu\text{g l}^{-1}$) and nitrate-nitrogen rich ($>300 \mu\text{g l}^{-1}$) (Angradi and Kubly, 1993; Benenati *et al.*, 2000). Hypolimnetic releases from Lake Powell reservoir determine initial thermal, optical, and nutrient characteristics (Blinn and Cole, 1991; Benenati *et al.*, 1998) and are responsible for extensive primary production occurring in this system (Blinn *et al.*, 1998).

The phytobenthic community consists of macroalgae (*C. glomerata*, *Ulothrix spp.*, *Mougeotia spp.*, *Spirogyra spp.*, and *Chara contraria*), cyanobacteria (*Oscillatoria spp.*), bryophytes (*Fontinalis spp.*), and macrophytes (*Potamogeton pectinatus*) (Benenati *et al.*, 2000). Epiphytes are composed almost entirely of diatoms (Hardwick *et al.*, 1992). Dominant taxa are *Diatoma vulgare*, *Cocconeis placentula*, and *Rhoicosphenia abbreviata* (Czarnecki and Blinn, 1978; Hardwick *et al.*, 1992; Benenati *et al.*, 2000).

Primary production experiments

Prior to conducting a series of photosynthetic-irradiance trials, algal-covered cobbles were collected locally and acclimated for at least 48h in recirculation containers (375L, 1.5 x 1m) at predetermined temperatures (11°, 16°, and 20°C) while exposed to natural nutrient and light levels. Recirculating pumps and periodic water changes were used to maintain flow, temperature, and nutrients during acclimation phase. We conducted experiments under natural sunlit conditions owing to difficulties simulating solar radiation in laboratory settings (Gomez *et al.*, 1998; Karsten *et al.*, 2001).

Three circular acrylic containers (25L), were used as primary production chambers (PPC) (Lexan[®], 35(h) x 35(w) cm). During each trial, three to four cobbles (10 x 15cm) were loaded in each PPC, filled, sealed, and purged of air. Phytobenthic material

consisted predominately of *C. glomerata* and its associated epiphytes. Cobbles were physically agitated (30s) to displace sediment, invertebrates, and senesced material to avoid changes in water clarity and obstructing flow. Water volume was determined by cobble displacement.

Photosynthetic photon flux density (PPFD) was measured with cosine corrected (LiCor, Inc., 190SA) and spherical quantum sensors (LiCor, Inc., 193SA). Underwater light was continuously monitored using three quanta sensors (LiCor, Inc., Li-1000). Sensors were externally mounted between PPC's on a triangular steel frame, 0.75m apart. For each temperature tested, 70 to 90 independent photosynthetic rates were made over a selected range of underwater PPFD levels (20-1600 $\mu\text{mol quanta m}^{-2} \text{s}^{-1}$). Oxygen and temperature were measured at 1-min intervals using calibrated dissolved oxygen probes and thermistors (YSI, model 52). To account for differential light absorption and scattering within PPC, external light measurements were calibrated to internal light environment. By taking advantage of underwater light-attenuation, PPFD levels were maintained at constant levels by lowering PPC's from a stationary boat deck using a bridge-boom and cable reel (vertical depth 5m).

Water was recirculated in a closed in-line system (flow rate: 11.6 L min⁻¹) using submersible pumps (Rule™, 1100-12V) allowing for rapid exchange and accurate measurements. Clear intake structures regulated outflow velocity and avoided internal light obstruction by routing water underneath and returning flow through base of each PPC. Internal temperatures were rheostatically regulated using in-line heating elements (1500W 120AC). Excess heat production was passively dissipated to external environment. A 30-min period was used to measure net photosynthesis. This was

repeated again during respiration phase by excluding light through use of external covers. Large volume and short-time interval avoided nutrient depletion (maximum incubation period was no greater than 1.5h). For pre- and post-incubation, water samples were collected, filtered (Whatman[®] GF/C 0.45 μm glass filters), stored in acid-clean polyethylene bottles, fixed (H_2SO_4), and refrigerated for later processing. Relative rates of net photosynthesis (*NP*) and community respiration (*CR*) were normalized per gram ash-free dry mass (AFDM), and are expressed as $\text{mgO}_2 \text{ gC}^{-1} \text{ m}^{-2} \text{ h}^{-1}$. Nutrient (NH_4^+ , $\text{NO}_3\text{-N}$, and O-PO_4) levels from each chamber were analyzed using a Technicon Auto Analyzer II [™]. Alkalinity and pH (2000 VWR Scientific) were measured in the field. Following each trial, cobbles were recovered and periphyton was scraped, brushed, dried (60°C for 24h), weighed ($\pm 0.001\text{g}$), and ashed (500°C for 1h) for AFDM (g m^{-2}) determination.

Production and Respiration Estimates

Production and respiration rates were calculated from the rate of change of dissolved oxygen. All production rates (net photosynthesis and community respiration) were normalized to account for differences in volume, substrate area, and biomass. For analytical purposes, we subdivided the photosynthetic-irradiance response into two regions (P-I curve) representing light-limited and light-saturated regions. A combination of multiple (MLR) and simple (SLR) linear regressions were used to evaluate effect of temperature, light and biomass on each region of the P-I curve. Photosynthetic parameters for maximum photosynthetic rate (NP_{MAX} : $\text{mgO}_2 \text{ gC}^{-1} \text{ m}^{-2} \text{ h}^{-1}$), onset of saturation (PPFD_{SAT} : $\mu\text{mol quanta m}^{-2} \text{ s}^{-1}$), and compensation point (C_P : $\mu\text{mol quanta m}^{-2}$

s^{-1}) were calculated as described by Kirk (1983). Multiple statistical packages were used for analyses (SAS Institute, Inc., 2000; Statistica StatSoft, Inc., 1997; Frontlines Systems, Inc. 1999).

Jassby and Platt's (1976) original function estimated net photosynthesis (NP , normalized to algal biomass):

$$NP = NP_{MAX} \tan\left(\frac{\alpha \cdot I}{NP_{MAX}}\right). \quad (1)$$

where, NP_{MAX} is the maximum net production rate at saturation, and α is the initial slope under light-limited conditions such that photosynthetic rate responded linearly to available underwater PPFD (I). Based on our results, Eq 1 was further parameterized by including other independent variables found to be statistically significant in explaining observed variability in NP . Coefficients were estimated using a non-linear optimization program that minimized residual sum of squares (Frontlines Systems, Inc. 1999) by fitting observed NP to Jassby and Platt's (1976) modified hyperbolic tangent function.

Using a MLR, we assessed the effect of temperature and biomass on CR_D rates. For our short-term experiment, we made the assumption that heterotrophic respiration remained constant between light and dark phases (Harris, 1978). Although, attempts were made to displace the heterotrophic component through agitation we were unable to distinguish quantitatively between heterotrophic and autotrophic respiration demands. Respiration rates are reported as daily community respiration (CR_D), (Jones, 1977).

Two types of gross primary production rates were estimated and defined as 1) biomass-specific gross primary production ($BSGP = NP + CR_D$), and 2) area-specific gross primary production ($ASGP = [NP + CR_D] \cdot B$). Both measures are interrelated

where $BSGP$ is the average gross production normalized per unit biomass ($\text{mgO}_2 \text{ gC}^{-1} \text{ m}^{-2} \text{ h}^{-1}$), and NP is the rate of net photosynthesis. $ASGP$ is the gross production per unit area ($\text{mgO}_2 \text{ m}^{-2} \text{ h}^{-1}$) where production rates were expanded by contribution of B , total photosynthetic biomass contained within an area (m^2).

We accounted for total metabolic costs from both CR_D and nightly respiration (CR_N) demands; however, no attempts were made to account for differences between autotrophic and heterotrophic community. Rather, we assumed equivalence between $CR_D \approx CR_N \approx CR$ and used respiration parameters interchangeably. Net primary production (NPP , $\text{gO}_2 \text{ m}^{-2} \text{ d}^{-1}$) is the resultant photosynthetic product after total respiration demands are accounted for over a 24-h period. The daily rate of change for NPP is expressed as:

$$NPP = (NP + CR) \cdot B \quad (2)$$

where: NP is net photosynthesis, CR is the combined daily and nightly respiration, and B is autotrophic biomass.

Although quantum yields are reported, we make no attempt to suggest that observed values represent a maximum quantum yield due to difficulties in distinguishing actual quantity of light absorbed by benthic autotrophs (Ramus, 1990). Rather, changes in oxygen rates reflect a photosynthetic response relative to the availability of PPFD measured (Rhee, 1982).

Primary production comparisons

Primary production has been sporadically studied in the Colorado River system with estimates derived from metabolic chambers that integrate production rates over

extended time intervals (Angradi and Kubly, 1993; Blinn *et al.*, 1998; Brock *et al.*, 2000). For comparative purposes we have attempted, where possible, to estimate these reported production rates using an independent method that takes into account environmental parameters. When pertinent data were not reported, environmental parameters (temperature, depth, day-length, PPFD) were reconstructed based on locality and date/time. Reconstructed values are reported in Table 1. Instantaneous PPFD was estimated using a relationship developed for predicting solar insolation (Chapter 2). Light-attenuation characteristics were determined by either direct measurements or derived from water quality relationships (Chapter 3) and monitoring data (USGS, 1990-2002).

RESULTS

Net Photosynthesis

Both regions of the P-I curve (light-limited and light-saturated conditions) were analyzed using a multiple linear regression approach; for light-limited region, results indicated that *NP* rates normalized to $\text{mgO}_2 \text{ gC}^{-1} \text{ m}^{-2} \text{ h}^{-1}$ were significantly affected by PPFD, temperature, and biomass ($F_{3,239} = 108$, $p < 0.01$). As expected, light-oxygen response demonstrated a kinetic effect, where under light-limited conditions *NP* rates for 11°C ($\alpha_{11} = 0.076$) and 16°C ($\alpha_{16} = 0.153$) had significantly different slopes ($p < 0.01$). Although the line intercept was not significant ($p > 0.05$) for C_p ($25\text{-}35 \mu\text{mol quanta m}^{-2} \text{ s}^{-1}$), the C_p intercept had a slightly elevated PPFD level for 16°C (Figure 2). Although light and temperature influenced *NP* rates at 11°C and 16°C , post-hoc tests indicated that biomass did not have a significant effect ($p = 0.1$) within the light-limited region.

However, once light-saturation was reached, further increases in PPFD levels no longer influenced oxygen production ($p > 0.8$) while temperature continued to have a positive kinetic effect on NP ($p < 0.01$). Also biomass was found to have a significant negative effect on NP ($p < 0.01$) within light-saturated region for both 11°C and 16°C (i.e., higher biomasses resulted in depressing production rates). Regardless of temperature (11°C and 16°C), light-saturation (PPFD_{SAT}) and maximum net photosynthetic (NP_{MAX}) levels shifted downward with increasing biomass. Because of normalized rates, once the sample's total biomass is accounted for the area-specific response results in elevating the NP rate overall.

NP rates measured at 20°C under similar light-limited conditions had an unexpected and spurious response where rates were significantly lower than other tested temperatures ($p < 0.01$). For light-limited conditions, light-oxygen slope at 20°C was depressed ($\alpha_{20} = 0.006$). C_p was elevated ($90\text{-}130 \mu\text{mol quanta m}^{-2} \text{s}^{-1}$) relative to lower temperatures. Biomass was not significantly correlated ($p > 0.05$) to NP ; however, response rate was different because PPFD_{SAT} shifted toward higher levels ($660\text{-}1000 \mu\text{mol quanta m}^{-2} \text{s}^{-1}$). NP_{MAX} remained low and constant ($9.2 \text{ mgO}_2 \text{ gC}^{-1} \text{ m}^{-2} \text{ h}^{-1}$) for changes in biomass.

Primary production model

Based on our statistical findings, we modified Eq 1 (Jassby and Platt, 1976). Independent variables used for estimating NP were: biomass = B (gC m^{-2} AFDM), temperature = T ($^\circ\text{C}$) and PPFD = I ($\mu\text{mol quanta m}^{-2} \text{ h}^{-1}$). Expression used was:

$$NP = (NP_{MAX} + (S_B \cdot B) + (S_T \cdot T)) \tanh\left(\frac{\alpha \cdot I + (L_T \cdot T)}{NP_{MAX} + (S_B \cdot B) + (S_T \cdot T)}\right). \quad (3)$$

For the light-saturated region the coefficients for the maximum net production rate (NP_{MAX}) is 19.1 mgO_2^{-1} ; saturation biomass coefficient (S_B) is $-1.62 \text{ gC}^{-1} \text{ m}^{-2} \text{ AFDM}$; and is saturation temperature coefficients (S_T) is $1.11 \text{ }^\circ\text{C}^{-1}$. For the light-limited region the coefficients for the initial photosynthetic response slope (α) is 0.184 mgO_2^{-1} ; and light-limited temperature coefficients (L_T) is $1.56 \text{ }^\circ\text{C}^{-1}$. Comparisons between estimated and observed NP rates are graphically depicted (Figure 2).

Community Respiration

Daily community respiration (CR_D) rates were positively correlated to increased temperature (SLR, $p < 0.001$) (11°C and 16°C). Post-hoc tests revealed that CR_D was positively correlated to biomass (SLR, $p < 0.001$) for both temperatures. Respiration rates ($\text{mgO}_2 \text{ gC}^{-1} \text{ m}^{-2} \text{ h}^{-1}$) were calculated using a MLR ($F_{2, 182} = 367$, $R^2_{Adj} = 0.80$) expressed as: $CR_D = (B_R \cdot B) + (T_R \cdot T)$ where B_R is the respiration biomass coefficient ($0.192 \text{ }^\circ\text{C}^{-1}$), and T_R is the respiration temperature coefficient ($0.083 \text{ }^\circ\text{C}^{-1}$). Biomass (B : g m^{-2}) and temperature (T : $^\circ\text{C}$) are required as independent variables.

Separate analyses were required to evaluate 20°C . Post-hoc tests indicated that CR_D rates were not significantly correlated to biomass (SLR, $p = 0.10$), but positively correlated to prior exposure levels of underwater incidence (SLR, $p < 0.01$). This antecedent effect was present even though PPC's were excluded from light during respiration phase. Underlying cause appeared related to photorespiration, therefore measured photosynthetic rates were considered inaccurate for 20°C experiment.

GPP and NPP estimates

Residual analysis indicated that most of the variation between observed and predicted *BSGP* ($r^2 = 0.86$) was explained by temperature, biomass, and PPFD. An inverse relationship existed between *BSGP* and biomass due to a corresponding reduction in oxygen production per gram of photosynthetic material. Predicted maximum *BSGP* rates under high light intensities and low biomass were 33 and 36 $\text{gO}_2 \text{gC}^{-1} \text{m}^{-2} \text{h}^{-1}$, for 11 and 16°C, respectively. Conversely, modeled results indicated that *ASGP* monotonically increased due to an additive effect from areal production (biomass adjustment); however, there was an apparent interference with further increases in biomass that were not compensated by increased metabolic demands. The cumulative affect from biomass and increased respiration reduced *NPP*, and ultimately constrained maximum net primary production (Figure 3). Table 1, reports *NP*, *ASGP*, CR_{N+D} , and *NPP* as a function of temperature and biomass. Predicted estimates were based on optimal light conditions for Lees Ferry, 21-June ($63.2 \text{ mol m}^{-2} \text{ da}^{-1}$), at 0.5m depth and $0.24 \text{ m}^{-1} K_N$.

A complex relationship between biomass, light, and temperature was found to influence carrying capacity of system, defined as maximum biomass (B_{MAX}). For simulated conditions, predicted B_{MAX} varied with temperatures, seasonal (June vs. December) solar insolation levels (63.2 to $25.2 \text{ mol m}^{-2} \text{ da}^{-1}$), and light-attenuation (0.24 to 3.0 m^{-1}). Under equivalent light conditions, B_{MAX} ranged seasonally from 185 to 140 g m^{-2} at 11°C (Figure 4C & 4D), and from 210 to 160 g m^{-2} at 16°C (Figure 4A & 4B).

Modeled results suggest that maximum daily *NPP* yield (NPP_{YIELD}) occurred at optimal biomass (B_{OPT}) and that these maximum rates varied as a function of PPFD and

temperature. Both NPP_{YIELD} and B_{OPT} were positively correlated to increased daily PPFD levels (Figure 4). At 16°C, NPP_{YIELD} varied seasonally (June and December) from 23.56 to 12.36 $gO_2 m^{-2} da^{-1}$ ($K_N = 0.24 m^{-1}$; 0.5m depth), whereas B_{OPT} ranged from 106 to 96 gC. Consequently, under identical seasonal PPFD levels, depths and optical conditions, NPP_{YIELD} and B_{OPT} decreased at lower temperatures. For 11°C, predicted NPP_{YIELD} decreased with reduced temperature, and seasonal irradiance levels from 19.17 to 10.39 $gO_2 m^{-2} da^{-1}$ for their respective B_{OPT} of 94 and 90 gC. Modeled results indicate that B_{OPT} levels can be depressed to almost negligible levels under conditions of high light-attenuation.

Other predicted estimates for equivalent springtime biomass and light conditions (autumnal equinox) were consistent with hourly and daily production rates reported from previous research (Brock *et al.* 2000; Angradi and Kubly 1993). Brock *et al.* (2000) reported daily production rates for ASGP as: 18.9 $gO_2 m^{-2} da^{-1}$ SE \pm 5.7, at 105 gC SE \pm 32; and 21.1 $gO_2 m^{-2} da^{-1}$ SE \pm 5.2, at 95 gC, SE \pm 19. In comparison, we predicted mean daily ASGP rates based on range of reported biomass, irradiance and temperature levels encountered in the field. Our mean predicted ASGP rates for the same time period, 27-March 1996, and 6-April 1996 were: 18.5 $gO_2 m^{-2} da^{-1}$ (range: 15.5 to 18.7); and 19.4 $gO_2 m^{-2} da^{-1}$ (range: 17.8 to 20.6), respectively (Table 2).

DISCUSSION

Production estimates varied as a function of light and temperature, and also depended on algal biomass. The influence biomass has on production in benthic environments has been long recognized (Auer and Canale, 1982; Stevenson and

Stoermer, 1982). There are a number of possible explanations for the negative biomass-specific primary production response, and include senescent growth, nutrient depletion, and light interference (Hill, 1996; Kalchev *et al.*, 1996; Falkowski and Raven, 1997; Spencer *et al.*, 1998). This allometric relationship appears due to resource acquisition since availability and reception of underwater light is an area relationship, and functional growth and biomass accrual is volumetric (Kalchev *et al.*, 1996). Once resources were limited by density, further growth would ultimately interfere with resource acquisition (Cuker, 1983; Guasch and Sabater, 1995).

In this river system, the standing biomass of the phytobenthic community decreases with distance from GCD (Stevens *et al.*, 1997). This relationship has significant implications for seasonal and spatial variability of autotrophic production occurring in the regulated Colorado River. Simulated results based on our field studies have indicated that phytobenthic community; consisting of filamentous algae, have a very high photosynthetic capacity. Photosynthetic differences in light acquisition were negatively correlated to biomass with highest *BSGP* rates occurring at lowest biomass levels. Alternately, *ASGP* rates had an inverse relationship attaining higher rates under moderate to high biomass levels. Typically, daily *ASGP* rates became asymptotic at moderate to high biomass levels. In the Colorado River during summer at 11 °C, predicted daily maximum *ASGP* may reach rates between 18 and 24 gO₂ m⁻²; however these estimates assume optimum instantaneous rates which are contingent on solar insolation, water clarity, depth, and biomass (60 to 140 gC AFDM) conditions. Other independent comparisons reinforce the commonly held thought that this upstream tail-water section is extremely productive (Blinn *et al.*, 1998; Brock *et al.*, 2000; Marzolf, 2000), (Table 2).

Variable pattern in *NPP* (Figure 4) suggests that algal standing biomass and disturbance history are useful for making inferences on production rates. Tett *et al.* (1978) identified that duration between flood events was a major determinant of algal biomass. Nutrients, light availability, temperature, hydraulic stress, sloughing, and grazing are other factors recognized for their effect on filamentous algae standing crop (Whitton, 1970; Cuker, 1983; Canale and Auer, 1982; Dudley, 1992; Nozaki, 2001). In the Colorado River, monitoring data indicate that the autotrophic communities in mid- and lower canyon sections (Figure 1) have lower standing biomass except after continued periods of flow stabilization or high clarity conditions (Benenati *et al.*, 2002). This photosynthetic-biomass response has been observed for other disturbed systems (Biggs and Thomsen, 1995; Dodds *et al.*, 1996). Therefore under frequent disturbance (Fayolle, 1998), *ASGP* should be reduced even though *BSGP* rates might remain high under decreased biomass.

Whereas, under environmentally stable conditions, continued growth should reduce daily, seasonal, and annual *NPP*, our predicted results indicate that increased growth beyond B_{OPT} resulted in decreased *NPP* and increased CR_{D+N} . Benthic communities are known to exhibit self-shading (Dudley, 1992; Hill, 1996; Nozaki, 2001). Reported values for carrying capacity in systems dominated by filamentous algae were found to be variable depending on light, temperature, and nutrients (Lekan and Coney, 1982; Guasch and Sabater, 1995; Nozaki, 2001). Filamentous algae have been shown to have a low photosynthetic capacity when senescent cells accumulate due to slow turnover rates (Biggs and Thomsen, 1995; Nozaki 2001). Our predicted B_{MAX} (150 to 200 g m⁻²) corresponded closely to carrying capacities reported in this system, 140-160 g m⁻² AFDM

(McKinney *et al.*, 2000), and 176 g m^{-2} AFDM, sd 74, $n = 220$, (Yard and Blinn 2001); and in other freshwater systems, $160\text{-}270 \text{ g m}^{-2}$ DW (Canale and Auer, 1982), and $150\text{-}225 \text{ g m}^{-2}$ DW (Lekan and Coney, 1982). Metabolic costs for maintenance should constrain growth and accrual under a standing biomass that approaches the carrying capacity even though *ASGP* remains high.

Predicted *NPP* were found to depend on biomass accrual (Figure 4). For this reason, intermittent disturbance and turnover rates might have profound effects on system-wide production. Studies specific to the Colorado River have observed production differences prior to, and following a hydrological disturbance that resulted in a 10% loss in mean standing biomass, with a corresponding increase in *ASGP* (Table 2) (Brock *et al.*, 2000). It has been shown that herbivory (Hart *et al.*, 1991; Dudley, 1992; Fayolle, 1998; Munoz *et al.*, 2000) and velocity (Dodds, 1991; Biggs and Thomsen, 1995) increased production rates through removal or prevention of excess growth. Hart *et al.* (1991) observed similar biomass-productivity responses relative to differences in herbivore disturbance; as have other studies where sloughing resulted in increased growth through reduced light-interference (Canale *et al.*, 1982; Dudley, 1992).

Photoinhibition was not detected below $1500 \mu\text{mol quanta m}^{-2} \text{ s}^{-1}$; however, if photoinhibition were to occur under higher irradiance levels, these intensities are limited seasonally to mid-day periods. Typical of summer periods, maximum solar incidence has been observed at 1950 to $2025 \mu\text{mol quanta m}^{-2} \text{ s}^{-1}$. Yet, because of Colorado River's normal light-attenuation characteristics, maximum intensities are usually less than $1500 \mu\text{mol quanta m}^{-2} \text{ s}^{-1}$, at depths equal to, or less than 0.75 m . This same upper surface zone is also influenced by daily flow fluctuations and desiccation (Blinn *et al.*, 1995;

Benenati *et al.*, 1998). Under present discharge regime, current daily stage change is 0.75 to 1.5m elevation (BOR, 1995), and is proportionally small relative to total channel area available for photosynthesis. However, because of light limitations in downstream sections, this varial zone may have greater areal importance for primary production. Excluding desiccation effects on algal production (Benenati *et al.*, 1998), *ASGP* differences at shallow depths will be related to seasonal changes in day-length. Filamentous algae, predominately *Cladophora*, appear well adapted to low light conditions ($PPFD_{SAT}$: 320-210 $\mu\text{mol quanta m}^{-2} \text{s}^{-1}$). Adams and Stone (1973) observed similar light saturation levels for this alga. Therefore, depending on light-attenuation, this portion of channel would be exposed to above light saturation levels. However, under turbid conditions ($K_N = 1.0 \text{ m}^{-1}$) at 2.5m depths, daily *NPP* would be seasonally limited by reduced day length and unsaturated light conditions.

Our results suggest that an increase in river temperature should result in greater algal production. Our measurements did not account for potential physiological adaptations to altered temperature (Spencer *et al.* 1998). Initial water temperature of the Colorado River originates from reservoir's hypolimnion as cold and seasonally constant (9°C , $sd \pm 2^\circ$). Even so, downstream temperature varies by season and distance from GCD (7.5° to 16°C), (USGS, water quality data). Although thermal differences have been observed for *C. glomerata* due to environmental conditions (Bellis, 1968; Whitton, 1970; Storr and Sweeney, 1971; Canale *et al.*, 1982), optimum temperatures typically extend between 16 - 18°C (Graham *et al.*, 1982; Wolfe and Sweeney, 1982). Another factor influencing thermal response is the epiphytic relationship between diatoms and *C. glomerata*, where epiphytes may represent 50 to 60% of total autotrophic biomass

(Stevenson and Stoermer, 1982; Dodds, 1991). Consequently, primary production may actually reflect physiological requirements of diatoms rather than epiphytic host. Blinn *et al.* (1989) has suggested that a thermal threshold of 17°C exists for multi-branched epiphytes in Colorado River system. His findings show that a physiognomic shift resulted in favoring adnate forms having lower biomass. Although these forms were capable of persisting at elevated temperatures, they represent a smaller proportion of the invertebrate diet (Pinney 1991).

A kinetic response was observed for photosynthesis under varying temperature. However, it remains unclear whether or not high and variable temperatures would result in greater primary production. Cold hypolimnetic releases may provide metabolic advantages to filamentous algae by reducing respiration requirements for maintenance, particularly at greater depths or higher light-attenuation (Salisbury and Ross, 1985). In canyon bound regions, vertical extent of algae may be constrained by light limitation and higher respiration rates. Reduced *NPP* was observed in modeled results where production rates at 16°C were less than rates at lower temperatures (Figure 4). Modeled results predicted that under conditions of $K_N = 1.0 \text{ m}^{-1}$ and 2.5m depths summer *NPP* would be significantly lower and thermally different, having reduced rates of 0.10 and 0.55 $\text{gO}_2 \text{ m}^{-2} \text{ da}^{-1}$ for 16°C and 11°C, respectively. Exposing algae to rapid or variable temperatures in excess of 8°C d^{-1} may also have negative effects. Negative results observed at 20°C, were considered due to photorespiration, since carboxylation and water splitting mechanism of photosystem II are heat sensitive (Jones, 1977; Falkowski and Raven, 1997). Therefore rapid thermal adjustments to river systems must be approached with forethought. Although it is reasonable to think that *Cladophora* might

function under much higher temperatures (Bellis, 1968; Whitton, 1970; Storr and Sweeney, 1971) a shift in epiphytic community might have trophic consequences (Blinn *et al.*, 1989).

Computational models are useful tools for addressing potential management prescriptions and engineering solutions (e.g., flow regulation, sediment augmentation and/or thermal control device), (Clarkson *et al.*, 1994; BOR, 1995). Purposeful alterations of the benthic food-base may be an effective method for controlling non-native fish, particularly visual sight feeders like trout (*Salmo trutta* and *Onchorhynchus mykiss*). Increased turbidity using sediment augmentation or other prescriptive measures will affect production, food availability, foraging behavior and reactive distance of piscivores (Shaver *et al.*, 1998; Barrett *et al.*, 1992); however, these actions may also impose trophic constraints on other more desirable components of the fish assemblage. Simulating Colorado River pre-dam characteristics should be cautiously approached, prior to altering the thermal and underwater light environment. For this reason, determining importance of allochthonous organics and trophic linkages remain paramount for understanding how this altered ecosystem might respond to prescriptive actions (Angradi, 1994; Thorp and Delong, 1994).

ACKNOWLEDGEMENTS

Research was funded by USGS Grand Canyon Monitoring and Research Center (CA: 98-FC-40-0540). Our gratitude goes to National Park Service (Glen Canyon National Recreational Area and Grand Canyon National Park) for providing necessary collection permits, facilities and assistance. We also express our appreciation to all staff,

students and volunteers who provided assistance during sampling periods, especially D.

Baker, A. Haden, A. Martinez, I. McKinnon, and H. Yard.

LITERATURE CITED

- Adams, M. S. and Stone, W. 1973. 'Field studies on photosynthesis of *Cladophora glomerata* (Chlorophyta) in Green Bay, Lake Michigan', *Ecology*, **54**, 853-862.
- Angradi, T. R. and Kubly, D. M. 1993. 'Effects of atmospheric exposure on chlorophyll-a, biomass and productivity of the epilithon of tailwater river', *Regul. Riv.*, **8**, 345-358.
- Angradi, T. R. 1994. 'Trophic linkages in the lower Colorado River: multiple stable isotope evidence', *N. Amer. Benth. Soc.*, **13**, 479-495.
- Auer, M. T., and Canale, R. P. 1982. 'Ecological studies and mathematical modeling of *Cladophora* in Lake Huron: 3. The dependence of growth rates on internal phosphorous pool size', *J. Great Lakes Res.*, **8**, 93-99.
- Barrett, J. C., Grossman, G. D., and Rosenfeld, J. 1992. 'Turbidity-induced changes in reactive distance of rainbow trout', *Trans. Amer. Fish. Soc.*, **121**, 437-443.
- Bellis, V. J. 1968. 'Unialgal cultures of *Cladophora glomerata* (L.) Kutz. II. Response to temperature', *J. of Phycology*, **4**, 19-23.
- Benenati, P., Shannon, J. P. and Blinn D. W. 1998. 'Desiccation and recolonization of phytobenthos in a regulated desert river: Colorado River at Lees Ferry, Arizona, USA', *Regul. Riv.*, **14**, 519-532.
- Benenati, E. P., Shannon, J. P., Blinn, D. W., Wilson, K. P., and Huftle, S. J. 2000. 'Reservoir-river linkages: Lake Powell and the Colorado River, Arizona', *N. Amer. Benth. Soc.*, **19**, 742-755.
- Benenati, E. P., Shannon, P. J., Haden, G. A., Straka, K., and Blinn, D. W. 2002. 'Monitoring and research: the aquatic food base in the Colorado River, Arizona during 1991-2001. Northern Arizona University, Flagstaff, AZ.
- Biggs, B. J. F., and Thomsen, H. A. 1995. 'Disturbance of stream periphyton by perturbations in sheer stress: time to structural failure and differences in community resistance', *J. Phycol.*, **31**, 231-241.
- Blinn, D.W., Truitt, R., and Pickart, A. 1989. 'Response of epiphytic diatom communities from the tailwaters of Glen Canyon Dam, Arizona, to elevated temperature', *Regul. Riv.*, **4**, 91-95.
- Blinn, D.W., and Cole, G. A. 1991. 'Algal and invertebrate biota in the Colorado River: Comparison of Pre- and Post-Dam Conditions', *In*. Marzolf, G.R. (Ed), *Colorado River Ecology and Dam Management: Proceedings of a Symposium*. National Academy Press, Washington, D.C.

- Blinn, D. W., Shannon, J. P., Stevens, L. E., and Carder, J. P. 1995. 'Consequences of fluctuating discharge for lotic communities', *N. Amer. Benth. Soc.*, **14**, 233-248.
- Blinn, D. W., Shannon, J. P., Benenati, P. L., and Wilson, K. P. 1998. 'Algal ecology in tailwater stream communities: the Colorado River below Glen Canyon, Dam', *Arizona. J. Phycol.*, **34**, 734-740.
- Boston, H. L. and Hill, W. R. 1991. 'Photosynthesis-light relations of stream periphyton communities', *Limnol. Oceanogr.* **36**, 644-656.
- Brock, J. T., Royer, T. V., Snyder, E. B., and Thomas, S. A. 2000. 'Periphyton metabolism: A chamber method', *In*. Webb, R. H., Schmidt, J. C., Marzolf, G. R., and Valdez, R. A. (Eds), *The controlled flood in Grand Canyon*. Geophysical Monograph, Am. Geophy. Union, Washington, D. C., **110**, 217-223.
- Bureau of Reclamation (BOR). 1995. *Final environmental impact statement: Operation of Glen Canyon Dam Colorado River Storage Project, Coconino County, Arizona*. U.S. Dept. of Interior, Bureau of Reclamation, Salt Lake City, UT.
- Canale, R. P., Auer, M. T., and Graham, J. M. 1982. 'Ecological studies and mathematical modeling of *Cladophora* in Lake Huron: 1. Seasonal and spatial variation in growth kinetics', *J. Great Lakes Res.*, **8**, 126-133.
- Canale, R. P., and Auer, M. T. 1982. 'Ecological studies and mathematical modeling of *Cladophora* in Lake Huron: 7. Model verification and system response', *J. Great Lakes Res.*, **8**, 134-143.
- Carpenter, S. R., Cole, J. J., Hodgson, J. R., Kitchell, J. F., Pace, M. L., Bade, D., Cottingham, K. L., Essington, T. E., Houser, J. N., and Schindler, D. E. 2001. 'Trophic cascades, nutrients, and lake productivity: whole-lake experiments', *Ecological Monographs.*, **71**, 163-186.
- Clarkson, R. W., Gorman, O. T., Kubly, D. M., Marsh, P. C., and Valdez, R. A. 1994. 'Management of discharge, temperature, and sediment in Grand Canyon for native fishes', Issue paper. Glen Canyon Environmental Studies, Flagstaff, AZ.
- Cuker, B. E. 1983. 'Grazing and nutrient interactions in controlling the activity and composition of the epilithic algal community of an arctic lake', *Limnol. Oceanogr.*, **28**, 133-141.
- Czarnecki, D. B., and Blinn, D. W. 1978. 'Diatoms of the Colorado River in Grand Canyon National Park and vicinity', *Bibl. Phycologia.*, **38**, 1-181.

- Dodds, W. K. 1991. 'Community interactions between the filamentous alga *Cladophora glomerata* (L) Kutzing its epiphytes, and epiphyte grazers', *Oecologia.*, **85**, 572-580.
- Dodds, W. K., and Gudder, D. A. 1992. 'The ecology of *Cladophora*', *J. Phycol.*, **28**, 415-427.
- Dodds, W. K., Hutson, R. E., Eichen, A. C., Evans, M. A., Gudder, D. A., Fritz, K. M., and Gray, L. 1996. 'The relationship of floods, drying, flow and light to primary production and producer biomass in a prairie stream', *Hydrobiologia.*, **333**, 151-159.
- Dudley, T. L. 1992. 'Beneficial effect of herbivores on stream macroalgae via epiphyte removal', *Oikos.*, **65**, 121-127.
- Dynesius, M., and Nilsson, C. 1994. 'Formation and flow regulation of river systems in the northern third of the world', *Science.*, **266**, 753-762.
- Falkowski, P. G., and Raven J. A. 1997. *Aquatic photosynthesis*. Blackwell Science, Malden, Mass.
- Fayolle, S., Cazaubon, A., Comte, K., and Franquet, E. 1998. 'The intermediate disturbance hypothesis: application of this concept to the response of epilithon in a regulated Mediterranean river (Lower-Durance, southeastern France)', *Arch. Hydrobiol.*, **143**, 57-77.
- Frontline Systems, Inc. 1999. Software NLP/NSP Solver DLL V 3.5. Incline Village, NV.
- Gomez, I., Perez-Rodriguez, E., Vinegla, B., Figueroa, F., and Karsten, U. 1998. 'Effects of solar radiation on photosynthesis, UV-absorbing compounds and enzyme activities of the green alga *Dasycladus vermicularis* from southern Spain', *J. Photochem Photobiol B Biol.*, **47**, 46-57.
- Graham, J. M., Auer, M. T., Canale, R. P., and Hoffman, J. P. 1982. 'Ecological studies and mathematical modeling of *Cladophora* in Lake Huron: 4. Photosynthesis and respiration as functions of light and temperature', *J. Great Lakes Res.*, **8**, 100-111.
- Guasch, H., and Sabater, S. 1995. 'Nutrient enrichment effects on biofilm metabolism in a Mediterranean stream', *Freshwat. Biol.*, **33**, 373-383.
- Haden, G. A., Blinn, D. W., Shannon, J. P., and Wilson, K. P. 1999. 'Driftwood: an alternative habitat for macroinvertebrates in a large desert river', *Hydrobiologia.*, **397**, 179-186.

- Haden, A. 1997. 'Benthic ecology of the Colorado River system through the Colorado Plateau region', *M.S. Thesis.*, Northern Arizona University, Flagstaff, AZ.
- Hardwick, G. G., Blinn, D. W., and Usher, H. D. 1992. 'Epiphytic diatoms on *Cladophora glomerata* in the Colorado River, Arizona: longitudinal and vertical distribution in a regulated river', *The Southwestern Naturalist*, **37**, 148-156.
- Harris, G. P. 1978. 'Photosynthesis, productivity and growth: The physiological ecology of phytoplankton', *Ergeb. Limnol.*, **10**, 1-171.
- Hart, D. D., Kohler, S. L., and Carlton, R. G. 1991. 'Harvesting of benthic algae by territorial grazers: the potential for prudent predation', *Oikos.*, **60**, 329-335.
- Hill, W. 1996. 'Factors affecting benthic algae. Effects of light', *In*. Stevenson, R. J., Bothwell, M. I., and Lowe, R. L. (eds.), *Algal ecology: freshwater benthic ecosystems.*, Academic Press, Inc., San Diego, Calif.
- Jassby, A. D. and Platt, T. 1976. 'Mathematical formulation of the relationship between photosynthesis and light for phytoplankton', *Limnol Oecnaogr.*, **21**, 540-547.
- Jones, R. I. 1977. 'The importance of temperature conditioning to the respiration of natural phytoplankton communities', *Br. Phycol. J.*, **12**, 277-285.
- Jordan, S., Shiozawa, D. K., and Schmid-Araya, J. M. 1999. 'Benthic invertebrates of a large, sandy river system: the green and Colorado Rivers of Canyonlands National Park, Utah', *Arch. Hydrobiol.*, **147**, 91-127.
- Kalchev, R. K., Beshkova, M. B., Boumbarova, C. S., Tsvetkova, R. L., Sais, D. 1996. 'Some allometric and non-allometric relationships between chlorophyll-a and abundance variables of phytoplankton', *Hydrobiologia.*, **341**, 235-245.
- Karsten, U., Bischof, K., and Wiencke, C. 2001. 'Photosynthetic performance of Arctic macroalgae after transplantation from deep to shallow waters', *Oecologia.*, **127**, 11-20.
- Kirk, J. T. O. 1983. '*Light and photosynthesis in aquatic ecosystems*', Cambridge University Press, Cambridge.
- Lekan, J. F. and Coney, T. A. 1982. 'The use of remote sensing to map the areal distribution of *Cladophora glomerata* at a site in Lake Huron', *J. Great Lakes Res.* **8**, 144-152.
- Ligon, F. K., Dietrich, W. E., and Trush, W. J. 1995. 'Downstream ecological effects of dams, a geomorphic perspective', *Bioscience.*, **45**, 183-192.

- Lowe, R. 1979. 'Phytobenthic ecology and regulated stream', *In* Ward, J. V. and Stanford, J. A. (eds), *The ecology of regulated streams*, Plenum Press, New York, NY.
- Marzolf, G., Bowser, C. J., Hart, R., Stephens, D. W., and Vernieu, W. S. 2000. 'Photosynthetic and respiratory processes: An open stream approach', *In* Webb, R. H., Schmidt, J. C., Marzolf, G. R., and Valdez, R. A. (eds), *The controlled flood in Grand Canyon.*, Geophysical Monograph, Am. Geophys. Union, Washington, DC., **110**, 205-215.
- McKinney, T., Rogers, R. S., Ayers, A. D., and Persons, W. R. 2000. 'Lotic community responses in the Lees Ferry Reach', *In* Webb, R. H., Schmidt, J. C., Marzolf, G. R., and Valdez, R. A. (Eds.), *The controlled flood in Grand Canyon.*, Geophysical Monograph, Am. Geophys. Union, Washington, DC., **110**, 249-258.
- Minckley, W. L. 1991. 'Native fishes of the Grand Canyon region: an obituary?', *In* National Academy of Sciences (eds.) *Colorado River ecology and dam management.*, NAS Press, Washington, D.C. pp. 124-177.
- Munoz, I., Real, M., Guasch, H., Navarro, E., and Sabater, S. 2000. 'Resource limitation by freshwater snail (*Stagnicola vulnerata*) grazing pressure: an experimental study', *Arch. Hydrobiol.*, **148**, 517-532.
- Nozaki, K. 2001. 'Abrupt change in primary productivity in a litoral zone of Lake Biwa with the development of a filamentous green-algal community', *Freshwater Biology.*, **46**, 587-602.
- Petts, G. E. 1984. *Impounded rivers*. Wiley Press, Chichester, England.
- Pinney, C. 1991. 'The response of *Cladophora glomerata* and associated epiphytic diatoms to regulated flow and the diet of *Gammarus lacustris*, in the tailwater of Glen Canyon Dam', *MS Thesis*, Northern Arizona University. pp. 94.
- Poff, N.L., Allan, D., Bain, M. B., Karr, J. R., Prestegard, K. L., Richter, B. D., Sparks, R. E., and Stromberg, J. C. 1997. 'The natural flow regime, a paradigm for river conservation and restoration', *BioScience.*, **47**, 769-784.
- Rader, R. B. and Ward, J. V. 1988. 'Influence of regulation on environmental conditions and the macroinvertebrate community in the upper Colorado River', *Regul. Riv.*, **2**, 597-618.
- Ramus, J. 1990. 'A form-function analysis of photon capture for seaweeds', *Hydrobiologia.*, **204/205**, 65-71.
- Rhee, G.-Yull. 1982. 'Effects of environmental factors and their interactions on phytoplankton growth', *Adv. Microb. Ecol.*, **6**, 33-74.

- Salisbury, F. B. and Ross, C. W. 1985. *Plant Physiology.*, Wadsworth Publishing Company, Belmont, CA.
- SAS, Inc., 1996. Version 6.12, SAS Institute, Inc. Cary, N.C. USA.
- Schmidt, J.C., Webb, R. H., Valdez, R. A., Marzolf, G. R., Stevens, L. E. 1998. 'Science and values in river restoration in the Grand Canyon', *BioScience.*, **48**, 735-747.
- Shannon, J. P., Blinn D. W., and Stevens, L. E. 1994. 'Trophic interactions and benthic animal community structure in the Colorado River, AZ, USA', *Freshwater Biology.*, **31**, 213-220.
- Shannon, J. P., Blinn, D. W., Haden, G. A., Benenati, E. P., and Wilson, K. P. 2001. 'Food web implications of $\delta^{13}\text{C}$ and $\delta^{15}\text{N}$ variability over 370 km of the regulated Colorado River USA', *Isotopes Environ. Health Stud.*, **37**, 179-191.
- Shaver, M. L., Shannon, J. P., Wilson, K. P., Benenati, P. L., and Blinn, D. W. 1998. 'Effects of suspended sediments and desiccation on the benthic tailwater community in the Colorado River, USA', *Hydrobiologia.*, **357**, 63-72.
- Spencer, W. E., Delaney, S. R., Rice, G. T., Johnston, K. L., Seither, R. and White, D. S. 1998. 'Optimum temperature for carbon assimilation in Kentucky Lake follows seasonal change in ambient temperature', *Arch. Hydrobiol.*, **141**, 389-401.
- Stanford, J. A. 1994. 'Instream flows to assist the recovery of endangered fishes of the Upper Colorado River Basin', Biological Report 24. DOI, National Biological Survey, Washington, D.C.
- Statsoft, Inc. 1997. Statistica for Windows., Version 5.1, Tulsa, O.K., USA.
- Stevens, L. E., Shannon, J. P., and Blinn, D. W. 1997. 'Colorado River benthic ecology in Grand Canyon, Arizona, USA: Dam, tributary and geomorphological influences', *Regul. Riv.*, **13**, 129-149.
- Stevens, L. E., Sublette, J. E., and Shannon, J. P. 1998. 'Chironomidae (Diptera) of the Colorado River, Grand Canyon, Arizona, USA, II: Factors influencing distribution', *Great Basin Naturalist.*, **58**, 147-155.
- Stevenson, R. J., and Stoermer, E. F. 1982. 'Seasonal abundance patterns of diatoms on *Cladophora* in Lake Huron', *J. Great Lakes Res.*, **8**, 169-183.

- Storr, J. F. and Sweeney, R. A. 1971. 'Development of a theoretical seasonal growth response curve of *Cladophora glomerata* to temperature and photoperiod', *In Proc. 14th Conf. Great Lakes Res., Internat. Assoc. Great Lakes Res.*, pp. 119-127.
- Sublette, J. E., Stevens, L. E. and Shannon, J. P. 1998. 'Chironomidae (Diptera) of the Colorado River, Grand Canyon, Arizona, USA, I: Systematics and ecology', *Great Basin Naturalist*, **58**, 97-146.
- Tett, P., Gallegos, C., and Kelly, M. G. 1978. 'Relationships among substrate, flow, and benthic microalgal pigment density in the Mechums River, Virginia', *Limnol. Oceanogr.*, **23**, 785-797.
- Thorp, J. H., and Delong, M. D. 1994. 'The riverine productivity model: an heuristic view of carbon sources and organic processing in large river ecosystems', *Oikos.*, **70**, 305-308.
- Valdez, R. A., Douglas, M. E., Ryel, R. J., Bestgen, K. R., and Wegner, D. L. 2000. *A program of experimental flows for endangered and native fishes of the Colorado River in Grand Canyon.*, Final Report, SWCA., Flagstaff, AZ.
- Ward, J. V. and Stanford, J. A. 1983. 'The serial discontinuity concept of lotic ecosystems', *In*. Fontaine, T.D. and Bartell, S.M. (eds), *Dynamics of lotic ecosystems*. Ann Arbor Science Publ., Ann Arbor, MI, pp. 29-42.
- Whitton, B. A. 1970. 'Biology of *Cladophora* in freshwaters', *Water Res.*, **4**, 457-476.
- Wolfe, T. L., and Sweeney, R. A. 1982. 'Laurentian Great Lakes *Cladophora* annotated bibliography', *J. Great Lakes Res.*, **8**, 201-237.
- Yard, M. D., and Blinn, D. W. 2001. 'Algal colonization and recolonization response rates during experimental low summer steady flows', Final Report, Grand Canyon Monitoring and Research Center, Flagstaff, AZ.

Table I. Predicted metabolic rates for net daily photosynthesis NP ; total 24-h community respiration, CR_{N+D} ; hourly biomass-specific gross primary production, $BSGP$; daily area-specific gross primary production, $ASGP$; and net primary production, NPP . Estimates were iteratively determined over a 5-min interval, based on optimal light conditions ($K_N = 0.24 \text{ m}^{-1}$) for Lees Ferry, 21-June ($63.2\text{-mol m}^{-2} \text{ da}^{-1}$), at 0.5-m depths.

AFDM g C m^{-2}	11°C					16°C				
	NP $\text{gO}_2\text{m}^{-2}\text{d}^{-1}$	CR_D $\text{gO}_2\text{m}^{-2}\text{d}^{-1}$	$BSGP_{AVG}$ $\text{gO}_2\text{gCm}^{-2}\text{h}^{-1}$	$ASGP$ $\text{gO}_2\text{m}^{-2}\text{d}^{-1}$	NPP $\text{gO}_2\text{m}^{-2}\text{d}^{-1}$	NP $\text{gO}_2\text{m}^{-2}\text{d}^{-1}$	CR_D $\text{gO}_2\text{m}^{-2}\text{d}^{-1}$	$BSGP_{AVG}$ $\text{gO}_2\text{gCm}^{-2}\text{h}^{-1}$	$ASGP$ $\text{gO}_2\text{m}^{-2}\text{d}^{-1}$	NPP $\text{gO}_2\text{m}^{-2}\text{d}^{-1}$
1	0.324	0.015	0.031	0.338	0.311	0.357	0.022	0.035	0.378	0.339
25	7.195	0.519	0.027	7.714	6.754	8.051	0.686	0.031	8.737	7.467
50	12.318	1.302	0.023	13.620	11.215	13.674	1.554	0.027	15.227	12.356
75	15.666	2.347	0.020	18.013	13.679	18.293	2.823	0.024	21.116	15.901
100	17.257	3.714	0.016	20.971	14.113	20.933	4.337	0.020	25.270	17.260
125	16.831	5.359	0.012	22.191	12.296	21.690	6.155	0.016	27.845	16.480
150	14.239	7.311	0.008	21.549	8.053	20.407	8.266	0.012	28.673	13.412
175	9.258	9.569	0.005	18.827	1.159	16.975	10.652	0.009	27.627	7.962
200	-	-	-	-	-	11.267	13.309	0.005	24.576	0.003

Table II. Summarized production estimates for measured and predicted: area-specific gross primary production, *ASGP*; biomass-specific gross primary production, *BSGP*; net photosynthesis, *NP*; daily community respiration, *CR_D*; and net primary production, *NPP*.

Literature Citation	Brock <i>et al.</i> 2000				Blinn <i>et al.</i> 1998			
	Production Estimates	Measured ⁽⁴⁾	Predicted	Measured ⁽⁴⁾	Predicted	Measured ⁽⁴⁾	Predicted	
<i>ASGP</i>	$\text{gO}_2 \text{ m}^{-2} \text{ d}^{-1}$	18.9	18.5	21.1	19.4	9.6	7.5	
<i>ASGP</i> ± SE	$\text{gO}_2 \text{ m}^{-2} \text{ d}^{-1}$	13.2–24.6	15.5–18.7 ⁽¹⁾	15.9–26.3	17.8–20.6 ⁽¹⁾	9.5–9.7 ⁽³⁾	6.5–8.4 ⁽¹⁾	
<i>ASGP</i> _{AVG}	$\text{mgO}_2 \text{ m}^{-2} \text{ h}^{-1}$	1,575 ⁽²⁾	1,680	1,758 ⁽²⁾	1,762	609 ⁽³⁾	553	
<i>BSGP</i> _{AVG}	$\text{mgO}_2 \text{ gC m}^{-2} \text{ h}^{-1}$	–	15.8	–	18.18	–	34.2	
<i>NPP</i>	$\text{gO}_2 \text{ m}^{-2} \text{ d}^{-1}$	12.4	11.3	16.6	13.0	–	5.5	
<i>NPP</i> ± SE	$\text{gO}_2 \text{ m}^{-2} \text{ d}^{-1}$	6.9–17.9	7.5–11.9 ⁽¹⁾	12.4–20.8	12.0–13.3 ⁽¹⁾	–	4.8–6.2 ⁽¹⁾	
<i>NP</i>	$\text{gO}_2 \text{ m}^{-2} \text{ d}^{-1}$	4.6	13.7	11.2	14.7	–	5.4	
<i>NP</i> ± SE	$\text{gO}_2 \text{ m}^{-2} \text{ d}^{-1}$	(-1.2)–10.4	12.2–14.7 ⁽¹⁾	6.8–15.6	14.0–14.9 ⁽¹⁾	–	4.7–6.0 ⁽¹⁾	
<i>CR</i>	$\text{gO}_2 \text{ m}^{-2} \text{ d}^{-1}$	14.3	3.5	9.8	3.3	–	0.73	
<i>CR</i> ± SE	$\text{gO}_2 \text{ m}^{-2} \text{ d}^{-1}$	11.0–17.6	2.0–5.5 ⁽¹⁾	5.1–14.5	2.6–4.4 ⁽¹⁾	–	0.62–0.84 ⁽¹⁾	
Parameters		Measured	Predicted	Measured	Predicted	Measured	Predicted	
Date		26-28 March	27-March	4-9 April	6-April	June	21-June	
Incubation time	h	Daily	Integrated	Daily	Integrated	10:00–14:00	4	
AFDM	g m^{-2}	105 g	–	95 g	–	15.8 g	–	
AFDM ± SE	g m^{-2}	73–137 g	–	81–114 g	–	13.7–17.9 g	–	
K_N	m^{-1}	–	0.24 ⁽⁴⁾	–	0.24 ⁽⁴⁾	–	0.25 ⁽⁴⁾	
Day-length	Hr	12.0	13.2 ⁽⁵⁾	12.0	13.5 ⁽⁵⁾	–	13.5 ⁽⁵⁾	
Daily Insolation	$\text{mol m}^{-2} \text{ da}^{-1}$	–	44.8 ⁽⁵⁾	–	47.7 ⁽⁵⁾	–	58.9 ⁽⁵⁾	
Surface PFD _{MAX}	$\mu\text{mol m}^{-2} \text{ s}^{-1}$	½ - Surface	1,810 ⁽⁵⁾	½ - Surface	1,867 ⁽⁵⁾	1800-2300	2,025 ⁽⁵⁾	
Water PFD _{MAX}	$\mu\text{mol m}^{-2} \text{ s}^{-1}$	–	902 ⁽⁵⁾	–	931 ⁽⁵⁾	–	1,650 ⁽⁵⁾	
Water Temp	°C	–	9.3° ⁽⁶⁾	–	10.5° ⁽⁶⁾	15.4–16.2° ⁽⁷⁾	–	
Depth	M	0-1-m	–	0-1-m	–	0-8-m ⁽⁷⁾	–	

¹ Range based on reported mean AFDM SE (±); ² Hourly rates estimated by dividing measured daily *ASGP* by the reported 12-hr incubation period (Brock *et al.* 2000); ³ Carbon *NPP* estimates converted back to original units ($\text{g-O}_2 \text{ m}^{-2} \text{ d}^{-1}$); (Blinn *et al.*, 1998); ⁴ Glen Canyon daily mean light attenuation coefficients (K_N : normalized for light refraction) estimated using water quality parameters at Lees Ferry (unpublished data); ⁵ Solar incidence at water surface (PFD, $\mu\text{mol m}^{-2} \text{ s}^{-1}$), (unpublished data); ⁶ Lees Ferry, mean daily temperatures (GCMRC 1990-2002 water quality data); ⁷ Personal communications with Shannon, J. P.

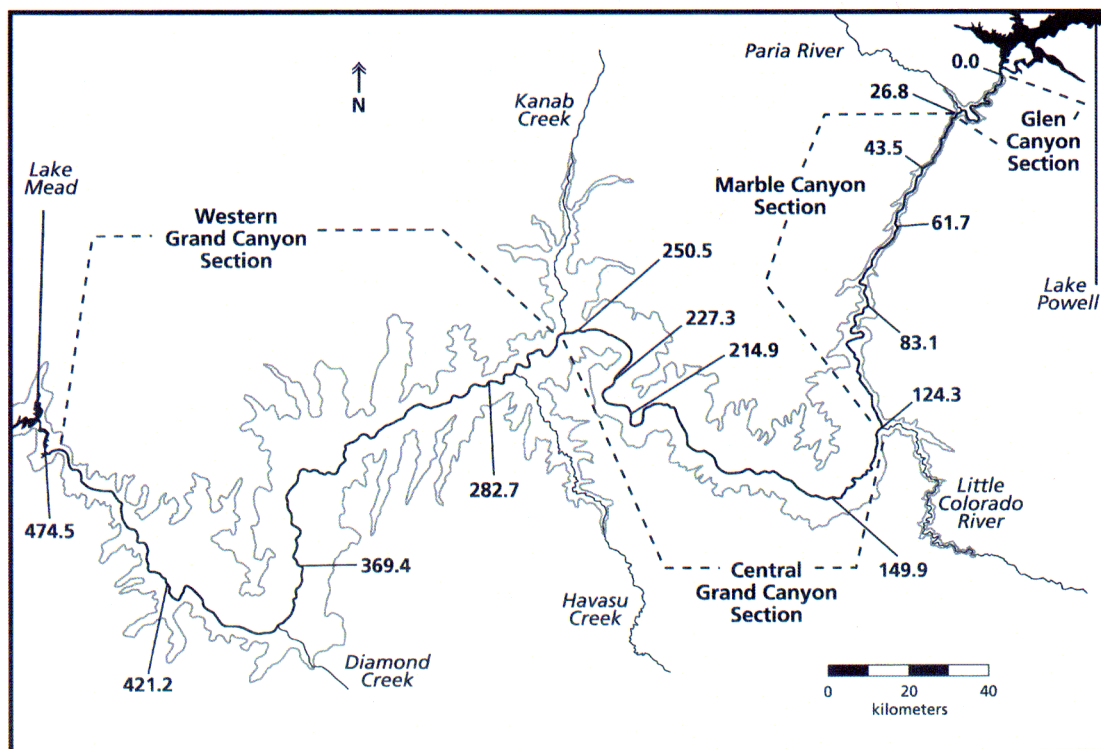


Figure 1. Map of the Colorado River, between Lake Powell and Lake Mead reservoirs the major canyon sections and tributaries are indicated.

Figure 2. Measured and predicted rates of net photosynthesis normalized per unit biomass (NP : $\text{mgO}_2 \text{ gC}^{-1} \text{ m}^{-2} \text{ h}^{-1}$) at two constant temperatures: Fig 2-A, 11°C ; and Fig 2-B, at 16°C . Net photosynthetic-irradiant response for estimates of oxygen generated at varying levels of underwater photosynthetic photon flux density (PPFD: $\mu\text{mol quanta m}^{-2} \text{ s}^{-1}$).

Figure 3. Predicted area-specific gross primary production ($ASGP$: $\text{mgO}_2 \text{ m}^{-2} \text{ h}^{-1}$) response and community respiration (CR_D : $\text{mgO}_2 \text{ m}^{-2} \text{ h}^{-1}$) over a range of standing biomass (g-AFDM) at two constant temperatures 11°C , and 16°C .

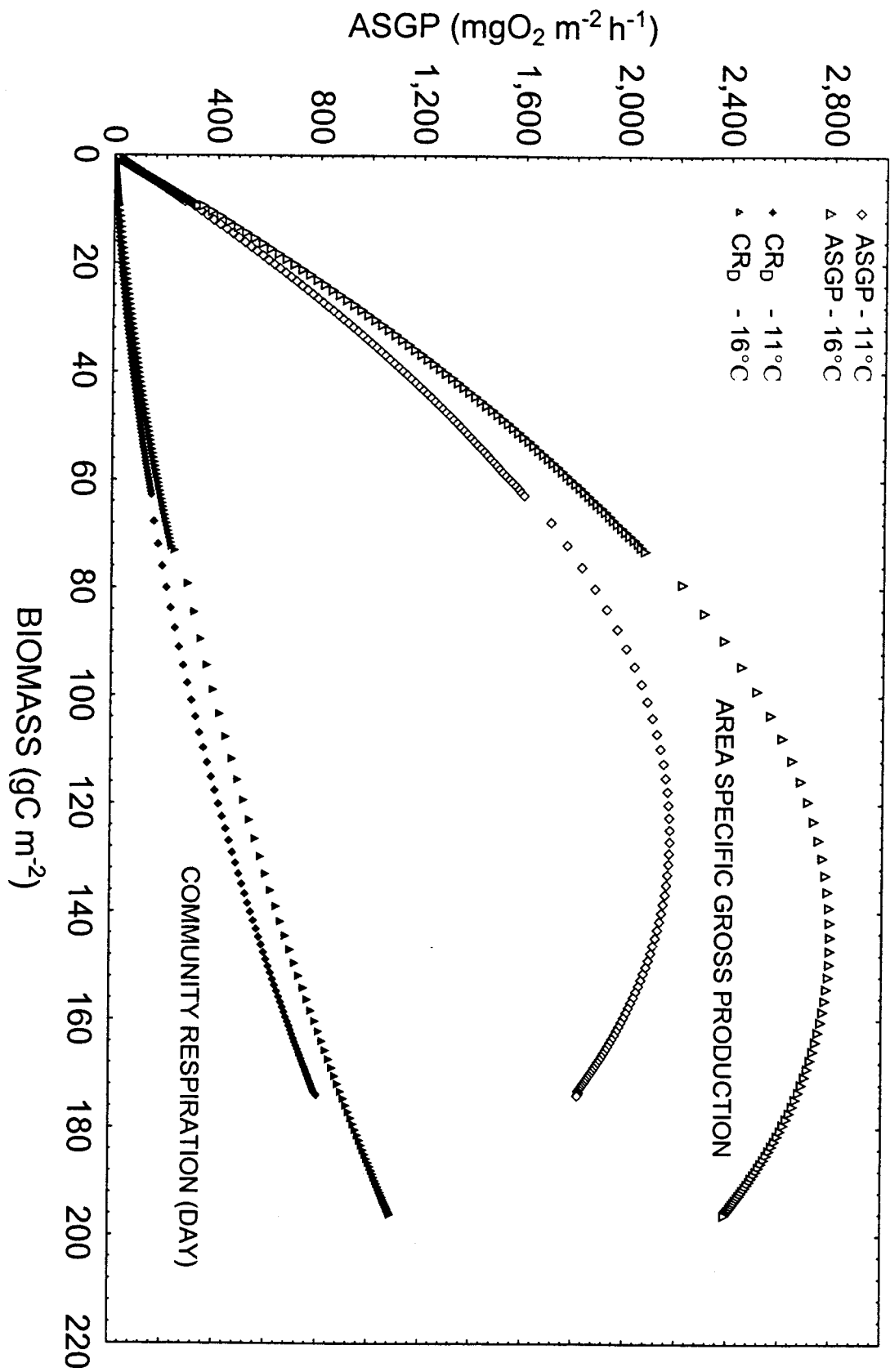


Figure 4. Predicted daily net primary production (NPP : $\text{gO}_2 \text{ m}^{-2} \text{ d}^{-1}$), and total community respiration, day and night (CR_{D+N} : $\text{gO}_2 \text{ m}^{-2} \text{ d}^{-1}$) response distributed over a range of standing biomass (g-AFDM). NPP were numerically solved for, estimating $ASGP$, CR_N , and CR_D under different biomass (g-AFDM), temperature ($^{\circ}\text{C}$), and seasonal light levels (PPFD) using a 5-min iterative process. Estimates were made for three different light-attenuation coefficients (K_N : 0.28, 1.5 and 3.0 m^{-1}) at underwater depths of 0.5-m. Seasonal and thermal comparisons were made between different surface irradiant (63.2 and $25.2 \text{ mol m}^{-2} \text{ da}^{-1}$) and temperature levels (11° – 16°C), Summer- 16°C (Fig 4-A), Winter- 16°C (Fig 4-B), Summer- 11°C (Fig 4-C), and Winter- 11°C (Fig 4-D).

